

ELUCIDATION OF PORCINE CORNEAL
ULTRASTRUCTURE TO INFORM
DEVELOPMENT OF CORNEAL XENOGRAFTS
OR BIOMIMETIC REPLACEMENTS

ASHLEY HOWKINS

*A thesis submitted in partial fulfilment of the
requirements of the University of Brighton for
the degree of Doctor of Philosophy*

June 2015

ABSTRACT

The transparent, anterior-most tissue of the eye globe, which allows light into the eye for sight, is the cornea. The main thickness of the cornea, known as the stroma, is a collagenous extra cellular matrix (ECM) that is comprised of fibrous collagen types I, V and VI along with keratan sulphate (KS) and chondroitin/dermatan sulphate (CS/DS) proteoglycans. These components maintain the collagen fibrils in a quasi-crystalline arrangement, which enables the tissue to be transparent.

Diseases or injuries to the cornea disrupt the ECM architecture resulting in visual impairment due to a loss of transparency with treatment often requiring transplantation of a corneal allograft. However, corneal allografts can fail and transmission of undetectable infective agents is also a potential risk.

Decellularised porcine corneal tissue and *in-vitro* produced stromal ECM replacements have shown great potential to generate tailor-made artificial corneal replacements. However, as yet no microscopic analysis of the porcine stromal ECM has been made and also *in-vitro* produced corneal biomaterials are often created solely using collagen type I.

This investigation used transmission electron microscopy to elucidate upon the full-depth three-dimensional architecture of the porcine stromal ECM; which provided a better understanding of the ECM architecture along with the mechanisms of transparency and the comparability of porcine stromal tissue to human stromal tissue. Moreover, decellularised and swollen porcine corneal stromal tissue was used as a scaffold to re-infiltrate primary human corneal keratocytes into the tissue to generate a humanised porcine corneal xenograft; with transparency being restored by dehydrating the tissue in dextran. Additionally, a novel biomimetic collagen types I and V and CS/DS hydrogel was created and possessed improved light transmission over a collagen type I only hydrogel as well as being able to host primary human corneal stromal cells.

It was concluded, that the corneal ECM architecture plays an important role in corneal transparency and future work into corneal replacements should consider utilising cues from the corneal stromal ECM architecture and components to generate enhanced artificial corneal stromal replacements.

CONTENTS

ABSTRACT	i
CONTENTS	ii
LIST OF TABLES	ix
LIST OF FIGURES	x
LIST OF ABBREVIATIONS.....	xvi
ACKNOWLEDGEMENTS	xviii
PRESENTATIONS.....	xix
DECLARATIONS.....	xx
CHAPTER 1: Introduction - The cornea and the need for a replacement cornea	1
1.1 ANATOMY OF THE EYE AND IMAGE FORMATION	1
1.2 THE CORNEA AND THE NEED FOR ARTIFICIAL CORNEAL REPLACEMENTs	4
1.3 TISSUES SURROUNDING THE CORNEA	8
1.4 CORNEAL STRUCTURE & TRANSPARENCY	12
1.4.1 Corneal Layers.....	12
1.4.2 Corneal Epithelium.....	14
1.4.3 Bowman’s Layer	21
1.4.4 Corneal Stroma	22

1.4.5	Corneal Descemet’s Membrane and Endothelium.....	34
1.5	CORNEAL BLINDNESS AND TREATMENTS.....	38
1.5.1	Surgical Intervention for Corneal Blindness	40
1.5.2	Development of a Novel Corneal Replacement.....	49
1.6	POTENTIAL FOR ARTIFICIAL CORNEAL REPLACEMENTs	52
CHAPTER 2:	Materials and Methods	54
2.1	Materials	54
2.1.1	Primary Human Corneal Fibroblast Culture Materials.....	54
2.2	Methods.....	56
2.2.1	Primary Human Corneal Fibroblast Cell Culture	56
CHAPTER 3:	Elucidation of the Porcine Corneal Stromal Architecture – Using transmission electron microscopy.....	61
3.1	INTRODUCTION.....	61
3.1.1	Corneal Stromal Architecture	62
3.1.2	Elucidation of the Porcine Corneal Stroma.....	63
3.2	EXPERIMENTAL Design.....	64
3.2.1	Sourcing Corneal Tissue	64
3.2.2	Location and Orientation of Stromal Tissue	64
3.2.3	Transmission Electron Microscopy of the Corneal Stroma.....	65
3.2.4	Hypothesis.....	68

3.3	EXPERIMENTAL PROCEDURE	69
3.3.1	Materials	69
3.3.2	Methods	72
3.4	RESULTS.....	76
3.4.1	Fibril Organisation	77
3.4.2	Lamella Organisation	79
3.5	DISCUSSION.....	87
3.5.1	Three-Dimensional Architecture of the Corneal Stroma	87
3.5.2	Comparability of the Architecture of Porcine, Rabbit and Human Corneal Stromal Extracellular Matrices.....	91
3.5.3	Ethical Issues Surrounding Xenografting	93
3.6	CONCLUSIONS	94
CHAPTER 4: Effects of Swelling and Dehydration on Decellularised Porcine Stromal Collagen Architecture for Humanising Corneal Xenografts.....		
4.1	INTRODUCTION	97
4.1.1	Corneal Xenotransplantation	98
4.1.2	Porcine to Human Corneal Xenograft Immunogenicity.....	99
4.1.3	Porcine Corneal Decellularisation	100
4.1.4	Potential for an Improved Corneal Xenograft	102
4.2	EXPERIMENTAL DESIGN	104

4.2.1	Objectives.....	104
4.2.2	Sourcing Porcine Corneal Tissue	105
4.2.3	Porcine Corneal Tissue Decellularisation and Swelling.....	105
4.2.4	Stromal Cellular Infiltration and Dehydration	106
4.2.5	Hypotheses.....	107
4.3	EXPERIMENTAL PROCEDURE	108
4.3.1	Materials	108
4.3.2	Methods	110
4.4	RESULTS.....	115
4.4.1	Corneal Decellularisation and Swelling.....	115
4.4.2	Transmission Electron Microscopy of Swollen and Dehydrated Decellularised Porcine Corneal Stromal Tissue.....	118
4.4.3	Infiltration of Human Corneal Fibroblasts	127
4.5	DISCUSSION.....	128
4.5.1	Corneal Decellularisation	128
4.5.2	Corneal Swelling.....	129
4.5.3	Corneal Dehydration	131
4.5.4	Infiltration of Primary Human Corneal Fibroblasts into Swollen Decellularised Corneal Stromal Tissue	132
4.6	CONCLUSIONS.....	134

CHAPTER 5: Development of a Novel Collagen Types I and V and Glycosaminoglycan Hydrogel as an Artificial Stromal Replacement	135
5.1 INTRODUCTION	135
5.1.1 <i>In-Vitro</i> Produced Artificial Corneal Replacements	136
5.1.2 Corneal Biomaterials & Tissue Engineered Constructs.....	136
5.2 EXPERIMENTAL DESIGN	140
5.2.1 Objectives.....	140
5.2.2 Sourcing Corneal Stromal Extra Cellular Components.....	141
5.2.3 Biomaterial Formulation – Component Ratios	142
5.2.4 Quantitative Biomechanical Analysis.....	144
5.2.5 Hypotheses.....	144
5.3 EXPERIMENTAL PROCEDURE	145
5.3.1 Materials	145
5.3.2 Methods	148
5.4 RESULTS.....	154
5.4.1 Transparency.....	154
5.4.2 Transmission Electron Microscopy	157
5.4.3 Biomechanical Analysis	159
5.4.4 Incorporation of Primary Human Corneal Fibroblasts into a Collagen Type I/V Hydrogel Matrix	161

5.5	DISCUSSION.....	163
5.5.1	Biomimetic Corneal Hydrogel Transparency	163
5.5.2	Biomechanical Analysis	166
5.5.3	Biomimetic Corneal Hydrogels as a Scaffold for Primary Human Corneal Fibroblasts.....	168
5.6	CONCLUSIONS.....	170
CHAPTER 6: Discussion – Elucidation of porcine corneal ultrastructure to inform the development of corneal xenografts or biomimetic replacements		
		172
6.1	INTRODUCTION	172
6.2	ELUCIDATION OF PORCINE CORNEAL ULTRASTRUCTURE	174
6.2.1	Porcine Corneal Stromal Architecture	174
6.2.2	Comparability of Porcine, Rabbit and Human Corneal Stromal Extra Cellular Matrix Architectures	176
6.2.3	Informing the Development of Artificial Corneal Replacements	177
6.3	DEVELOPMENT OF A HUMANISED PORCINE CORNEAL XENOGRAFT.....	178
6.3.1	Porcine Corneal Decellularisation	179
6.3.2	Infiltration of Human Cells into Decellularised Porcine Cornea Tissue	179
6.4	DEVELOPMENT OF BIOMIMETIC CORNEAL REPLACEMENTS	182
6.4.1	Potential for an Improved Artificial Corneal Replacement.....	183
6.4.2	Biomimetic Corneal Replacements.....	184

6.5 CONCLUDING REMARKS	187
REFERENCES	189
APPENDICES	205
APPENDICES	205
APPENDIX A	206
APPENDIX B	210
APPENDIX C	213

LIST OF TABLES

Table 1:	Components of the corneal stromal extra cellular matrix	25
Table 2:	Common examples of corneal ailments	39
Table 3:	Relative composition of corneal stroma extra cellular matrix components.....	142

LIST OF FIGURES

Figure 1:	Schematic representation and image of the eye globe	2
Figure 2:	Schematic flow chart of the penetrating keratoplasty procedure.....	5
Figure 3:	Schematic representation of the anterior eye tissues.....	7
Figure 4:	Schematic representation of the corneal periphery and surrounding tissues.....	9
Figure 5:	Image and schematic representation of the five corneal layers in cross section	13
Figure 6:	Schematic representation of the corneal epithelium in crosssection.....	15
Figure 7:	Schematic representation of the epithelial adherence mechanisms.....	19
Figure 8:	Transmission electron microscope micrograph of the orthogonally arranged collagen lamellae of the corneal stroma.....	24
Figure 9:	Transmission electron microscope micrograph of the uniform arrangement of collagen fibrils within the corneal stromal extra cellular matrix.....	27
Figure 10:	Chemical structure of the stromal extra cellular matrix proteoglycans	29

Figure 11:	Schematic representation of collagen-proteoglycan-collagen bridges within the corneal stromal interstitial fluid	30
Figure 12:	<i>In-situ</i> confocal microscope image of the corneal endothelial cells.....	36
Figure 13:	Schematic flow chart of the limbal epithelial stem cell graft procedure	42
Figure 14:	Schematic representation of the Boston KPro keratoprosthesis.....	45
Figure 15:	Schematic representation of the Osteo-odontal keratoprosthesis	47
Figure 16:	Transmission electron microscope micrograph of porcine corneal stromal extra cellular matrix fibrils	77
Figure 17:	Transmission electron microscope micrograph of rabbit corneal stromal extra cellular matrix fibrils	78
Figure 18:	Mean diameter and spacing of porcine and rabbit corneal stromal collagen fibrils	79
Figure 19:	Transmission electron microscope micrograph of porcine corneal stromal extra cellular matrix orthogonal lamellae.....	81
Figure 20:	Transmission electron microscope micrograph of rabbit corneal stromal extra cellular matrix orthogonal lamellae.....	82
Figure 21:	Transmission electron microscope micrograph of porcine corneal stromal extra cellular matrix interweaving lamellae	83
Figure 22:	Transmission electron microscope micrograph of rabbit corneal stromal extra cellular matrix interweaving lamellae	84

Figure 23:	Transmission electron microscope micrograph of porcine corneal stromal extra cellular matrix anterior and posterior lamellae.....	85
Figure 24:	Transmission electron microscope micrograph of rabbit corneal stromal extra cellular matrix anterior and posterior lamellae.....	86
Figure 25:	Visual inspection of decellularised porcine corneal stromal transparency.....	116
Figure 26:	Cryo-histology images of decellularised porcine corneal tissues	117
Figure 27:	Transmission electron microscope micrograph of swollen decellularised porcine corneal stromal extra cellular matrix fibrils....	120
Figure 28:	Transmission electron microscope micrograph of dehydrated decellularised porcine corneal stromal extra cellular matrix fibrils....	121
Figure 29:	Mean diameter and spacing of swollen and subsequently dehydrated decellularised porcine corneal stromal collagen fibrils....	122
Figure 30:	Transmission electron microscope micrograph of swollen decellularised porcine corneal stromal extra cellular matrix lamellae	125
Figure 31:	Transmission electron microscope micrograph of dehydrated decellularised porcine corneal stromal extra cellular matrix lamellae	126
Figure 32:	<i>In-situ</i> image of primary human corneal fibroblast infiltration into swollen decellularised porcine corneal stromal tissue	127

Figure 33:	Visual inspection of the transparency of artificial biomimetic corneal replacements	154
Figure 34:	Percentage light transmission of biomimetic corneal replacements.....	156
Figure 35:	Transmission electron microscope micrographs and mean fibril diameter and spacing of the collagen fibrils of artificial biomimetic corneal replacements	158
Figure 36:	Biomechanical analysis of artificial biomimetic corneal replacements.....	160
Figure 37:	<i>In-situ</i> image of primary human corneal fibroblasts within artificial biomimetic corneal replacements	162
Appendix A(i):	Composite TEM micrograph taken in low magnification mode of the full depth profile of the porcine corneal stroma	206
Appendix A(ii):	Composite TEM micrograph taken in low magnification mode of the full depth profile of the rabbit corneal stroma.....	207
Appendix A(iii):	Diameter and spacing of the collagen fibrils from porcine and rabbit corneal stromal extra-cellular matrices.....	208
Appendix A(iv):	Boxplot of the collagen fibril diameters of porcine versus rabbit corneal stromal tissues.....	209
Appendix A(v):	Boxplot of the collagen fibril spacing of porcine versus rabbit corneal stromal tissues.....	209

Appendix B(i):	Diameter and spacing of the collagen from swollen porcine corneal stromal tissue extra cellular matrices	210
Appendix B(ii):	95% confidence interval plot of the mean collagen fibril diameter of swollen porcine stromal tissues	211
Appendix B(iii):	95% confidence interval plot of the mean collagen fibril spacing of swollen porcine stromal tissues	211
Appendix B(iv):	95% confidence interval plot of the mean collagen fibril diameter of swollen porcine stromal tissues after dextran treatment	212
Appendix B(v):	95% confidence interval plot of the mean collagen fibril spacing of swollen porcine stromal tissues after dextran treatment	212
Appendix C(i):	Mean absorbance and % light transmittance of biomimetic artificial corneal replacements.....	213
Appendix C(ii):	95% confidence interval plot of the mean % light transmittance of biomimetic artificial corneal replacements at 405nm.....	214
Appendix C(iii):	95% confidence interval plot of the mean % light transmittance of biomimetic artificial corneal replacements at 450nm.....	214
Appendix C(iv):	95% confidence interval plot of the mean % light transmittance of biomimetic artificial corneal replacemenst at 490nm.....	215
Appendix C(v):	95% confidence interval plot of the mean % light transmittance of biomimetic artificial corneal replacements at 595nm.....	215
Appendix C(vi):	95% confidence interval plot of the mean % light transmittance of biomimetic artificial corneal replacements at 750nm.....	216

Appendix C(vii):	Mean fibril diameters of novel biomimetic corneal replacements	217
Appendix C(viii):	95% confidence interval plot of the mean fibril diameters of novel biomimetic corneal replacements.....	218
Appendix C(ix):	Shear stress sweep test of biomimetic corneal collagen hydrogels ...	219
Appendix C(x):	Storage modulus (G') for biomimetic corneal collagen hydrogels	220
Appendix C(xi):	Loss modulus (G'') for biomimetic corneal collagen hydrogels	221
Appendix C(xii):	Complex modulus ($ G^* $) for biomimetic corneal collagen hydrogels	222
Appendix C(xiii):	95% confidence interval plot of the storage modulus (G') for biomimetic corneal collagen hydrogels	223
Appendix C(xiv):	95% confidence interval plot of the loss modulus (G'') for biomimetic corneal collagen hydrogels	223
Appendix C(xv):	95% confidence interval plot of the complex modulus ($ G^* $) for biomimetic corneal collagen hydrogels	224

LIST OF ABBREVIATIONS

NAME	ACRONYM
1-ethyl-3-(3-dimethyl-aminopropyl-carbodiimide)	EDAC
Analysis of variance	ANOVA
Ascorbic acid	Vitamin C
Chondroitin sulphate (Chondroitin sulphate A) (Chondroitin sulphate C)	CS CS _A CS _C
Complex modulus	G*
Deep anterior lamella keratoplasty	DASK
Dermatan sulphate (Chondroitin sulphate B)	DS
Dimethylsulphoxide	DMSO
Dulbecco's modified Eagle's medium	DMEM
Embryonic keratocytes	EK1Br
Extra cellular matrix	ECM
Foetal calf serum	FCS
Glycosaminoglycan	GAG
Haematoxylin and eosin stain	H & E stain
Keratan sulphate	KS
Limbal ring fibroblasts	LRF
Loss modulus	G''
Matrix metalloprotease-2	MMP-2
N-hydroxysuccinimide	NHS

Optimum cutting compound	OCT
Osmium tetroxide	OsO ₄
Osteo-odontal keratoprosthesis	OOKP
Phosphate buffered saline	PBS
Poly-methyl methacrylate	PMMA
Proteoglycan	PG
Queen Victoria Hospital	QVH
Sodium dodecyl sulphate	SDS
Sodium hydroxide	NaOH
Sodium/potassium adenosine triphosphatase	Na ⁺ /K ⁺ ATPase
Storage modulus	G'
Thiazolyl Blue Tetrazolium Bromide assay	MTT
Transmission electron microscope	TEM
World Health Organisation	WHO

ACKNOWLEDGEMENTS

The author wishes to acknowledge the kind contributions made by the following individuals for their help during the research carried out during this thesis:

Dr. S. E. (Liz) James and Dr. Stuart L. James, both formerly of the University of Brighton, for their supervision, guidance, expertise, training and the opportunity to conduct this research project.

Dr. S.E. (Liz) James, formerly of the Queen Victoria Hospital and Blonde McIndoe Research Foundation and Dr. Angela (Angie) Sheerin of the University of Brighton for kindly gifting the limbal ring fibroblasts and embryonic keratocytes, respectively, utilised during this thesis.

Dr. Ross Shevchenko, Dr. Iain U. Allan, Dr. Matthew Illsley, all of the University of Brighton, Dr. Badr Ibrahim, formerly of the University of Brighton, and the technical staff (including but not limited to Anna Blunden and Jenny Holtier) from the School of Pharmacy and Biomolecular Sciences of the University of Brighton for their help, training and expertise of tissue culture, tissue engineering and biomaterials.

Dr. Julian R. Thorpe of Sussex University and Prof. Ian W. Boyd and Dr. Alan J. Reynolds of Brunel University for kindly making available the Hitachi-7100 and Jeol-2100, respectively, Transmission Electron Microscopes utilised during this thesis as well as their training and expertise of electron microscopy and ultra-microtomes.

Dr. Che J. Connon, of the Reading University and his team, for their guidance and expertise of collagen hydrogels and fibrillogenesis.

PRESENTATIONS

The following presentations were made to disseminate the findings of the research results presented herein:

Howkins, A.J. (2014); Modelling porcine corneal tissue to inform xenograft and *in-vitro* produced biomimetic corneal replacement development; Presented at the TEM – Research at ETC Brunel Open Day, Brunel University

Howkins, A.J. (2013); Artificial Corneal Replacements: Decellularised porcine corneal tissue as a xenografts & A novel collagen type I/V hydrogel biomaterial; Presented at the Experimental Techniques Centre Seminar Series, Brunel University

Howkins, A.J. (2010); Analysis of a *De Novo* Extra Cellular Matrix Produced by Human Corneal Fibroblasts Compared with Porcine and Rabbit Stromal Tissue Models; Poster presented at the European Tissue Engineering and Regenerative Medicine International Society, Galway University, Ireland

Howkins, A.J. (2009); An investigation into the corneal structure using a porcine model and the development of a stromal replacement using biomaterials; Poster presented at the Postgraduate Annual Research Presentation Day, University of Brighton

Howkins, A.J. (2008); An investigation into the detailed structure of the corneal stroma with a view to the development of a full thickness corneal replacement; Presented at the 1st Limbal Stem Cell Forum, Newcastle

Howkins, A.J. (2007); Artificial Corneal Replacements; presented at the Postgraduate Annual Research Presentation Day, University of Brighton

DECLARATIONS

I declare that the research contained within this thesis, unless otherwise formally indicated within the text, is the own work of the author. The thesis has not been previously submitted to this or any other university for a degree and does not incorporate any material already submitted for a degree.

Signed:

A handwritten signature in black ink, consisting of a stylized initial 'A' followed by a horizontal line with a small vertical tick at the end.

Date:

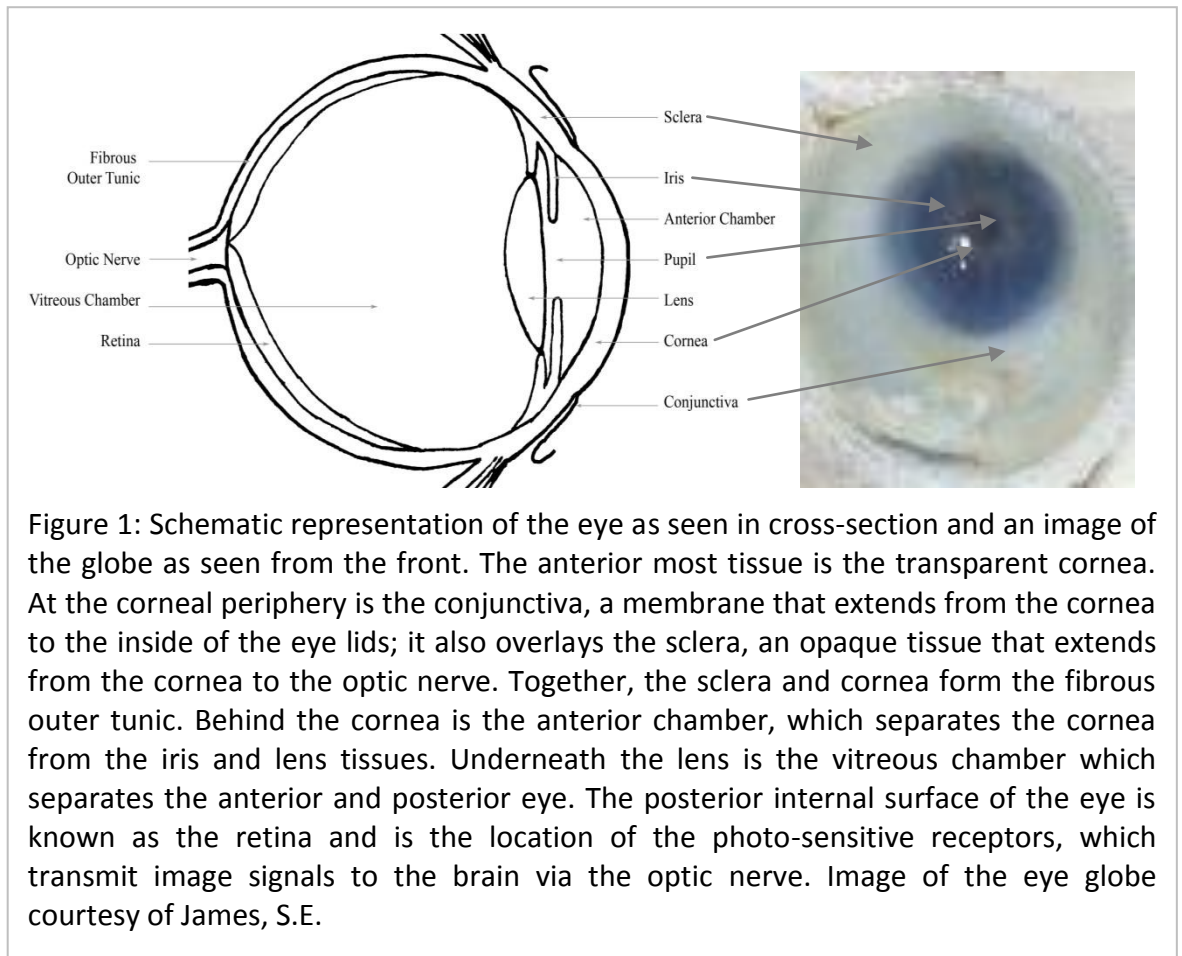
June 2015

CHAPTER 1: Introduction - The cornea and the need for a replacement cornea

The cornea is the anterior tissue of the eye and the first tissue through which light must pass in order to enable vision. However, when this tissue does not function correctly vision will inevitably become impaired, even if the rest of the eye is functioning normally. In order to correct the problem some kind of surgical intervention will be required; yet the current treatment options are not always satisfactory hence more research is required to develop better treatments and improve the prognosis for corneal blindness sufferers.

1.1 ANATOMY OF THE EYE AND IMAGE FORMATION

The eye enables humans and animals to visualise the surrounding environment by detecting visible electromagnetic wavelengths and transmitting them into electro-chemical signals which the brain uses to form an image. This is achieved by multiple tissues working together to capture, focus and transmit light (Figure 1). The anterior most tissue of the eye is the fibrous and transparent cornea. Being transparent the cornea is a window through which light passes into the eye while the fibrous nature is used to form part of the fibrous outer tunic that encases the eye organ.



At the periphery of the cornea is the conjunctiva and sclera. The conjunctiva is a membrane that covers the anterior surface of the sclera and the inside of the eye lids and is involved with tear film production, which lubricates eye-lid movement. Beneath the conjunctiva is the opaque sclera, which makes up the remaining portion of the fibrous tunic and extends from the corneal round to the optic nerve at the back of the eye.

Behind the cornea are the anterior chamber, iris and pupil tissues. The anterior chamber is filled with a watery liquid known as aqueous humour, which provides nutrition to the cornea and its volume aids with maintaining the intra-ocular pressure within the eye globe. The iris is the coloured portion of the eye and controls the size of the pupil, which is seen as the “black hole” in the centre of the eye. The iris will dilate or contract the pupil

according to the light conditions to allow more or less light into the eye, respectively; analogous to a camera shutter controlling the exposure time.

Beneath the iris and pupil is the lens, a transparent tissue that focuses light onto the retina at the back of the eye. It is a flexible structure that is suspended within an elastic capsule. The flexible nature of the tissue enables it to change shape so it may focus light rays onto the retina (Marieb, 2004).

Between the lens and retina is a vacuous space known as the vitreous chamber. This space is filled with a viscous, jelly-like, liquid known as vitreous humour, which creates the majority of the intra-ocular pressures to prevent the eye structure from collapsing.

The tissue at the back of the eye is the retina, which is an area rich in photo-receptor cells. The photo receptor cells detect the beam of light and create an electro-chemical potential that is transmitted along the optic nerve, situated at the back of the eye, to the brain, where the image is interpreted.

In order for the eye to form an image, there is a cascade of events that must take place so that light waves from the external environment can be transmitted into electro-chemical signals. Firstly, light waves enter the eye globe through the transparent cornea. At the posterior surface of the cornea the light rays are refracted so they will pass through the anterior chamber and pupil and on to the lens. Once the light rays hit the lens they are further refracted to focus the light rays onto the back of the eye. At the back of the eye the light rays strike the photo-sensitive receptors within the cells of the retina, which will stimulate an electro-chemical signal (known as an action potential) to be sent along the optic nerve to the brain, where the signal is interpreted and formed into an image.

1.2 THE CORNEA AND THE NEED FOR ARTIFICIAL CORNEAL REPLACEMENTS

The cornea makes up approximately the anterior one-sixth of the fibrous outer tunic, which maintains the eye globe structure, as well as aiding light refraction into a focal point on the retina; although, its main function is to be transparent.

Corneal transparency can be attributed to an organised collagen architecture, whereby collagen fibrils are very thin and evenly spaced at less than half the wave-length of light apart (Benedek, 1971, Maurice, 1957), this is discussed in more detail in subsequent sections, (*see section 1.4.4 Corneal Stroma*). In addition to providing transparency, the collagenous architecture maintains the structure of the eye globe, through an interweaving fibrous network (Radner & Mallinger, 2002). Furthermore, the cornea has a convex geometry that allows it to refract light onto the retina. Human corneas have a thickness that varies from 0.7mm at the periphery to 0.5mm centrally (Nishida et al., 1997), analogous to a convex camera lens.

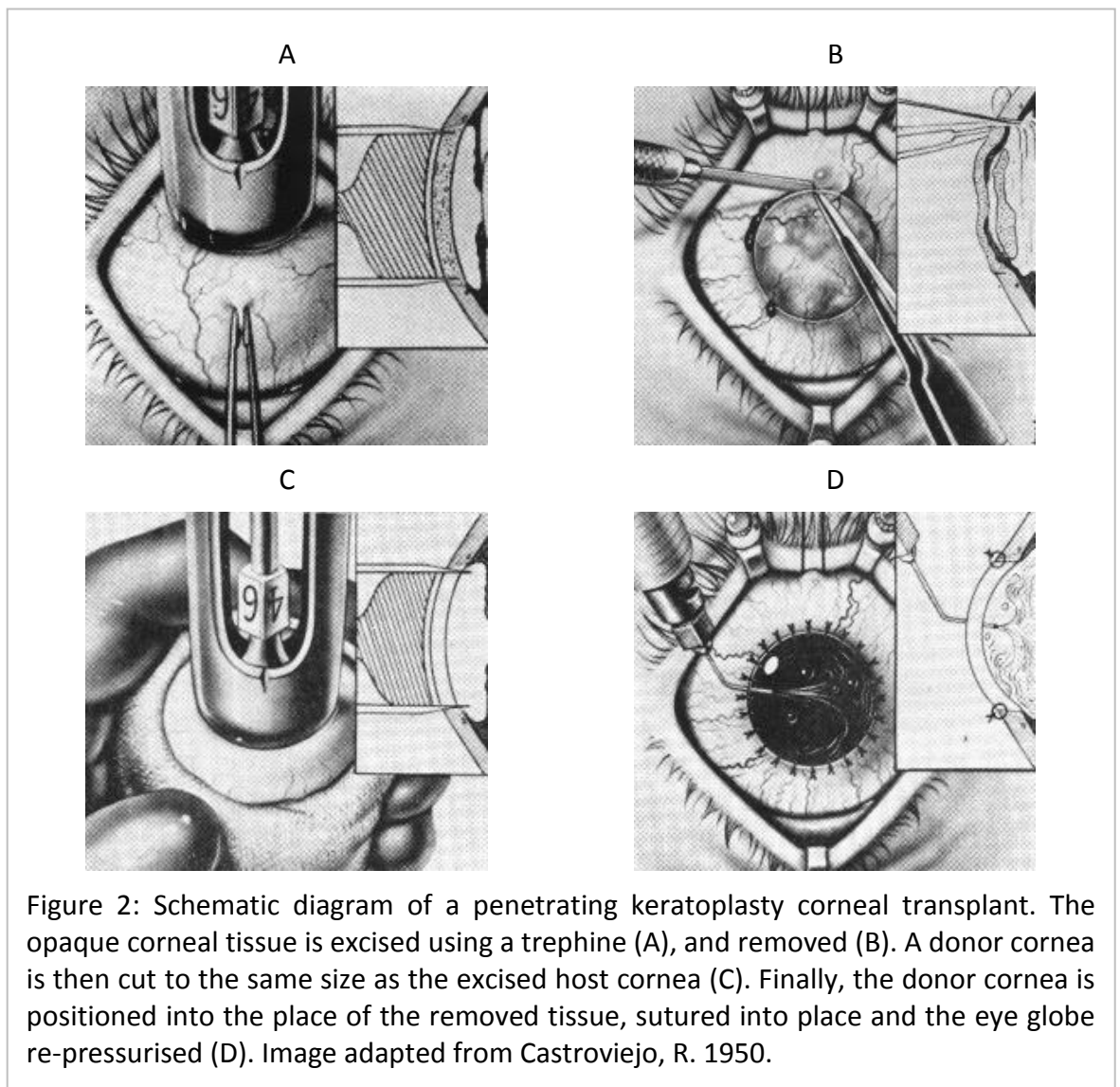
The need for corneal transparency is essential for vision, since a loss of corneal transparency will prevent light entering the eye resulting in blindness even if the remaining eye tissues are functioning.

Certain diseases or injury to the cornea may result in decreased tissue transparency or even tissue opacity, resulting in impaired vision since light rays will not be able to enter the eye. According to the World Health Organisation (WHO) blindness caused by corneal opacities affects 1.56 million individuals and accounts for an additional 2.46 million visually impaired individuals (Pascolini and Mariotti, 2012).

Curing corneal blindness does not currently have an easy solution and corrective surgery is often the only option available to a clinician. The most common and successful surgery

employed to treat corneal opacities is a corneal transplant where a donated cornea is grafted in the place of the diseased or injured tissue. The procedure, known as keratoplasty, involves excision of the central portion of an opaque cornea and then a donor cornea is cut to the same size as the removed portion and sutured onto the recipient eye (Figure 2) (Castroviejo, 1950).

Corneal transplantation was first successful in 1905 (Armitage et al., 2006) and the principle of the technique has changed very little since then and modern keratoplasties have survival rates after five-years of 72-74% (NHS Blood & Transplant, 2014, Williams et



al., 2006). Moreover, corneal keratoplasty does not require immune suppression due to the avascular nature of corneal tissue, since the central portion of the cornea, which is the portion replaced during keratoplasty, is devoid of any blood vessels. Hence the donated corneal tissue is hidden from the immune system and does not provoke an immunological reaction to attack the foreign donor tissue.

Keratoplasty is deemed to be a successful procedure; however looking at the figures from above, donor corneas are subject to failure in over a quarter of cases (26-28%) after five years and clinicians are wary that transplant rejection remains a risk. This is particularly so where vascular in growth from the conjunctiva into the cornea has taken place or where corneal endothelial cell numbers have declined to a level which results in a loss of hydration control (see section 1.4.5 – Corneal Descemet’s Membrane and Endothelium). Additionally, in the UK, demand for corneal donor tissue only just matches its supply, which is not an ideal situation. In 2013/14 5440 corneas were donated, of which 3580 were suitable for penetrating keratoplasty and 3313 corneas were supplied for donation by eye banks – corneas were deemed to be unsuitable due to medical contraindications, poor tissue quality, microbial contamination or stored for longer than 28 days (NHS Blood and Transplant, 2014).

At present, corneal transplantation remains the best treatment option for corneal blindness. However, the rates of graft failure rates and the supply of tissue are currently not satisfactory. Furthermore, future supply of donor corneal tissue may come under pressure due to an ageing population since increasing rates of dementia and stringent organ donor exclusion policies introduced to prevent the transmission of non-detectable variant-Creutzfeldt-Jakob disease prions may prevent individuals with dementia from

donating their organs (NHS Executive, 1999). Therefore research, including this thesis, is being focused on novel ways of reducing, and even eliminating, the need for human donor corneal tissue.

Creating novel approaches to curing corneal blindness is not a simple undertaking, and requires a detailed understanding of the healthy cornea and the mechanisms that allows for the cornea to function correctly. Furthermore, an appreciation of the tissues surrounding the cornea (Figure 3), including the sclera and conjunctiva, is necessary because peripheral vascular in-growth has been shown to contribute heavily to graft

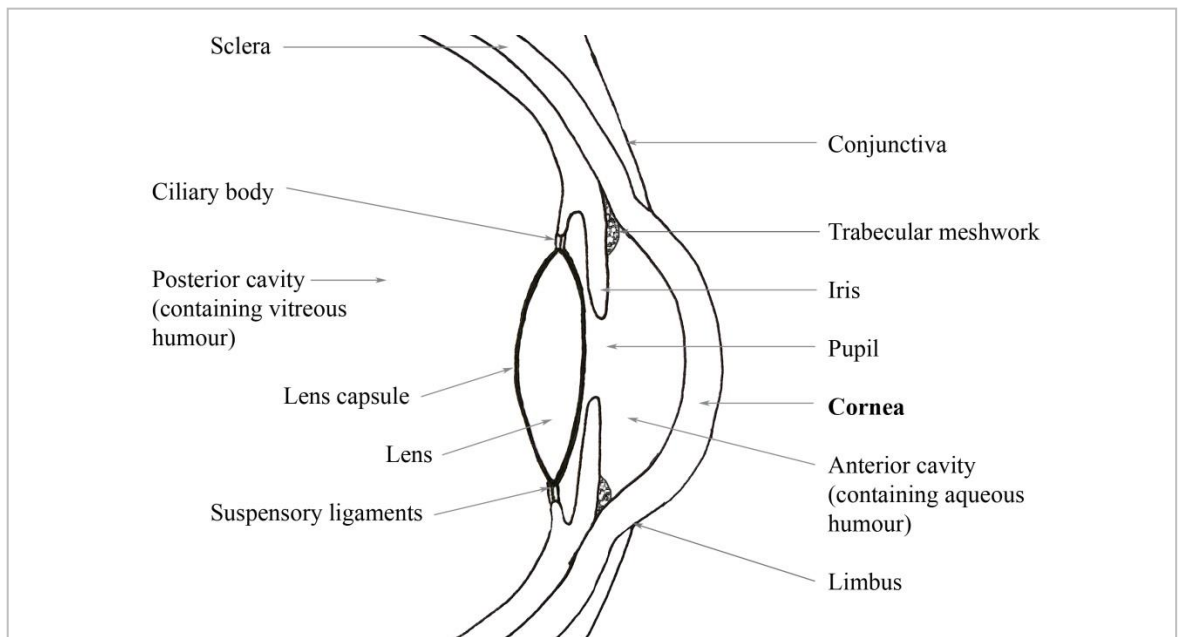


Figure 3: Schematic diagram of the anterior portion of the eye as seen in cross-section. The cornea is the anterior most transparent window; the conjunctiva is a membrane the meets the periphery of the cornea and extends round to the inside of the eye lids. Beneath the conjunctiva is the sclera, which forms the remainder of the fibrous tunic. The posterior surface of the cornea interfaces with the anterior chamber, which is filled with aqueous humour. Posterior to the anterior chamber is the iris and pupil. The iris controls the size of the pupil. Where the iris meets the corneal-scleral junction there is a region known as the trabecular meshwork. Beneath the iris is the lens that is suspended within the lens capsule. The lens capsule attaches to the suspensory ligaments and the ciliary body, which contracts or relax in order to change the shape of the lens tissue in order to focus light onto the retina.

rejection episodes in corneal transplantations (Williams et al., 2006) and the same would be true for any novel artificial cornea.

1.3 TISSUES SURROUNDING THE CORNEA

The cornea interfaces with a number of surrounding tissues which play a role in maintaining the cornea (Figure 4). The main thickness of the cornea, known as the stroma, merges into the fibrous sclera. The anterior surface of the cornea, known as the corneal epithelium, interfaces with the conjunctiva; while the posterior surface, known as the corneal endothelium, interfaces with the trabecular meshwork at the peripheral cornea edge, as well as the anterior chamber in the central portion of the cornea.

The sclera is the white of the eye and forms the majority of the fibrous outer tunic that extends from the optic nerve to the corneal-sclera junction. The role of this tissue is to encapsulate the eyeball and shape the eye into its distinct globe-like shape. At the corneal-sclera junction the collagen extra cellular matrices of the cornea and sclera form continuous fibres; however scleral collagens are disorganised and have a tendon-like composition making the sclera completely opaque (Marieb, 2004).

The sclera has some level of vascularisation, mostly, in its two anterior-most regions; the Tenon's capsule, which tightly interfaces with the posterior surface of the conjunctiva, and episclera, a region below the Tenon's capsule. At the corneal-sclera junction the vasculature of the episclera forms a circumferential capillary network that surrounds the cornea. The vascular architecture will function to provide nutrition to the sclera, and

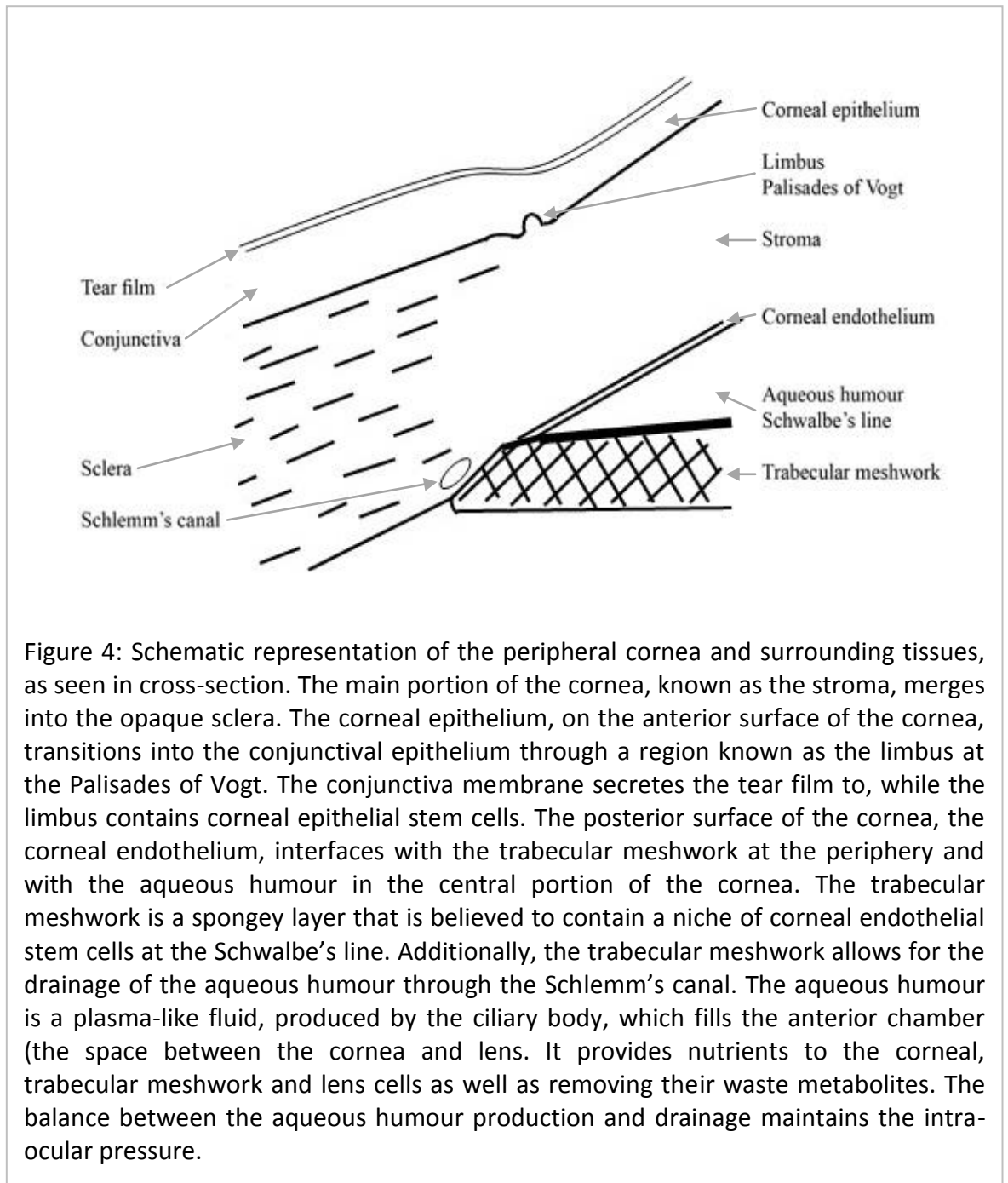


Figure 4: Schematic representation of the peripheral cornea and surrounding tissues, as seen in cross-section. The main portion of the cornea, known as the stroma, merges into the opaque sclera. The corneal epithelium, on the anterior surface of the cornea, transitions into the conjunctival epithelium through a region known as the limbus at the Palisades of Vogt. The conjunctiva membrane secretes the tear film to, while the limbus contains corneal epithelial stem cells. The posterior surface of the cornea, the corneal endothelium, interfaces with the trabecular meshwork at the periphery and with the aqueous humour in the central portion of the cornea. The trabecular meshwork is a spongy layer that is believed to contain a niche of corneal endothelial stem cells at the Schwalbe's line. Additionally, the trabecular meshwork allows for the drainage of the aqueous humour through the Schlemm's canal. The aqueous humour is a plasma-like fluid, produced by the ciliary body, which fills the anterior chamber (the space between the cornea and lens). It provides nutrients to the corneal, trabecular meshwork and lens cells as well as removing their waste metabolites. The balance between the aqueous humour production and drainage maintains the intra-ocular pressure.

peripheral cornea, in addition to providing some level of immunity. However, the posterior layers of the sclera are avascular for reasons that are unknown (Watson and Young, 2004).

At the corneal-sclera junction a potential niche of corneal stromal stem cells exist around the Palisades of Vogt (Pinnamaneni and Funderburgh, 2012, Du et al., 2005). Within this

region are a number of cells that express characteristic proteins which are associated with other stem cells. One such protein (known as a differentiation marker) these cells express is PAX6 (McGowan et al., 2007, Cvekl and Tamm, 2004). PAX6 is expressed by haematopoietic stem cells and is also an embryological transcription factor and functions as a gene activator to control DNA translation into proteins during eye development (Ramaesh et al., 2003). Within the corneal-sclera limbus a small number of cells express this protein; whereas differentiated corneal stromal cells (keratocytes) do not express this differentiation marker suggesting a potential niche of corneal stromal stem cells.

Overlaying the sclera and protecting the sclera collagenous matrix is the conjunctiva. The conjunctiva is a mucous membrane consisting of stratified epithelial cells interspersed with mucous producing goblet cells. This membrane forms a sac which covers the sclera (Figure 4), known as the bulbar conjunctiva, and inside of the eye-lids, known as the palpebral conjunctiva. The conjunctival epithelia are stratified in order to provide a barrier to protect the scleral surface; additionally the goblet cells contribute to the production of a tear-film which lubricates eye movements and eye-lid blinking.

The production of a tear film is important for maintaining a healthy corneal epithelium, since the tear film provides water and nutrients to the corneal epithelium (Meng and Kurose, 2013, Dartt, 2009), and it lubricates blinking. In addition the lymphatic drainage of the tear film plays a role in the immunological defence of the eye by recruiting immunological cells to the area and stimulating inflammation when an infection occurs, this is commonly seen as conjunctivitis (Marieb, 2004, Nelson and J.D., 1997), also abnormal secretion of the tear film will cause dry-eye syndrome which can cause abrasions to the corneal surface during blinking (Meng and Kurose, 2013, Dartt, 2009).

At the border between the conjunctiva and the cornea is a transitional region, known as the limbus. Specifically the limbus is the transitional epithelia around the Palisades of Vogt (Figure 4). This region is important since it marks the change in phenotype of the epithelial cells from those that are conjunctival and those that are corneal. Additionally the limbus also contains a niche of stem cells for the corneal epithelium.

Epithelial cells express cyto-skeletal proteins known as cytokeratins but different epithelial cells phenotypically express different cytokeratins depending on their location and level of differentiation. Hence the expression pattern of cytokeratins defines whether an individual cell originates from the conjunctiva, cornea or is a stem cell. Conjunctival epithelial cells express CK4, CK7 and CK13 cytokeratins (Krenzer and Freddo, 1997), while corneal epithelial cells express CK3 and CK12 cytokeratins (Kivela and Uusitalo, 1998). Finally corneal epithelial stem cells express CK19 and vimentin (Schermer et al., 1986, Davanger and Evensen, 1971). The corneal limbal stem cell niche is discussed further in the following section (*see section 1.4.2*).

At basal layer of the cornea, the peripheral corneal endothelium interfaces with a spongy tissue known as the trabecular meshwork at a region known as the Schwalbe's line. The function of the trabecular meshwork is to drain the aqueous humour from the anterior cavity into the Schlemm's canal. This function is vital for the maintenance of the intra-ocular pressures (Abad et al., 2008). Like other peripheral region interfaces, the corneal endothelium-Schwalbe's line border contains a possible source of corneal endothelial progenitor cells (Whikehart et al., 2005); however this potential source of stem cells is less well defined and understood since corneal endothelial cells do not readily divide.

Below the central posterior surface of the cornea is the anterior cavity of the eye. This cavity is filled with a fluid known as aqueous humour. The composition of the aqueous humour is much like that of the blood plasma. Hence, the function of the aqueous humour is to provide nutrients for the avascular cornea and lens cells as well as removing waste metabolites. In addition the aqueous humour maintains the intra-ocular pressure within the eye globe (Marieb, 2004).

1.4 CORNEAL STRUCTURE & TRANSPARENCY

In order to develop a functional and successful corneal replacement, it is important to understand the architecture and composition of the cornea. This is required because the unique composition and highly organised structure dictates and controls the optical clarity of the tissue. Such an understanding of the corneal architecture and mechanisms of transparency will inform the best potential avenues for the development of an artificial corneal replacement.

1.4.1 Corneal Layers

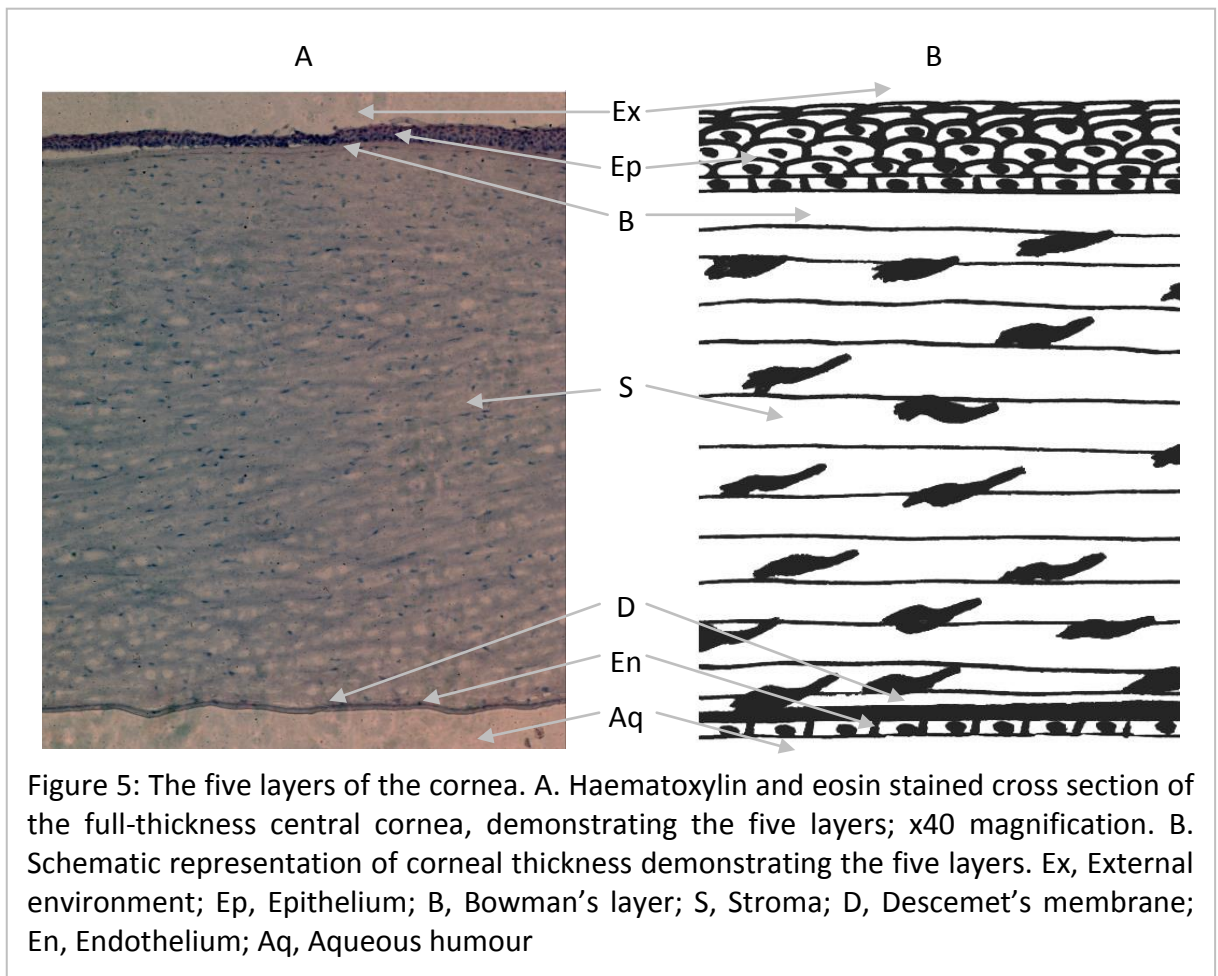
The cornea is comprised of five layers:

1. An epithelium, consisting of stratified epithelial cells
2. A thin acellular extra-cellular matrix layer known as the Bowman's layer

3. A thick extra-cellular matrix layer, known as the stroma, which contains corneal specific fibroblasts
4. An enlarged acellular basal lamina known as the Descemet's membrane
5. And an endothelium, consisting of uniform cuboidal endothelial cells

Figure 5 shows a cross-sectional micro-graph and schematic representation of the cornea demonstrating the 5 different layers. The epithelium sits atop the Bowman's layer, which is continuous with the stroma. At the posterior of the stroma there is the Descemet's membrane followed by the endothelium.

The corneal epithelium is comprised of stratified epithelial cells, which act as a barrier between the external environment and the underlying tissues. The Bowman's layer is the

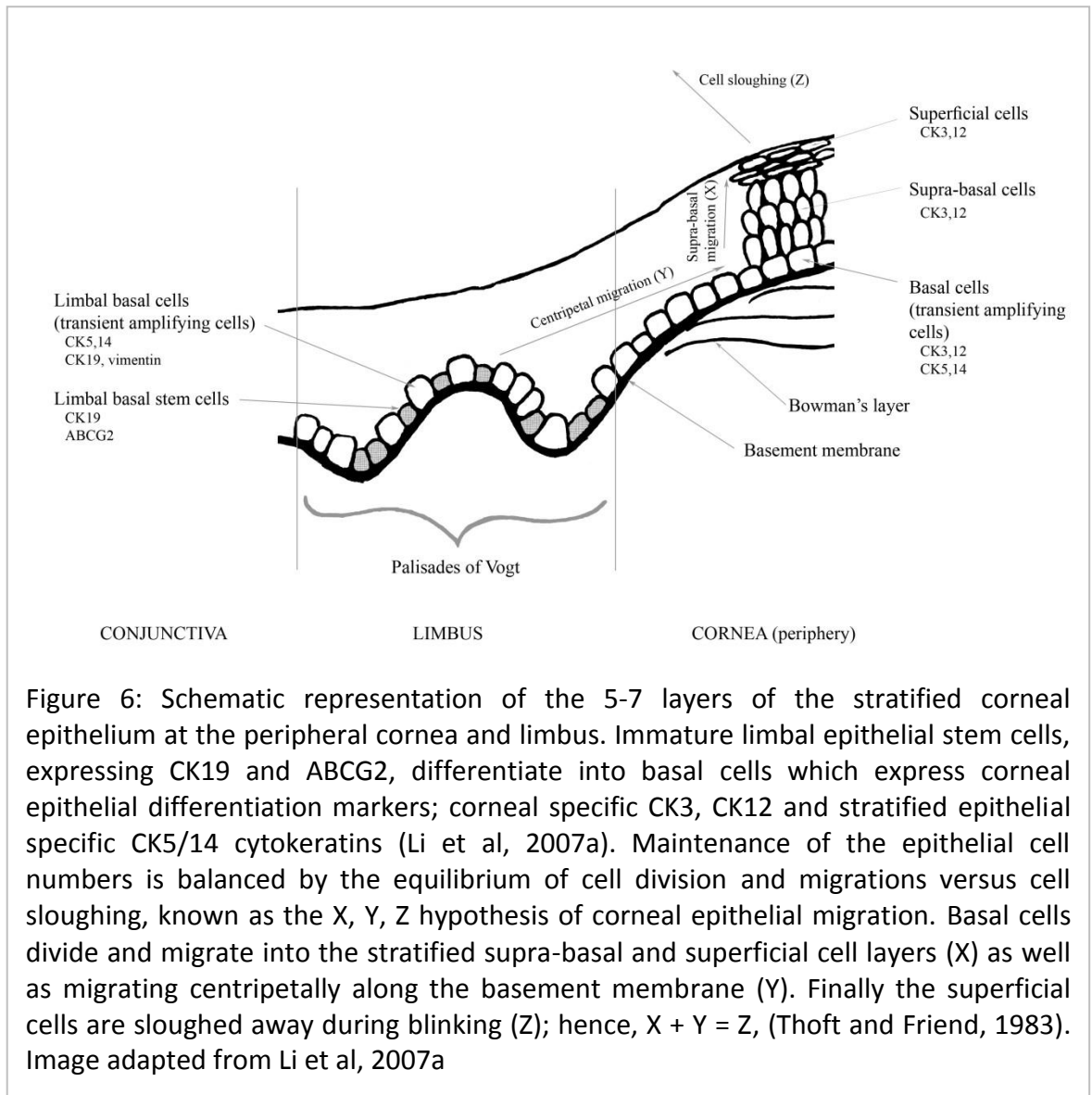


start of the transparent collagenous matrix and is an acellular collagen matrix, approximately 12µm thick in humans that is continuous with the stromal extra cellular matrix. The stroma makes up 90% of the corneal thickness and is comprised of the highly organised collagen extra cellular matrix along with corneal fibroblasts, known as keratocytes. The Descemet's membrane is an enlarged basal lamina, to which the endothelium attaches to the posterior surface of the cornea. Finally the endothelium is a layer of uniform endothelial cells, which function to maintain the stromal hydration (Nishida et al., 1997).

1.4.2 Corneal Epithelium

The corneal epithelium is the outermost layer of the cornea which functions to act as a barrier to the external environment, much like other external stratified epithelial layers, for example skin and gut epithelia and the conjunctiva. This is achieved by forming a layer of tightly packed, stratified, non-keratinising squamous epithelial cells, between 5-7 cells thick and sloughing away of the cells from the external corneal surface during blinking.

Each cell will go through four stages of differentiation before getting sloughed away in order to balance the lost cells. Figure 6 schematically depicts the differentiation and migration of corneal epithelial cells. The cells start out as immature corneal stem cells, residing within the corneal-conjunctival limbal stem cell niche. The limbal epithelial stem cells will divide and then begin differentiating and migrating along the epithelial basement membrane, replacing basal cells. Next, the basal cells will migrate into the



supra-basal cell layer, and will eventually migrate towards the epithelial surface where they become superficial cells.

1.4.2.1 Limbal Epithelial Stem Cells

Corneal epithelial stem cells are located within the corneal limbus and function to replenish desquamated corneal epithelial cells. Specifically, corneal epithelial stem cells

exist as a small side population within the basal layer of the epithelium in the Palisades' of Vogt, (Schermer et al., 1986, Davanger and Evensen, 1971); although, distinguishing the limbal epithelial stem cells from the surrounding population is difficult because the differences between the limbal epithelial cells and the surrounding basal epithelial cells are subtle and there is no definitive differentiation marker (Figure 6) (Ahmad, 2012, O'Sullivan and Clynes, 2007).

Davanger and Evensen (1971) were the first to propose the possibility of corneal epithelial stem cells within the limbus due to the centripetal (peripheral to central) migration of basal epithelial cells from the limbus into the central cornea. This led to further studies that found a small portion of limbal cells distinct from the basal cell population with certain characteristics that are similar to stem cells found within other stem cell niches. These characteristics (Ordonez and Di Girolamo, 2012, O'Callaghan and Daniels, 2011, O'Sullivan and Clynes, 2007, Schlotzer-Schrehardt and Kruse, 2005, Dua and Azuara-Blanco, 2000, Kivela and Uusitalo, 1998) included:

1. A low level of differentiation - limbal epithelial stem cells express membrane bound ABCG2, p63 transcription factor and the cytokeratin CK19, which are commonly associated with stem cell phenotypes, but they do not express the differentiated corneal epithelial cell cytokeratins CK3 and CK12 nor do they express stratified epithelial cytokeratins CK5 or CK14.
2. Limbal basal stem cells are slow cycling, that is they divide at a much slower rate than the basal epithelial cells.
3. Cells from the limbal basal region have a greater *in-vitro* proliferation capacity compared with centrally located basal cells.

Additionally a loss of the limbal basal cells as a result of injury or certain diseases results in decreased epithelial wound healing (Ahmad, 2012, Huang and Tseng, 1991, Chen and Tseng, 1991, Chen and Tseng, 1990, Kruse et al., 1990), a condition known as limbal stem cell deficiency, which can be treated by transplanting limbal basal epithelial cells (Ahmad, 2012, O'Callaghan and Daniels, 2011, Pellegrini et al., 1997, Tsai et al., 1990, Kenyon, 1989, Kenyon and Tseng, 1989).

1.4.2.2 *Basal Cells*

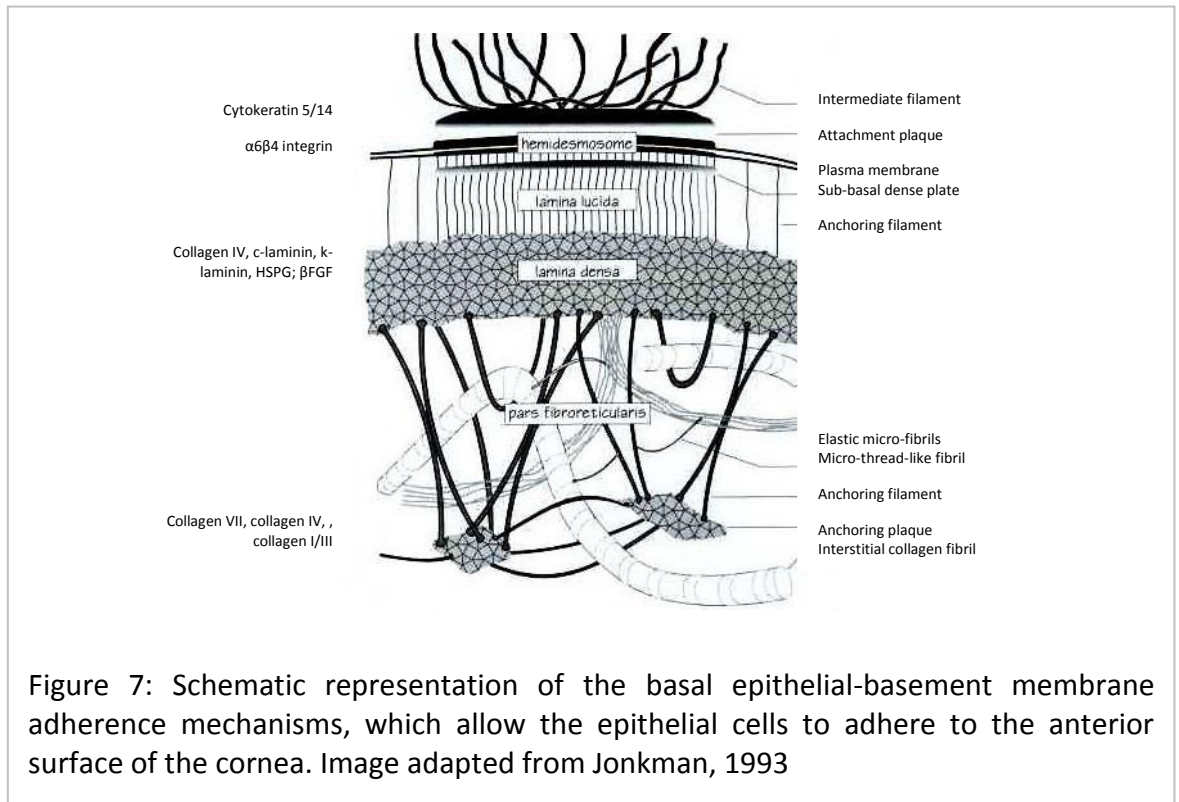
Corneal basal epithelial cells are derived from the limbal stem cells that have begun differentiating into corneal epithelial cells. These cells are cuboidal, transient amplifying cells that make up the foundation of the stratified corneal epithelium which covers the entire corneal surface and anchors the epithelium to the anterior surface of the cornea. In order to cover the central cornea, the cells migrate from the periphery of the cornea in a centripetal fashion; whilst to anchor the epithelium to the anterior corneal surface, the basal corneal cells will secrete and attach to the basement membrane (Figure 7).

Corneal basal epithelial cells are not terminally differentiated cells and they maintain the majority of their cellular organelles and metabolic activity (Nishida et al., 1997). Additionally, corneal basal epithelial cells retain their ability to replicate; hence these cells are often referred to as transient amplifying cells (Ahmad, 2012, Dua and Azuara-Blanco, 2000) and they will complete additional rounds of division in order to replenish desquamated corneal epithelial cells without depleting the limbal stem cell population.

An interesting property of the two daughter cells from basal cells division is that they will either jointly remain as basal cells, or both cells will migrate vertically into the supra-basal layers (i.e. the daughter cells will synchronise when they differentiate), (Beebe and Masters, 1996). Intuitively, limbal and peripheral located corneal basal cells are more likely to remain as basal cells and migrate further towards the centre of the corneal surface, completing additional rounds of division along the way. Whereas central corneal basal cells are more likely to migrate vertically and differentiate (Lehrer et al., 1998). This has lead researchers to call limbal basal cells early-TACs while corneal basal cells are late TACs, due to their respective proliferative capacity, proximity to the stem cell population and centripetal migration (Li et al., 2007a, Li et al., 2007b).

The rate of division, differentiation, centripetal and vertical migration of the basal cells is determined by the equilibrium established between superficial cell desquamation and basal cell division. This equilibrium is described by the X, Y, Z hypothesis of epithelial homeostasis. If you consider the number of basal cells dividing and migrating to the superficial epithelial layers to be X; the centripetal migration of basal cells to be Y; and the number of superficial cells lost to be Z; then $X + Y = Z$ (Figure 6) (Thoft and Friend, 1983); hence basal cell division and centripetal migration is equal to desquamated superficial cells. In cases of limbal stem cell deficiency $X+Y<Z$, hence the epithelial cell population becomes deficient.

A secondary role of corneal basal epithelial cells is to secrete and maintain the basement membrane and aid the adherence of the epithelium to the anterior surface of the cornea. The basement membrane is a continuous membrane that lies between the epithelial and Bowman's layers and is comprised of collagen types IV and VII, laminin and fibronectin,



(Fukuda et al., 1999). In order for the epithelium to adhere to the corneal surface the basal cells form tight cell-cell and cell-basement membrane links (Figure 7) (Jonkman and Bouwes Bavinck, 1993). The junctions formed between adjacent basal cells, as well as with adjacent supra-basal cells, are a mixture of inter-digitations, desmosome links and gap junctions; while the basal cells also form hemi-desmosome-collagen VII links with the basement membrane. These hemi-desmosomes link with collagen type VII anchoring filaments of the basement membrane and the collagen type VII anchoring filaments penetrate through the basement membrane and into the Bowman's layer. In the Bowman's layer, the collagen type VII filaments form anchoring plaques with the collagen type I matrix, (Swamynathan et al., 2011, Gipson et al., 1987).

1.4.2.3 *Supra-Basal Cells*

Overlying the basal cells are supra-basal cells, which is a layer of 2-3 cells. Supra-basal cells are intermediate cells between superficial cells and basal cells committed to differentiating into superficial cells. They express high level of corneal specific CK3 and CK12 cytokeratins, and they also lose mitotic activity; however sparse cellular organelles remain, suggesting these cells maintain a degree of metabolic activity. Supra-basal cells are characterised by having a wing-like appearance, due to remnant links with the basement membrane that have yet to be severed, though as the cells migrate towards the superficial corneal cells, the hemi-desmosome links do detach. Like basal cells, supra-basal cells form tightly packed cell-cell junctions, including desmosome links, gap-junctions and inter-digitations with adjacent cells, in order to provide the epithelial barrier function to the cornea (Nishida et al., 1997).

1.4.2.4 *Superficial Cells*

The outermost layer of the epithelium, which overlies the supra-basal cells, is the superficial layer – comprised of superficial epithelial cells. Superficial cells are terminally differentiated squamous epithelial cells, expressing corneal specific CK3 and CK12 and are tightly packed together in 2-3 layers. The terminally differentiated nature of these cells makes superficial cells less metabolically active and so they have few organelles or RNA (Nishida et al., 1997). Superficial cells are very important in providing the barrier function to the cornea due to the formation of tight junctions with adjacent cells in addition to desmosome (Swamynathan et al., 2011) which helps to form a protective barrier between

the cornea and the external environment. Additionally, the outer-most superficial cells will get desquamated from the corneal surface due to abrasion caused during blinking. These two features act to protect the underlying cornea since they prevent particulates or micro-organisms penetrating into the epithelium and the rest of the cornea.

1.4.3 Bowman's Layer

Posterior to the corneal epithelium is the Bowman's layer which is a transparent collagen extra cellular matrix (ECM) that is continuous with the underlying stromal layer. The Bowman's layer is distinct from the stroma, because the Bowman's' layer is acellular, the collagen fibrils are thinner than stromal fibrils, 20-30nm thick versus 22-35nm thick, respectively, and the collagen fibrils lack the uniformity seen in the stroma – i.e. the collagen fibrils are randomly arranged (Germundsson et al., 2013, Akhtar, 2012, Nishida et al., 1997, Komai and Ushiki, 1991).

The Bowman's layer is theorised to be the remnants of a primary stromal ECM deposited during foetal development. During early corneal development, surface ectoderm cells will deposit a disorganised primary ECM, which is then swollen and infiltrated by stromal fibroblasts (keratocytes). The keratocytes will then deposit the organised secondary ECM seen in the mature cornea. However, the primary corneal ECM is comprised of collagen fibrils measuring approximately two-thirds the diameter of mature collagen fibrils, and it is also acellular until keratocyte infiltration – making primary corneal tissue very similar to the Bowman's layer (Wilson and Hong, 2000, Bard and Higginson, 1977) and hence

explaining the difference between the architecture of the Bowman's and stromal extra-cellular matrices.

The thin nature of the Bowman's layer collagen fibrils is one of the factors that allows for transparency. They are the product of the specific ECM composition, including collagen, proteoglycans (PGs) and glycosaminoglycans (GAGs), which work together to limit the collagen fibril diameter to 20-30nm. A more thorough explanation of the detailed collagen-PG/GAG ECM composition, their interactions and mechanisms of transparency, will be considered when discussing the stromal composition, since the Bowman's layer ECM and stromal ECM compositions are the same and the collagen fibrils are continuous between the two layers.

1.4.4 Corneal Stroma

Posterior to the Bowman's layer is the stroma, which makes up the majority, ~90%, of the corneal thickness. Since it makes up 90% of the corneal thickness, transparency of the stroma is fundamental for the transparency of the cornea, and is the product of a highly organised stromal extra cellular matrix structure that is maintained by corneal specific fibroblasts, known as keratocytes.

1.4.4.1 *Stromal Extra Cellular Matrix Composition*

The extra cellular matrix (ECM) of the corneal stroma consists of fibrous structural proteins known as collagens associated with proteoglycans and their glycosaminoglycan side chains.

Collagen is the most abundant protein of the body; it is found within the cornea, scleral tissue, ligaments, bones and all other ECM tissues that provide a structural function. However, the collagen make-up within different tissues is not ubiquitous; moreover the relative abundance of different collagen types, of which there are over twenty, as well as the architecture of the collagen bundles enables collagenous tissues to behave in very different ways in order for them to best perform their function. In the case of the corneal stromal ECM, stromal collagens are specialised in order to provide transparency to corneal tissue, hence the collagen composition is different when compared with the collagens found with the opaque sclera.

The most abundant of all the collagens is collagen type I, which makes up ~68% (dry weight) of stromal collagens (Robert et al., 2001). Collagen type I neatly follows the basic collagen structure consisting of three, glycine and proline rich, poly-peptide chains coiled together into a triple helix. The collagen type I triple helix will then form into fibrous networks, through a process known as fibrillogenesis. These networks interweave and interconnect and provide the necessary structural properties required by a tissue. In the case of the corneal stroma, collagen type I forms into sheet-like bundles with varying thicknesses 0.2-2.5 μm and widths 0.5-250 μm (Komai and Ushiki, 1991), known as lamellae (Figure 8). These lamellae are arranged into orthogonal arrays which interlace and interweave laterally, longitudinally and vertically thus providing structural integrity to

the cornea by dispersing the pressures exerted on the cornea (Radner and Mallinger, 2002). The orthogonal arrangement of the collagen lamellae has been shown to be preferentially orientated in the superior-inferior and nasal-temporal directions, which is hypothesised to be due to the forces exerted upon the cornea by the rectus tendons and the movement of the eye (Meek and Boote, 2009, Hayes et al., 2007, Boote et al., 2005)

The collagen type I lamellae of the corneal stroma provides the necessary scaffold to withstand, and maintain, the intra-ocular pressures exerted upon the fibrous outer tunic by the eye humours. However, considering that the opaque sclera, which must also maintain intra-ocular pressure, is also predominantly a collagen type I lamella matrix

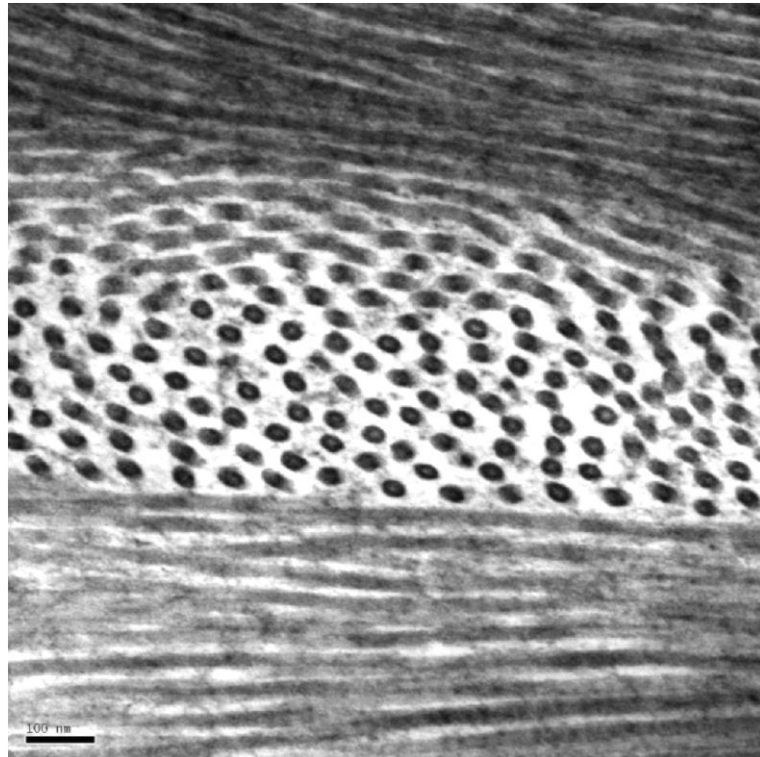


Figure 8: TEM micrograph demonstrating the orthogonal lamella arrangement of collagen bundles within the corneal stroma; Micrograph taken by Howkins, A. J. (scale bar = 100nm)

(~95% dry weight) (Watson and Young, 2004) it is the remaining stromal collagen types that facilitate stromal transparency.

Table 1 demonstrates the various different types of collagens found within the corneal stromal ECM and the relative proportions of each type of collagen. Collagen type I makes up only 68% of the stromal dry-weight (Meek and Fullwood, 2001) – a relatively low figure when compared with other fibrous tissues; whilst collagen types V (15-20%) and VI (7-10%) along with trace amounts of collagen type III make up the remaining dry weight percentages (McLaughlin et al., 1989, Zimmermann et al., 1986).

Collagen type V is the secondary collagen protein found within the corneal stroma,

ECM component	Quantity (% dry weight)	Distribution & function within the corneal stroma
Collagen type I	68%	Fibrous structural collagen
Collagen type III	Varies (trace)	Fibrous structural collagen; deposited as part of the wound healing process
Collagen type V	15-20%	Fibrous structural collagen; associated with type I collagen; limits fibril growth
Collagen type VI	7-10%	Fibril-associated collagen; forms links between type I collagen fibrils; interact with proteoglycans to limit fibril diameter and fibril spacing
Keratan sulphate	<1%	Short chain proteoglycan; forms bridging links between adjacent collagen fibrils limiting collagen fibril spacing
Chondroitin/dermatan sulphate	<1%	Long chain proteoglycan; forms bridging links between collagen fibrils limiting collagen fibril spacing

Table 1: Corneal stroma extra cellular matrix components along with their relative abundances (Robert et al., 2001, Scott and Bosworth, 1990)

constituting 15-20% of the stromal collagens. The concentration of collagen type V within the corneal stroma is much greater than within other fibrous tissues, e.g. the sclera only has trace levels, whilst dermal collagen type V constitutes ~1.6% of the collagen ECM dry-weight (Watson and Young, 2004, McLaughlin et al., 1989, Hashimoto et al., 1986, Tseng et al., 1982). Collagen type V, like type I collagen, is a fibrous collagen, though it has the ability to form heterotypic fibres with collagen type I during fibrillogenesis. However, collagen type V has a specialised globular amino-acid sequence at the N-terminal domain of the protein which protrudes out into the inter-fibrillar space of the heterotypic fibrils (Smith and Birk, 2012). The presence of the globular domain within the interfibrillar space acts to inhibit additional fibrillogenesis onto the collagen fibril through electrochemical repulsion and stereochemical inhibition of collagen deposition (Smith and Birk, 2012, Gordon and Hahn, 2010, Birk, 2001, Fitch et al., 1998); the result being uniformly thin collagen fibrils, with a diameter of 22-35nm (Figure 9) (Akhtar, 2012, Parfitt et al., 2010, Komai and Ushiki, 1991).

Coupled to the uniformly thin collagen type I/V fibrils are collagen type VI fibrils. Type VI collagen is a fibril associated collagen with a short (~100nm) non-striated morphology. One end of a type VI collagen fibril will bind to a type I collagen fibril in a perpendicular fashion (Robert et al., 2001, Meek and Fullwood, 2001, Hirsch et al., 2001), whilst the other end binds to a proteoglycan core proteins. This coupling mechanism acts as a spacer for the collagen fibrils, aiding the bridging role of the PGs, in order to keep the collagen fibrils regularly spaced, 39-53nm apart (Akhtar, 2012, Hirsch et al., 2001, Nishida et al., 1997, Bidanset et al., 1992).

The other major collagen to consider within the corneal stromal ECM is collagen type III. Its presence within a healthy stromal ECM is usually only in trace quantities; although, upon wounding, quiescent keratocytes transform their phenotype into activated myofibroblasts, and type III collagen synthesis is heavily up-regulated (Janin-Manificat et al., 2012, Robert et al., 2001) in order to quickly heal the wound. Thus, collagen type III is commonly found within scar tissue and scar tissue is not transparent, due to the disruption of the uniformly thin fibrils and equal spacing provided by collagens and PGs when scar tissue is laid down (Janin-Manificat et al., 2012).

Associated with the fibrous collagens are proteoglycans (PGs), which are a protein core molecule bound to a repeating linear sulphated disaccharide side-chain, known as a

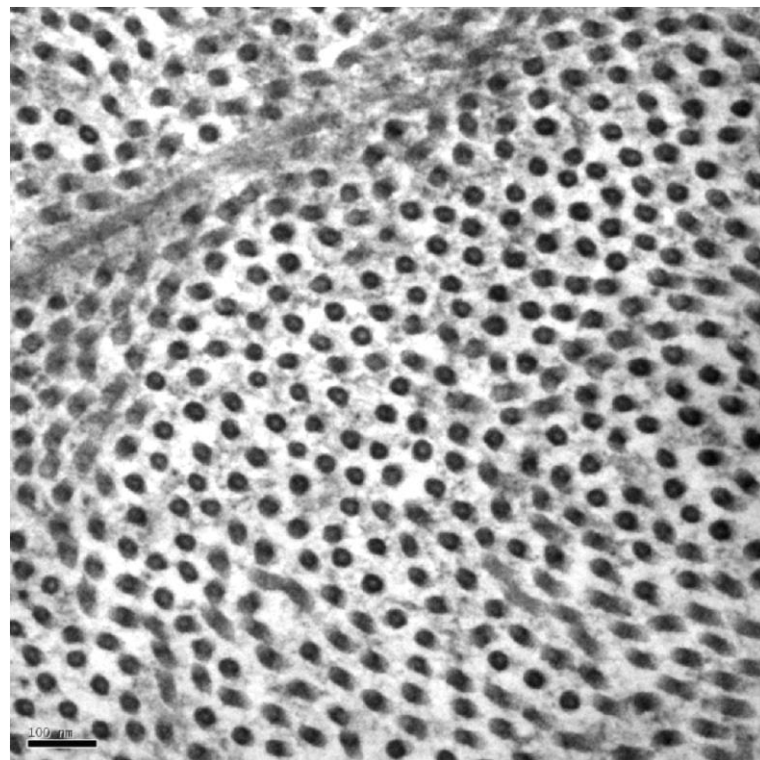


Figure 9: TEM micrograph demonstrating the quasi-crystalline organisation of collagen fibrils within the stroma; Micrograph taken by Howkins, A.J. (Scale bar = 100nm)

glycosaminoglycan (Gregory et al., 1982, Muller et al., 2004). Within the corneal stroma PGs, along with collagen type VI, are used as spacers for the collagen fibrils, keeping the collagens fibrils evenly distributed (Figure 9) (Parfitt et al., 2010, Bairaktaris et al., 1998, Scott and Bosworth, 1990). This is achieved by the GAG side chains extending into the interstitial fluid where they may form bridges with other GAG side chains, while the PG core protein binds to the collagen fibrils (Scott and Haigh, 1985).

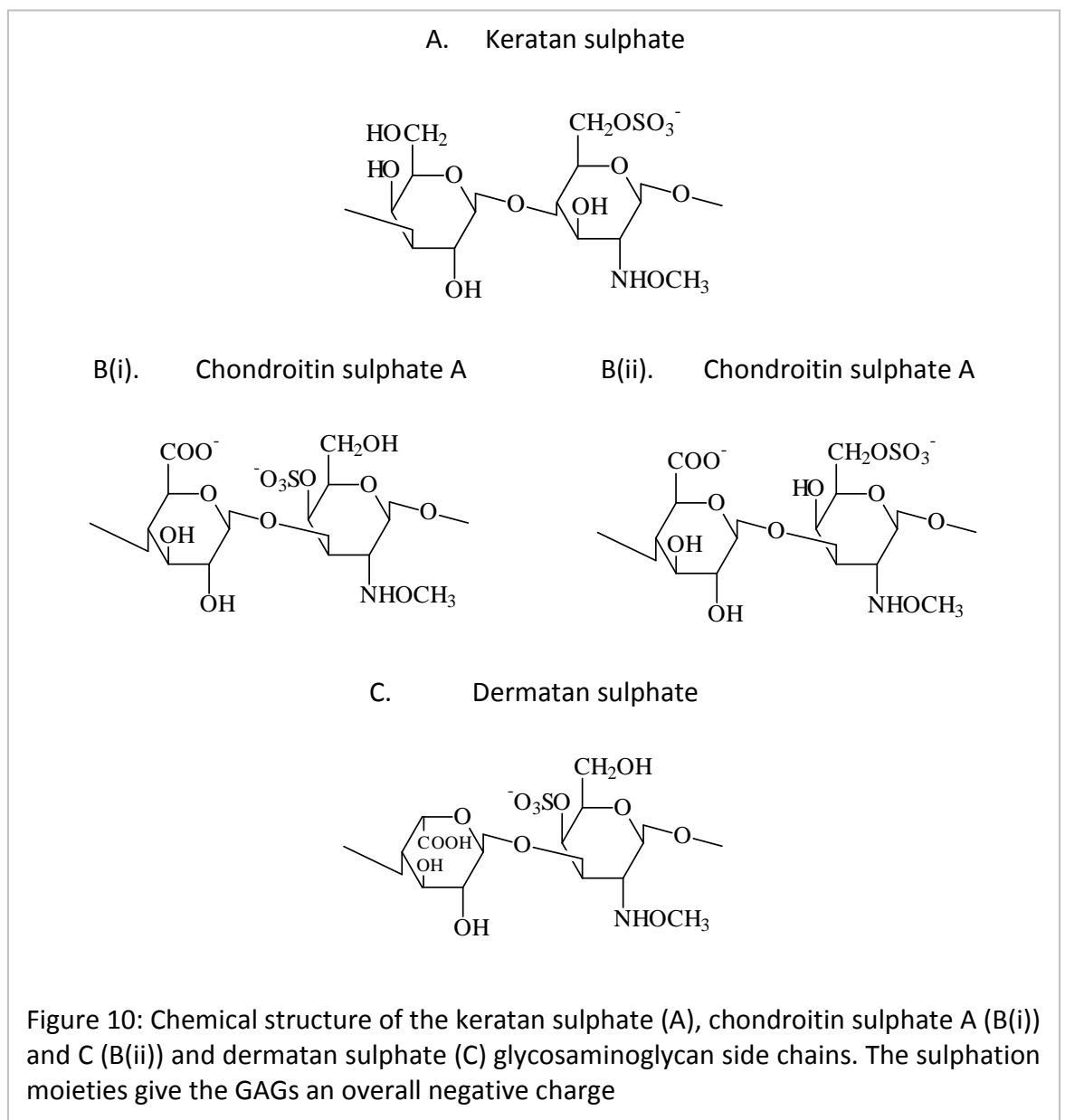
There are two forms of proteoglycans present within the corneal stroma, keratan sulphate (KS) and chondroitin/dermatan sulphate (CS/DS). They have subtle structural differences with regard to their core protein and sulphated GAG side chains (Figure 10), though they work in synergy to maintain the collagen spacing whilst creating a fluidic system.

Keratan sulphate PG is the more abundant of the two PGs. It is formed from a keratocan, lumican or mimecan core protein linked to repeating KS GAGs lactosamine (3Gal β 1-4GlcNAc β 1) sugars sulphated on the carbon-6 moieties of the GlcNAc hexose rings (Figure 10a) (Funderburgh, 2000). The KS core proteins adhere to the α - and c -periodic bands of the collagen fibrils (Scott and Haigh, 1985), while the GAG side chains form short, \sim 31.4nm, perpendicular arrays into the interstitial fluid (Parfitt et al., 2010).

Chondroitin sulphate/dermatan sulphate PGs are formed from a decorin core protein linked to chondroitin sulphate, CS, (alternating N-acetyl-D-galactosamine (GalNAc) and D-glucuronic acid (GlcA) hexose rings) or decorin sulphate, DS, (alternating GlcNAc and L-iduronic acid (IdoA) hexose rings) GAG side chains. CS is sulphated at various different points making different species, of which CS_A and CS_C are present within the cornea (Figure 10b(i) and 10 b(ii)); additionally DS (Figure 10c) was previously known as CS_B due

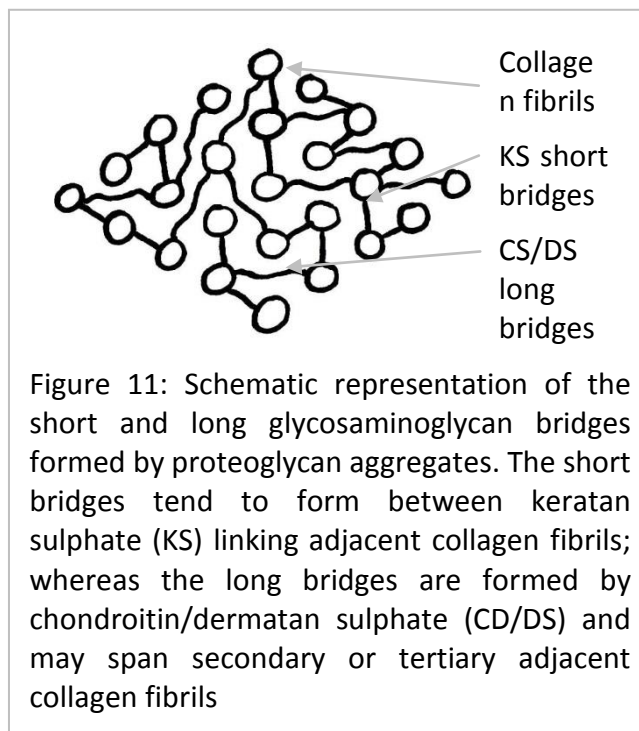
to its structure being very similar to other CS species (Trowbridge and Gallo, 2002). Hence these GAG side chains are able to connect to the same core protein, decorin. The decorin core protein will then bind to the collagen fibrils at the *d*- and *e*-periodic band of the collagen fibrils (Scott and Haigh, 1985) with the CS/DS GAGs forming two longer, 64.5nm and 122.5nm, sinuous arrays extending into the interstitial fluid (Parfitt et al. 2010).

Within the interstitial fluid the GAG side chains laterally aggregate as a result of hydrogen bonding and electrochemical attraction to negatively charged sulphation moieties (Scott,



2001, Scott, 1995) (Figure 11). The aggregates that form tend to be in the form of dimer bridges that occur perpendicular to the collagen fibrils and with adjacent fibrils; this is particularly so for short KS GAGs. Alternatively, the longer CS/DS GAGs bridges may interlink neighbouring or next-but-one neighbouring collagen fibrils; furthermore CS/DS GAGs may form multiple aggregates, with two, four or more GAG chains participating in the fibril bridges (Parfitt et al., 2010) (Figure 11). This is, in part, due to their longer nature, but also due to the dimerisation of GAGs at the binding site with decorin. Conceivably, this may result in four closely positioned CS/DS GAGs on two neighbouring collagen fibrils (Scott, 2001) being able to; 1, span three collagen fibrils; 2, form oblique and sinuous orientated GAG bridges with GAGs at different axial positions along collagen fibrils; and 3, form heterotypic aggregates with KS GAG (Knupp et al., 2009, Lewis et al., 2010).

The nature of hydrogen bonding and electrochemical attraction between all GAG bridges



result in weak linkages between the GAGs. This means that GAG bridges are constantly formed, broken and reformed – potentially with differing GAG chains, creating a fluidic system within the stroma (Scott, 2001).

However, where two GAG chains meet at their maximal length and can form multiple bonds, more stable aggregates will occur. It is hypothesised that where these more stable GAG aggregates form the GAGs exert equally opposed attractive and repulsive forces on the collagen fibrils to uniformly space the collagen fibrils (Figure 9) (Lewis et al., 2010, Parfitt et al., 2010). The attractive forces exerted on the collagen fibrils are due to thermal-kinetic motion shortening the GAG bridges from their maximal lengths – pulling the fibrils closer together (analogous to the elastic recoil of a bungee cord pulling the ends together). At the same time, the GAG bridges elicit an opposing force on collagen fibrils due to osmotic swelling around the negatively charged sulphation moieties – the negative charge of the GAGs recruit cations to the surrounding area, creating a localised concentration of ions around GAG bridges. In turn this will attract water into the area, through osmosis and the Donnan effect, and swell the space between adjacent collagen fibrils (Lewis et al., 2010, Parfitt et al., 2010, Knupp et al., 2009).

1.4.4.2 Stromal Collagen Organisation and Transparency

Considering the uniform diameter and spacing of the collagen fibrils and the underlying mechanisms that result in the uniform nature of collagen fibrils, it suggests that the regular collagen arrangement may be required for stromal transparency. This purports an idea that collagen fibrils will have an ordered crystalline arrangement. However, Figure 9

clearly demonstrates that the collagen fibrils do not have such a long-range order; instead collagen fibrils have a short range, quasi-crystalline, arrangement.

To best explain the quasi-crystalline collagen fibril arrangement, consider the collagen fibrils as individuals and how each individual fibril relates to its adjacent fibrils over short and long distances. Over short distances, i.e. adjacent collagen fibrils; an individual fibril is surrounded by six other collagen fibrils, in a hexagonal arrangement. However, over longer distances, i.e. secondary-adjacent, tertiary-adjacent and beyond-adjacent collagen fibrils; this six-fold arrangement is not present and the collagen fibrils become increasingly random in relation to the initial collagen fibril. Putting this into the context of the entire corneal stroma, which is comprised of millions of collagen fibrils, the collagen fibrils have a 'quasi-crystalline organisation', i.e. over short distances, the collagen fibrils have a crystalline order, but over longer distances, the collagen fibrils are randomly ordered (Parfitt et al., 2010, Komai and Ushiki, 1991, Cox et al., 1970). Taking this pseudo-lattice arrangement into account and the nanometre scale between collagen fibrils, one can theorise the mechanisms of stromal transparency.

Experimentally it is very difficult to prove the mechanisms of stromal transparency; however, information from the normal and opaque stromal architecture and the wave nature of light has lead scientists to hypothesise that stromal transparency is based on the destructive interference of scattered light, and the collagen fibrils having an overall spacing of less than half the wave-length of visible light (Maurice, 1957).

Stromal collagens have a centre-to-centre spacing of approximately 73.4nm (median value published by Akhtar, 2012), which is important because the centre-to-centre collagen spacing is less than half the wavelength of the shortest wavelength of visible

light (i.e. 200nm), which enables light waves in the forward direction to pass, uninterrupted, through the ECM since the visible light waves will miss the collagen fibrils (Benedek, 1971, Goldman et al., 1968, Goldman and Benedek, 1967). However, where the light waves hit a collagen fibril, resulting in the light wave getting scattered, the scattered light is destructively interrupted by the scattered light from other collagen fibrils due to sufficient homogeneity between adjacent fibrils in the quasi-crystalline collagen organisation (Lewis et al., 2010, Parfitt et al., 2010, Freegard, 1997, Komai and Ushiki, 1991, Cox et al., 1970, Goldman et al., 1968, Maurice).

1.4.4.3 Maintaining Stromal Organisation – Stromal Keratocytes

Keratocytes are corneal specific fibroblasts found encapsulated between stromal lamellae and comprise approximately 3-5% of the stromal mass (Beuerman and Pedroza, 1996). Being fibroblastic cells, keratocytes form long, spindleform, pseudopodia that orientate in the same direction as the collagen lamellae. This is due to a cellular motility phenomenon known as contact guidance, whereby cells move along a plane in the direction of greatest tension; in this case the collagen fibrils.

The spindleform pseudopodia are important for the keratocytes, because they enable the formation of a cellular network within the stroma as a result of gap junctions that form where the pseudo-podia of one cell meets another. Thus, keratocytes are able to communicate across the stroma (Nishida et al., 1988, Ueda et al., 1987) and cellular signalling pathways can induce increased matrix degradation/synthesis within the

quiescent stroma, or, where apoptosis or necrosis has occurred, induce the wound repair and matrix synthesis processes (Dupps and Wilson, 2006, Nishida et al., 1997).

Within the quiescent stroma, keratocytes maintain the stromal collagen-proteoglycan matrix by balancing ECM synthesis against protease degradation (Nishida et al., 1997, Muller et al., 1995). This is a slow, controlled process, with the turnover of collagen taking years to fully remodel (Davison and Galbavy, 1986). Quiescent ECM synthesis involves the synthesis and secretion of the various collagen types and proteoglycans by the cells, as well as the secretion of extra cellular enzymes that are involved in collagen fibrillogenesis and matrix organisation; e.g. lysyl oxidase which cross-links collagen fibrils, and sulfotransferases that add sulphate groups to proteoglycans (Funderburgh, 2000), respectively. Quiescent ECM degradation is utilised to break-down and reabsorb areas of the matrix which are damaged or old, and is carried out by matrix-metalloprotease-2 (MMP-2 (also known as gelatinase A)). MMP-2 exists within the corneal stroma in an inactive form, but once activated it degrades and denatures ECM collagens and proteoglycans which are reabsorbed by the keratocytes (Fini et al., 1992, Matsubara et al., 1991a, Matsubara et al., 1991b).

1.4.5 Corneal Descemet's Membrane and Endothelium

Posterior to the stromal extra cellular matrix are the layers of the Descemet's membrane and endothelium. The endothelium is the posterior-most layer of the cornea while the Descemet's membrane is an enlarged basal lamina, to which the endothelial cells adhere to the posterior corneal surface. The Descemet's membrane is considered a basal lamina

since the composition is similar to other basement membrane tissues, i.e. it is made-up of collagen type IV, laminin and fibronectin, which is secreted by the corneal endothelial cells, however it is an enlarged since it measures approximately 10µm thick, which is thicker than other basement membranes (Nishida et al., 1997, Beuerman and Pedroza, 1996, Ishizaki et al., 1993, Fitch et al., 1990). The enlarged nature of the Descemet's membrane is due to the lack of anchoring mechanism between the Descemet's membrane and the endothelial cells – the endothelium is held in place by the intra-ocular pressure and aqueous humour (Beuerman and Pedroza, 1996) and the lack of endothelial cell attachment mechanisms means the Descemet's membrane is not sheared away when endothelial cells are lost (Johnson et al., 1982).

The corneal endothelium is a single layer of uniform hexagonal endothelial cells (Figure 12). At birth corneal endothelial cell numbers can be as many as 500,000 cells with a density of 7,500cells/mm², though there is a decline in cells numbers until adulthood where the cell density is approximately 2,500cells/mm² (Tuft and Coster, 1990). Once the corneal endothelium has matured there is an estimated 0.52% per year decrease in endothelial cell density (Tuft and Coster, 1990) due to endothelial cells being terminally differentiated, meaning they do not readily replicate (Mimura et al., 2013). Where cell loss occurs, adjacent endothelial cells enlarge and migrate over the denuded area in order to maintain the endothelial layer integrity (Whikehart et al., 2005, Gain et al., 2002, Singh et al., 1985; Bourne and Kaufman, 1976).

Individual endothelial cells measure approximately 20µm in diameter and 5µm in depth, are rich in cytoplasmic organelles, including mitochondria, smooth and rough endoplasmic reticulum, and Golgi apparatuses, and exhibit microvilli that project into the anterior chamber. Adjacent endothelial cells form fine interdigitations together and are separated by 3µm gap junctions towards the anterior chamber, though this expands to approximately 30µm towards the Descemet's membrane (Nishida et al., 1997, Tuft and Coster, 1990).

The high density of cytoplasmic organelles relates to the function of the endothelial cells, since the endothelial layer is required to maintain a constant level of hydration within the

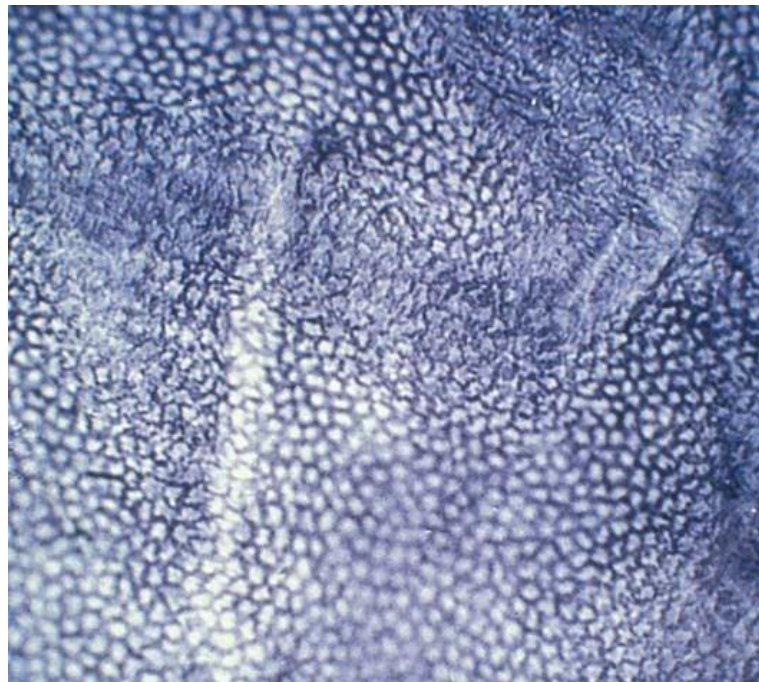


Figure 12: *In-situ* confocal microscope image of the endothelium of the cornea. The endothelium is comprised of a layer of uniform hexagonal endothelial cells that maintain a constant level of hydration within the stroma by creating an osmotic gradient between the stroma interstitial fluid and aqueous humour, which enables the cornea to be transparent. Image courtesy of James, S.E. (x400 magnification)

stroma, which maintains the collagen spacing, as well as providing nutrients to, and taking waste metabolites away from, the stroma. This is achieved by the equilibrium between the passive imbibing of aqueous humour into the stroma and endothelial active transport of interstitial fluid out of the stroma (Nishida et al., 1997, Beuerman and Pedroza, 1996).

Aqueous humour is passively imbibed into the stroma, known as the stromal swelling pressure, through gap junctions between adjacent endothelial cells. This is due to an overall negative charge within the stroma, attributable to the sulphation moieties on the ECM glycosaminoglycans (Zhang et al., 2006, Bairaktaris et al., 1998, Nishida et al., 1997, Scott and Bosworth, 1990). However, if the stromal GAG swelling pressure imbibes too much interstitial fluid into the stroma it will become over-hydrated, and the resulting oedema will cause the stromal ECM to become disorganised and to scatter more light, hence transparency will be decreased (Bonanno, 2012, Freegard, 1997, Benedek, 1971, Goldman et al., 1968).

In order to balance the stromal swelling pressure the endothelial cells create an osmotic gradient at their posterior membrane, which draws interstitial fluid out of the stroma. This is achieved by sodium/potassium adenosinetriphosphatase (Na^+/K^+ ATPase) pumps which create a concentration of sodium ions within the aqueous humour at the endothelial cell membrane. The concentration of ions creates an osmotic gradient where interstitial fluid flows from the stroma into the aqueous humour (Nishida et al., 1997, Herse, 1990, O'Neal and Polse, 1985, Baum et al., 1984, Dikstein and Maurice, 1972).

A supplementary function of the corneal endothelium and the hydration control mechanisms is to provide nutrients to the corneal cells and to remove waste metabolites (Bonanno, 2012). Glucose transporter mechanisms are present at anterior and posterior

endothelial cell membranes, which transport glucose across the cell and into the stroma; additionally the swelling pressure enables nutrients to osmotically diffuse through the gap junctions into the stroma. Conversely waste metabolites, such as lactate will also diffuse across the endothelium, away from the stroma and into the aqueous humour due to the Na⁺/K⁺ ATPase pump osmotic gradient.

1.5 CORNEAL BLINDNESS AND TREATMENTS

Injuries and diseases will cause disruption to the corneal structure, resulting in decreased visual clarity. Table 2 demonstrates a few examples of the diseases and injuries which can affect the cornea, resulting in visual impairment along with the treatment options and prognosis.

The progression of degenerative corneal disorders will often result in the need for surgical intervention, such as penetrating keratoplasty to replace the tissue. Whereas, in the case of corneal trauma, wound healing mechanisms are employed to protect the eye, however wound repair mechanisms are result in fibrous scar tissue deposition, which is detrimental to stromal transparency. Fibrous scar tissue is fundamentally different to the quasi-crystalline stromal ECM since collagen type V and KSPG production is down-regulated (Cho et al., 1990, Cintron et al., 1982, Cintron et al., 1981), while collagen types I and III and CS/DS PG production is up-regulated (Rawe et al., 1992, Cintron et al., 1990, Hassell et al., 1983). This results in scar tissue that is opaque and may require also surgical intervention in order to return transparency to the cornea, i.e. a corneal transplantation.

Fuchs' Endothelial Dystrophy

Pathology	An inherited degenerative disorder of the corneal endothelial cells that results in over-production of the Descemet's membrane, a loss endothelial cell morphology and ion-pump function
Treatment	Penetrating keratoplasty before the final stages of the disease
Prognosis	Prognosis is good, provided the graft is not rejected

Interstitial Keratitis (Stromal infection)

Pathology	Areas of opaque tissue necrosis within the stroma due to a systemic micro-organism infection e.g. syphilis
Treatment	Anti-microbial agents to treat the systemic infection and corticosteroids to reduce corneal inflammation
Prognosis	Vision is likely to return to normal after treatment; though severe cases may require a limbal stem cell graft or even a corneal transplant

Keratoconus

Pathology	The underlying causes for keratoconus are poorly understood, however this disease will commonly presented as a progressive thinning of the peripheral cornea, giving a cone-like shape to the tissue
Treatment	Early stages can be treated with corrective lenses. Moderate stages are treated by stromal collagen crosslinking using riboflavin and UV-light to prevent degradation of the collagenous ECM. Later stages require a corneal transplantation
Prognosis	Prognosis is good, provided the graft is not rejected

Corneal Trauma

Pathology	Mechanical, chemical burn or thermal burn injury
Treatment	Less severe injuries may be patched with a corneal bandage or corneal limbal stem cell graft. The most severe will require corneal transplantation or prosthetic corneal graft
Prognosis	Largely depends on the severity. Less severe injuries have a good prognosis; but chemical burns, particularly alkaline burns have a very poor prognosis due to melting of the tissue. Additionally, those who retain an intact limbal region have a better prognosis since the epithelial can be restored during healing

Table 2: Some examples of the common corneal ailments presented to clinicians, along with their pathology, treatment and prognosis (Kaufman, 2000)

1.5.1 Surgical Intervention for Corneal Blindness

A loss of corneal transparency can result in visual impairment and, in severe cases, blindness to the affected eye, even if the rest of the eye functions normally. However, if corneal transparency (or transparency to the anterior of the eye) can be restored, vision may be improved or restored.

In order to treat for corneal blindness surgical intervention is often required, which at present, is limited to the replacement of the diseased or injured tissue. The extent of the damage to the corneal structure will determine the treatment option utilised, though at present ophthalmologists have three main treatment options; 1, engraftment of limbal epithelial stem cells; 2, transplantation of a corneal allograft (keratoplasty) or; 3, a prosthetic cornea (keratoprosthesis).

Limbal stem cell grafts are utilised to treat limbal stem cell deficiencies, where the epithelial limbal stem cell niche has become compromised. Keratoplasty is used to treat corneas where the stromal tissue has become opaque. Keratoprosthesis is used to treat the most extreme cases of corneal blindness, where a corneal transplant would be unsuitable.

1.5.1.1 Limbal Epithelial Stem Cell Grafts

Injuries, traumas, multiple surgeries or microbial infections that affect the corneal anterior surface can cause destruction to the corneal-conjunctival limbus and the corneal epithelial stem cells within this niche region, resulting in a condition known as Limbal

Stem Cell Deficiency. Individuals suffering from limbal stem cell deficiency have insufficient epithelial stem cells to restore the corneal epithelium; hence the corneal epithelium loses its ability to act as a barrier to the external environment and the underlying tissue may become ulcerous. If the condition is left unchecked, conjunctival epithelial cells surrounding the cornea will migrate onto the denuded cornea, in order to re-establish an epithelial barrier. However, conjunctival in-growth is detrimental to corneal transparency because the in-growth stimulates neovascularisation and inflammation (Levis and Daniels, 2009, Sharpe et al., 2007).

In order to treat limbal stem cell deficiency, an ophthalmologist may use a limbal stem cell graft (Figure 13), where cultured corneal limbal epithelial stem cells are grafted onto the anterior surface of the eye (Sharpe et al., 2007, Daya et al., 2005). The process of engraftment begins with the harvesting and isolation of limbal epithelial stem cells from the anterior surface of a donor corneal limbus that has been discarded after penetrating keratoplasty. The cells are then expanded *in-vitro* on a denuded amniotic membrane substrate, which is transparent and has non-immunogenic properties, and then grafted onto the surface of the eye with epithelial deficiency (Sharpe et al., 2007, Daya et al., 2005, Tsai et al., 2000).

The use of limbal stem cell grafts to treat limbal stem cell deficiency is a useful technique where the underlying corneal stroma remains transparent. Additionally, if the other eye of the afflicted individual is un-affected, limbal epithelial stem cells may be harvested from the healthy eye to produce a stem cell autograft (James et al., 2001); though an allograft, produced from cadaveric or a living donor source may be used if harvesting cells

for an autograft is not viable (Levis, 2009; Sharpe, 2007; Daya et al 2005 James et al 2001).

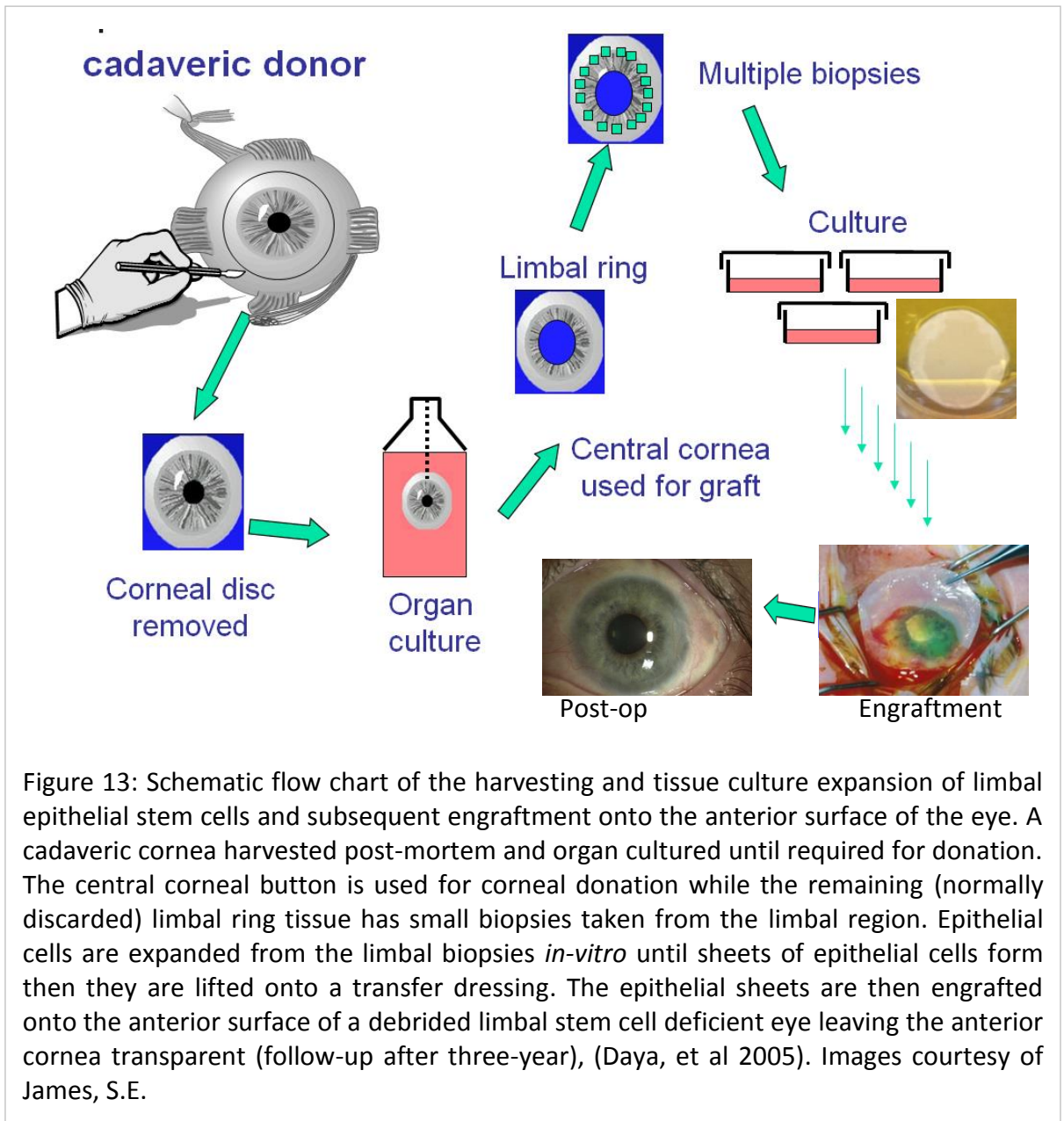


Figure 13: Schematic flow chart of the harvesting and tissue culture expansion of limbal epithelial stem cells and subsequent engraftment onto the anterior surface of the eye. A cadaveric cornea harvested post-mortem and organ cultured until required for donation. The central corneal button is used for corneal donation while the remaining (normally discarded) limbal ring tissue has small biopsies taken from the limbal region. Epithelial cells are expanded from the limbal biopsies *in-vitro* until sheets of epithelial cells form then they are lifted onto a transfer dressing. The epithelial sheets are then engrafted onto the anterior surface of a debrided limbal stem cell deficient eye leaving the anterior cornea transparent (follow-up after three-year), (Daya, et al 2005). Images courtesy of James, S.E.

1.5.1.2 *Keratoplasty – Corneal Transplantation*

Corneal transplantation is the replacement of an opaque cornea with a cadaveric cornea, in either a partial thickness graft, known as a lamella keratoplasty; or a full thickness transplant, known as a penetrating keratoplasty.

The variation between each keratoplasty relates to the depth of the stromal tissue which is opaque and requiring replacement, though the procedure follows the same basic method:

1. A trephine is used to excise the central portion of the opaque corneal tissue
2. A donor cornea is then cut to the same size as the excised tissue using a second trephine
3. The donor tissue is sutured into the place of the excised tissue

The choice between whether to employ lamella keratoplasty or penetrating keratoplasty is subject to the extent of corneal blindness and the graft prognosis; though of vital importance is the state of the corneal endothelial cells and their ability to maintain the stromal hydration. Partial thickness lamella keratoplasty removes the anterior portions of the corneal stroma which have become opaque leaving the hosts' posterior stromal lamellae, Descemet's membrane and endothelium intact – hence, partial thickness lamella grafts are suitable for individuals who retain a functioning endothelium. Penetrating keratoplasty replaces the entire cornea and is suitable for individuals who have suffered a loss of endothelial cell numbers (to below 500cells/mm² (Engelmann et al., 2004)) and stromal swelling is a problem (Verdier, 1997).

1.5.1.3 *Keratoprosthesis – Corneal Prosthetics*

Prosthetic corneas are transparent devices, usually created from a synthetic polymer or partially synthetic polymer, which is used to replace an opaque cornea with the sole purpose of restoring anterior globe transparency, thus allowing light into the eye (McLaughlin et al., 2009b, Duan et al., 2006). Ophthalmologists generally consider keratoprotheses to be an option of last resort for end-stage corneal blindness, where the prognosis for keratoplasty is poor, for example in cases of repeated corneal graft rejection, or a severely compromised corneal epithelium with conjunctival in-growth, neo-vascularisation and poor tear-film production, e.g. Stevens-Johnson Syndrome, or severe burns that have compromised the anterior eye globe. This is due to the following reasons:

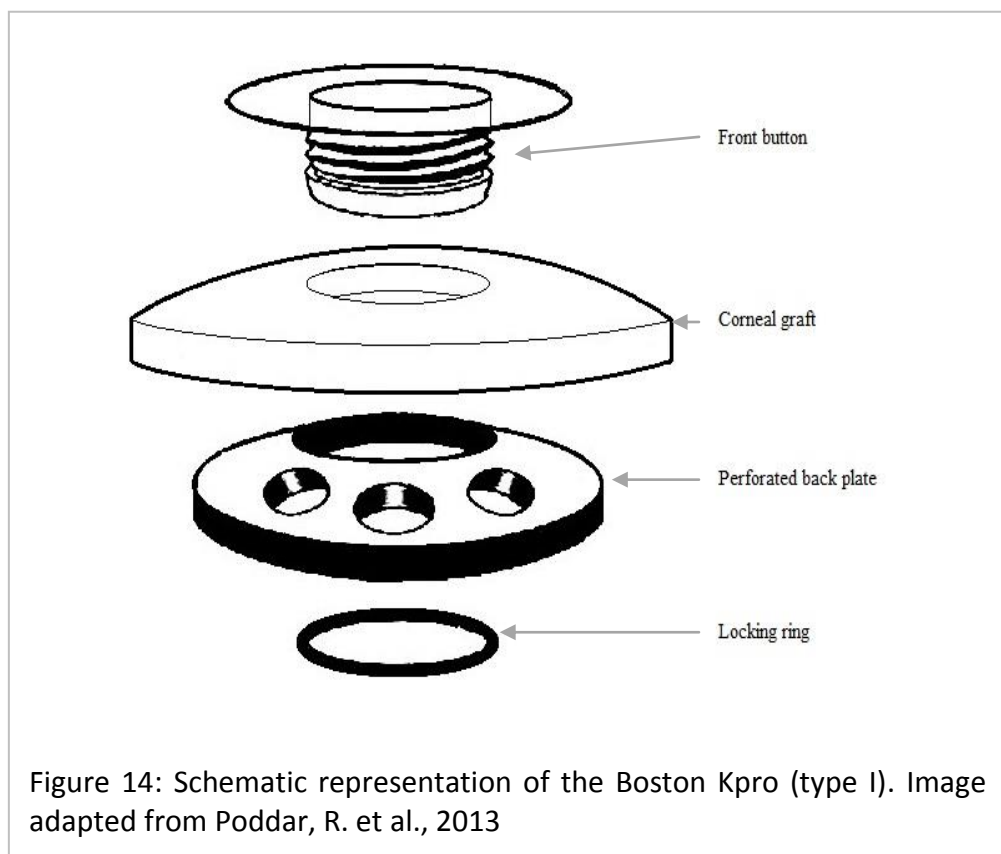
1. Implantation can require multiple surgeries and potentially the removal of the anterior eye structures, including the iris and anterior chamber
2. Individuals with Keratoprosthetic implants require life-long follow-ups by the ophthalmologist, since the implants are subject to complications such as glaucoma and corneal-melt which can lead to total loss of the eye.
3. The results are not aesthetically pleasing.

At present there are a few keratoprotheses available, from the simple type I Boston KPro, to the highly complex osteo-odontal keratoprosthesis (OOKP). A brief summary of the Boston KPro and OOKP are given below since they are the most established corneal prosthetics and they succinctly demonstrate the role of corneal prosthetics in the treatment of corneal blindness (for a more detailed review of keratoprosthesis see; Gomaa, 2010; McLaughlin, 2009; Duan 2006).

Boston KPro

The Boston KPro is a completely synthetic keratoprosthesis with two available designs, type I and type II. The type I Boston KPro has a collar-button design with three parts, a central poly-methyl methacrylate (PMMA) optical stem, a titanium back-plate and a titanium locking ring (Figure 14), and the type II Boston KPro has the same design with an additional anterior nub that projects out from the front button (Khan et al., 2007, Doane et al., 1996).

The type I device is used as a direct corneal replacement for individuals that have had repeated graft failure. The failed corneal graft is excised and then a second donor cornea, often not of donor quality, i.e. with a low endothelial cell count, is cut to the same size of the hole. The second donor tissue subsequently has a 3.5mm ring cut out from the central



portion. Through this hole the optical stem of the front button is positioned and then screwed into the back-plate. Next the locking ring is clipped onto the end of the optical stem that protrudes through the back-plate. Finally the graft tissue is sutured into place in the same manner as a penetrating keratoplasty procedure (Khan et al., 2007, Duan et al., 2006).

The addition of the anterior nub on the front button of the type II device was designed to protrude through the eye-lids, which is sewn shut, or a buccal-mucosal auto-graft that is grafted onto the anterior eye. This has allowed for the Boston KPro to be selected for patients with severe corneal blindness and with a poor tear film and compromised epithelium, e.g. Stevens Johnson syndrome; and corneal trauma, e.g. chemical burns, (Khan et al., 2007, Duan et al. 2006).

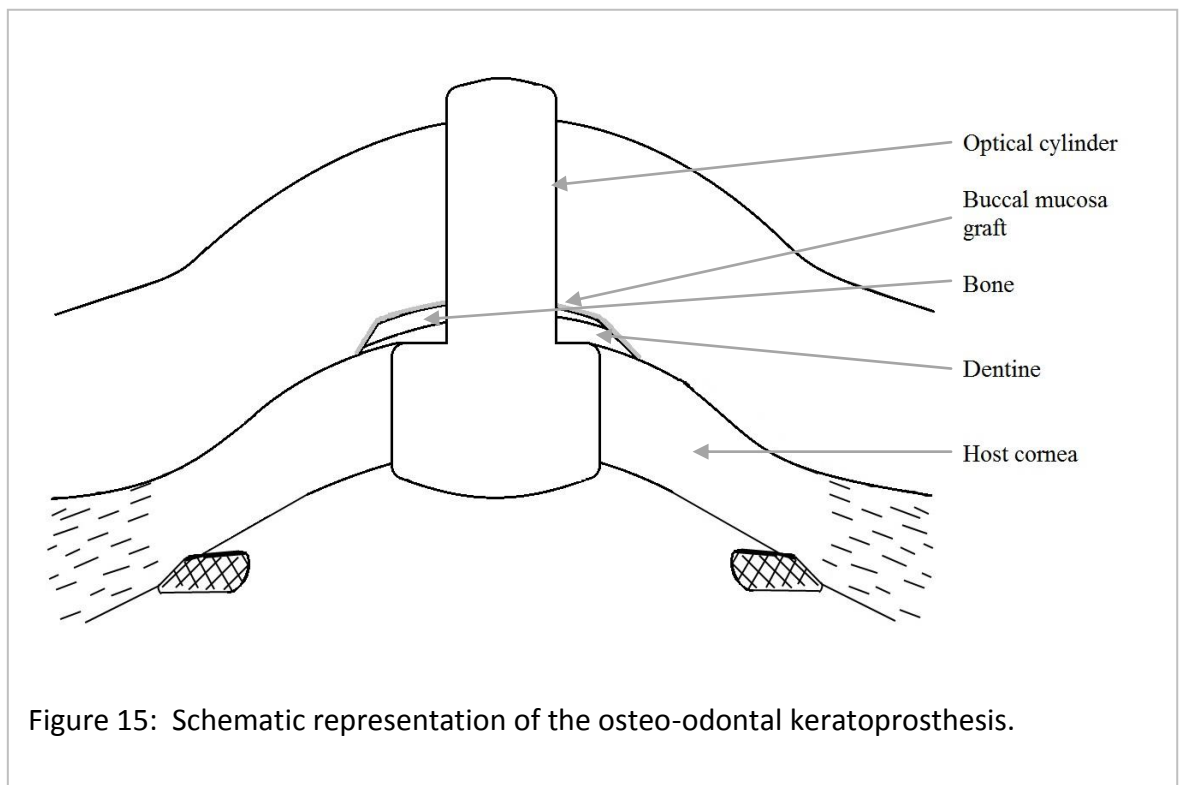
In clinical practice the majority of Boston Type I keratoprotheses have been implanted into patients diagnosed with repeated corneal graft rejection (54%), though other diagnoses include chemical injury, bullous keratoplasty and viral herpes simplex keratitis. In the majority of cases visual acuity improved to 6/60 (56%) and graft retention was ~95% after (an average) 8.5 month post-operative follow-up (Gomaa et al., 2010). However, the Boston Kpro has a number of complications that can occur as a result of its implantation. The two most common complications include the formation of a retroprosthetic membrane and glaucoma; both of which may require additional surgical intervention to prevent total blindness. Retroprosthetic membrane formation can cause the implant to extrude, thus YAG-laser membranectomy is often used to remove the membrane, or where the membrane cannot be removed the implant is replaced. In order

to treat the glaucoma medication is prescribed or a tube shunt can be implanted (Gomaa et al., 2010).

Osteo-Odontal Keratoprosthesis

The osteo-odontal keratoprosthesis is a highly complicated and two-stage surgical procedure with the end product being a transparent poly(methyl methacrylate) (PMMA) optical cylinder being cemented into a patient's own canine tooth root and alveolar bone, which is then sutured into the anterior of the eye globe and covered by a buccal mucosal membrane auto-graft (Figure 15). The procedure described herein is the modified Falcinelli procedure utilised by Mr. Christopher Liu of the Sussex Eye Hospital (Gomaa et al., 2010).

During the first surgery of the OOKP procedure two steps are carried out; i) a canine tooth



along with its alveolar bone is prepared to become a receptacle for the PMMA optic; and
ii) the buccal mucosal membrane autograft is placed over the cornea.

During surgery 1(i), a canine tooth, along with the dentine bone is harvested from the patients jaw. The tooth root and dentine is shaped and a hole is drilled through the root and dentine bone of the tooth, into which the PMMA optic is cemented into place, producing the OOKP lamina. Once the lamina is formed the crown of the tooth is removed and the lamina is then buried within a sub-muscular pouch in the lower lid of the fellow eye (which is not operated on).

In surgery 1(ii), the defective cornea is exposed and debrided of epithelial cells and the Bowman's layer. Next a full thickness mucous membrane auto-graft is harvested from the inside of the cheek from the patient and sutured onto the sclera of the patient at the rectus muscle insertions.

The OOKP lamina and buccal mucosal grafts are then left for approximately four-months in order for the buccal mucosal graft to become vascularised, and to ensure that the optic is stable within the OOKP lamina and that a fibrovascular capsule has formed around the lamina.

During the second stage of surgery the buccal mucosal graft is pulled back to expose the eye. The central 5mm of the cornea as well as the whole iris and lens are then excised from the eye, and some anterior vitreous humour is also removed. The lamina is then recovered from the sub-muscular pocket. Any excess tissue and the fibrovascular capsule are trimmed away from the PMMA optic, and the lamina is then sutured to the remaining corneal tissue. Finally the buccal mucosal graft is placed back over the eye and a hole is cut through the mucous membrane through which the optic stem will protrude.

Although this procedure requires the removal of the iris and lens, it is effective because the osteo-odontal support allows for the active integration of the OOKP into the pre-existing corneal tissue (Stoiber et al., 2002). In clinical practice the multi-stage surgery and life-long follow-ups required in order to detect and correct any complications that can occur with this type of keratoprosthesis means the OOKP is reserved for the most severe cases of corneal blindness such as Stevens' Johnson syndrome, severe chemical or thermal burns, multiple graft failures where dry-eye is a problem and other cases where the prognosis is poor. In the majority of cases (60%) visual acuity improves to 6/18 and after 20-years OOKP retention rates are approximately 80%. However, the OOKP is commonly complicated by glaucoma, in approximately one-third of cases, and requires topical and systemic glaucoma medication, or may require a tube shunt to be implanted. Additionally, the mucous membrane can grow over the optic stem, hence it requires trimming back to prevent this from happening. The most severe complication of the OOKP is extrusion of the implant due to retroprosthetic membrane formation or mucosal ulceration and can require a repeat OOKP implantation.

1.5.2 Development of a Novel Corneal Replacement

At present there is no "gold-standard" solution for treating corneal blindness, moreover, the complex nature of the cornea, the multitude of pathologies and requirement for tissue transparency demands a wide range of treatments option.

When treating corneal blindness a clinician has to consider the availability of tissue and its quality (when considering corneal transplantation), the invasiveness of the surgery as well

as the prognosis of the treatment. However at present the most common treatment is keratoplasty; although limbal stem cell grafts are a useful tool for limbal stem cell deficiency and keratoprotheses can save the sight of individuals with severe corneal blindness where the prognosis for other treatments would be poor.

Corneal transplantation like all forms of tissue donation, has the potential to fail, and a five year follow-up study of corneal donation in Australia revealed that 1-in-4 grafts will fail during this period (Williams et al., 2006). This can be due to a loss of endothelial cells and stromal hydration control which results in swelling and opacity to the stroma; however it highlights the need for better treatment options. Additionally, corneal transplantation within England is reliant upon the good will of others since tissue donation is currently run as an “opt-in” system, where donors, or their families, must volunteer their organs for donation upon death. In 2013/14, corneal donation only just matched the demand for corneal transplants (NHS Blood and Transplant, 2014) although in previous years demand has out-stripped supply (NHS Blood and Transplant, 2012). However, the donor pool may decline in the future due to an ageing population and stringent regulations regarding donation in order to prevent CJD-prion transmission (NHS Executive, 1999). Within an ageing population the corneal tissue supplied to the eye banks may not be suitable for donation due to reduced endothelial density, since corneal tissue harvested from older individuals have a lower endothelial cells density than corneas yielded from younger donors (Gal et al., 2008, Gain et al., 2002). Also, guidelines were introduced within the UK after the discovery that vCJD was transmitted in corneal tissues by prions that cannot be easily detected. The guidelines currently exclude donations from individuals with dementia of unknown origin; but Britain has an ageing

population, with increasing rates of dementia in the elderly and the end result may be a decline in the number of available corneal donors.

Alternatives to keratoplasty are valuable tools to treat corneal blindness, but at present they are not ideal. Corneal prosthetics are not the first choice a surgeon will take to treat corneal blindness even though they are useful to treat extreme cases of corneal blindness including where a corneal transplant is unsuitable or has repeatedly failed. Their use is reserved for these cases because in the majority of cases visual acuity improves to only 6/60 for the Boston KPro (Gomaa et al., 2010) and 6/18 for the OOKP (Tan et al., 2012) whilst implantation can be a long and invasive process. Additionally keratoprosthetics will require lifelong follow-ups because complications are common-place. For example, patients with the Boston and OOKP keratoprosthetics frequently have glaucoma that requires additional medication or surgery; while a less common, but more serious complication, is extrusion of the implant which will require immediate surgery to save the eye (Gomaa et al., 2010, Khan et al., 2007).

Limbal stem cell grafts have given ophthalmologists a novel alternative to corneal transplantation for limbal stem cell deficiency, which offers clinicians the opportunity to produce autograft donor material as well as allogeneic grafts. However its use is limited to treating limbal stem cell deficiency, where the underlying stroma remains transparent. In addition, the amniotic membrane used to replace damaged stromal tissue in some instances is highly variable with regard to transparency (Connon et al., 2010).

Limbal stem cell grafts highlight the emerging field of tissue engineering and regeneration for the treatment of corneal blindness, furthermore, through research into the mechanisms of corneal transparency and development of novel corneal replacements,

there is potential to provide regenerative treatment options for treating corneal blindness and even autograft analogous materials.

1.6 POTENTIAL FOR ARTIFICIAL CORNEAL REPLACEMENTS

Artificial corneal replacements are man-made corneal replacements used to replace the native corneal tissue. The Boston and osteo-odontal keratoprosthetics and limbal stem cell grafts are examples of artificial corneal replacements, and these examples nicely highlight two possible ways of approaching artificial corneal replacements – to fully replace the cornea with a polymeric ‘biomaterial’, or regenerate the corneal tissue with an *in-vitro* produced tissue engineered construct. In addition to biomaterials and tissue engineered constructs, there is the potential to utilise corneal xenografts, donor corneal tissue sourced from animal tissue as a corneal replacement, due to the immune privileged nature of the cornea.

For an artificial corneal replacement to be considered successful the corneal replacement must be able to fulfil the following criteria:

- First and foremost, any corneal replacement must be transparent and maintain transparency after long-term engraftment
- Secondly, the corneal replacement must be able to withstand the intra-ocular pressures exerted upon it once implanted
- Finally, the replacement should become suitably incorporated into the host tissue, without causing damage to the host tissue

In order to produce an artificial corneal replacement, it is intended to utilise the cornea itself and take cues from the collagenous stromal architecture in order to produce an enhanced transparent structure that mimics the cornea. Hence, the aims of this thesis are:

- To elucidate upon the corneal ultrastructure and gain an understanding of how the stromal extra-cellular matrix composition and architecture enable the tissue to be transparent.
- Utilise the knowledge gained to inform the development a “humanised” porcine corneal xenograft through the use of tissue engineering.
- Additionally, the knowledge of the corneal stromal ECM structure and composition will be used to inform the development of an *in-vitro* produced artificial corneal biomaterial in order to generate a biomaterial that mimics the stromal ECM composition.

CHAPTER 2: Materials and Methods

2.1 MATERIALS

Below are the generic tissue culture materials used to maintain the cells throughout this thesis; additional materials used for the development of specific methodologies are contained within the relevant chapter materials sections.

2.1.1 Primary Human Corneal Fibroblast Culture Materials

Primary human corneal fibroblasts were obtained from explant cultures of discarded corneal limbal rings of tissue (Figure 1.13) where there was specific consent and approval for use for research purposes, following corneal transplantation operations at the Queen Victoria Hospital NHS Foundation Trust, East Grinstead, UK and kindly gifted to the University of Brighton, a Human Tissues Authority Licenced premises. Primary human embryonic keratocyte cells from research approved sources were isolated in-house and kindly gifted for this study by Dr. Angela Sheerin of the University of Brighton (Kipling et al., 2009, Dropcova et al., 1999).

Materials	Source
Primary Human Corneal Fibroblast – isolated from corneal limbal explant cultures (designated; LRF207)	Queen Victoria Hospital NHS Foundation Trust, East Grinstead, UK
Primary Human Embryonic Keratocytes (designated EK1Br)	Kindly gifted to this study by Dr. Angela Sheerin, University of Brighton
CellStar, 75cm ² Tissue Culture Flasks, with filter cap	Greiner BioOne Ltd., Stonehouse, Glos, UK
CellStar, 1ml, 2ml, 5ml, 10ml and 25ml, sterile, serological pipettes	
30ml sterile plastic universal tubes	
50ml falcon tubes	Nunc Brand from Thermo Fisher Scientific UK, UK
Pre-plugged and non-plugged glass Pasteur pipettes	Thermo Fisher Scientific UK, UK
Dulbecco's Modified Eagle's Media (DMEM) + 1000mg/l glucose + GlutaMAX™ + pyruvate	Gibco, Invitrogen Life Technologies Ltd. Paisley, UK
Foetal Calf Serum (FCS)	
Hank's Balanced Salt Solution without CaCl ₂ and MgCl ₂	
0.05% Trypsin-EDTA	
Dimethyl Sulphoxide (DMSO) Hybri-Max	Sigma-Aldrich Company Ltd., Dorset, UK
Nunc CryoTube 1.8ml Vials	Thermo Fisher Scientific UK, UK
Haemocytometer	Nunc Brand from Thermo Fisher Scientific UK, UK
Isopropyl Alcohol	Thermo Fisher Scientific UK, UK
Motic AE31 inverted light microscope Moticam 2000, 2.0M pixel USB digital camera and Motic Image Plus imaging software	Available in laboratory

2.2 METHODS

Below are the generic tissue culture protocols used to maintain the cultured cells throughout this thesis; more specific culturing techniques used during the development of specific methodologies are contained within the relevant chapter methods sections.

2.2.1 Primary Human Corneal Fibroblast Cell Culture

All *in-vitro* cellular manipulations e.g. media preparation, routine cell culture (i.e. Passage or media changes) and studies using corneal fibroblasts, were carried out in a class II laminar flow hood.

2.2.1.1 Primary Limbal Ring Fibroblasts

Corneal limbal ring fibroblasts, (LRFs) were isolated from limbal tissue supplied by the Queen Victoria Hospital (QVH) NHS Foundation. The fibroblast explant cultures were established by Dr S.E. James and the primary culture (LRF207) expanded with aliquots frozen in DMEM + 10% FCS + 10% DMSO at 3-million cells/ml and stored in liquid nitrogen vapour until thawed. A frozen vial containing 1.52-million (1.52×10^6) cells at Passage 5, 67 days in culture, and 14.56 cumulative population doublings were received, with the cells having previously been cultured in growth medium consisting of DMEM +10% FCS and in a humid atmosphere at 37°C and 10% CO₂. The thawed cells continued to be grown under the same conditions.

2.2.1.2 *Primary Human Embryonic Keratocytes*

Embryonic keratocytes (EK1Br) were kindly donated to this study by Dr. Angela Sheerin of the University of Brighton. The cells were isolated from an aborted foetus, which had been ethically cleared for research purposes and the cells have been well characterised in previous studies (Kipling et al., 2009, Dropcova et al., 1999). Two vials containing 1.8×10^6 and 1.1×10^6 cells, respectively, frozen in MEM + 30% FCS + 10% DMSO + penicillin (100units/ml) + streptomycin (0.1mg/ml) were received and stored in liquid nitrogen vapour until thawed. The cells in both vials were received at Passage 16, had completed 26.9 and 28.1 cumulative population doublings, respectively and had been cultured in MEM + 10% FCS and in a humid atmosphere at 37°C and 5% CO₂.

2.2.1.3 *Cell Thawing*

Thawing of LRF207 and EK1Br cells were carried out as per the standard operating procedures described here-in. The frozen cell pellet was transferred into a 30ml universal tube and thawed by adding 20ml of cold DMEM in a drop-wise fashion. The cell suspension was thoroughly mixed and a single cell suspension was created using a pipette to gently draw-up and blow-out the liquid. The cell suspension was then centrifuged at 1500rpm (equivalent to 412g) for 4-minutes resulting in cellular pellet. The supernatant was aspirated off using a glass pipette attached to a vacuum pump, and then the cellular pellet was re-suspended in 10ml of cold DMEM with 10% FCS. The suspension was centrifuged a second time, at 1500rpm for 4-minutes, and the supernatant aspirated away from the pellet to remove any remaining DMSO. The pellet was re-suspended in a

10ml aliquot of DMEM + 10% FCS at ambient temperature and then seeded into a 75cm² flask with filter-cap at a total of 2x10⁵ cells in each flask.

2.2.1.4 Cell Culture

LRF207 and EK1Br cells were cultured in a humid environment at 37°C and 10% or 5% CO₂, respectively, and had a medium change every 2-3 days. Culture media was changed by aspirating off the old media and adding 10ml of fresh growth media to the flasks.

2.2.1.5 Cell Expansion, Passage & Harvest

When both cell types reached approximately 85% confluence, the cells were Passaged and harvested using the following standard operating procedure. The media was aspirated out of the flask using a glass Pasteur pipette attached to a vacuum pump, and then the flask was washed with 5ml HBSS. The HBSS was removed and 2ml of 0.05% trypsin-EDTA was added to the flask. The flask was incubated at room temperature for ~5-minutes (or until all the cells had been removed from the flask surface determined by microscopic examination). Once all the cells had detached, the trypsin was neutralised with 3ml DMEM + 10% FCS, and the cells were transferred to a 30ml universal tube. The flask was rinsed with an addition 5ml DMEM + 10% FCS, in order to collect any remaining cells in the flask, with the rinsing 5ml of media being transferred to the 30ml universal tube containing the cells. The cellular suspension was evenly distributed, to give

a single cell suspension, and ~20µl was loaded into a haemocytometer to count the number of cells in the suspension. Cell counting was carried using a Motic AE31 inverted phase contrast light microscope at x400 magnification. The harvested cells were then sub-cultured into multiple 75cm² flasks with 1x10⁵ cell aliquots seeded into each flask.

The process of cell culturing, Passage and harvesting was continued for the LRF207 cells until a large quantity (>5x10⁷) of cells had been established, which was at Passage 9, or 88 days in culture and 23.1 cumulative population doublings. After which time the cells were frozen down in 1ml aliquots (*see below*) until required. This ensured that all aliquots of cells used experimentally throughout the project were from the same source material.

For the infiltration into decellularised porcine corneal tissue studies 1 vial of cells was thawed and grown for one passage and before seeding the cells with decellularised porcine corneal tissue.

The EK1Br cells were grown up for one Passage after thawing and then utilised in the novel collagen I/V-GAG biomaterial studies.

2.2.1.6 *Cell Freezing*

LRF207 cells were frozen by substituting the culture medium for a freezing medium of DMEM + 10% FCS + 10% DMSO using the following standard operating procedure. Trypsinised cells were centrifuged at 1500rpm for 4-minutes, and the supernatant was aspirated away from the pellet. The cell pellet was re-suspended in cold freezing medium at a cellular concentration of 3x10⁶cells/ml, and then 1ml volumes of the suspension were

aliquoted into multiple freezing vials. The freezing vials were stored at -80°C , in a freezing tub containing isopropyl alcohol, which established a controlled freezing rate of 1°C per minute down to -20°C . After ~ 12 -hours, the frozen vials were transferred to the liquid nitrogen vapour cell bank within the laboratory. Aliquots from the same frozen batch were used throughout this thesis.

CHAPTER 3: Elucidation of the Porcine Corneal Stromal Architecture – Using transmission electron microscopy

3.1 INTRODUCTION

The success of modern medicine has enabled the transplantation of organs from person to person, known as allografting. However, in many instances, there is a deficit in the number of organ donors when compared to the clinical need (NHS Blood and Transplant, 2014) and as such the transplantation of organs or tissues from animals to humans, known as xenografting, has often been considered as a source of donor material or an alternative *in-vitro* product has needed to be produced, i.e. biomaterials and tissue engineered regenerative constructs.

The cornea has been identified as an area where an artificial replacement may be beneficial for the treatment of corneal opacity, since an artificial corneal replacement could be designed to regenerate the tissue, as well as to eliminate the needs for cadaver corneal tissues. However, the complex nature of the cornea and, more specifically, the corneal stromal extra cellular matrix needs to be thoroughly understood in terms of its architecture and the mechanisms of transparency in order to inform the development of an artificial corneal replacement. Hence the aim of this chapter is to elucidate upon the corneal stromal architecture and utilise the information to inform the development of an artificial corneal stromal replacement.

3.1.1 Corneal Stromal Architecture

The corneal stroma makes up 90% of the corneal thickness (Nishida; 1997) and is required to be transparent as well as maintain the structure of the eye globe. It is comprised of an organised collagen and proteoglycan extra cellular matrix (ECM), which is maintained by corneal fibroblasts (keratocytes).

The mechanisms that allow for the corneal stromal ECM to be transparent include thin collagen fibrils that are uniformly spaced (Akhtar, 2012, Knupp et al., 2009, Lewis et al., 2010, Freegard, 1997, Komai and Ushiki, 1991, Cox et al., 1970, Maurice, 1957) between adjacent fibrils that are arranged into a quasi-crystalline hexagonal arrangement (Parfitt et al., 2010, Cox et al., 1970). This arrangement of stromal collagen fibrils is the product heterogeneous collagen type I and type V fibrils that restrict the diameter of the collagen fibrils (Smith and Birk, 2012, Birk, 2001, Robert et al., 2001) and the keratan sulphate (KS) and chondroitin/dermatan sulphate (CS/DS) proteoglycans that act to evenly space the collagen fibrils (Parfitt et al., 2010, Scott, 2001, Scott and Bosworth, 1990).

In addition to the uniform nature of adjacent collagen fibrils, the corneal stromal ECM also exhibits a second level arrangement, whereby the collagen fibrils are grouped into sheets known as lamellae (Komai and Ushiki, 1991). These sheets are stacked into orthogonal arrays, which are preferentially orientated in the superior-inferior and nasal-temporal orientations (Meek and Boote, 2009, Hayes et al., 2007) though they interweave and interlace throughout the stroma and provide the structural integrity that enables the cornea to maintain the shape of the eye globe (Radner and Mallinger, 2002).

3.1.2 Elucidation of the Porcine Corneal Stroma

Porcine tissues are a common model for human tissues due to structural similarities between the tissues of the two species and they are also currently used as a xenograft material for animal to human engraftment, e.g. for dermal tissue and heart valves (Crapo, 2011; Gilbert, 2006). Additionally porcine tissue is deemed ethically acceptable for use as a model or xenograft since pork is a common foodstuff. For these reasons porcine tissue has been considered as a potential source of xenograft material for the cornea (Oh et al., 2009a, Oh et al., 2009b, Oh et al., 2009c, Ahmadiankia et al., 2009). However, there has been limited data published regarding the three-dimensional architecture of the porcine corneal stroma and there has yet to be a full depth microscopic analysis of the porcine corneal stroma despite investigations of porcine stromal tissue as a potential corneal xenograft. Therefore the porcine corneal stromal architecture needs elucidating.

Due to the lack of published three-dimensional data on porcine stromal architecture, a comparison between porcine and human stromal tissues has yet to be made. However, previous studies between rabbit and human corneal stromal tissues have been carried out and the differences between the species are well known and documented, with the collagen fibrils of both species having a uniform architecture while the collagen lamellae of the human tissue was demonstrated to interweave and interlace more-readily than the rabbit tissue (Radner and Mallinger, 2002, Radner et al., 1998, Komai and Ushiki, 1991). Hence, in order to assess the suitability of porcine stromal tissue to be a xenograft for human donation a direct comparison of porcine and rabbit corneal stromal tissues will be made after which an indirect comparison of porcine versus published data of the human corneal stroma can be made.

3.2 EXPERIMENTAL DESIGN

3.2.1 Sourcing Corneal Tissue

Pork and rabbit are common foodstuffs, and as such porcine and rabbit tissues can be readily sourced from abattoirs and meat processing factories or from other scientific investigations.

3.2.2 Location and Orientation of Stromal Tissue

The corneal stromal ECM architecture is commonly assumed to have the orthogonal arrangement with regularly spaced and diameter collagen fibrils as described within the introduction. However, there have been various studies that have revealed that stromal tissues from various species do not necessarily conform to this strict orthogonal arrangement and the direction of collagen fibrils become less organised at the periphery (Meek and Boote, 2009, Hayes et al., 2007).

Knowing that the collagen fibril orientation is less defined than previously thought is important since any three-dimensional modelling may be affected by lamella orientation changes; hence the most appropriate area to model the porcine and rabbit stromal ECM architecture would be from the central region. Additionally, the central region would be the area excised during keratoplasty and as such this region would also be used if porcine corneal tissue were to be used as a xenograft. In addition to selecting the central portion of the cornea, the tissue was orientated in such a way that best demonstrates the orientation of the lamellae and enabled visualisation of the orthogonal collagen

arrangement; i.e. the tissue were orientated in such a way as to give a vertical cross-section through the tissue.

3.2.3 Transmission Electron Microscopy of the Corneal Stroma

Studying corneal tissue, and the stromal ECM, has been carried out for over a century, first using light microscopy and then using more advanced microscopy techniques, such as electron microscopy. Light microscopes were first used to investigate the cornea at the turn of the 20th century; and through light microscope investigations, the lamella sheet arrangement of the stromal extra cellular matrix was well defined by the middle of the 20th century (Maurice 1957). Nevertheless, light microscopes have a limited resolution and cannot resolve nanometre scale structures, such as individual corneal stromal collagen fibrils. However, more advanced microscopy techniques, such as transmission electron microscopy (TEM), have a greater resolving power and are able to image the nanometre scale stromal collagen fibrils (Goodhew et al., 2001).

The ability of a microscopy system to distinguish two distinct objects, known as the resolution, of an optical system can be defined by Abbe's equation (Goodhew et al., 2001):

$$d = (0.612\lambda) \div (n \sin \alpha)$$

Where: d , is the achievable resolution; λ , is the wavelength of light; n , is the index of refraction of the medium and the lens(es); and α is half the angle of cone formed by the aperture (in radians).

From looking at the functions of Abbe's equation, the resolving power of an optical system can be improved by two factors – decreasing the wavelength of light ($0.612 \times \lambda$) or increasing the lens and aperture assembly ($n \sin \alpha$).

Practically, scientists and engineers have improved the apertures and use oil immersion lenses to yield a value of ~ 1.6 for the lens and aperture assembly, and as the numerical aperture approaches 1 the resolving power is determined by the wavelengths function of the equation. Considering visible light has a wavelength of 400-700nm within the electromagnetic spectrum, 400nm is the smallest possible wavelength usable for light microscope imaging. Therefore, in this instance, λ is the limiting factor of light microscope imaging systems and the best possible resolving power of a light microscope may only be ~ 150 nm.

In order to improve upon the resolving power of a microscopy system shorter wavelengths are required. Fortunately, electron sub-atomic particles have a waveform nature when they pass through a directed magnetic field within a vacuum, and the achievable wavelengths are much smaller than those of visible light; as determined by de Broglie's equation (Goodhew et al., 2001):

$$\lambda = h \div mv$$

Where: λ , is the wavelength (in nanometres); h , is Planck's constant (6.6×10^{-27}); m , is the mass of an electron (9.1×10^{-28}); and v , is the velocity of the electron.

Due the charged nature of electron, the de Broglie's equation can be manipulated using Einstein's mass-energy equivalence equation ($e = mc^2$) to express the velocity of the particles as a function of the potential energy (voltage) exerted upon the electron, hence:

$$\lambda = 1.23 \div \sqrt{V}$$

Where: λ , is the wavelength (in nanometres) and V is the accelerating voltage exerted upon the electrons.

This equation can be substituted into Abbe's equation, to give the theoretical resolving power of electron microscopes, hence:

$$d = 0.753 \div (\alpha \sqrt{V})$$

Where, d , is the resolution; α , is the half aperture angle; V , is the accelerating voltage.

The majority of TEMs used for biological imaging are set to 100kV; therefore the theoretical resolving power of an electron microscope is 0.24nm, if α is similar to that of light microscopes (for a more detailed knowledge of the theory of electron microscopy see (Goodhew et al., 2001)).

In reality lens aberrations do not quite allow α to be at the same level as light microscopes, hence the resolution is practically $\sim 0.5\text{nm}$. However; given what we know from the literature of human corneal stromal fibre size (22-35nm), electron microscopy is a highly suitable technique for resolving the porcine stromal structure.

3.2.4 Hypothesis

The following hypotheses were formulated for the comparison of porcine with rabbit tissue:

1. There is no significant difference between the diameter and spacing of collagen fibrils between porcine and rabbit corneal stromal tissues.
2. There is no significant difference in the arrangement of the lamella sheets between porcine and rabbit corneal stromal tissues.

Additionally the following qualitative assessments will be made regarding the arrangement of the collagen fibrils of both porcine and rabbit corneal tissues:

1. The arrangement of the collagen lamellae in terms of interweaving and orthogonal arrangement throughout the stromal depth.

2. The organisation of the collagen fibrils in terms of uniformity and hexagonal arrangement.

Finally, the following hypothesis was formulated for the indirect comparison of porcine and human corneal stromal tissues

1. Porcine corneal stromal tissue is not significantly different from human corneal stromal tissue, in terms of the collagenous fibrils' diameter and spacing

3.3 EXPERIMENTAL PROCEDURE

3.3.1 Materials

3.3.1.1 Corneal Tissue Dissection

Porcine and rabbit tissue for studying the corneal structure by TEM, along with the dissection equipment and consumables for excising the corneas were obtained from the following sources:

Materials	Source
Porcine eyes (3) (for the study of the corneal stromal structure)	Northwick Park Institute for Medical Research, Harrow, London
Rabbit eyes (3) (for the study of the corneal stromal structure)	Rabbit eye tissues were kindly supplied from Oxford University
Sterile disposable scalpels size 22A	Thermo Fisher Scientific UK, UK
100mm Petri-dishes	Thermo Fisher Scientific UK, UK
Forceps & tweezers	Available in laboratory
Phosphate buffered saline (PBS) tablets – 1	Thermo Fisher Scientific UK, UK

tablet makes 100ml PBS, pH7.4	
Sterile 30ml Universal Tubes	Gibco, Invitrogen Life Technologies Ltd. Paisley, UK

3.3.1.2 Processing Materials for Transmission Electron Microscopy

All processing for TEM and analysis using TEM was carried out using the following materials, equipment and software packages:

Materials	Source
TEM fixative – 2.5% gluteraldehyde (v/v) + 2% formaldehyde (v/v) in 0.1M phosphate buffer (pH7.4)	Prepared in lab by mixing 25% gluteraldehyde and 10% formaldehyde (from Thermo Fisher Scientific UK, UK) with 0.2M phosphate buffer (pH7.4) (prepared in laboratory – see below) and distilled water
0.1M phosphate buffer (pH7.4)	Prepared in lab by mixing sodium dihydrogen phosphate (0.2M) and disodium hydrogen phosphate (0.2M) (both prepared in laboratory – see below) with distilled water
0.2M sodium dihydrogen phosphate	Prepared in lab by dissolving sodium dihydrogen phosphate (from Thermo Fisher Scientific UK, UK) in distilled water
0.2M disodium hydrogen phosphate	Prepared in lab by dissolving sodium dihydrogen phosphate (from Thermo Fisher Scientific UK, UK) in distilled water
Sterile disposable scalpels size 15	Thermo Fisher Scientific UK, UK
100mm Petri-dishes	Thermo Fisher Scientific UK, UK
Sterile 30ml Universal Tubes	Gibco, Invitrogen Life Technologies Ltd. Paisley, UK
1% Osmium tetroxide (OsO ₄) in distilled	Prepared in laboratory by dissolving a 0.25g

water	ampoule of OsO ₄ crystals (Agar Scientific, Essex UK) in 25ml of distilled water
Distilled Water	Available in laboratory
Graded alcohols (10%, 20%, 30%, 50%, 75% & 90%, 100%)	Prepared in the lab from absolute ethanol (Thermo Fisher Scientific UK, UK) diluted in distilled water
Propylene oxide	Thermo Fisher Scientific UK, UK
TAAB low viscosity resin kit	TAAB, UK
Beem Capsules	Agar Scientific, UK
Glass Knives	Prepared in the laboratory using an RMC Products Glass Knife Maker and Ultramicrotome Glass (Agar Scientific, UK)
Diatome Ultra 35 ^o	TAAB, UK
RMC Powertome-PC Ultramicrotome; Leica Ultracut Ultramicrotome	Kindly made available by Brunel University; RMC Products (UK); Kindly made available by the University of Sussex; Leica Microsystems (UK), UK;
Copper 200-mesh TEM grids	Agar Scientific, UK
1% (w/v) aqueous uranyl acetate, (0.22µm filtered)	Prepared in laboratory by mixing 1g uranyl acetate (Agar Scientific, UK) with 100ml distilled water and filtering through a 0.22µm filter
Lead citrate (saturated)	Prepared in laboratory with the following protocol: Dissolve 33.1g Lead nitrate (Agar Scientific, UK) in 100ml distilled water (Sol. A), 37.7g tri-sodium citrate in 100ml distilled water (Sol. B), 4g sodium hydroxide in 100ml distilled water (Sol. C). Then, mix 16ml distilled water with 3ml Sol. A and 2ml Sol. B and stir for 30minutes. Then add 4ml Sol. C until the precipitate dissolves. Finally filter through 0.22µm filter
Potassium hydroxide	Thermo Fisher Scientific UK, UK

Jeol 2100F FEG TEM, with axially mounted Gatan Orius camera;	Kindly made available by Brunel University;
Hitachi-7100 Transmission Electron Microscope, with axially mounted Gatan Ultrascan 1000 CCD camera	Kindly made available by the University of Sussex
Gatan Digital Micrograph Software Suite	Gatan UK, UK
Adobe Photoshop CS3 Extended	Adobe System Inc.

3.3.2 Methods

3.3.2.1 Corneal Tissue Processing for Transmission Electron Microscopy

Whole porcine eyes (Northwick Park Hospital) and rabbit eyes (Oxford University) were excised immediately post mortem and stored at 4°C and transported to the University of Brighton. Three pig eyes and 3 rabbit eyes were received, and the corneas, plus a 2mm scleral ring, were dissected away from the remaining eye tissue.

Fixation

The corneas were placed into a TEM fixative solution consisting of 2.5% gluteraldehyde (v/v) + 2% formaldehyde (v/v) in 0.1M phosphate buffer (pH 7.4), where they were further dissected into 1-2mm cubes. After which, the corneal cubes were kept in the TEM fixative solution at room temperature for 2 hours, and then at 4°C overnight in order to fix the proteins.

After 12-hours the tissue cubes were removed from the TEM fixative solution and given at least two rinses in 0.1M phosphate buffer solution. Next the tissue blocks were post-fixed

in 1% osmium tetroxide (OsO_4) in distilled water for 4-hours at room temperature, in order to fix any lipid structures; after which they were rinsed twice in distilled water.

Dehydration ad solvent exchange

Once the tissue cubes were thoroughly rinsed in distilled water, they were dehydrated by rinsing the tissue in the following series of alcohol concentrations: 10%, 20%, 30%, 50%, 75%, 90% (v/v in distilled water) and finally two 100% ethanol rinses. Once the tissue blocks were fully dehydrated in the second 100% ethanol rinse, the alcohol solvent was exchanged for propylene oxide in preparation for resin embedding.

Resin embedding

A resin stock solution of TAAB low viscosity resin was prepared according the standard protocol; 48g of LV resin was mixed with 16g VH1 hardener, 36g of VH2 hardener and 2.5g of LV accelerator. A small aliquot (~10ml) of this resin stock solution was separated from the stock solution and mixed with an equal quantity of propylene oxide to give a 50:50 propylene oxide/resin intermediary solution.

The propylene oxide solution around the tissue blocks was then exchanged for the 50:50 propylene oxide/resin intermediary solution in order to aid the penetration of the resin into the tissue due to the lower viscosity of the 50:50 solution.

Next, the 50:50 propylene oxide/resin intermediary solution was exchanged for the stock resin solution and the tissue blocks were placed into Beem Capsules and orientated in such a way that the tissue would be sectioned in cross-section, so as to reveal the

orthogonal arrangement of the collagen lamellae and fibrils. Finally the tissue blocks were then left to polymerise over-night at 70°C and resulted in the tissue being embedded within the resin.

Tissue sectioning

After polymerization, the tissue blocks were removed from the Beem capsules and any excess resin surrounding the tissue was trimmed away using a scalpel. The resin block was then placed in either a Leica Ultracut Ultramicrotome or RMC Power-Tome PC ultra-microtome and the block-face was trimmed and shaped, until the full depth of the cornea was exposed, using a glass knife.

A second glass knife was then used to smooth down the cutting surface, until the block face was smooth and then the tissue was sectioned into 100nm thin sections using a Diatome Ultra 35° diamond knife. The tissue sections were floated out onto distilled water and mounted onto the shiny side of copper 200 mesh grid by dabbing the grid onto the surface of the water.

Contrast staining

Due to the nature of biological material, contrast within the TEM may be difficult, therefore the tissue sections were contrast stained using the following protocol. The TEM grids were floated, section-side down, on top of a 20µl droplet of 1% (w/v) aqueous uranyl acetate (0.22µm filtered) and incubated for 1 hour at ambient temperature in the dark. After 1 hour the sections were rinsed with distilled water and then floated onto a

droplet of saturated lead citrate for 15 minutes in the same manner as before, after which the sections were rinsed and then left to air-dry.

3.3.2.2 *Transmission Electron Microscopy and Micrograph Analysis*

Tissue sections were viewed using either a Hitachi-7100 Transmission Electron Microscope, with imaging carried out on an axially-mounted Gatan Ultrascan 1000 CCD camera or a Jeol 2100F FEG TEM and imaged with a Gatan Orius camera. Micrograph analysis was carried out using accompanying Gatan Digital Micrograph Software Suite or Photoshop CS3 Extended. Statistical analysis was carried out using a Student's T-test on Microsoft Excel 2003 SP3. Data was considered to be statistically significant where $p \leq 0.05$.

The full depth of the corneal stromal ECMs from porcine and rabbit tissues were imaged – from the anterior Bowman's layer to the posterior Descemet's membrane. From the images generated, the morphology of the architecture of the porcine and rabbit corneal stromal ECMs were noted.

Additionally, measurements of the diameter and spacing of the collagen fibrils from both species were taken from cross-sectioned fibrils. Measurements of the fibril diameters were carried out by measuring the fibrils from edge to edge and through the centre of the fibril at the thinnest part of the fibril. Measurements were carried out in this way since it was assumed that the collagen fibrils are cylindrical and when cross-sectioned any obliqueness from the sectioning would be eliminated since the shortest length, edge to

edge, through the centre of a cylinder should be equivalent to the diameter. After this was carried out, the fibril spacing was determined by measuring the distance between the central points of two fibrils, minus the radii of the two fibrils.

To compare the diameter and spacing of the collagen fibrils of the porcine and rabbit stromal tissues a two-way Student's T-Test was performed. Additionally, in order to compare the diameter and spacing of the porcine tissue with the published data of the human tissue a one-sample sample T-test was carried out. Mean values were considered statistically significant where the difference between the two values had a $p \leq 0.05$.

3.4 RESULTS

Transmission electron microscopy was able to resolve the stromal organisation of the pig and rabbit corneal tissues. Under low powered TEM the micrometre scale architecture of the porcine and rabbit stromal lamellae was revealed, whereas under higher magnification TEM the nanometre scale organisation of individual collagen fibrils from both species were resolved. Additionally, the software packages used were able to quantify the arrangement of the corneal stroma from both species and the three-dimensional architecture of porcine and rabbit stromal extra cellular matrices were elucidated.

3.4.1 Fibril Organisation

High powered TEM of the stroma from pig and rabbit corneas was able to resolve the individual fibrils which make-up the stromal ECMs of both species (Figures 16 & 17). Sectioning of the corneal stroma in cross-section revealed various en-face fibrils, i.e. the collagen fibrils were sectioned perpendicular to the cylinder length. When viewed under higher magnification TEM, these en-face fibrils are useful for describing the arrangement of adjacent collagen fibrils as well as quantifying the uniform nature of the fibril matrix.

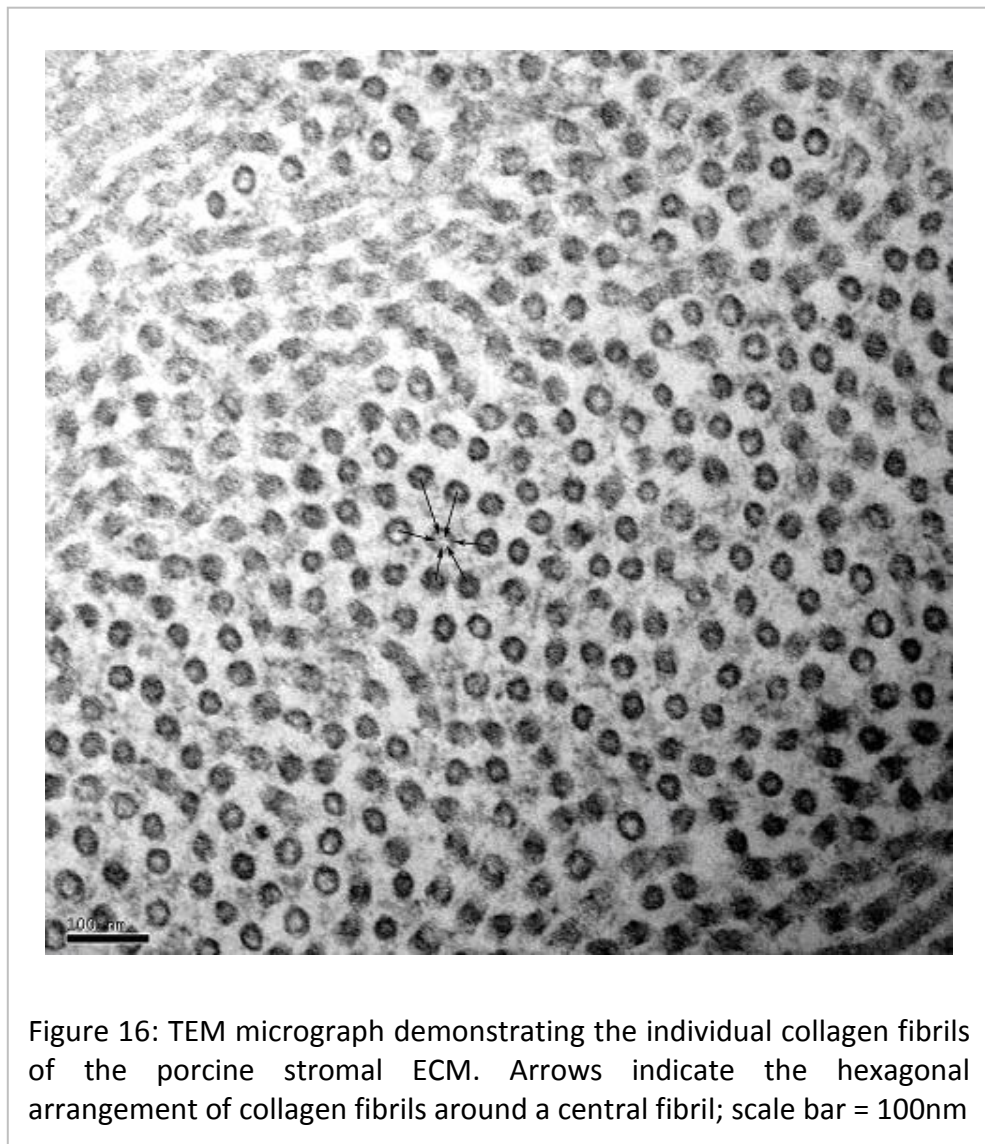


Figure 16: TEM micrograph demonstrating the individual collagen fibrils of the porcine stromal ECM. Arrows indicate the hexagonal arrangement of collagen fibrils around a central fibril; scale bar = 100nm

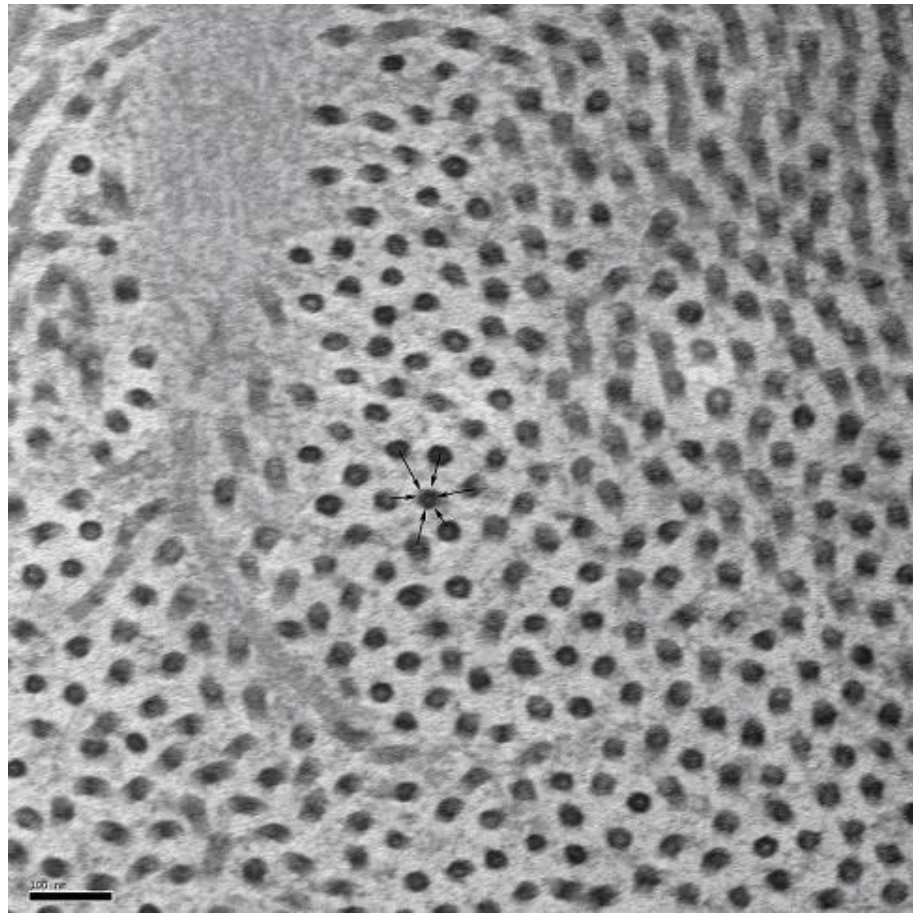
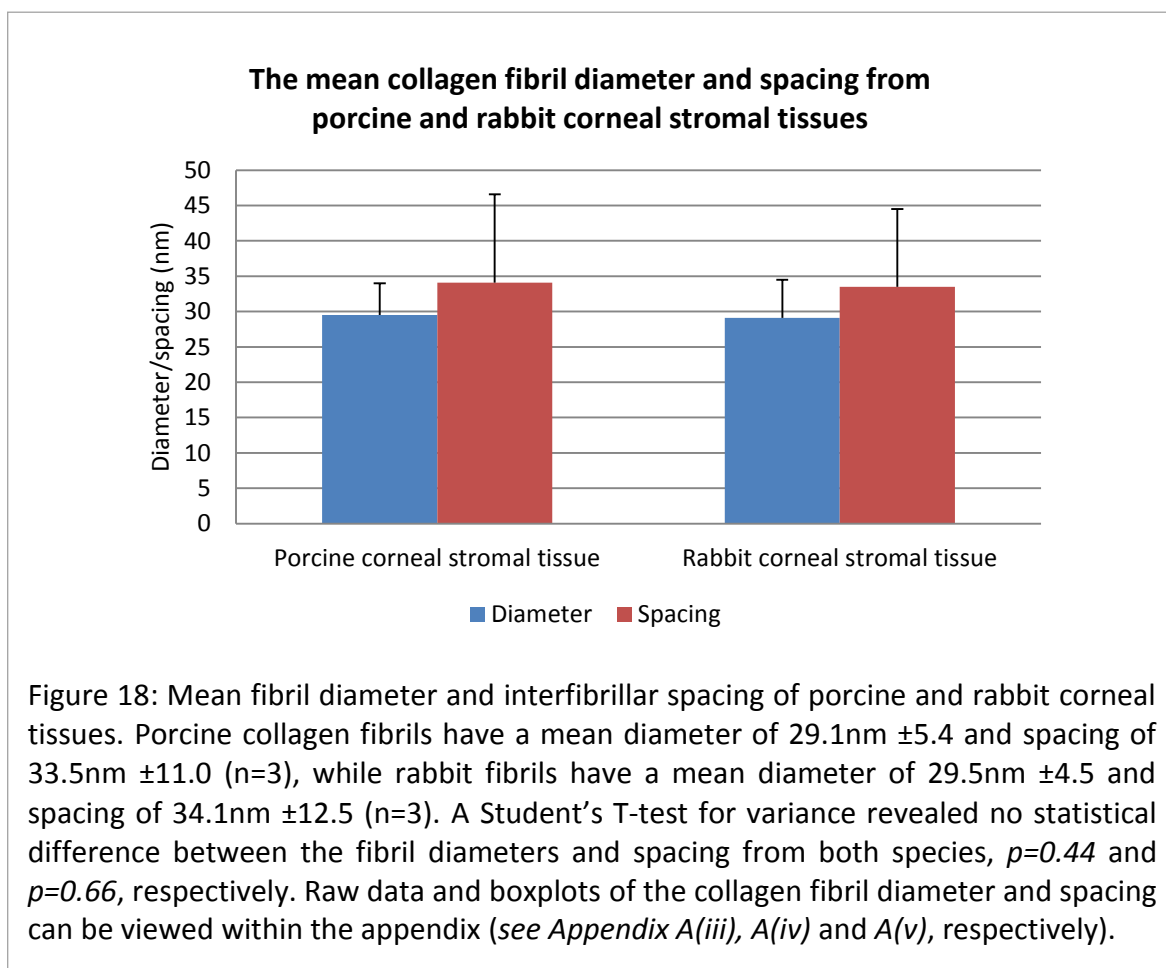


Figure 17: TEM micrograph demonstrating the individual collagen fibrils of the rabbit corneal stroma ECM. Arrows indicate the hexagonal arrangement of collagen fibrils around a central fibril; scale bar = 100nm

The mean corneal stromal collagen fibril diameter and interfibrillar spacing are given in Figure 18 as determined by measuring the en-face fibril. The mean diameter of the porcine collagen fibrils was $29.5\text{nm} \pm 4.5$ and the mean interfibrillar spacing for porcine tissues was $34.1\text{nm} \pm 12.5$, while the rabbit fibrils have a diameter and spacing of $29.1\text{nm} \pm 5.1$ and $33.5\text{nm} \pm 10.7$, respectively. En-face fibrils of the porcine and rabbit stromal ECMs were viewed to have a quasi-hexagonal arrangement, whereby a central fibril is surrounded by six other fibrils (Figures 16 & 17 arrows). However, a distinct crystalline



ordering of the collagen fibrils was not observed when looking at the secondary and tertiary adjacent collagen fibrils and in certain cases, it was difficult to distinguish the hexagonal arrangement.

3.4.2 Lamella Organisation

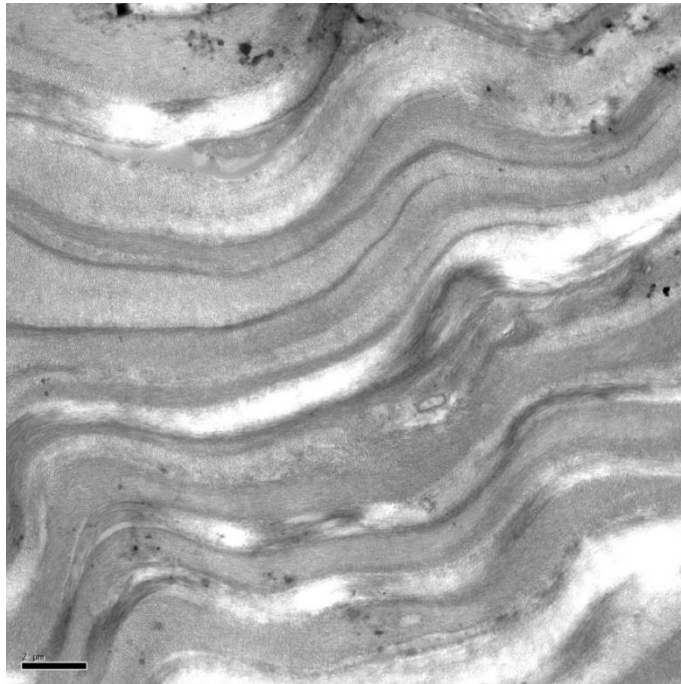
Using the TEM in a low magnification mode enabled the generation of a full depth profile of the corneal stroma from both porcine and rabbit corneas (Appendices A(i) and A(ii), respectively) as well as visualisation of the collagen lamellae of the corneal stroma for both species (Figures 19 & 20, respectively). The collagen fibrils from the porcine and

rabbit corneal stromal ECMs are formed into lamella sheets with the classically described stacked arrangement (Figures 19a & 20a), with a thickness range of the stromal lamellae for porcine lamellae measuring between 0.2 – 9.5 μm and 0.5 – 20.8 μm for rabbit lamellae.

When viewed under higher magnification the stacked lamellae from both species were observed to have the typical orthogonal arrangement of the stroma (Figures 19b & 20b); although the collagen fibrils do not strictly conform to the orthogonal collagen arrangement within both species (Figures 21 & 22), with many adjacent lamellae demonstrating fibril orientation changes (Figures 21a & 22a) or convergence/divergence (Figures 21b & 22b) as the lamellae interweave past one another and interlace together, respectively.

By looking at the full depth of the corneal stroma developed for both species (Appendices A(i) and A(ii)), the differences between the anterior and posterior lamella sizes and level of interweaving were revealed (Figure 23 & 24). From the full depth profile the anterior stromal lamellae had a mean depth of 1.8 μm \pm 1.3 and 3.3 μm \pm 2.0, for porcine and rabbit tissues respectively. The posterior stromal lamellae have a mean lamella depth of 3.1 μm \pm 2.2 and 4.3 μm \pm 3.6, for porcine and rabbit tissues, respectively. Statistically these results are not significantly different, $p=0.49$ for porcine tissue and $p=0.71$ for rabbit tissue, though the trend suggests that posterior lamellae are thicker than anterior lamellae.

A



B

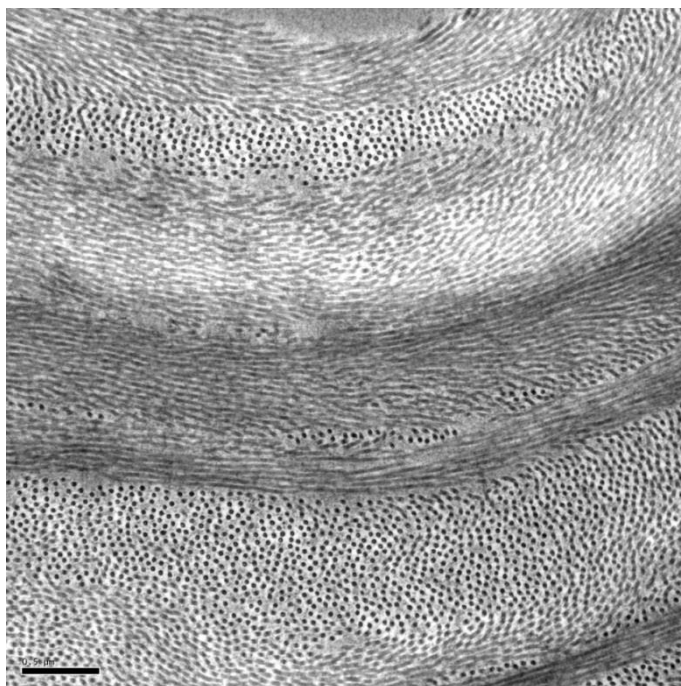
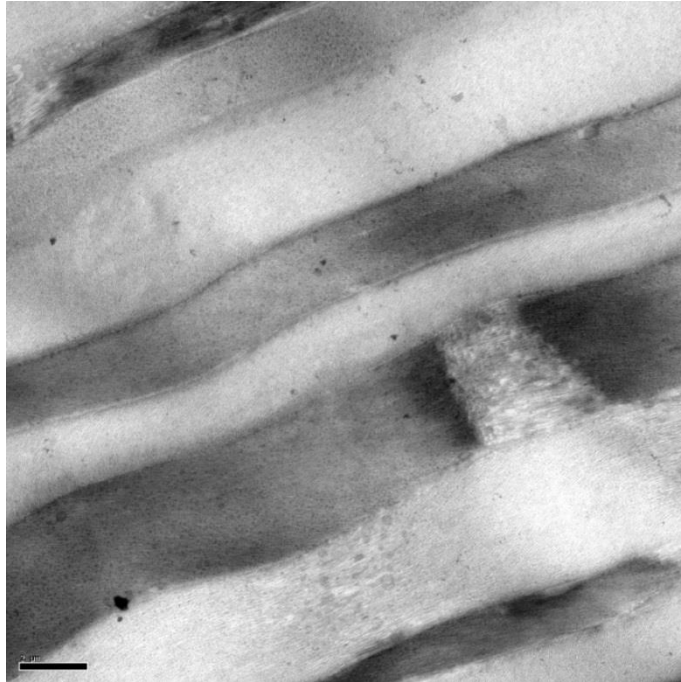


Figure 19: TEM micrograph demonstrating the stacked lamella arrangement of collagen bundles within the porcine stroma (A) and the orthogonal arrangement of the collagen lamellae (B). Porcine corneal lamellae measure between 0.2-9.5μm in depth. A, scale bar = 2μm; B; scale bar = 0.5μm.

A



B

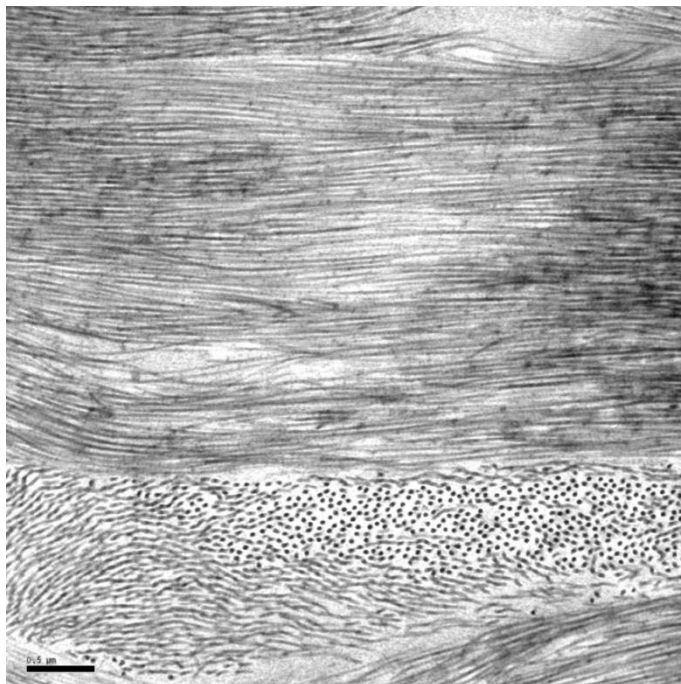
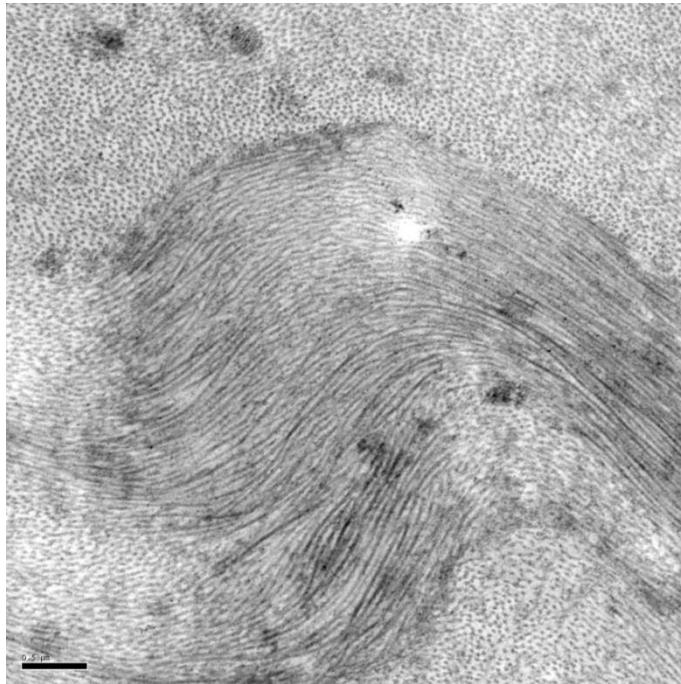


Figure 20: TEM micrograph demonstrating the stacked lamella arrangement of collagen bundles within the rabbit stroma (A) and the orthogonal arrangement of the collagen lamellae (B). The rabbit stromal lamella sheets measure between 0.5-20.8 μm in depth. A scale bar = 2 μm; B scale bars = 0.5 μm.

A



B

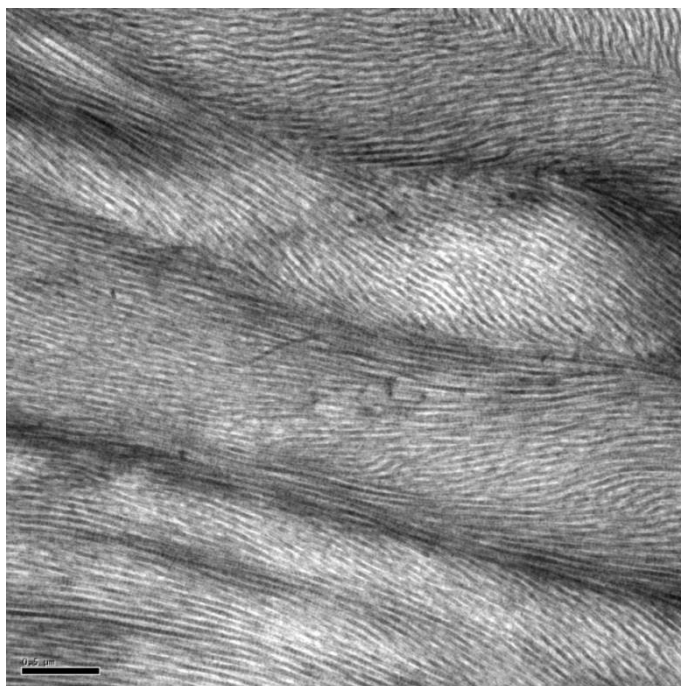
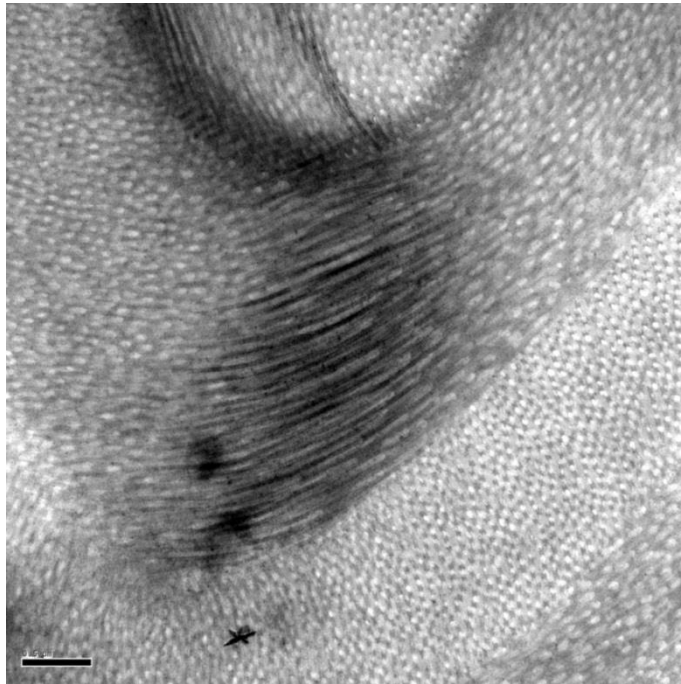


Figure 21: TEM micrograph demonstrating the interweaving (A) and converging/diverging of collagen lamellae (B) within the porcine stroma. The orientation changes of the collagen fibrils demonstrate that this feature is 3D property, occurring throughout the stromal depth. A scale bar = 0.5μm; B scale bar = 0.5μm.

A



B

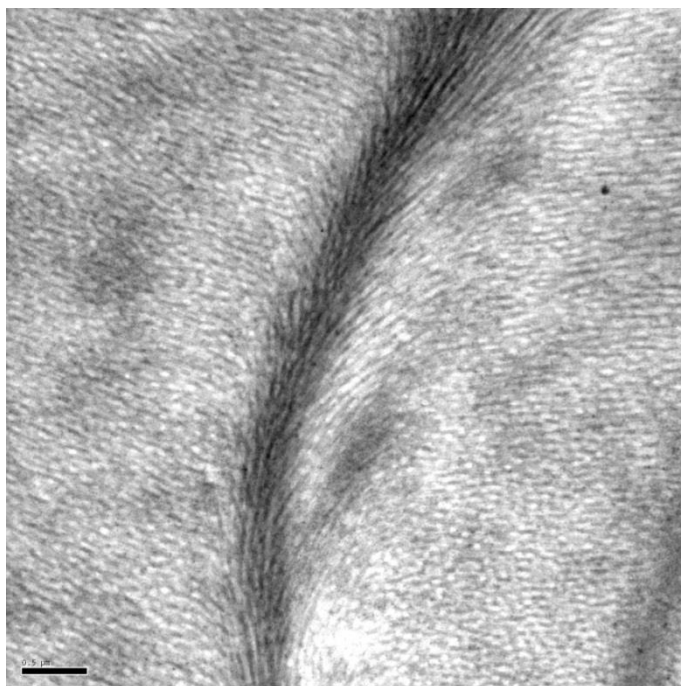


Figure 22: TEM micrograph demonstrating the interweaving (A) and converging/diverging of collagen lamellae (B) within the rabbit stromal ECM. The orientation changes of the collagen fibrils demonstrate that this feature is 3D property, occurring throughout the stromal ECM. A scale bar = $0.5\mu\text{m}$; B scale bar = $0.5\mu\text{m}$.

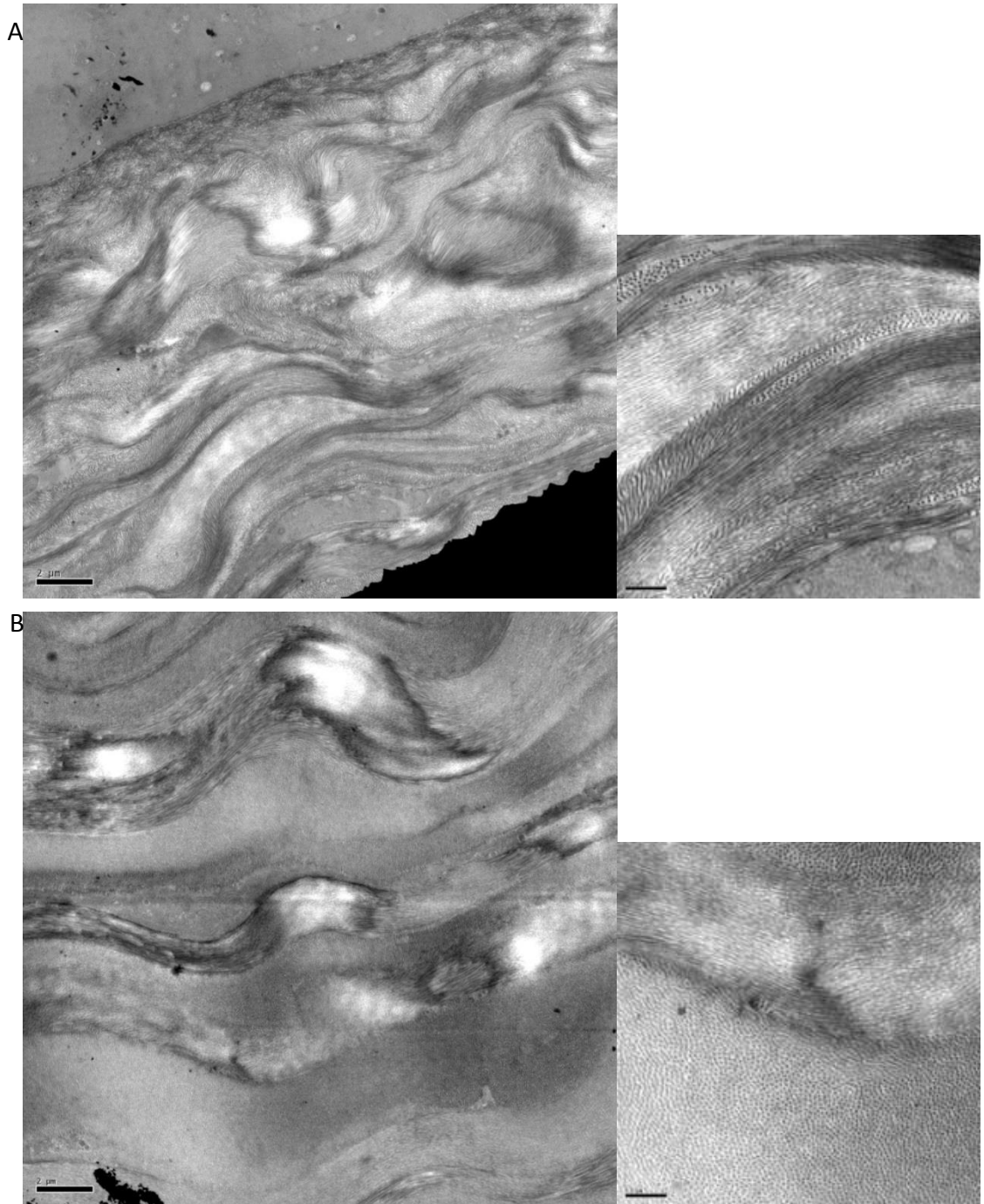


Figure 23: TEM micrograph representation of the differences between anterior and posterior lamella interweaving within the porcine corneal stroma. The lamellae of the anterior stroma (A) interweave more readily than the lamellae of the posterior stroma (B). In addition, anterior collagen lamellae (insert A) tend to be thinner than the posterior lamellae (insert B), $1.8\mu\text{m} \pm 1.3$ and $3.1\mu\text{m} \pm 2.2$, respectively, $p=0.49$. A scale bar = $2\mu\text{m}$; A insert scale bar = $0.5\mu\text{m}$; B scale bar = $2\mu\text{m}$; B insert scale bar = $0.5\mu\text{m}$.

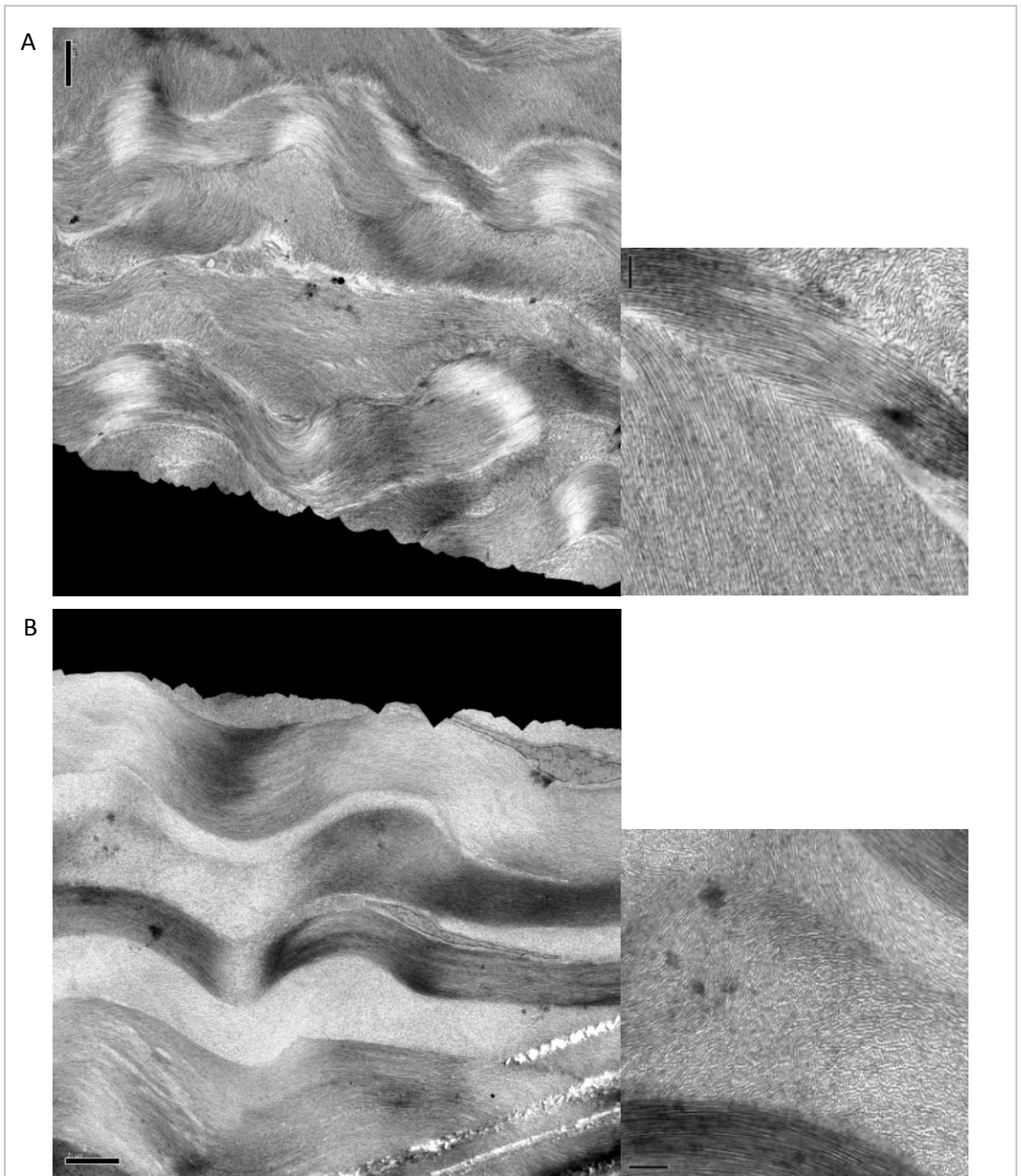


Figure 24: TEM micrograph representation of the differences between anterior and posterior lamella interweaving within the rabbit corneal stroma. The lamellae of the anterior stroma (A) interweave more readily than the lamellae of the posterior stroma (B). In addition, anterior collagen lamellae (insert A) tend to be thinner than the posterior lamellae (insert B), $3.3\mu\text{m} \pm 2.0$ vs. $4.3\mu\text{m} \pm 3.6$, respectively, $p=0.71$. A scale bar = $2\mu\text{m}$; A insert scale bar = $0.5\mu\text{m}$; B scale bar = $2\mu\text{m}$; insert B scale bar = $0.5\mu\text{m}$.

3.5 DISCUSSION

3.5.1 Three-Dimensional Architecture of the Corneal Stroma

3.5.1.1 Fibril Organisation

Upon Initial inspection the collagen fibrils from porcine and rabbit tissues were observed to have a regular and uniform arrangement (Figures 16, 17, 19 & 20) with porcine collagen fibril diameter and spacing measured to be $29.5\text{nm} \pm 4.5$ and $34.1\text{nm} \pm 12.5$, respectively, and rabbit collagen fibril diameter and spacing measures $29.1\text{nm} \pm 5.4$ and $33.5\text{nm} \pm 11.0$ respectively (Figure 18; Appendix A(iii)). These figures demonstrate the small and tightly compacted nature of the corneal stromal collagen fibrils and the mechanisms that allow for the uniform nature of the collagen fibrils are most likely due to heterogeneous collagen type I and V collagen fibrils as well as KS and CS/DS proteoglycans (Robert et al., Birk, 2001, Meek and Fullwood, 2001).

However from the micrographs taken, it was often difficult to distinguish a fully crystalline organisation of collagen fibrils and little crystallinity was observed between secondary and tertiary adjacent collagen fibrils. The lack of regularity can be observed in Figures 16 & 17, whereby the hexagonal arrangement around a central fibril is elongated (arrows). Additionally, the standard deviations from the mean values for porcine and rabbit tissues, $\pm 12.5\text{nm}$ and ± 11.0 , respectively, indicates 95% of the collagen fibrils can be spaced between 9.1nm and 59.1nm within porcine tissues and 11.5nm and 55.5nm for rabbit corneal tissues, along with the minimum and maximum values for the collagen spacing of porcine collagen fibrils, 7.5nm and 8.4nm , respectively, and rabbit collagen fibrils, 17.5nm and 65.5nm , respectively (Appendix A(iii) and A(v)), reveals that there is a great deal of variation in the spacing of the fibrils.

The lack of overall crystallinity between collagen fibrils is most likely a result of a fluid system within the stroma. Knupp, (2009) investigated the relationships of the proteoglycans (PGs) on the collagen architecture. They proposed that stromal PGs hold the collagen fibrils in a dynamic system whereby PGs continually form bridges that break and reform, generating repulsive and attractive forces between adjacent collagen fibrils. This theory also explains how there is a lack of crystalline order between secondary adjacent fibrils, and the high degree of spacing variability between adjacent collagen fibrils.

When considering the lack of crystallinity in terms of stromal transparency, porcine and rabbit stromal collagens express the quasi-crystalline – quasi-random collagen fibril arrangement hypothesized by Cox (1970). This is where the collagen fibrils have a crystalline arrangement over short distances, i.e. adjacent collagen fibrils, but over greater distances, i.e. non-adjacent collagen fibrils, the collagen fibrils do not demonstrate a crystalline lattice. Therefore, the sum of the diameter and spacing of two adjacent collagen fibrils i.e. 64.6nm and 62.6nm for porcine and rabbit corneal tissues, respectively, is less than half the wavelength of visible light (200nm). This allows light waves to pass over the fibrils without interruption and this short-range ordering is sufficient to negate the need for a crystalline lattice throughout the tissues.

3.5.1.2 *Lamella Organisation*

Visualising the corneal stroma using the TEM set to lower magnifications enabled the imaging of the stromal lamellar structure and the expected stacked orthogonal arrangement rabbit tissues (Figure 19 & 20). The mechanisms governing fibril orientation are poorly understood, though some work has been carried out using optical coherence tomography and x-ray diffraction of corneal stromal tissue (Hayes et al., 2007). These techniques are useful in looking at the orientation of collagen fibrils across the whole cornea and demonstrated that the preferential orientation of porcine and rabbit collagen fibrils within the central corneal stroma is along the axes of the four orbital tendons. However, these studies found that the lamella orientation of both species are not strictly orthogonal; which is also something that we observed, since a number of obliquely sectioned fibrils and weaving lamella bundles were observed (Figure 21a and 22a), additionally, the lamellae were observed to converge/diverge at various points through the stroma (Figure 21b & 22b). This interweaving and merging of the collagen fibrils were seen in all three planes of movement, i.e. the x, y and z axes, as observed by the fibril orientation changes within adjacent lamellae, meaning the collagen lamella orientation changes are a three dimensional feature.

Looking at the difference in thickness between anterior and posterior stromal lamellae, there was no significant difference, however, there was a trend to suggest that posterior lamellae are thicker than anterior lamellae, which has previously been demonstrated within human corneal tissues (Meek and Boote, 2009, Radner et al., 1998). The mechanisms that govern anterior and posterior stromal lamella thickness may be due to the corneal stroma development. During development, a primary ECM structure is laid

down and then expanded and infiltrated by primary keratocytes. Next, the collagen ECM is remodelled and compacted into the mature transparent ECM (Ruberti and Zieske, 2008). As the stroma develops the amount of primary stromal tissue laid down before the tissue is expanded ready for keratocyte infiltration decreases, hence the lamella thickness decreases from posterior to anterior

Recently, there has been a controversial suggestion of a pseudo-layer at the posterior of the corneal stromal extra cellular matrix, where the stroma meets the Descemet's membrane, known as the Dua's Layer (Dua et al., 2013). This is a layer of acellular collagen lamellae approximately 6-15 μ m thick that originates from the trabecular meshwork and spans the entire of the posterior cornea (Dua et al., 2014). It is theorised that this layer is important for deep anterior lamella keratoplasty (DASK), where an opaque corneal stroma is excised and replaced with donor tissue leaving the host endothelium and Descemet's membrane in-tact. During DASK excision, air is injected into the stroma, known as the big-bubble technique, and it is proposed that the point of separation of the excised tissue and the remaining tissue is where the Dua's Layer meets the stroma proper. Our results cannot confirm or denounce this layer, since no separation of the tissue was observed in the vicinity of the Descemet's membrane. Therefore, perhaps, in order to accentuate the presence of this layer the big-bubble technique may need to be employed during TEM preparation. In addition to this, the sections for this study were taken from a vertical slice through the central portion of the cornea, rather than the width of the posterior cornea. However, recently another study investigating the Dua's layer has discredited this layer as they demonstrated the distance between the Descemet's membrane and stromal keratocytes is highly variable and host keratocytes

remained posterior to the big-bubble separation point after excision of the tissue (Schlötzer-Schrehardt et al., 2014).

3.5.2 Comparability of the Architecture of Porcine, Rabbit and Human Corneal Stromal Extracellular Matrices

Porcine corneal tissue has been proposed as a suitable alternative for human corneal xenografting, even though its comparability to human tissue has yet to be established. However, by comparing the architecture of porcine corneal stroma tissue against the well published architecture of rabbit corneal stromal tissues, which has already been compared with human corneal stromal tissues (Komai and Ushiki, 1991), an indirect comparison with published human tissue data can be made.

Within the published literature, rabbit and human corneal stromal tissues are comparable in terms of their individual collagen fibril arrangement and the orthogonal lamella arrangement; however, the main difference of note was the level of lamellae interweaving between the two species, with human tissue being much more interwoven than that of rabbit tissue and the level of interweaving increases in the anterior one third of the tissue (Meek and Boote, 2004, Radner and Mallinger, 2002, Hirsch et al., 2001, Beuerman and Pedroza, 1996, Komai and Ushiki, 1991).

A direct comparison of fibril diameter and spacing between porcine and rabbit corneal stromal tissues shows no significant difference, $p=0.44$ and $p=0.66$, respectively. When compared against human corneal stromal tissues, with a mean diameter and spacing

28.4nm \pm 5.8 and 45.0 \pm 4.6 (n=4), respectively (Akhtar, 2012), the porcine and human collagen fibrils diameter and spacing is not significantly different, $p=0.82$ and $p=0.27$, respectively. Hence, the fibril results presented here demonstrate that the porcine fibril arrangement is comparable with that of human tissue, and the collagen fibril organisation is comparable across all three species.

When comparing the lamellae architecture of porcine and rabbit corneal stromal tissues, the architecture of both the porcine and rabbit tissues were generally observed to have an orthogonal arrangement, though a number of lamellae from both species did not strictly conform to this arrangement, furthermore the lamellae were observed to interweave and interlace in a three-dimensional manner. Additionally the posterior lamellae tend to be thicker than anterior lamellae in both species, porcine tissue anterior lamellae were approximately 1.8 μ m and posterior lamellae were approximately 3.1 μ m, while rabbit anterior and posterior lamellae were 3.3 μ m and 4.3 μ m respectively. This may make the porcine a more suitable model than the rabbit model, since previous comparisons (Komai & Ushiki, 1991) of rabbit and human tissue have shown that the rabbit stroma interweaves less than human tissue. The level of interweaving and merging of bundles appears to be greater in the anterior stroma than the posterior stroma within both species; although the porcine lamellae interweave more readily than the rabbit lamellae, which also appeared to be the case when human and rabbit tissue were compared, (Komai & Ushiki, 1991).

3.5.3 Ethical Issues Surrounding Xenografting

The results presented herein demonstrate the potential of porcine tissue to act as a xenograft replacement for human cadver corneal transplantation; however, raising animals for the purposes of medical treatments throws up a number of ethical and moral issues that must be considered to ensure any future work into the development of a porcine derived artificial corneal replacement is conducted in an ethically approved manner. Such ethical and moral issues include:

- Animal welfare, including the treatment of the animal during its life-cycle and slaughter
- Cultural issues, i.e. the use of porcine tissue and the prohibition of its consumption by Islamic and Hebrew cultures
- And, the psychological impact of the recipient receiving the xenograft

Animal Welfare

Within the United Kingdom and European Community there have been a number of legislative guidelines have been created to ensure the welfare of any animal, whether it is a domestic pet, farmed animal or animal raised for medical research, (Home Office, 2013; DEFRA, 2006). The Animal Welfare Act legislates that animals are provided with a suitable environment, nourishment and care during their lifetime and at the end of their lifetime they are euthanized without causing undue stress or pain to the animal and covers domestic and farm animals. While the Animals (Scientific Procedures) Act legislates the same for animals raised for medical research, but more importantly, it ensures that

research conducted upon animals is only carried out where no other suitable *in-vitro* model is available.

In the context of the work carried out within this chapter and in the subsequent chapters, the corneal tissue has been acquired from licensed sources, i.e. Northwick Park Institute for Medical Research, Harrow, and Cherryfields, Croydon (*see section 4.3.1*). These licenses ensure that all legislative guidelines have been met and the welfare of the animals has been considered.

Cultural & Psychological Issues of Xenografts

In many Western cultures pork is a common foodstuff, however, in other cultures, such as Islamic and Hebrew communities, pork is prohibited as pigs are considered to be a “dirty” animal. Additionally, studies on attitudes towards xenograft transplantation have shown that 7% of individuals are against implantation of xenograft tissues (Schlitt et al., 1999) and there is a preference for allograft material over xenograft material (Rubaltelli et al., 2009). Hence, a porcine derived artificial corneal replacement would not be ethically suitable for all faiths and all individuals. Therefore, informed choice should always be obtained before using such grafts, were they to be made clinically available

3.6 CONCLUSIONS

Using transmission electron microscopy to image the ultrastructure of the porcine corneal stroma has elucidated upon the three-dimensional organisation of the porcine corneal

stromal extra cellular matrix and how the ECM relates to the transparency of the tissue. Porcine stromal collagens exhibit a quasi-crystalline arrangement that maintains adjacent collagen fibrils at less than half the wavelength of light, which enables the tissue to be transparent; however, the collagen fibrils are not strictly crystalline owing to the fluidic nature of the tissue. Additionally the collagen fibrils are grouped together into lamella sheets that are generally stacked into orthogonal arrays; though the lamellae will interlace and interweave in a three-dimensional fashion, especially within the anterior stroma, in order to provide structural integrity to the tissue.

By comparing porcine and rabbit corneal stromal tissues, an indirect comparison of porcine and human corneal tissues could be made. This was possible due to previously published data comparing rabbit and human tissues and from the comparison made within this chapter it was concluded that porcine corneal tissue is comparable with human tissue; though further work is required in order to establish whether the controversial Dua's Layer is present within porcine corneal tissues. It is suggested that, due to the greater extent of interweaving seen in the anterior stroma of the porcine tissue, the porcine corneal structure is a closer match to the human structure than rabbit tissue.

These results are useful for informing the development of an artificial corneal replacement since any artificial corneal replacement will need to have thin fibrils that allow light waves to pass by without becoming disrupted, while the lamella architecture could enable for structural integrity. In addition, porcine tissues would make for a suitable xenograft alternative to cadaver corneal tissue and the development of an artificial corneal replacement. Hence further work will be aimed at the development of an *in-vitro*

produced artificial corneal replacement with thin fibrils, in order to improve their transparency, as well as the use of porcine tissue as an artificial corneal replacement.

CHAPTER 4: Effects of Swelling and Dehydration on Decellularised Porcine Stromal Collagen Architecture for Humanising Corneal Xenografts

4.1 INTRODUCTION

The cornea is the transparent tissue at the anterior of the eye which allows light into the eye for sight; however in states of disease or injury it will lose transparency, become opaque and impair vision with treatment often requiring a corneal transplant. Within the UK, corneal donor supply only just matches its demand (NHS Blood and Transplant, 2014) and throughout the world the demand for donor tissue often out-strips its supply, particularly in Asia (Lee et al., 2014). In order to reduce the reliance on human cadaver corneal tissue, and give clinicians an additional option to treat corneal blindness, corneal tissues that have been harvested from animal sources, such as pigs, may provide a ready-made and off-the-shelf functional scaffold that can be called upon to use whenever necessary. Additionally, utilising tissue-engineering protocols there is the potential to “humanise” the corneal xenograft by introducing human corneal cells into the animal tissue.

4.1.1 Corneal Xenotransplantation

In order to give a corneal xenograft the best chance of being accepted by the graft recipient careful consideration of the donor species needs to be made in terms of tissue compatibility and tissue transparency, and in addition the donated corneal tissue needs to be obtained from ethically approved sources.

Studies of mammalian stromal tissues have shown that the corneal stromal extra cellular matrices from different species are very similar in terms of their composition, architecture and mechanisms of transparency (Hayes et al., 2007, Scott and Bosworth, 1990). Comparisons made in the previous chapter demonstrate the potential for porcine tissue to provide a xenograft alternative for corneal transplantations and are supported by the literature (Radner and Mallinger, 2002, Zeng et al., 2001, Radner et al., 1998, Komai and Ushiki, 1991). Additionally, clinical evidence has shown the comparability of porcine tissue to human tissue and there are a wide variety of commercially available porcine xenograft products. Such products include, dermal tissue, urinary bladders, small intestines and heart valves for various clinical applications (Crapo, 2011; Gilbert, 2006). Furthermore, pork is a common food-stuff and as such deemed ethically acceptable to be utilised for xenografting. Hence, using donor corneal material from porcine xenograft sources may provide a very suitable replacement for human corneal tissue for transplantation.

When researching porcine corneal xenotransplantation an important study to consider is that corneal xenotransplants from porcine to cynomolgus monkeys have been shown to elicit an immune reaction (Zhiqiang et al., 2007, Amano et al., 2003). This immune reaction was directed towards the cellular components of the foreign tissue, thus, at

present, porcine xenografts are not suitable for direct corneal transplantation into humans. Conversely, a decellularised porcine xenograft, which has been infiltrated with human corneal cells may be a valid alternative.

4.1.2 Porcine to Human Corneal Xenograft Immunogenicity

The cornea is often described as an immunologically privileged site due to the avascular nature of the tissue; however, the immunological reaction of cynomolgus monkeys to porcine corneal xenograft transplantations was the result of immunological cell infiltration into the corneal lamellar grafts (Amano et al., 2003), while penetrating keratoplasty results in a complete rejection episode directed against the endothelial layer (Zhiqiang et al., 2007). Hence the immune privilege nature of the cornea is not an absolute and does not guarantee graft success.

The mechanisms that result in an immune reaction within corneal lamella-grafts are poorly understood, though it is hypothesised that lymphatic drainage of the aqueous humour and a small number of immature Langerhans cells play a part within the process (Pleyer and Schlickeiser, 2009). Yet, from studies of other porcine xenografts, the major molecular structure that invokes an immunogenic response within humans is known to be a cell surface glycoconjugate, Gal α 1-3Gal β 1-4GlcNAc-R, and specifically, it is the α -Gal epitope on the galactose molecule. Humans (and higher apes) cannot naturally synthesise α -Gal as a result of an evolutionary mutation to the α 1,3-galactosyltransferase encoding gene, which rendered the gene useless, meaning higher apes and humans cannot synthesise the α 1,3-galactosyltransferase enzyme, and consequently cannot produce α -

Gal. With α -Gal being absent from their own cell surface make-up, humans recognise α -Gal expressing cells as non-self and consequently α -Gal epitopes are immunogenic to the human immune system (Cooper, 2003, Tanemura et al., 2000, Stults et al., 1999).

Therefore, any porcine corneal xenografts expressing α -Gal epitopes could be recognised by a human recipient as foreign and elicit an immune response, which would be detrimental to the tissue transparency as demonstrated by Zhiqiang (2007). Hence, all immunogenic material from a xenograft will need to be removed in order to prevent an immunological response being invoked.

4.1.3 Porcine Corneal Decellularisation

Gal α 1-3Gal β 1-4GlcNAc-R glycoconjugates are expressed on the surface of porcine stromal keratocytes within the cornea (Amano et al., 2003). Therefore, if all the cellular material was removed from the tissue, there is the potential to negate an immunological response; and currently decellularisation of porcine heart-valves, dermal tissue and ligaments has been successfully reported (Sasaki et al., 2009). Once the stromal extra cellular matrix is devoid of cellular material, it may be used as a biomaterial scaffold that may be seeded with human corneal fibroblasts in order to humanise the tissue.

The most logical technique for the removal of α -Gal is to decellularise the tissue and ensure complete removal of cell membranes. Successful techniques to decellularise porcine corneal tissues are of great interest to scientists in order to provide corneal

xenograft material; however, treatments to decellularise corneal xenograft material must preserve tissue transparency, whilst completely removing any immunogenic material.

The most common ways to remove keratocytes from the corneal stroma involve lysing the cells with various different treatments, or combinations of treatments, and then thoroughly washing the tissue to remove the cellular debris. However, decellularising corneal tissue is not selective, so the anterior and posterior stromal surfaces will have their epithelial and endothelial cells stripped away, respectively (if not already done so by scraping the cells off prior to treatment (Shao et al., 2010, Oh et al., 2009a, Oh et al., 2009b, Oh et al., 2009c)). Below is a selected list of treatments reported in the literature (Lee et al., 2014, Lynch and Ahearne, 2013, Fu et al., 2010, Hashimoto et al., 2010, Oh et al., 2009a, Oh et al., 2009b, Oh et al., 2009c):

- Detergents, e.g. triton-X100 or sodium-dodecyl-sulphate (SDS)
- Hypertonic solutions, e.g. hypertonic saline or hyper-osmolar glycerol
- Hydrostatic pressure – pressurised solutions
- Enzymatic degradation e.g. DNase/RNase or trypsin/dispase
- Freeze-thawing

These studies have identified some of the least and most effective ways of decellularising porcine corneal tissue as revealed by optical observations and transmission electron-microscopy (Oh et al., 2009c). Enzymatic treatments resulted in a complete loss of corneal transparency due to severe disruption of the stromal extra cellular matrix with the collagen fibrils being severely fragmented. Treatments using freeze thawing and hypertonic solutions were not detrimental to the collagenous architecture, however they did not completely remove the cells and cellular debris remained within the stroma. The

most successful techniques for decellularising porcine corneal tissues were those that used detergents and hydrostatic pressure to firstly lyse the cells and then thoroughly rinsed to completely remove the keratocyte cellular material from the stroma without being visibly detrimental to tissue transparency (Hashimoto et al., 2010, Fu et al., 2010).

4.1.4 Potential for an Improved Corneal Xenograft

Once porcine corneas have been decellularised, they can potentially be used as an acellular corneal xenograft available for immediate engrafted. Acellular porcine corneal lamella grafts have been engrafted into rabbits, with survival rates of at least 3 months for triton-X100 decellularised corneas (Luo et al., 2013, Fu et al., 2010) and at least one-year for corneas decellularised with SDS (Zhou et al., 2011). The use of acellular porcine corneal tissue may provide an easily accessible stromal replacement for human use; however, there is potential to provide an improved corneal replacement that has been humanised by incorporating human cells into the acellular matrix. Moreover, keratocytes may be harvested from the recipient and infiltrated into the acellular stromal scaffold *in-vitro*; thus, the corneal xenograft could be considered as an autograft analogue and a more enhanced corneal graft in comparison with an acellular graft.

Reintroducing cellular material into the decellularised corneal tissue may not be a simple undertaking since the tightly packed, orthogonal arrangement of the stromal tissue may not allow the free movement of cells between the collagen fibrils and lamellae. Some studies have injected rabbit corneal fibroblasts directly into decellularised porcine corneal tissue and subsequently engrafted the construct into a rabbit recipient, demonstrating

graft survival rates of more than 24-weeks (Yoeruek et al., 2012, Pang et al., 2010). However, these studies randomly injected cells into the decellularised tissue without considering their location and cell numbers, since there is potential to over-saturate the tissue with cells that could result in apoptosis and even scar tissue formation.

An alternative method, that could better limit the number of cells within the decellularised corneal tissue, would be to look at the corneal foetal development (Ruberti and Zieske, 2008). During foetal development, an immature primary stromal matrix consisting of collagen types I, II & IX is laid down by corneal epithelial cells (Fitch et al., 1994, Chen et al., 1993, Linsenmayer et al., 1990, Hayashi et al., 1988). This extra cellular matrix is tightly compacted by the collagen type IX, until corneal endothelial pre-cursor cells begin to secrete a collagenase enzyme (matrix-metallo-protease 2, MMP-2) that degrades collagen type IX (Ruberti and Zieske, 2008, Huh et al., 2007, Fitch et al. 1998). Once this occurs, the primary stromal matrix swells and allows a controlled infiltration of neural crest-derived mesenchymal cells (stromal fibroblast precursors) into the matrix. Once these cells have infiltrated the matrix, they secrete mature stromal extracellular matrix components, collagen types I, V & VI and KSPG and CS/DSPGs (Ruberti and Zieske, 2008, Linsenmayer et al., 1998, Gordon et al., 1996, Funderburgh et al., 1986, Bard and Higginson, 1977). With the secretion of these components, together with the maturation of the corneal endothelium hydration control mechanisms, the corneal stroma compacts to become the transparent window that allows for vision.

Corneal fibroblast cells have been shown to naturally infiltrate into an acellular matrix through a phenomenon known as contact guidance, whereby fibroblasts migrate along an axis of greatest tension (Friedrichs et al., 2007, Cisneros et al., 2006), i.e. they will migrate

along collagen fibres. Thus the natural infiltration of cells into a decellularised cornea may be possible. However, mimicking corneal foetal development and encapsulating corneal stromal fibroblasts by swelling and re-compacting the tissue *in-vitro* will require some consideration since the lack of endothelial control means the stroma will naturally imbibe water and swell when it is placed into a solution that has an osmolarity greater than the aqueous humour (Zhang et al., 2006). Additionally, the effect of swelling the corneal tissue on the fine collagenous extra cellular matrix architecture and tissue transparency will require studying.

4.2 EXPERIMENTAL DESIGN

4.2.1 Objectives

With the advancing knowledge of cell culture and tissue engineering there is the opportunity to humanise acellular porcine stromal tissue by re-introducing human cells into the matrix. In order to achieve this, it is intended to mimic the corneal foetal development by swelling decellularised porcine corneal tissue and then dehydrating the ECM once cells have been introduced.

In order to determine the effects of both the decellularisation and re-compacting processes on the stromal extra cellular matrices and tissue transparency, the tissues will need to be modelled using transmission electron microscopy and the techniques described within the previous chapter. Cultured primary human corneal fibroblasts will be

incubated with the decellularised tissue and allowed to infiltrate into the tissue *in-vitro* and the infiltration of the cells into the matrix visualised *in-situ*.

4.2.2 Sourcing Porcine Corneal Tissue

Porcine tissue is currently used as xenograft material for heart valve and dermal grafts (Sasaki et al., 2009), and it is also a common foodstuff, hence porcine tissue may be suitable for use as a potential corneal xenograft. For this investigation porcine corneal tissue was sourced from abattoirs and meat processing factories.

4.2.3 Porcine Corneal Tissue Decellularisation and Swelling

Careful consideration of the decellularisation process needed to be taken in order to preserve the highly organised stromal extra cellular matrix and retain tissue transparency as well as potentially removing all immunogenic antigens, for these reasons Triton X100 was selected since it has shown great potential for removing porcine cellular material while maintaining tissue transparency (Luo et al., 2013, Fu et al., 2010).

In order to allow for cells to re-infiltrate into the decellularised extra cellular matrix the stromal tissue needed to be swollen. This step was carried out in conjunction with the decellularising process, since swelling the tissue should also aid the diffusion of cellular debris out of the tissue. Swelling was achieved by placing the stromal tissue into a solution with greater osmolarity than the aqueous humour, thus causing the fibril spacings to increase (Zhang et al., 2006, Doughty, 2000) and allow for the maximal

removal of porcine cellular materials. To achieve this, the corneas were incubated for a number of days in decellularising triton X-100 solution in a hypo-osmolar solution, such as phosphate buffered saline (PBS). Additionally, the epithelial and endothelial layers were removed prior to exposure to the triton X-100 in order to overcome the hydration control mechanisms.

4.2.4 Stromal Cellular Infiltration and Dehydration

Once the stromal tissue had been decellularised and swollen human corneal fibroblasts were incubated with the tissue in order to re-populate the extra-cellular matrix scaffold with human cells. However, it was expected that the tissue would lose transparency, due to the oedema; hence the tissue would be required to be dehydrated in order to restore transparency.

Eye banking protocols routinely swell and dehydrate corneal tissue to re-establish size and transparency when preparing corneal tissue for transplantation. During organ culture the cornea is kept in hypo-osmolar organ culture solutions, where it naturally swells and opacifies. Then, prior to engraftment the corneas are placed into a dehydrating dextran solution, which re-establishes normal size and transparency to the corneal tissue (Armitage, 2011, Pels and Schuchard, 1983). Therefore, for this study, a 5% dextran (v/v) solution was used to dehydrate the processed cornea, and the collagenous extra cellular matrix assessed for transparency.

4.2.5 Hypotheses

The following statistical hypotheses were created in order to prove the study objectives:

1. Swelling of the porcine corneal tissue during decellularisation in a hypo-osmolar solution will result in a significant increase to collagen fibril spacing
2. Dehydration of the collagenous extra cellular matrix will result in;
 - i. a significant reduction in collagen fibril spacing.
 - ii. no significant difference to the fibril spacing when compared with normal corneal tissue
3. No change will be observed to the diameter of the collagen fibrils during any stage of the process

Additionally, the following qualitative assessments will be made:

1. The ability of the cell lysing detergent triton X-100 to decellularise corneal tissue
2. The ability of dextran to dehydrate the swollen, decellularised corneal tissues and re-establish corneal transparency
3. The arrangement of the collagen lamellae in terms of interweaving and orthogonal arrangement after swelling and re-compacting the tissue
4. The organisation of the collagen fibrils in terms of uniformity and hexagonal arrangement after swelling and re-compacting the tissue
5. The ability of cells to re-infiltrate the acellular extra cellular matrix

4.3 EXPERIMENTAL PROCEDURE

4.3.1 Materials

4.3.1.1 Corneal Dissection

Freshly excised whole porcine eyes, 23 in total, were purchased from a local meat processing factory (Cherryfields, Croydon, UK). The corneal tissue was then dissected from the eye globe using the same materials as listed in the previous chapter, *see section 3.3.1.1*.

4.3.1.2 Corneal Decellularisation, Swelling & Dehydration

Once the porcine corneal tissues had been dissected from the eye globe, they were decellularised, swollen and dextran dehydrated using the following materials:

Materials	Source
Sterile disposable scalpels size 22A	Thermo Fisher Scientific UK, UK
Phosphate buffered saline (PBS) tablets – 1 tablet makes 100ml PBS, pH7.4	Thermo Fisher Scientific UK, UK
Sterile 30ml Universal Tubes	Gibco, Invitrogen Life Technologies Ltd. Paisley, UK
1% triton X-100 in PBS (v/v)	Prepared in laboratory by diluting triton X-100 (Sigma-Aldrich, UK) in PBS
Rotary table	Available in laboratory
5% Dextran in PBS (v/v)	Prepared in laboratory by diluting High Molecular Weight Dextran (Sigma-Aldrich) in PBS

4.3.1.3 Histology

The following materials were used to histologically assess the decellularised porcine corneal tissues:

Materials	Source
Optimum cutting compound (OCT)	Leica Microsystems, UK
Liquid Nitrogen	BOC Group PLC. UK
Leica CM1510S cryostat microtome	Leica Microsystems, UK
Haematoxylin	Sigma-Aldrich, UK
Eosin	Sigma-Aldrich, UK
Glass slides	Fisher-Scientific, UK
Motic AE31 inverted light microscope Moticam 2000, 2.0M pixel USB digital camera and Motic Image Plus imaging software	Available in laboratory

4.3.1.4 Transmission Electron Microscopy

The materials used to fix, embed, section, contrast stain and image the decellularised porcine corneal tissue were the same as those used in the previous chapter; *see section 3.3.1.2.*

4.3.1.5 *Tissue Culture*

Primary human corneal fibroblasts harvested from the limbal region of the stroma, designated limbal ring fibroblasts, LRF207 cells, were cultured during cellular infiltration into the decellularised corneal tissue, *in-vitro* using the same equipment as previously described *see section 2.1.1*.

4.3.2 Methods

4.3.2.1 *Corneal Dissection, Decellularisation and Swelling*

Whole porcine eyes, 23 in total, were received from the local meat processing factory, (Cherry Fields, Croydon, UK) and were transported to the laboratory. Upon arrival, the corneas were dissected as previously described, *see Section 3.3.2.1*, and then split into the following three groups:

Group 1 – Triton X100 decellularised, and PBS swollen cornea group

Ten corneas had their anterior and posterior surfaces scraped with a scalpel blade to remove the epithelial and endothelial layers, respectively, and rinsed in PBS. After which they were placed in a decellularising solution containing 1% triton X-100 in phosphate buffered saline (PBS).

Group 2 – PBS swollen cornea group

Ten corneas had their anterior and posterior surfaces scraped with a scalpel blade to remove the epithelial and endothelial layers, respectively, and rinsed in PBS. After which they were placed into fresh PBS.

Group 3 – Normal cornea control group

Three corneas were rinsed in PBS to act as normal control corneas for qualitative transparency and histological analysis. In order to prevent swelling, these corneas had their transparency assessed immediately after excision by the ability to see text through the corneas and were then processed for histology as per the protocol described below.

Corneas from groups 1 and 2 were then left for 48 hours at ambient temperature on a rotary table. After 48 hours the treated stromal tissues were thoroughly rinsed in PBS, with each cornea given three rinses and at least 30 minutes per rinse. The transparency of each corneal sample was then assessed qualitatively by the ability to read text through the cornea.

4.3.2.2 Histology of Decellularised Porcine Corneal Tissues

The effectiveness of the decellularising process was assessed by histological analysis. For this analysis three whole corneas from groups 1, 2 and 3 were embedded in optimum cutting temperature compound (OCT) and frozen in liquid nitrogen and then stored at -

80°C. Each OCT embedded cornea was then sectioned into 10µm tissue sections using a Leica CM1510S cryostat microtome set to -24°C. Sections were collected onto glass slides and allowed to warm up to ambient temperature. Excess OCT was gently washed away from the tissue sections using distilled water and the sections were stained with haematoxylin and eosin (H&E stain) then visualised using a Motic AE31 inverted light microscope with attached Moticom 2000, 2.0M pixel USB digital camera and Motic Image Plus imaging software.

4.3.2.3 Corneal Dehydration

The ability of dextran to dehydrate the corneal tissue and re-establish transparency was qualitatively assessed using four corneas from groups 1 and 2 in the following way. Three corneas from groups 1 and 2 were cut into two halves; one half of each cornea was placed into a dehydrating solution of 5% dextran in PBS and the other half placed into a PBS solution as a control. The corneas were then incubated for 24 hours at ambient temperature, after which their transparency was qualitatively assessed by the ability to see text through the corneas. Subsequently these corneas were processed for TEM as described below.

The fourth swollen cornea from each group was left whole and had their transparencies qualitatively analysed in the manner described, then placed in the dextran solution for 24 hours and had their transparencies re-analysed in order to demonstrate whether dextran was able to restore transparency to the whole cornea.

4.3.2.4 *Transmission Electron Microscopy of Dextran-Treated, Decellularised Porcine Stromal Tissue*

The collagenous architecture of the decellularised porcine stromal tissue was assessed by imaging the tissue using TEM. For this analysis the half corneas that had been immersed in 5% dextran in PBS as well as the half corneas not immersed in dextran were processed for TEM as previously described in section 3.3.2.

Briefly; each corneal half was dissected into ~2mm cubes and placed into a fixative solution consisting of 2.5% glutaraldehyde (v/v) + 2% formaldehyde (v/v) in 0.1M phosphate buffer (pH 7.4) for 2 hours at ambient temperature and then overnight at 4°C. The cubes were rinsed in 0.1M phosphate buffer then post-fixed in osmium tetroxide for four hours and then thoroughly rinsed in distilled water twice. Subsequently the tissue cubes were dehydrated in a graded series of alcohols, (10%, 20%, 30%, 50%, 75%, 90%, and 2x100%) and then placed in propylene oxide followed by 50:50 propylene oxide and low viscosity resin mixture and left over-night to allow the resin to impregnate into the tissue. The following day the tissue cubes were placed into Beem capsules containing 100% resin, mixed to a medium-hard hardness, and cured at 70°C over-night. After polymerisation, 100nm ultra-thin sections were cut using an RMC Power-Tome PC ultra-microtome with a Diatome 35° diamond knife and collected onto 200-mesh copper grids and allowed to dry overnight. Tissue sections were contrast stained with 1% (w/v) uranyl acetate for 1 hour and saturated lead citrate for 15 minutes, with distilled water rinses after each stain was applied. Finally the tissues were imaged using a Jeol 2100F FEG TEM with a Gatan Orius camera and micrograph analysis was carried out using Gatan Digital Micrograph.

Micrographs were taken through the full depth of the corneal stroma from each cornea and a qualitative morphological analysis of the collagenous architecture was made, in terms of the fibril architecture and lamella arrangement. Additionally measurements of the diameter and spacing of the stromal collagen fibrils were made on collagen fibrils cut in cross-section. The fibril diameter was measured at the thinnest point through the cross-sectioned fibrils while the spacing between adjacent fibrils was determined by measuring the central points between two fibrils and subtracting the radii of the fibrils. In order to compare the data collected herein with that of normal porcine corneal tissue, the data presented in the previous chapter for the porcine corneal stroma will be used as a control.

Statistical analyses were carried out using a two-way analysis of variance (ANOVA) where more than two data sets were compared or a two-way Student's T-test where only two data sets were compared – the specific test used is stated within the results section; data was considered to be statistically significant where $p \leq 0.05$. Confidence interval plots for all ANOVA tests can be observed within *Appendix B*.

4.3.2.5 *Infiltration of Primary Human Corneal Fibroblasts into Decellularised Porcine Stromal Tissue*

In order to assess the infiltration of primary corneal fibroblasts into the decellularised stromal extra cellular matrix, the remaining three corneas from groups 1 and 2 were incubated with limbal ring fibroblasts, LRF207 cells, using the following protocol. After decellularising treatments, the swollen corneal stromal ECMs were sterilised by

immersion in DMEM + 10% FCS dosed with 5x concentrated penicillin (500units/ml), streptomycin (0.5mg/ml) and fungizone (12.5µg/ml) antimicrobial agents for 30 minutes at 37°C in a 5% CO₂ atmosphere. After this time the treated matrices were placed into six-well tissue culture plates and a suspension of 1x10⁵ cells/ml LRF207 cells was introduced into each well. The tissue culture medium was exchanged for fresh medium every 2-3 days, as per the routine tissue culture protocols described in chapter 2 (*see section 2.2.1*), and the cells were allowed to infiltrate the tissue over the following 14-days. At 7 and 14 days the cellular infiltration into the corneal tissue was monitored *in-situ* and imaged using a Motic AE31 inverted light microscope with attached Moticom 2000, 2.0M pixel USB digital camera and Motic Image Plus imaging software.

4.4 RESULTS

4.4.1 Corneal Decellularisation and Swelling

Representative images of the transparency of the corneas treated with decellularising solution and dextran can be seen in Figure 25. Immediately after the corneal tissue had been excised the tissue was transparent and the text can clearly be seen through the tissue (Figure 25c). The porcine corneal stromal tissues decellularised and swollen in 1% triton X-100 in phosphate buffered saline and swollen in PBS can be seen in Figures 25a and 25b, respectively. Tissues Decellularised and swollen using 1% triton X-100 in PBS and tissues swollen using PBS resulted in the tissue becoming equally translucent and hazy, but the text was discernible (Figure. 25a and Figure. 25b, respectively).

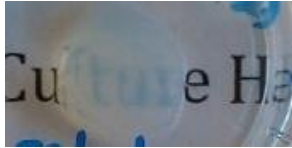



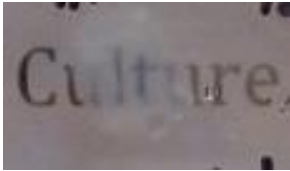
	Decellularising/swelling treatment		Normal Cornea
	1% triton X100	PBS	
After swelling	<p>A</p> 	<p>B</p> 	<p>C</p> 
After dextran treatment	<p>D</p> 	<p>E</p> 	

Figure 25: Visual inspection of the transparency of decellularised corneal tissue. Corneas decellularised and swollen using 1% triton X100 in PBS (A) and corneas swollen PBS alone (B) resulted in the cornea becoming less transparent than immediately excised corneal tissue (C), though incubating the swollen stromal tissue with 5% dextran restored some level of transparency to the triton X-100 in PBS and PBS treated tissues (D and E, respectively).

The ability of dextran to re-establish transparency to the swollen stromal tissue was assessed in the same manner. Dextran dehydration resulted in an improvement to the transparency of both the 1% triton X100 and PBS swollen corneal tissues as observed by the ability to visualise text through the corneas (Figures 25d and 25e, respectively). However, both corneas had some level of haziness and the transparency was inferior to the normal corneal tissue. No differences were observed whether the corneas were cut in half or kept whole.

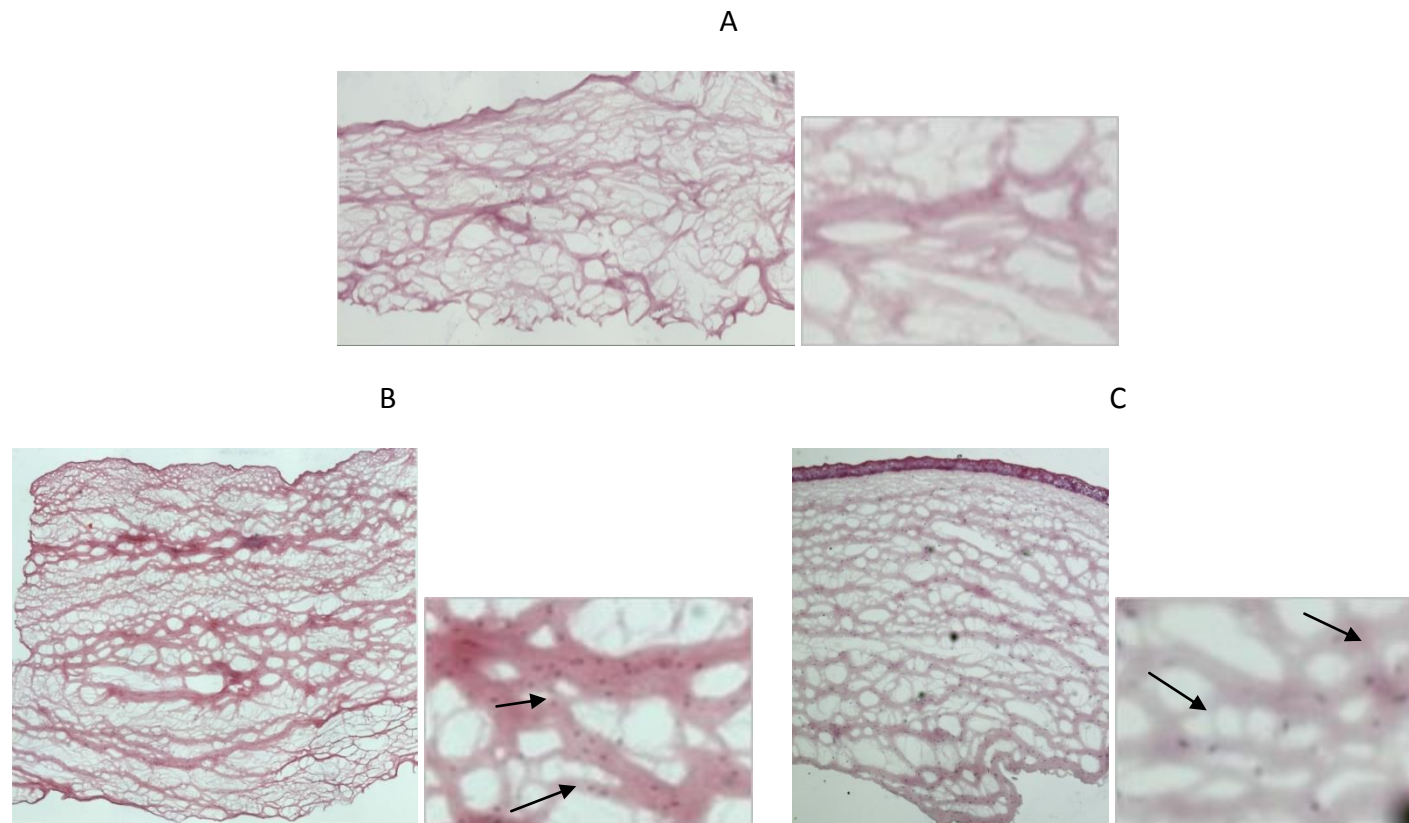


Figure 26: Cryo-histological sections stained with haematoxylin (purple) and eosin (pink) of the porcine corneal tissue after incubation in 1% triton X100 in PBS and PBS alone revealed the extent to which the treatments had removed the porcine cellular material (A and B, respectively) in comparison with the normal porcine corneal tissue (C). Treating the tissue with 1% triton X100 resulted in the complete removal of the porcine cellular material from the full corneal thickness (A) whereas the PBS treated corneal tissues had heavy haematoxylin staining for cellular material (B); as did the normal cornea (C). *Inserts are digitally zoomed-in images of the central portion of the images to emphasise presence of cellular material (arrows).* x40 magnification

Cryo-histological sectioning of the tissue revealed the extent to which the tissue had been decellularised in comparison with normal porcine corneal tissue (Figure 26). Staining with haematoxylin and eosin of the normal corneal tissue showed the dispersion of keratocytes through the cornea as well as the epithelial and endothelial cell layers (Figure 26c). Stromal tissues decellularised with 1% triton X100 were devoid of detectable cellular material, as determined by the lack of purple haematoxylin staining (Figure 26a); while the heavy purple haematoxylin staining of the PBS treated corneal tissues (Figure 26b) indicating little cellular material was removed.

4.4.2 Transmission Electron Microscopy of Swollen and Dehydrated Decellularised Porcine Corneal Stromal Tissue

Using transmission electron microscopy to image the decellularised/swollen corneal tissue and subsequent dextran dehydration revealed the effects of each treatment on the organised collagenous extra cellular matrix ultra-structure.

4.4.2.1 Fibril Organisation

The nano-scale organisation of collagen fibrils are demonstrated by the TEM micrographs in Figure 27. Decellularisation and swelling of porcine corneal tissue using 1% triton X100 in PBS and swelling corneal tissue in PBS only (Figure 27a and 27b, respectively) had a negligible effect on the individual collagen fibrils, compared with normal porcine corneal

tissue (Figure 27c). The mean diameter of the collagen fibrils was $28.7\text{nm} \pm 1.5$ for 1% triton X100 in PBS decellularised/swollen tissues, $29.3\text{nm} \pm 2.6$ for PBS swollen tissues and $29.5\text{nm} \pm 4.5$ for the normal corneal tissue (Figure 28). A two-way ANOVA test comparing the mean diameter of groups 1, 2 and 3 revealed that the diameter of the collagen fibrils are not significantly different for either treatment, $p=0.33$ ($n=3$, with a minimum of 34 fibril diameters measured for each cornea, *see Appendix B(ii)*). However, immediately after swelling, the stromal tissues from groups 1 and 2 had an increase in the spacing between adjacent collagen fibrils – the mean collagen fibril spacing for corneal tissue treated with 1% triton X100 in PBS was $71.0\text{nm} \pm 27.7$, while those treated with PBS alone had their collagen fibrils spaced $76.2\text{nm} \pm 55.5$ (Figure 28). The increase in collagen fibril spacing was observed to be comparable between both groups 1 and 2, $p=0.52$, when compared using a Student's T-test. However both treatments resulted in the spacing of the collagen fibrils more than doubling in distance, $p<0.0001$, than the collagen fibril spacings of a normal cornea, $34.1\text{nm} \pm 12.5$ when compared using a two-way ANOVA, ($n=3$, with a minimum of 53 fibril spacings measured for each cornea, *see Appendix B(iii)*).

Re-compacting the swollen corneal tissues using 5% dextran also had a negligible effect on the diameter of the collagen fibrils of the 1% triton X100 in PBS treated corneal tissues (Figure 30a) and the PBS treated corneal tissues (Figure 28b) since the mean collagen diameters for each treatment were $29.3\text{nm} \pm 2.6$ and $28.6\text{nm} \pm 2.2$, respectively (Figure 28).

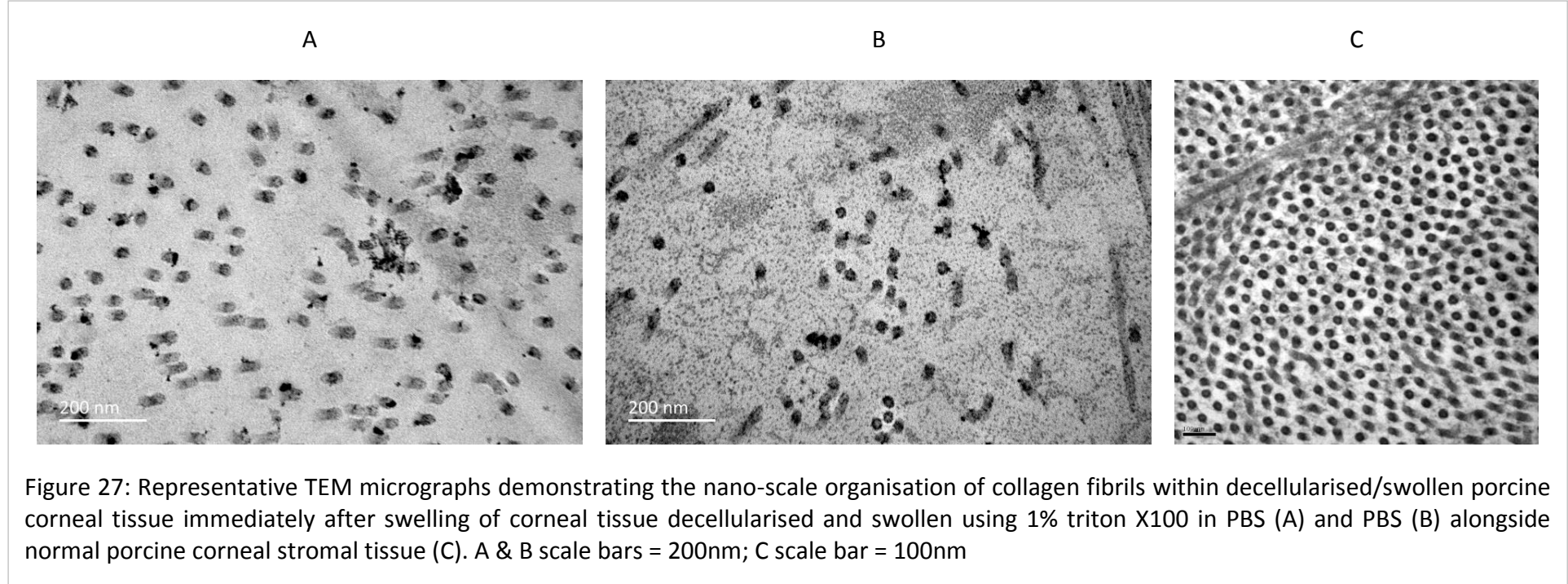
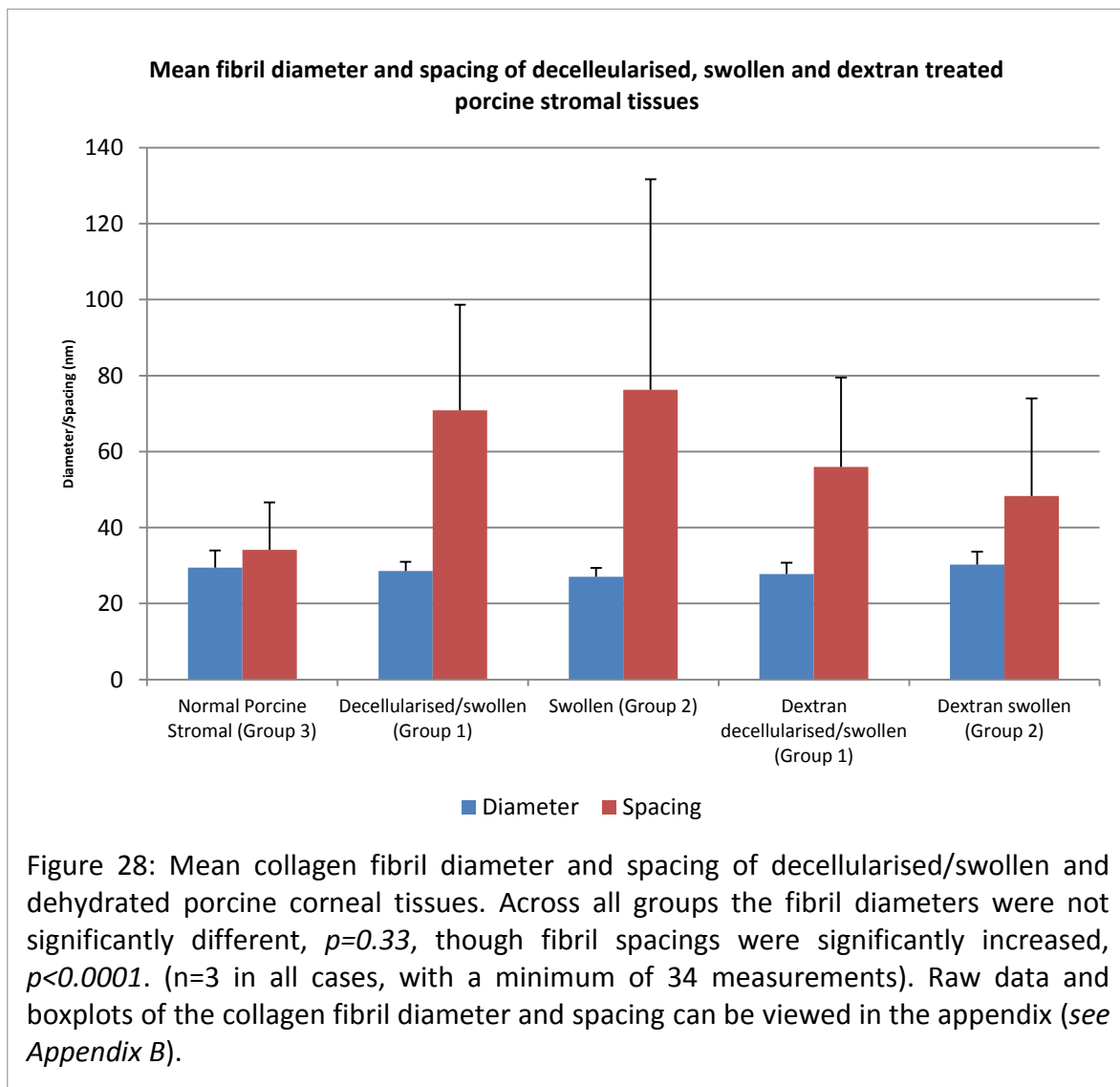
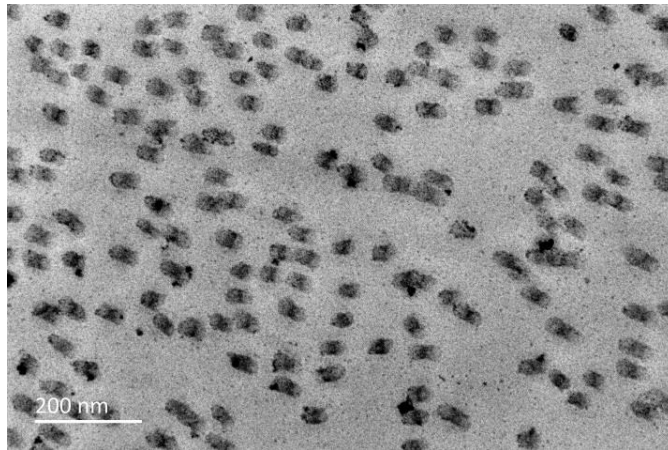


Figure 27: Representative TEM micrographs demonstrating the nano-scale organisation of collagen fibrils within decellularised/swollen porcine corneal tissue immediately after swelling of corneal tissue decellularised and swollen using 1% triton X100 in PBS (A) and PBS (B) alongside normal porcine corneal stromal tissue (C). A & B scale bars = 200nm; C scale bar = 100nm



A



B

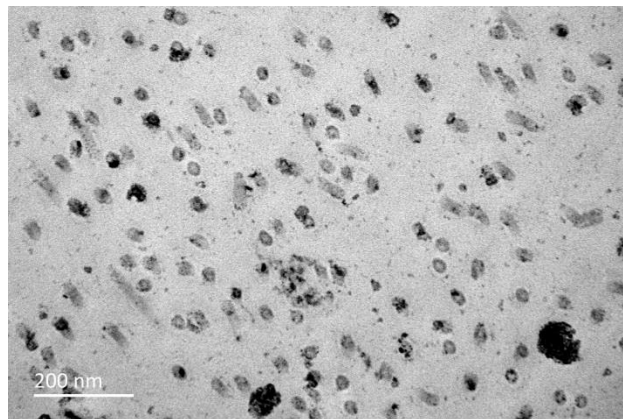


Figure 29: Representative TEM micrographs demonstrating the nano-scale organisation of collagen fibrils within porcine corneal tissue after treatment and dehydration using 5% (v/v) dextran. The collagenous fibrils of corneal tissue treated with dextran having been swollen with 1% triton X100 in PBS (A) and PBS alone (B). The diameter of the collagen fibrils did not significantly change; however the spacing between collagen fibrils decreased after dextran treatment (n=3 in all cases). A & B scale bars = 200nm

Again, this was not significant when compared to the diameter of collagen fibrils from normal corneal tissue, $p=0.20$, using an ANOVA, ($n=3$, with a minimum of 88 fibril diameters measured for each cornea, *see Appendix B(iv)*). The addition of 5% dextran to the solution did have an effect on the spacing of collagen fibrils, since after treatment with dextran the mean collagen fibril diameter decreased to $52.8\text{nm} \pm 27.4$ and $53.1\text{nm} \pm 23.5$ for 1% triton X100 in PBS treated corneal tissues and PBS treated corneal tissues, respectively (Figure 28). These two values were not significantly different $p=0.94$, ($n=3$, with a minimum of 138 fibril diameters measured for each cornea, *see Appendix B(i)*). Comparing swollen and dextran dehydrated tissues demonstrated a significant reduction in fibril spacing after dextran treatment, though, the collagen fibril spacing still remain significantly larger than normal porcine corneal tissue fibril spacing, $p<0.0001$, (as revealed by an ANOVA statistical test and 95% confidence interval plot *see Appendix B(v)*).

4.4.2.2 Lamella Organisation

The organisation of the collagenous lamella sheets within the PBS swollen and dextran dehydrated porcine corneal stromal tissues are demonstrated by the TEM micrographs in Figures 30 and 31, respectively. Decellularisation and swelling the porcine corneal tissue using 1% triton X100 in PBS and swelling porcine corneal tissue in PBS (Figure 30a and 30b, respectively) resulted in a marked decrease in organisation and definition of the collagenous lamellae, in terms of orthogonal arrangement and compaction of the

collagen fibrils within individual lamellae, for both treatments when compared to that of the normal cornea (Figure 30c).

After treatment of the swollen corneal tissue with 5%(v/v) dextran the interweaving and orthogonally orientated lamella sheets were much more distinguishable for both the 1% triton X100 in PBS decellularised and swollen stromal tissues (Figure 31a) and the PBS swollen corneal tissues (Figure 31b) when compared with the immediately decellularised corneal (Figures 30a and 30b), and appears to be similar the normal porcine stromal tissue lamella arrangement (Figure 31c).

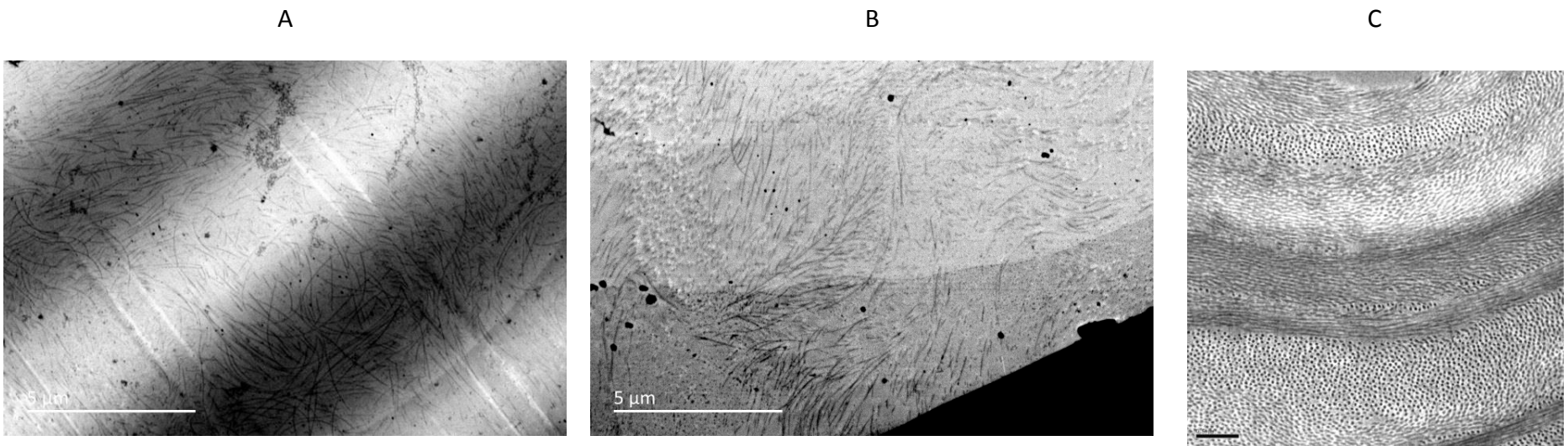


Figure 30: Representative TEM micrographs demonstrating the organisation of the collagenous stromal lamellae within swollen porcine corneal tissue immediately after swelling. Treatment using 1% triton X100 in PBS (A) and PBS alone (B) caused a great deal of disruption to the lamellae, making the sheets difficult to distinguish. The level of disruption was such that the normal orthogonal lamella arrangement (C) was not observed. A & B scale bars = 5 μ m; C scale bar = 0.5 μ m

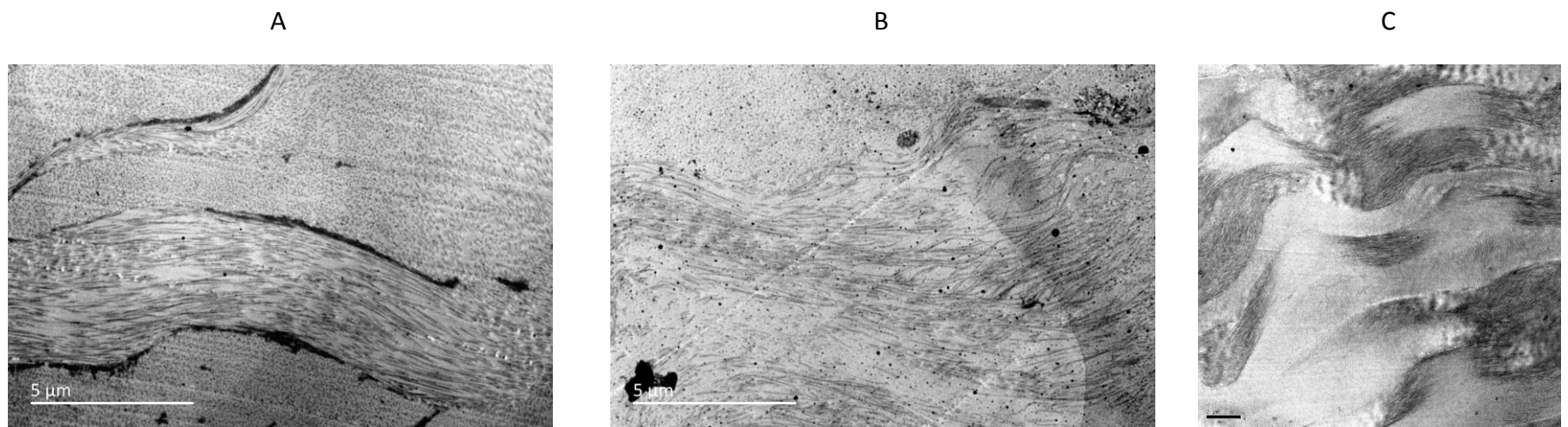
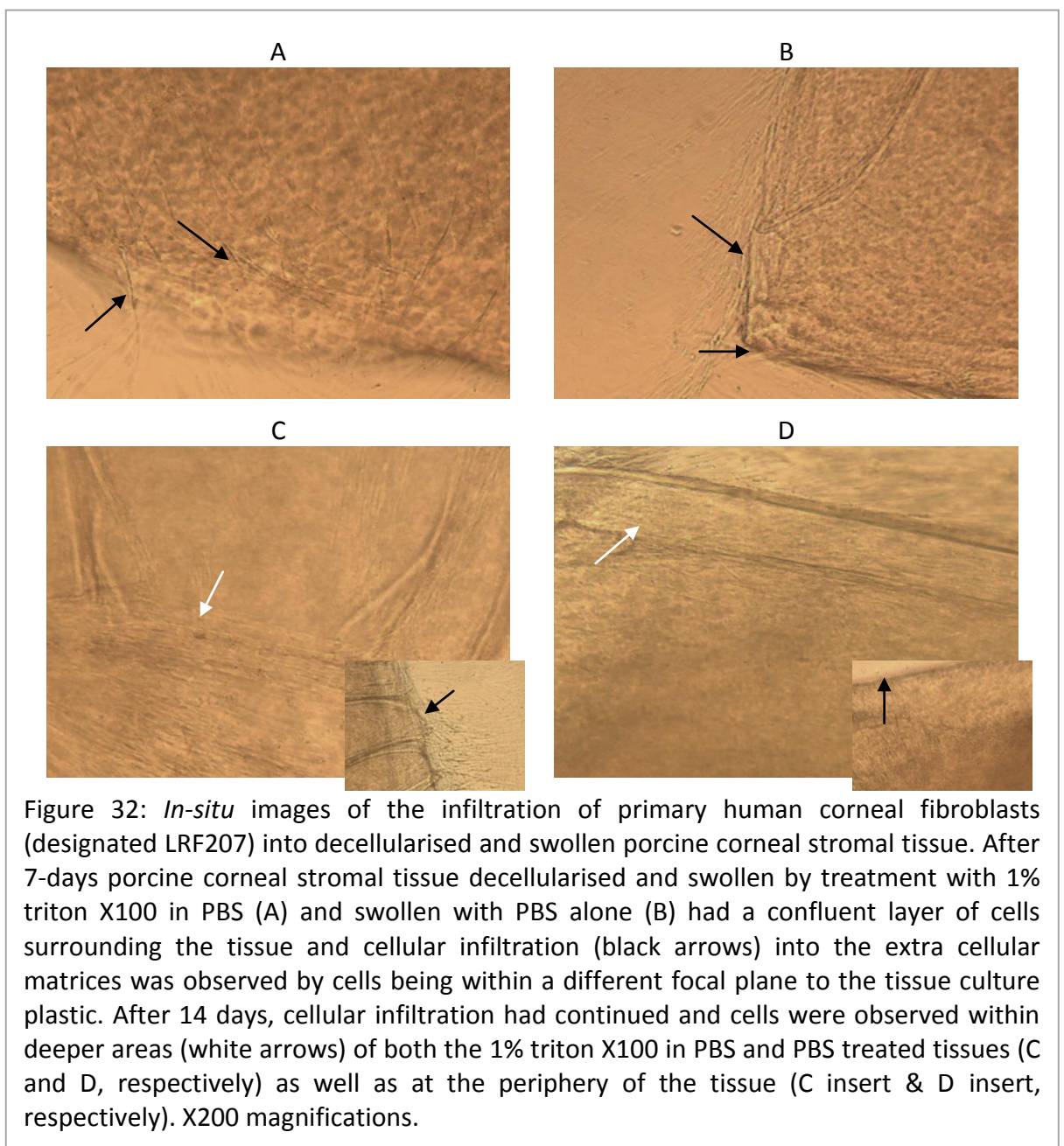


Figure 31: Representative TEM micrographs demonstrating the organisation of the collagenous stromal lamellae within swollen porcine corneal tissue after dehydration using 5% dextran. Dextran dehydration of 1% triton X100 in PBS (A) and PBS (B) swollen porcine stromal tissue improved the ordering of the collagen fibrils and re-established the orthogonal and interweaving arrangement of the lamella sheets of both tissues, which appears to be comparable to the orthogonal and interweaving lamella arrangement of normal porcine corneal tissue (C). A & B scale bars = 5μm; C scale bar = 2μm

4.4.3 Infiltration of Human Corneal Fibroblasts

The infiltration of primary human corneal fibroblasts into the decellularised swollen extra cellular matrices was assessed *in-situ* by imaging the decellularised stromal tissue following incubation with primary limbal ring fibroblasts (LRF207 cells) after 7 and 14 days (Figure 32). After 7 days a fully confluent layer of cells were observed on the tissue culture plastic of the wells for corneal tissues treated with 1% triton X100 in PBS and PBS



alone (Figure 32a and 32b, respectively). Additionally, at this time point, cells were observed to be infiltrating into the swollen collagenous extra cellular matrices of both tissues, as determined by the cells at the periphery of the tissue being observed to be at a different focal point to those on the tissue culture plastic. After 14 days, the cells had continued to infiltrate into both of the corneal extra cellular matrices and were visible at deeper points within the tissue (Figure 32c and 32d) as well as at the periphery (Figure 32c and 32d inserts).

4.5 DISCUSSION

Transparent corneal tissue is of vital importance for vision and hence transparency must be preserved within any artificial corneal replacement. However, porcine tissue intended for use as a corneal xenograft replacement must be devoid of α -Gal epitopes that are present on keratocyte cell membranes, hence the tissue should be decellularised in order for the recipient to accept the tissue. Additionally, by utilising tissue culture techniques and infiltrating cells into decellularised porcine corneal tissue there is the potential to provide humanised porcine corneal xenografts.

4.5.1 Corneal Decellularisation

The technique for decellularising porcine corneal tissue needed some consideration because the decellularising processes had to be able to completely remove the cellular

material without disrupting the corneal architecture as this may be detrimental to the transparency of the tissue. Previous work into decellularising porcine corneal tissue has shown detergents to be the best agents to use to remove the cells while not being too detrimental to the stromal architecture. So for this study the detergent triton-X100 was selected since it has shown great potential for removing porcine cellular material while maintaining tissue transparency (Luo et al., 2013, Fu et al., 2010).

Triton X100 is a detergent which causes disruption to cell membranes resulting cell lysis and the ability of triton X100 to decellularise corneal tissue has been previously reported (Fu et al., 2010, Sasaki et al., 2009), and the results presented herein are in accordance with the published data. By treating the tissue with a non-selective cell lysing detergent such as triton X100, as well as denuding the posterior and anterior corneal surfaces has produced an acellular stromal extra cellular matrix that is potentially suitable for engrafting as a corneal xenograft. However preparing the tissue in this manner is not be suitable for penetrating keratoplasty, due to the decimation of the endothelial and the loss of the stromal hydration control mechanisms which these cells provide. Nevertheless, a decellularised stromal extra cellular matrix would be suitable as a lamellar graft, where the recipients endothelial remains in-tact and functional.

4.5.2 Corneal Swelling

This investigation deliberately set about to swell the corneal tissue with a view to mimicking corneal foetal development. Phosphate buffered saline solution was chosen as the medium to swell the corneal tissue since it has been demonstrated to swell corneal

tissue to three to four times its normal wet mass (Doughty, 2000). While the triton X-100 was lysing the corneal cells, the hypo-osmolar PBS caused the extra cellular matrix to swell as a result of the stromal swelling pressure caused by imbibition of water into the stroma by the hydrophobic proteoglycans. Thus, by immersing the corneal tissue in PBS during the decellularising incubation time, corneal swelling was achieved. However, the gross swelling of corneal tissue in PBS affected the collagenous architecture of the stromal tissue, with collagenous lamella sheets becoming disordered and lacking the interweaving and orthogonal arrangement of the normal corneal stroma, while the collagen fibrils lost their quasi-crystalline uniform arrangement, which was detrimental to the tissue transparency.

The corneal tissue became swollen as a result of the PBS being hypo-osmolar when compared to the aqueous humour and also due to the imbibition of fluid into the stromal extra cellular matrix, which is the result of the swelling pressure exerted upon the stroma due to the sulphation of the ECM proteoglycans (Zhang et al., 2006). Additionally, the removal of the endothelial cells from the posterior surface of the cornea prior to decellularisation also removed the Na⁺/K⁺ ATPase pumps that create an osmotic gradient to counter-act the swelling pressure. Conversely, the consistency of the decellularised collagen fibril diameters with that of normal corneal tissue demonstrates that neither the decellularising nor the swelling processes, i.e. the 1% triton X100 detergent or PBS, respectively, had an effect on the heterogeneous type I and type V collagen fibrils.

4.5.3 Corneal Dehydration

In order to restore transparency to the swollen decellularised corneal tissues, the tissues were immersed in 5% dextran since dextran has been demonstrated to re-establish the transparency of corneal tissue kept in organ culture by dehydrating the tissue to a level that enables for tissue transparency (Armitage, 2011, Pels and Schuchard, 1983). Other investigations into decellularising corneal tissues have used 100% glycerol to return the corneal tissue to transparency after decellularisation (Lynch and Ahearne, 2013). However, glycerol concentrations of 12% have been shown to affect cell viability (Wiebe and Dinsdale, 1991) due to the osmotic pressure exerted on the cells; which may also be detrimental to infiltrated corneal cells, hence 100% may result in damage to the corneal cells infiltrated into the decellularised matrix.

After treatment with dextran some level of transparency was returned to the tissue; however some haziness remained. The improved transparency of the dextran treated corneal tissues, compared to the swollen corneal tissues can be explained by the significant reduction in spacing of the collagen fibrils. However, the tissues did remain oedematous in comparison with the normal corneal stromal, hence the observed haziness within the tissues. Nevertheless by dehydrating the swollen stromal tissue with dextran the collagen fibril spacing was reduced and the interweaving and orthogonal lamellae architecture returned to a level that is similar to the normal cornea. Furthermore, the collagen fibrils were not affected by the dextran, since the collagen fibril diameters remained the same.

The reduced response of decellularised porcine stromal tissue to 5% dextran, in comparison with organ cultured corneal tissue may be due to a lack of endothelial

hydration control because within organ culture systems the corneal tissues have an intact endothelium, complete with hydration control mechanisms. Further investigation into the correct dehydrating solution and concentration of solution is required in order to fully re-establish transparency and the quasi-crystalline nature of collagen fibril. Additionally care would need to be taken in any future work using dehydrating solutions, such as dextran or glycerol, since they can exert osmotic stress upon cells infiltrated into the swollen extra cellular matrix if their concentration is too high.

4.5.4 Infiltration of Primary Human Corneal Fibroblasts into Swollen Decellularised Corneal Stromal Tissue

Over the course of two weeks primary human corneal fibroblasts were observed to infiltrate into the swollen corneal tissue, which suggests mimicking what occurs during foetal development of the cornea, since keratocyte progenitor cells migrate from the periphery of swollen primary corneal tissue (Ruberti and Zieske, 2008). After 14-days the LRF207 cells were observed to be well infiltrated into the swollen corneal tissue. This is evidence that decellularised and swollen porcine corneal tissue would provide a suitable host for humanising corneal xenograft material.

Previous investigations have implanted acellular porcine corneal constructs, decellularised using triton-X100 into intra-stromal pockets of healthy rabbits with graft survival rates of at least 3-months (Fu et al., 2010). However, there was only limited cellular infiltration of keratocytes into the decellularised porcine stromal discs. Additionally, caution must be taken when considering these results as rabbits are not

suitable models for human studies in this instance because rabbit cells express the α -Gal epitope (Shao et al., 2012); i.e. the porcine α -Gal epitope may not be immunogenic to rabbits. When decellularised porcine corneal stromal tissues were implanted into unhealthy (alkali burned) rabbit corneas, the grafts underwent a rejection episode that caused the corneal tissue to become cloudy (Luo, 2013). Additionally, when normal porcine corneal stromal discs were implanted into intra-stromal pockets of healthy α -Gal negative cynomolgus monkeys immunological cellular infiltrations were observed (Amano et al., 2003). Therefore, within an unhealthy human cornea, which may have inflammation and neo-vascularisation, it is likely that the human immune system would elicit a greater reaction.

Nevertheless, this investigation has presented a viable way of introducing human cells into decellularised porcine corneal, and the inclusion of cultured cells has presented the opportunity of creating a humanised porcine corneal xenograft. Furthermore, if keratocytes can be harvested from a patient's unaffected eye, there is the potential to provide an autograft-like xenograft that may reduce an immunological reaction to the graft. This could be achieved using established regenerative medicine techniques for harvesting limbal epithelial cells (Daya et al., 2005, James et al., 2001); briefly, a small limbal biopsy could be taken from the unaffected eye, expanded *in-vitro* until they form sheets of epithelial cells and then grafted onto the corneal surface at the time of corneal reconstruction surgery.

To create an autograft-like xenograft, corneal fibroblasts from the same biopsy could also be harvested and expanded *in-vitro* and then infiltrated into decellularised porcine corneal tissues. Furthermore, epithelial sheets formed from the same biopsy could be

seeded onto anterior surface of the fibroblast repopulated stromal scaffold, thus creating a partial thickness autograft-like corneal replacement.

4.6 CONCLUSIONS

By incorporating primary human limbal ring fibroblasts into a decellularised porcine corneal extra cellular matrix the tissue has the potential to provide artificial corneal replacements that have allograft properties, or even potentially pseud-autograft qualities if a recipient own cells are used. The results presented herein demonstrate the ability of fibroblasts to infiltrate a decellularised swollen porcine stromal scaffold, which can then have its transparency restored to acceptable levels by utilising currently employed corneal organ culture techniques. Further work may be required to optimise the protocol for restoring complete tissue transparency, although once the reconstructed tissue is incorporated as a lamella graft into a recipient, the host's normal hydration control mechanisms may complete the process.

Furthermore, there is the potential to take decellularised porcine corneal tissues one stage further by utilising the decellularised stromal tissue as a scaffold onto which autologous cells are seeded – making porcine corneal xenografts into autograft-like corneal replacements.

CHAPTER 5: Development of a Novel Collagen Types I and V and Glycosaminoglycan Hydrogel as an Artificial Stromal Replacement

5.1 INTRODUCTION

In instances of corneal blindness, often the only treatment option for clinicians is a corneal transplantation; however an artificially produced corneal replacement would be an ideal alternative to donor corneal tissue since it could be an “off-the-shelf” product that can tailored to a specific size or shape, which could be seeded with an individual’s own cells to generate a tissue engineered autograft corneal replacement. Moreover, the production of an artificial corneal replacement can be stringently controlled resulting in less product-to-product variation than cadaver corneal tissue, and less potential for transmission of non-detectable infective agents, e.g. CJD-prions. Additionally, an off-the-shelf product that mimics the natural cornea may also reduce or eliminate the need for tests to be carried out on corneal tissues from live animals during the development of novel drug therapies.

5.1.1 *In-Vitro* Produced Artificial Corneal Replacements

Over approximately 50 years a large amount of research and development has been carried out to create artificial corneal replacements to treat corneal blindness. The early work into the development of artificial corneal replacements produced prosthetic transparent polymers that are implanted with the intention of enabling light to enter the eye, e.g. the Osteo-odontal keratoprosthesis (*see section 1.5.1.3*) implantation, which was first described in 1963 (Gomaa et al., 2010).

Over time, and with increased knowledge of the corneal architecture and tissue culture techniques, the use of naturally occurring biomaterials, such as collagen derived scaffolds, were investigated to generate biomaterials that mimic the natural cornea (Germain, L. et al., 2000; Griffith, M. et al., 1999). Modern techniques are attempting to use tissue engineering, a techniques that is still in relative infancy, to grow *in-vitro* corneal replacements. Such corneal replacements made from naturally occurring biopolymers and tissue engineered products have shown great potential for providing the superior artificial corneal replacements required by clinicians (Lagali, et al., 2011; Fargerholm, et al. 2010; Proulx et al., 2010).

5.1.2 Corneal Biomaterials & Tissue Engineered Constructs

Biomaterial science and tissue engineering are very closely related fields with many similarities in terms of their processes and goals; therefore, it is worth discussing each term, and where possible we will try to use the correct term. Biomaterials are usually

considered to be an 'off the shelf' product that a clinician can call upon when required and consists of polymers artificially prepared to mimic, replace or regenerate a tissue or organ. They can be created from a range of substrates such as biological or synthetic polymers, such as collagen or poly-methyl methacrylate (PMMA), respectively, which can be polymerised on their own or in mixtures known as co-polymerised or hybridised biomaterials.

Tissue engineering is an off-shoot of biomaterial science that has developed into a field of science in its own right and is the process of using cultured cells to form *in-vitro* tissues or organs with the purpose of replacing or initiating regeneration of a tissue or organ when placed *in-vivo*. Often, for the cultured cells to produce an *in-vitro* tissue they will require some kind of external stimuli, hence it is not uncommon for tissue engineered constructs to require a biomaterial substrate, or scaffold, to provide such stimuli. More recently, the process of implanting a biomaterial with biological cues in order to promote the host's own cells, or stem cells supplied externally, to regenerate a tissue or organ, has led to a further term, regenerative medicine.

There is a lot of cross over between biomaterial science and tissue engineering that makes defining each field difficult, however for either field of study to be successful in providing clinicians with an artificial corneal replacement the product created must fulfil three corneal functions of the cornea:

1. First and foremost, the corneal replacement must be transparent and maintain transparency after long-term engraftment
2. The corneal replacement must be able to withstand the intra-ocular pressures exerted upon it once implanted

3. The replacement should become suitably incorporated into the host tissue without causing damage to the host

A significant amount of tissue engineering and biomaterial research has taken place in order to produce artificial constructs with these properties. Corneal tissue engineers use corneal fibroblasts to produce their own extra cellular matrix in order to produce a novel stromal matrix with an organised collagen arrangement. Hence, they will use corneal cells with specialised culture techniques and manipulations in order to produce such a *de novo* construct that mimic the natural cornea.

Culturing fibroblasts in serum transforms the cells into an “activated” state, with a repair phenotype. These activated cells will divide and deposit extra cellular matrix materials more readily than quiescent cells, and when they are maintained at confluence they will secrete their own transparent *de novo, in-vitro* ECM (Guo et al., 2007). Additionally, supplementing the culture medium with extra cellular matrix synthesis associated co-enzymes, for example, ascorbic acid (vitamin C) increases the rate of extra-cellular matrix production. After ~4-weeks in culture corneal fibroblasts form stratified layers (~36µm thick) with a collagenous ECM separating the cells with the collagen bundles forming into orthogonal arrays and being comprised of stromal ECM components (Proulx et al., 2010, Guo et al. 2007). However, by transforming the cells, with the use of serum, the collagen matrix deposited is phenotypically different to the normal corneal stromal collagens since they have an enlarged diameter and spacing, 39.5nm ±4.3 and 25.0nm ±5.8, (Boulze Pankert et al., 2014).

Biomaterials created for artificial corneal replacements are most commonly created from collagen type I. This collagen is used since it is the most abundant protein within mammals and the most abundant component of the corneal stroma. It is also non-immunogenic in allografts and commercially available to scientists.

Collagen type I can be reconstituted with specific dimensions and has a level of malleability that allows many techniques to be employed in creating collagen type I biomaterials, from simple gels that take advantage of the natural fibrillogenesis properties of collagen (Liu et al., 2006a, Liu et al., 2006b) to more complex magnetically aligned collagen matrices (Torbet et al., 2007) or electro-spun collagen matrices (Wray and Orwin, 2009) to name a few examples. However, the constructs produced using these techniques are not necessarily transparent, with large collagen bundles and non-uniform diameter collagen fibrils observed and the addition of glycosaminoglycans decreased collagen orientation (Torbet 2007).

Using collagen type I for artificial corneal replacements because the corneal stromal ECM is a combination of collagen types I, V and VI along with KS and CS/DS PGs. Therefore, inclusion of the additional collagen types and proteoglycans into a corneal biomaterial, to produce a biomimetic corneal stromal analogue, should be considered. The inclusion of the additional stromal components could potentially enhance the transparency of a replacement corneal biomaterial, since the uniform nature of collagen fibrils elucidated upon in Chapter 3 attribute the architecture to ECM composition, and thus enables tissue transparency.

5.2 EXPERIMENTAL DESIGN

5.2.1 Objectives

The corneal stroma is a complex extra cellular matrix and is comprised of collagen types I and V together with the proteoglycans keratan sulphate and chondroitin/dermatan sulphate, which ensures a uniform nature in terms of collagen fibril diameter and spacing and maintains the fibrils less than half the wavelength of light. In spite of that, a homogenous biomaterial, with a composition similar to that of the corneal stromal extra cellular matrix has yet to be attempted. Therefore, the intention of this study was to create a novel artificial corneal stromal replacement that better mimics the natural cornea by including collagen type V and glycosaminoglycans into the biomaterial structure in ratios which are proportional to the percentages found within the natural cornea.

With the inclusion of collagen type V and GAGs into the biomaterial structure it was envisaged that this novel corneal mimicking biomaterial will provide enhanced optical properties, due to the formation of heterogeneous collagen type I/V fibrils that have a thinner diameter than a control collagen type I, alone, biomaterial. Additionally the structural properties of the biomaterial products were tested as well as the viability primary human corneal fibroblasts incorporated into the novel collagen type I/V-GAG biomaterial demonstrated.

5.2.2 Sourcing Corneal Stromal Extra Cellular Components

Collagen types I and V, along with the GAGs chondroitin and dermatan sulphate are all commercially available to purchase. There is wide range of collagen type I products commercially available, which have been harvested from a variety of tissues and species; but due to the non-specificity of collagen type I, the location and species from which the collagen was harvested does not show any significant difference in its performance as a biomaterial (Torbet et al., 2007). Therefore high concentration (5.2mg/ml) collagen type I from rat tail tendon, pre-sterilised using chloroform (FirstLink, UK), was selected since it is a collagen type I product that has been well studied for its use as a corneal biomaterial and its gel forming properties are well known and established (Connon et al., 2010, Levis et al., 2010).

Collagen type V and CS/DS GAGs are also commercially available as lyophilised products. The collagen type V used was harvested from human amniotic membrane tissue, which is the transparent sac that encloses the embryo and later the foetus during gestation. The CS GAGs used were isolated from bovine tracheal cartilage, while the DS GAGs were isolated from porcine intestinal mucosa (Sigma-Aldrich, UK).

Collagen type VI and keratan sulphate GAGs are not available commercially at this time and could not be reliably harvested for this investigation.

5.2.3 Biomaterial Formulation – Component Ratios

It is believed that a novel biomaterial that mimics the compositional proportions of the natural corneal stroma will have enhanced optical properties over that of a control collagen type I hydrogel; hence, the proportions within the cornea must be considered.

Fortunately there is a wealth of published data on the stromal composition, along with the relative concentrations of each component (Table 3), which was used to determine the ratios of each lyophilised product required for the biomaterial.

From the information within the literature, the relative ratios of each component were determined as follows:

Stromal Extra Cellular Matrix Component	Relative Percentage
Collagen Type I	68% (dry-weight)
Collagen Type V	15% (dry-weight)
Chondroitin/Dermatan Sulphate	30mg/g of dry weight
Chondroitin Sulphate	~75% of the CS/DS total weight*
Dermatan Sulphate	~25% of the CS/DS total weight*

Table 3: The relative concentrations of commercially available corneal stromal extra cellular matrix components as reported in the literature (Meek and Fullwood, 2001, Robert et al., 2001, Scott and Bosworth, 1990). *The proportion of CS/DS of 75% CS and 25% DS was taken from the data of the higher mammals within the cited study.

Collagen type I:V ratio

- Collagen types I and V make up ~68% and 15% of the corneal stroma, respectively, (Meek and Fullwood, 2001, McLaughlin et al., 1989) which equates to an approximate ratio of 4.5:1 of collagen type I:V.

Total collagen:chondroitin/dermatan sulphate ratio

- The chondroitin/dermatan sulphate (CS/DS) proteoglycans are found at a concentration of 30mg/g of dry weight within the cornea, (Robert et al., Scott and Bosworth, 1990) which is equivalent to a ratio of 33.3:1 total collagen:CS/DS. For the purposes of ease of calculation, a ratio of 30:1 total collagen:CS/DS was used.

Chondroitin sulphate:dermatan sulphate ratio

- Chondroitin sulphate (CS) proteoglycan makes up ~75% of CS/DS PG total weight, while dermatan sulphate (DS) proteoglycan makes up 25%; (Scott and Bosworth, 1990) hence the ratio of CS/DS is 3:1.

From these figures it was determined that all the collagen biomaterials that were to be created would be produced from a 3mg/ml working stock solution of collagen as it would make the dilution of each product relatively simple.

5.2.4 Quantitative Biomechanical Analysis

Determining the biomechanical properties of the hydrogels is important, since it is not known whether the inclusion of collagen type V into a collagen type I hydrogel will weaken the hydrogel structure, due to the heterogeneous nature of collagen type I/V fibrils that could form. Therefore rheology was performed on the gels as this technique can quantitatively measure the visco-elastic properties of the hydrogels by measuring the storage modulus (G') and loss modulus (G'') These relate to the dynamic elasticity and viscosity of the hydrogels, respectively. Moreover, when the values of G' and G'' are combined ($G'+G''$), the product is known as the complex modulus ($|G^*|$), which is an indication of the stiffness of the gel, i.e. how firm the gels are.

5.2.5 Hypotheses

The following hypotheses were formulated for the comparison of a novel collagen type I/V-GAG biomaterial with that of a control collagen type I biomaterial:

1. A collagen type I/V-GAG hydrogel will have a statistically significant increase in light transmission over a collagen type I hydrogel.
2. A collagen type I/V-GAG hydrogel will have a statistically significant increase in mechanical complex modulus over a collagen type I hydrogel.
3. A collagen type I/V-GAG hydrogel will statistically have significant thinner diameter fibrils than those of a collagen type I hydrogel.

Additionally, the following qualitative assessments will be made:

1. The ability of the collagen type I/V-GAG hydrogel to provide a suitable environment for corneal fibroblast survival

5.3 EXPERIMENTAL PROCEDURE

5.3.1 Materials

5.3.1.1 *Collagen Type I/V-Chondroitin/Dermatan Sulphate Glycosaminoglycan Hydrogels*

A novel collagen type I/V-CS/DS GAG hydrogel was created from materials from the following sources:

Materials	Source
High concentration (5.2mg/ml) collagen type I from rat tail tendon, pre-sterilised using chloroform	FirstLink, UK
Collagen type V, isolated from human placenta – lyophilised powder	Sigma-Aldrich, UK
0.6% acetic acid	Prepared in laboratory by dilution of glacial acetic acid (Fisher Scientific, UK) in distilled water (available in laboratory)
Chondroitin sulphate A (CS _A) – lyophilised powder	Sigma-Aldrich, UK
Chondroitin sulphate B (dermatan sulphate, DS) – lyophilised powder	Sigma-Aldrich, UK
Nunc 24 well tissue culture plates	Fisher Scientific, UK
10x concentrated phosphate buffered saline (PBS), with 10µg/ml phenol red indicator	Prepared in laboratory by dissolving 10 PBS tablets (Fisher Scientific, UK) and phenol red indicator (Sigma-Aldrich, UK) in 100ml

	distilled water (available in laboratory)
1.0M & 0.5M Sodium Hydroxide (NaOH)	Prepared in Laboratory by dissolving sodium hydroxide pellets (Fisher Scientific, UK) in distilled water
Dulbecco's Modified Eagle's Media (DMEM) + 1000mg/l glucose + GlutaMAX™ + pyruvate	Gibco, Invitrogen Life Technologies Ltd. Paisley, UK
Ice	Available in laboratory

5.3.1.2 *Light Transmission*

The transparency of the hydrogel products were established using the following equipment:

Materials	Source
Biotek ELX800 plate reader	Available at University of Brighton
Microsoft Excel 2010	Microsoft Corporation

5.3.1.3 *Rheology*

The structural properties of the hydrogel products were tested using the following equipment:

Materials	Source
HAAKE Rheostress 1 Rheometer, with 35mm plate	Available at University of Brighton
Microsoft Excel 2010	Microsoft Corporation

5.3.1.4 *Transmission Electron Microscopy*

The preparation and imaging for transmission electron microscopy was carried out using the same equipment as described previously (*see section 3.3.1.2*).

5.3.1.5 *Tissue Culture*

Embryonic corneal keratocytes, designated EK1Br, were grown *in-vitro* and then seeded into the collagen scaffolds and fed during the incubation period using the same equipment as previously described (*see section 2.1.1*).

5.3.2 Methods

5.3.2.1 Collagen Type I/V-Chondroitin/Dermatan Sulphate Hydrogel Formation

Working Solution Preparation

The following working solutions were created in order to generate collagen hydrogels with a total collagen concentration of 3mg/ml, with collagens type I and types V at a ratio of 4.5:1, and a CS/DS glycosaminoglycan concentration of 0.1mg/ml, with a CS and DS ratio of 3:1.

3mg/ml Collagen Type I

A working collagen type suspension, with a concentration of 3mg/ml, was created by diluting the collagen type I stock solution with 0.6% acetic acid.

3mg/ml Collagen Type I/V

A stock collagen type V suspension, with a concentration of 3mg/ml, was prepared by reconstituting lyophilised collagen type V in 0.6% acetic acid in distilled water (v/v). Then, a working 3mg/ml collagen type I/V solution was created by mixing 1ml of collagen type V suspension with 4.5ml of the working collagen type I suspension (i.e. a ratio of 1:4.5, respectively) – the concentration of collagen types I and V within this working solution were 2.45mg/ml and 0.55mg/ml, respectively.

10mg/ml Chondroitin Sulphate A/Dermatan Sulphate

A 10mg/ml (x100 concentrated) CS/DS stock solution, with concentration ratio of 3:1, respectively, was created by dissolving 75mg Chondroitin sulphate A (CS_A) and 25mg DS in 10ml of PBS. This solution was then diluted down during the hydrogel formation.

Hydrogel Formation

Collagen type I/V hydrogels were cast using the following published protocol (Levis et al., 2010, Mi et al., 2010a, Mi et al., 2010b, Brown et al., 2005). All solutions were cooled to ~4°C prior to forming the collagen gels, and all mixing was carried out on ice so as to keep the solutions cool. The solutions were kept on ice to slow the collagen gelation process and to enable transference into a suitable casting mould, in this case 24-well tissue culture plates, since they have a similar diameter to the cornea, 1.5cm.

A 4ml aliquot of the working collagen type I/V collagen solution was mixed with 0.5ml of x10 PBS with phenol red indicator. The acetic acid was neutralised with 1M sodium hydroxide which was added in a drop-wise fashion, until the phenol red indicator began to change colour. At this point the neutralising agent was switched to 0.5M sodium hydroxide, which was again added in a drop-wise fashion, until the phenol red indicated that the pH was 7.4 (just pink).

Once the acid was neutralised, 40µl of the 10mg/ml CS_A/DS GAG and 0.5ml of DMEM were added to the collagen mixture, finally the gels were cast as 1ml aliquots in 24-well tissue culture plates and the transparency of the gels was noted by the ability to see text through the gel matrix.

As controls, a collagen type I only gel and a collagen type I/V gel without the CS/DS GAGs were also cast. In order to ensure that the gels had the same volumes, the gels that did not have GAGs added to their mixtures had a 40µl aliquot of PBS added to the mixture after the acid was neutralised, while the collagen type I gels were made using the working stock collagen solution.

5.3.2.2 *Ultra-Violet/Visible Light Spectroscopy*

The collagen hydrogels that were created were subjected to ultra-violet/visible wavelength spectroscopy using a Biotek ELX800 spectrometer plate reader in order to determine the optical properties of the biomaterials. The absorbance of wavelengths of light across the visible spectrum, including; 405nm (violet), 450nm (blue), 490nm (green), 595nm (yellow) and 750nm (red), were measured using the spectrometer. As a reference, a 0.6% acetic acid solution was neutralised and placed into a 24-well plate as described in the previous section.

The absorbance results for each wavelength were then converted to percentage light transmission using the following formula:

$$\% \text{ Light Transmittance} = (10^{-\text{Absorbance}}) * 100$$

After which, a two-way analysis of variance (ANOVA) was carried out to determine whether there was a statistical difference between the mean light transmission values. Data was considered to be statistically different where $p \leq 0.05$.

5.3.2.3 *Transmission Electron Microscopy*

Transmission electron microscopy was carried out on the gels to determine the diameter of the collagen fibrils. The preparation for TEM and imaging were carried out as previously described (*see section 3.3.2*). Briefly; the collagen hydrogels were cast as described above and then diced into ~2mm cubes and placed into a TEM fixative of 2.5% gluteraldehyde + 2% formaldehyde (v/v) in 0.1M phosphate buffer (pH 7.4) for 2 hours at room temperature and then overnight at 4°C. After rinsing in 0.1M phosphate buffer, the biomaterials were post-fixed in osmium tetroxide for four hours and then dehydrated in a graded series of alcohols (10%, 25%, 50%, 75%, 90%, 100%x2 ethanol). The ethanol was then exchanged for propylene oxide, followed by 50:50 propylene oxide-low viscosity resin and then 100% TAAB low viscosity, mixed to a medium-hard hardness, and left to cure overnight at 70°C.

Once in resin, 100nm ultra-thin sections were cut using a RMC Power-Tome PC ultra-microtome with a Diatome 35° diamond knife and mounted onto 200 mesh copper TEM grids. Next the sections were contrast stained using 1% uranyl acetate in distilled water (0.22µm filtered) for 1 hour and saturated lead citrate (0.22µm filtered) for 15 minutes, with distilled water rinses after each stain was applied, and then left to air dry. Finally, the hydrogel sections were imaged using a Jeol 2100F FEG TEM with a Gatan Orius camera and micrograph analysis was carried out using accompanying Gatan Digital Micrograph software.

Micrographs of the collagen fibrils were taken, from which the diameter of collagen fibrils was measured by measuring the widest point of longitudinally orientated collagen fibrils. Additionally the data presented in the previous chapter for the porcine corneal stroma

was used in order to compare the data collected herein with that of normal porcine corneal tissue.

Statistical analyses were carried out using a two-way analysis of variance (ANOVA); data was considered to be statistically significant where $p \leq 0.05$. Confidence interval plots for all ANOVA tests can be observed within *Appendix C*.

5.3.2.4 *Rheology*

The biomechanical properties of the collagen type I/V-GAG hydrogel were determined using a HAAKE Rheostress 1 rheometer with a 35mm plate. In order to optimise the system and determine the linear viscoelastic range of the complex modulus an oscillating shear stress sweep test was performed on the hydrogels. From the results of this test (*see Appendix C(viii)*) it was determined to exert 0.2Pa of shear stress upon the gels while subjecting the gels to an oscillating sinusoidal frequency sweep test with a range of 0.1-10Hz in exponential steps.

As a statistical comparison, a two-way ANOVA was carried out to determine whether there was a significant difference between the complex modulus of the collagen type I/V-GAG hydrogel versus the control gel from the data collected at 1Hz. Data was considered to be statistically different where $p \leq 0.05$.

5.3.2.5 *Incorporation of Primary Corneal Fibroblasts into the Hydrogel Matrix*

In order to test the viability of cells within the collagen type I/V-GAG hydrogel, embryonic corneal keratocytes, EK1Br cells, were incorporated into the gels during the casting process as follows. The gels were cast as described above, however, the 0.5ml of DMEM added after the acid was neutralised was substituted with 0.5ml of embryonic keratocytes suspended in DMEM at a concentration of 2×10^5 cells/ml; i.e. a total number of 1×10^5 cells were encapsulated within the collagen type I/V-GAG hydrogel matrix.

Once the hydrogels had been cast, the gels were sterilised by incubating the gels in DMEM + 10% FCS dosed with 5x concentrated penicillin (500units/ml), streptomycin (0.5mg/ml) and fungizone (12.5 μ g/ml) antimicrobial agents for 30 minutes at 37°C in a 5% CO₂ atmosphere. After this time the sterilising medium was aspirated away from the gels and any excess medium was removed by rinsing the gels with HBSS.

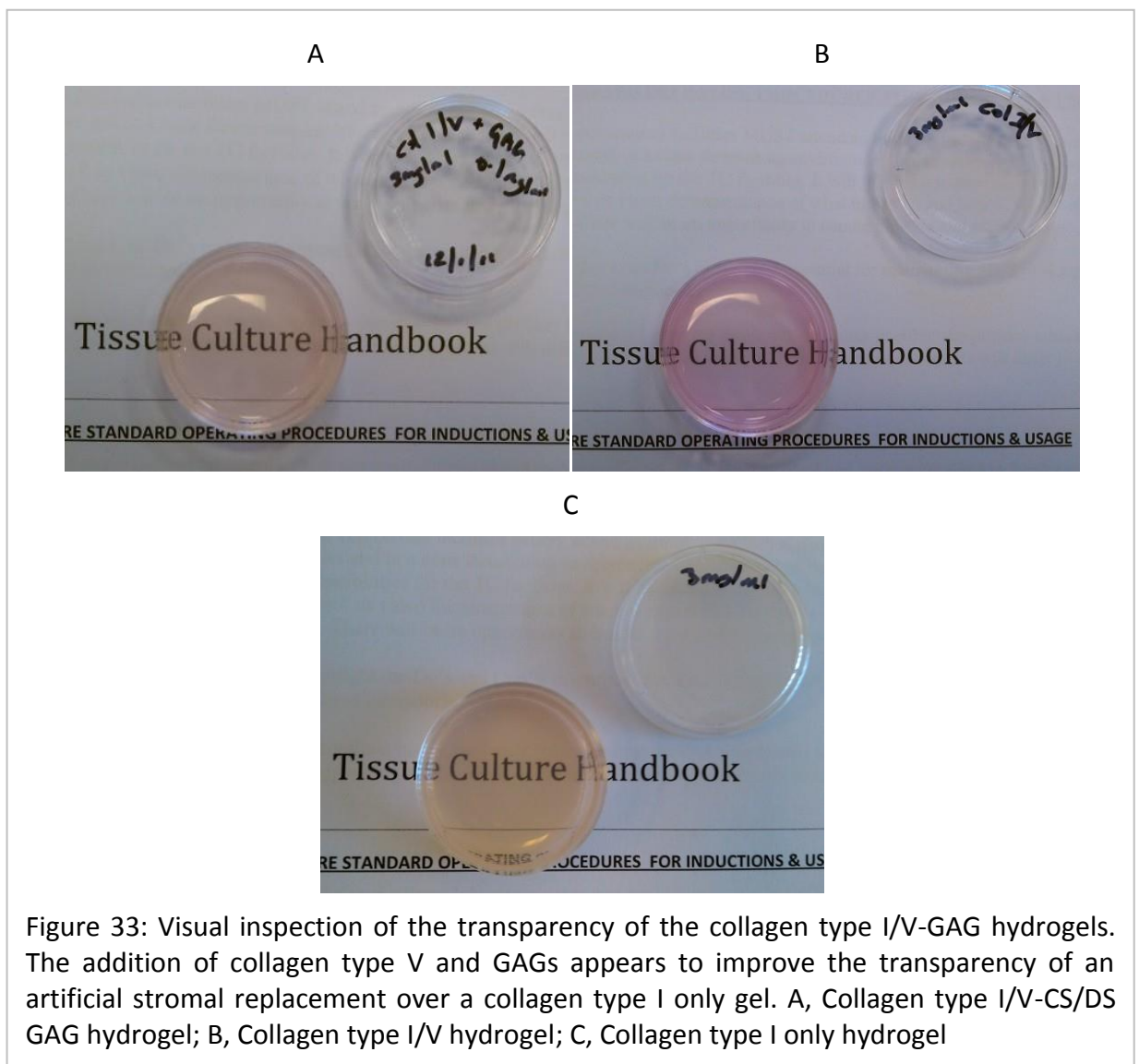
Once the gels were sterilised the cells were cultured in DMEM + 10% FCS dosed with 1x concentrated penicillin (100units/ml), streptomycin (0.1mg/ml) and fungizone (2.5 μ g/ml) in a tissue culture incubator set to 37°C with a 5% CO₂ atmosphere. The gels were cultured for a total of 7 days with the medium being exchanged every 2-3 days to ensure adequate nutrients for the cells as per the standard tissue culture protocols previously described (*see section 2.2.1*).

Over the 7 day culture period the cells within the gel matrix were monitored and imaged *in situ* using a Motic AE31 inverted light microscope with attached Moticam 2000, 2.0M pixel USB digital camera and Motic Image Plus imaging software. Additionally the transparencies of the gels were noted by the ability to visualise a text through the gels while the contraction of the gels was noted by measuring the gel diameter using a ruler.

5.4 RESULTS

5.4.1 Transparency

Upon initial inspection, all three gel type had a good level of transparency, since text was discernible through all gel matrices (Figure 33). However, the collagen type I/V only hydrogel was, subjectively, the most transparent of all the gels (Figure 33b), followed by the collagen type I/V-CS/DS GAG gel (Figure 33a) and finally the collagen type I gel (Figure 33c) appeared to be the least transparent of the three gels that were created and the text appeared slightly hazy.



The visual observations regarding the gel transparency were quantified by the percentage light transmission data that were obtained by ultra-violet/visible light spectroscopy (Figure 34). The collagen type I hydrogel was the least transparent of the four types of gel, allowing for only 9.9% \pm 3.5 light transmittance at 405nm, 16.8% \pm 5.3 at 450nm, 21.8% \pm 5.5 at 490nm, 36.4% \pm 6.1 at 595nm and 57.0% \pm 7.2 light transmittance at 750nm.

Adding collagen type V to the hydrogel matrix, yielded a marked improvement in transparency when compared to the collagen type I gels. In the case of the collagen type I/V hydrogel the percent light transmittance improved to 25.8% \pm 4.5, 38.0% \pm 5.8, 39.6% \pm 5.4, 51.5% \pm 6.1 and 69.0% \pm 7.3 at 405nm, 450nm, 490nm 595nm and 750nm, respectively.

The addition of CS/DS GAGs to the collagen type I/V gel matrix also resulted in an improved level to transparency over the collagen type I alone gel; though it was not as transparent as the collagen type I/V hydrogel matrix, since the gels transmitted 14.9% \pm 2.3, 24.9% \pm 4.2, 32.4% \pm 5.5, 48.5% \pm 8.2 and 67.9% \pm 11.4 at 405nm, 450nm, 490nm 595nm and 750nm wavelengths, respectively.

ANOVA statistical analyses of the percent light transmittance revealed that the transparency of the collagen type I/V and collagen type I/V-CS/DS GAG hydrogels is significantly more than the collagen type I hydrogel for all wavelengths of light; $p < 0.0001$ at 405nm; $p < 0.0001$ at 450nm; $p = 0.0002$ at 490nm; $p = 0.004$ at 595nm; $p = 0.05$ at 750nm; although the collagen type I/V hydrogel was significantly greater than the collagen type I/V-CS/DS GAG hydrogel ($n = 6$ in all cases, see Appendix C for 95% confidence interval plots).

% Light transmittance of collagen hydrogels across the wavelengths of white light

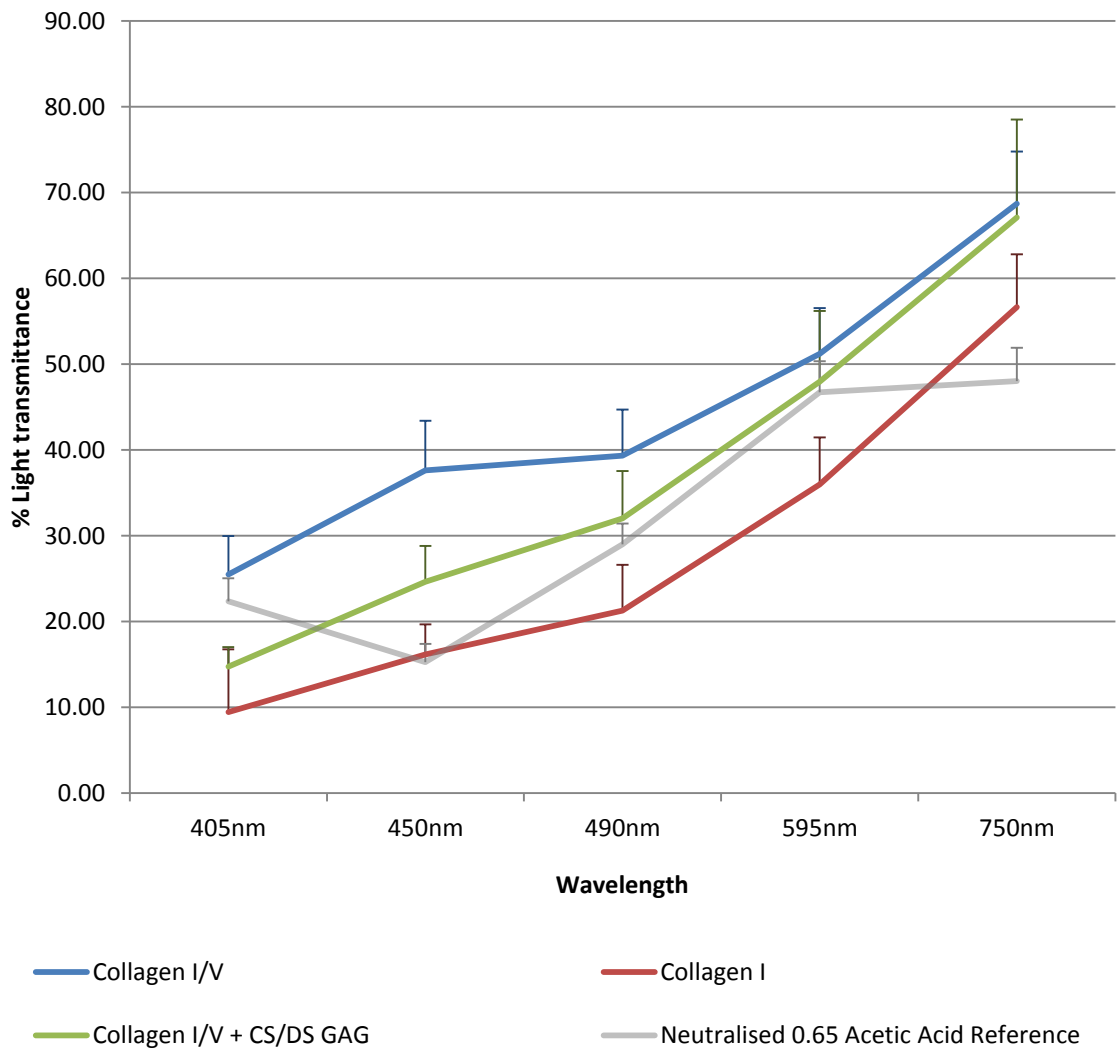


Figure 34: The percentage light transmission of collagenous hydrogels across wavelengths of white light. The collagen type I/V has significantly greater light transmission over the remaining gels, $p < 0.0001$ at 405nm; $p < 0.0001$ at 450nm; $p = 0.0002$ at 490nm; $p = 0.004$ at 595nm; $p = 0.05$ at 750nm ($n = 6$ in all cases; see Appendix C for raw data and 95% confidence interval plots).

5.4.2 Transmission Electron Microscopy

Transmission electron microscopy was able to reveal the individual fibrils of the collagen hydrogels (Figure 35) and also allowed for the measurement of the collagen fibril diameters of the hydrogels (Figure 35d).

The collagen types I/V plus CS/DS GAG (Figure 35a) had the thinnest collagen fibril diameters, with the mean fibril diameter measured to be $26.5\text{nm} \pm 6.3$. The collagen type I/V hydrogel fibrils (Figure 35b) had a mean fibril diameter of $38.5\text{nm} \pm 17.5$. While the collagen types I hydrogel (Figure 35c) had the thickest collagen fibrils, with a mean collagen fibril diameter of $64.4\text{nm} \pm 26.5$. A two-way ANOVA statistical test revealed the fibril diameter of the collagen type I/V-CS/DS GAG and collagen type I/V hydrogels to be significantly thinner than the collagen type I gels, $p < 0.0001$, which is most likely due to the collagen type V fibrils and the CS/DS GAGs within the hydrogel matrix ($n=3$ in all cases, with a minimum of 45 fibrils measured, raw data and 95% confidence interval plots are included in *Appendix C*).

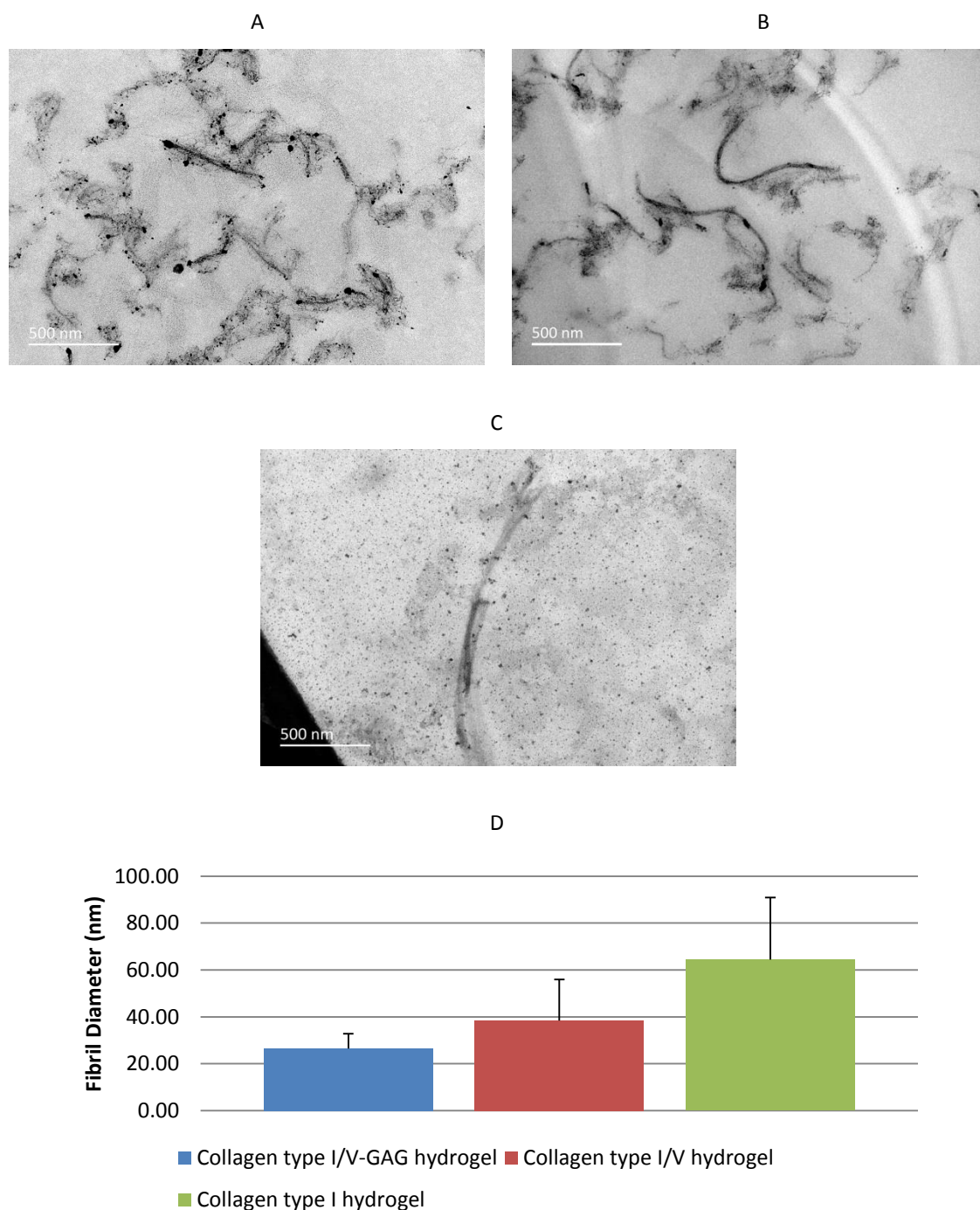


Figure 35: Representative transmission electron microscopy micrographs of the collagen fibres of collagen type I/V-CS/DS GAG (A), collagen type I/V (B) and collagen type I (C) hydrogel matrices, and a chart demonstrating the mean fibril diameters (D). The collagen type I/V-GAG hydrogel had the smallest diameter fibrils with a mean diameter of 26.52nm \pm 6.25, the collagen type I/V hydrogel mean fibril diameter measured 38.46nm \pm 17.48, while the mean fibril diameter of the collagen type I hydrogels was 64.39nm \pm 26.45; (n=3 in all cases; $p < 0.0001$). Raw data and 95% confidence interval plots can be seen in *Appendix C*.

5.4.3 Biomechanical Analysis

Figure 36 demonstrates the storage modulus (G' ; Figure 36a), loss modulus (G'' ; Figure 36a) and complex modulus ($|G^*|$; Figure 36c) for the each of the hydrogels. At 1Hz, the mean G' for the collagen type I/V, collagen type I/V-CS/DS GAG and collagen type I hydrogels were, 4006mPa \pm 4620, 1086mPa \pm 887 and 4796mPa \pm 7468, respectively.

The mean G'' , at 1Hz, was 3031mPa \pm 2387 for the collagen type I/V hydrogels, 1279mPa \pm 1130 for the collagen type I/V-CS/DS GAG hydrogels and 2335mPa \pm 3254 for the collagen type I hydrogels. Finally, the mean $|G^*|$ at 1Hz was 5353mPa \pm 8119, 5100mPa \pm 5090 and 1679mPa, \pm 1435 for the collagen type I/V, type I/V-CS/DS GAG and type I hydrogels, respectively. Statistical analyses using a two-way ANOVA of the mean G' , G'' and $|G^*|$, at 1Hz, for each hydrogel revealed no significant difference during the frequency sweep test, $p=0.66$, $p=0.69$ and $p=0.68$, respectively ($n = 3$ in all cases; raw data and 95% confidence interval plots of this data are in *Appendix C*)

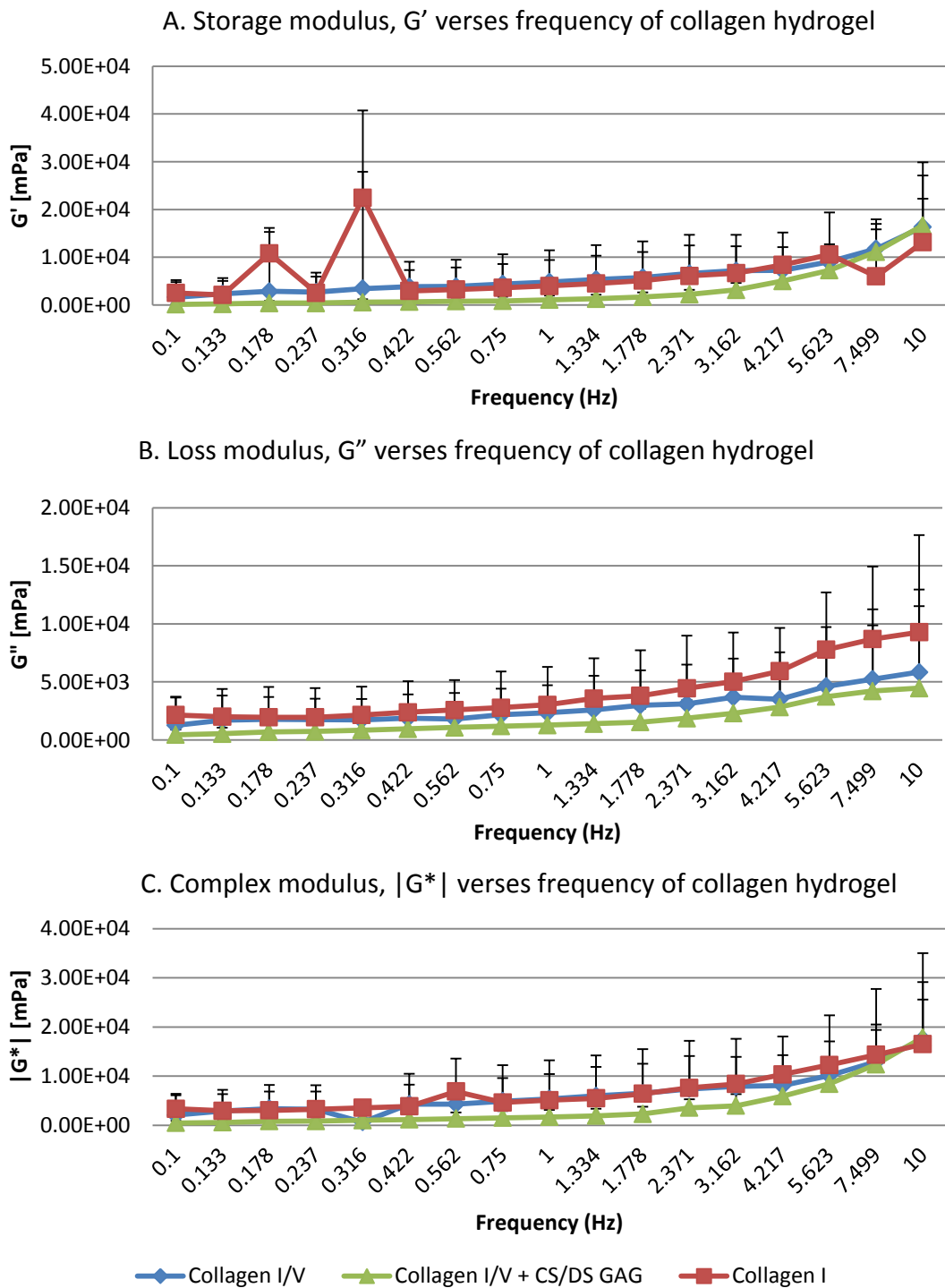


Figure 36: Biomechanical properties of collagenous hydrogels as determined by oscillating frequency sweep rheology. At 1H there was no significant difference in the storage modulus G' (A), ($p=0.66$); the loss modulus, G'' (B) ($p=0.69$) or the complex modulus $|G^*|$ (C) ($p=0.68$). ($n=3$ in all cases) (see Appendix C for raw data and 95% confidence interval plots).

5.4.4 Incorporation of Primary Human Corneal Fibroblasts into a Collagen Type I/V Hydrogel Matrix

Encapsulating EK1Br cells into the hydrogel matrices demonstrated the ability of the hydrogels to provide a suitable environment for the cells. Thirty minutes after, casting the gels had cured as previously described and the EK1Br cells began to change their morphology from round cells, as in suspension, to that of elongated cells with form pseudopodia that are typically observed by fibroblastic cells that are attaching to surfaces when in *in-vitro* culture (Figure 37), moreover the cells were observed to be within different focal planes meaning the cells were throughout the depth of the gel matrix for all types of gel.

After 4-days, *in-situ* imaging of the EK1Br cells within all gels was observed to have a typical fibroblastic morphology, while still being observed at different focal planes through the gels. Additionally the density of cells appeared to have increased.

After 7-days the EK1Br cells continued to demonstrate the typical fibroblastic morphology, increased density and three-dimensional positions. However, the gels had contracted from their original size; all gels had an initial diameter of 15.5mm but by day 7 the collagen type I/V-CS/DS GAG gel has contracted to 12.0mm \pm 0.0, the collagen type I/V gel measured 8.3mm \pm 0.6 and the collagen type I gel was 9.0mm \pm 0.0 (n=3 in all cases). The contraction caused the hydrogels to lose transparency and the collagen type I and collagen types I and V became completely opaque (Figure 37), which also prevented further *in-situ* imaging of the EK1Br cells. However, the decreased level of contraction within the collagen type I/V and CS/DS GAG hydrogel allowing the hydrogel to maintain some level of transparency, since text could be visualised through the hydrogel.

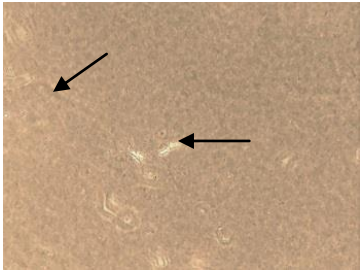
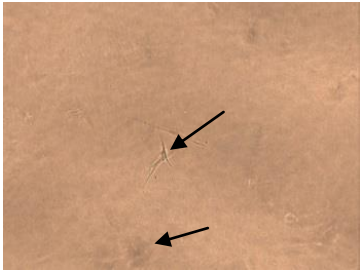

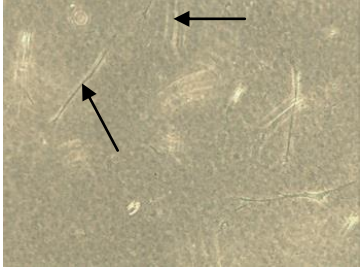
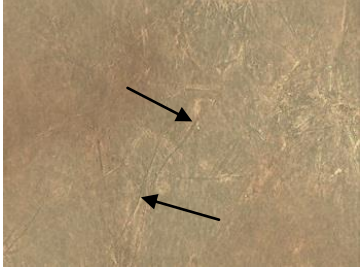
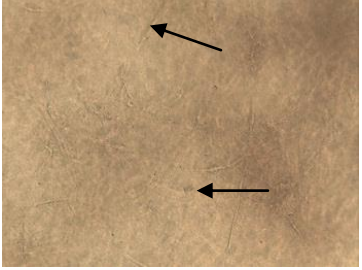
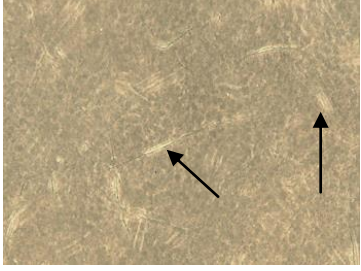

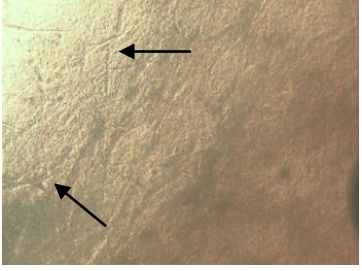



Time	Collagen type I/V-CS/DS GAG	Collagen type I/V	Collagen type I
0-days			
4-days			
7-days			
Gel contraction (day 7)			

Figure 37: In situ tissue culture images of corneal embryonic keratocytes (EK1Br, arrows) incorporated into collagen type I/V-CS/DS GAG, collagen type I/V, collagen type I-CS/DS GAG and collagen type I hydrogels. Images were taken 30-minutes after casting (0-days), after 4 days and after 7-days (all images taken at x400 magnification). After 7-days the gels had significantly contracted from their original size; 22.6% for the collagen type I/V-CS/DS GAG gel, 46.2% for the collagen type I/V gel and 41.9% for the collagen type I gel.

5.5 DISCUSSION

Artificial corneal stromal replacements made from collagenous biomaterials have been studied for over 15-years (Acun and Hasirci, 2014, Levis et al., 2010, Mi et al., 2010a, Mi et al., 2010b, Crabb et al., 2006, Griffith et al., 1999); however many of the artificial stromal replacements that have been created were produced using simple collagen type I or III matrices even though the corneal stroma is comprised of a complex of collagen types I/V/VI with keratan and chondroitin/dermatan sulphate proteoglycans extra cellular matrix, and from the results presented herein the inclusion of corneal stromal extra cellular matrix components should be considered in the development of an artificial stromal replacement since they have provide enhanced transparency to simple collagen type I hydrogel matrices.

5.5.1 Biomimetic Corneal Hydrogel Transparency

Upon casting the hydrogels, all gel types showed good overall transparency; although the hydrogels with collagen type I/V matrices were visibly clearer than the hydrogels created with collagen type I, alone, while the addition of the chondroitin/dermatan sulphate glycosaminoglycans did not appear to reduce the clarity of the collagen I/V matrix significantly, and was still visibly clearer than the collagen type I alone.

Quantitative analysis of the hydrogel transparency, determined by ultra-violet visible spectroscopy, confirmed our visual observations, which suggests that using collagen type

I alone as a biomaterial matrix for an artificial corneal replacement can be improved upon by the addition of corneal stromal ECM components.

Transmission electron microscopy was used to visualise and measure the collagen fibres of the hydrogels and to determine the state of the collagen fibrils. The addition of the collagen type V and GAGs to the hydrogel matrices resulted in thinner diameter fibrils probably as a result of collagen type V forming heterogeneous collagen fibres with collagen type I and the globular protein domain of the collagen type V inhibiting the aggregation of additional collagen fibrils onto the fibre (Smith and Birk, 2012), additionally, the GAG protein cores binding to the collagen fibrils may also prevent aggregation of additional collagen fibrils (Quantock and Young, 2008). Therefore, these thinner diameter fibrils are likely to be associated with the enhanced optical properties observed during light transmission testing, and the inclusion of collagen type V and CS/DS GAGs into the hydrogel matrix resulted in collagen fibrils that are comparable to the thickness of normal corneal collagen fibrils, which have a diameter of $29.5\text{nm} \pm 4.5$ (see *Chapter 3*).

The enhanced transparency of the collagen type I/V hydrogels over the collagen type I only hydrogels highlights the potential advantages of a collagen type I/V hydrogel as artificial stromal replacement, since collagen type V is the secondary fibrous collagen of corneal stromal tissue (Robert et al., 2001) and by incorporating this collagen into the gel matrix transparency of the collagen type I gels has improved, since collagen type I is not inherently transparent and in tissues where it is the sole component, e.g. sclera, dermal and tendon tissues; the tissue is completely opaque.

Furthermore, considering that stromal collagen fibrils have a uniform diameter, which is the product of the interactions of all parts of the stromal ECM, simple collagen type I biomaterials are susceptible to a lack of transparency. This is not a problem for the current crop of collagen corneal biomaterials (Levis et al. 2010, Mi et al., 2010, Vrana et al., 2008, Torbet et al., 2007), since they have a relatively low concentration of collagen, up to 10mg/ml, whereas the normal cornea has a total collagen concentration of more than 100mg/ml (Torbet et al., 2007). Hence, the additional ECM components have provided the mechanisms to maintain the collagen type I fibril diameters.

Counter intuitively, adding chondroitin/dermatan sulphate glycosaminoglycans into the hydrogel matrices slightly reduced the transparency of collagen type I/V hydrogels. It is unclear why this is the case, although within the normal corneal stroma keratan sulphate GAGs work in synergy with CS/DS GAGs to maintain the stromal collagen spacing in a dynamic and fluidic state (Lewis et al., 2010, Parfitt et al., 2010) as well as being involved in maintaining stromal hydration through imbibing aqueous humour into the cornea (Zhang et al., 2006). However, investigations into the disruption of the normal KS GAG-CS/DS GAG concentrations have shown that the cornea becomes less transparent due to stromal over hydration as a result of atypical stromal imbibition (Quantock and Young, 2008). Hence, it is plausible that the lack of keratan sulphate (KS) GAGs has caused the decreased transparency, though further investigation would be required to determine whether the inclusion of KS GAGs would improve the hydrogel transparency.

5.5.2 Biomechanical Analysis

Biomechanical analyses, using rheology, were carried out on all the hydrogels in order to assess the comparability of the hybridised collagen type I/V and collagen type I/V-CS/DS GAG hydrogels with simple collagen type I hydrogels. Rheology was selected for this process as it is a non-destructive technique and can quickly generate results. However, rheology is limited by specimen thickness and the stiffness of the gels (Zuidema, J. M. et al., 2013). Nevertheless statistical analyses of the mean values for G' , G'' and $|G^*|$ demonstrated that there was no significant difference between the data sets. However, care needs to be taken when interpreting these results, because the data set was small and there was a great deal of variation between the samples that appears to skew the data; *Appendix C* demonstrates the 95% confidence limits of the data set.

Further investigation is required to establish better statistical evidence regarding the comparability between the collagen hydrogels; however the evidence suggests that the collagen type I/V and collagen type I/V + CS/DS GAG hydrogels have biomechanical properties that are within the same order of magnitude as the collagen type I hydrogel, i.e. the storage, loss and complex moduli for each hydrogel is within the order to $\times 10^3$ mPa.

The reason for the large amount of variation in the moduli of all three gel types is unclear. The shear rate used is low, as are the values for the moduli themselves, and small variations in gel structure from gel to gel may display large percentage variation in viscoelastic moduli. It could be argued that the variability in rheological measurements is due to localised cross linking between adjacent collagen fibrils a free fluid in a rigid matrix of cross-linked collagen fibres. The fluid therefore, will flow between the more rigid cross-

linked fibrils during deformation, rather than the whole material acting as a truly viscoelastic body. The very small amplitude of deformation would still allow any viscoelastic properties to be revealed, although it could be argued that the properties are not strictly defined by G' and G'' . Adopting this view, it is still valid to suggest the data indicates that there is no difference in properties between the three materials.

Nevertheless, when considering this evidence in comparison with other published data of collagenous hydrogels intended for use as corneal replacements, it is likely that a collagen type I/V hydrogel or collagen type I/V-GAG hydrogel will require some kind of cross-linking agent in order to improve their biomechanical properties. Un-cross-linked collagen hydrogels maintain their structure through hydrogen-bonding of adjacent collagen fibrils; however the collagen fibrils are often disperse and hydrogen-bonds are inherently weak (Xiao et al., 2014, Chandran and Barocas, 2004), hence simple collagen hydrogels are structurally weak materials. Therefore it is likely that the collagen type I/V and collagen type I/V-GAG hydrogels produced herein will require cross-linking in order to improve the structural integrity and in order to overcome the structural weakness of simple collagen hydrogels, these hydrogels could be cross-linked using various techniques; such as, chemical cross-linkers, e.g. carbodiimide (Liu, et al. 2006; Griffith et al. 1999) or dehydration, e.g. plastic compression (Xiao et al., 2014) to name two examples.

This is because rheology factors the fluidic properties of the hydrogels into the measurements, but by stiffening the hydrogels with a cross-linking agent the hydrogels will lose their fluidity. Therefore other mechanical testing techniques may need to be considered, such as tensile testing (Brown, R.A. et al., 2005).

5.5.3 Biomimetic Corneal Hydrogels as a Scaffold for Primary Human Corneal Fibroblasts

In order for any artificial corneal replacement to be considered as a suitable replacement for allograft corneal tissue, the replacement must be able to host corneal cells and not be toxic to the cells. Since collagen is a naturally occurring protein structure that is common to mammals, it is not inherently toxic to cells as well as being non-immunogenic upon engraftment; however, any toxicity introduced during the manufacturing process as well as the ability of the formed hydrogels to accommodate cells within the matrix structure needs to be established. The results presented herein demonstrated that corneal stromal cells, namely embryonic keratocytes, were successfully incorporated into the gel matrices and were observed on different focal planes when viewed using phase contrast light microscopy. This demonstrated that the cells were encapsulated throughout the thickness of the collagenous matrix and over a period of 7-days the cells maintained the morphology typical of fibroblastic cells. Further work is required though to validate the *in-situ* behaviour of the cells as well as quantify the cells within the hydrogels in order to assess any cytotoxic effects the hydrogels have on the cells. Finally the phenotype of the cells within the matrices should also be characterised.

Visualisation of the cells was carried out *in-situ* in order to detect the in-growth of the cells within the biomaterial matrix. However, in order to validate these subjective results, live cell imaging may be required. This can be achieved by using live cell dyes, such as Hoechst 33342 fluorescent dye. Additionally, to quantify the cells numbers and cell proliferation within the hydrogels, a technique such as by a Thiazolyl Blue Tetrazolium

Bromide (MTT) assay or trypan blue assay could be employed (Shevchenko, R. V. et al., 2014). The MTT assay measures the activity of mitochondrial dehydrogenase enzymes which cleaves the Thiazolyl Blue Tetrazolium into formazan – a water insoluble purple dye. Therefore cells that are metabolically active will produce the purple dye, and where there are increased numbers of metabolically active cells the dye will develop quicker. Hence, the number of cells can be quantified by the creation of a calibration curve, of known cell number against light absorbance using UV/visible spectroscopy, and then the cell numbers within the hydrogel matrices extrapolated from the curve.

In order to assess the phenotype of the cells immunolabelling of certain proteins associated with the keratocyte phenotype can be employed, for example, identification of secreted proteoglycans and collagens, i.e. keratan sulphate secretion and collagen type I and V secretion versus collagen type III, as well as α -smooth muscle actin (α -SMA), which is a cyto-skeletal protein associated with myofibroblast phenotype cells.

Over the course of the culture period, the hydrogels all experienced a significant level of contraction, which resulted in a decrease to the transparency of the gels. This contraction was not unexpected and the level of contraction between the collagen type I/V and collagen type I hydrogel appears to be comparable, while the level of contract of the collagen type I/V-CS/DS GAG hydrogels was significantly less. Without further investigation it would be difficult to ascertain why the addition of the CS/DS GAGs to the hydrogels decreases the level of contraction. It could even be suggested that with the inclusion of the components found in normal corneal stromal ECM, i.e. collagen type VI and keratin sulphate, it may be possible to reduce the contraction further.

In order to minimise or eliminate the hydrogel contraction, cross-linking the collagen fibres, with a cross-linking agent such as carbodiimide or gluteraldehyde treatment could be considered as has been carried within other studies (Liu, Y. W. et al. 2006; Germain, L. et al. 2000). By introducing a cross-linking agent the collagen fibres form covalent bonds between adjacent collagen fibrils, giving greater structural integrity to the fibrils. However, it is known that some cross-linking agents are cyto-toxic, particularly gluteraldehyde (Gough et al., 2002), which would mean that encapsulating the cells in the manner carried out in this investigation may not be possible. Alternatively dehydrating the hydrogel matrix could also reduce the gel contraction since the collagen fibrils are more tightly compacted together and form additional hydrogen-bonded cross-links during fibrillogenesis. One way to do this would be to compress the hydrogels, as has already been carried out (Xiao et al., 2014, Levis et al., 2010, Mi et al., 2010a, Mi et al., 2010b, Brown et al., 2005).

5.6 CONCLUSIONS

The intention of this chapter was to develop a novel biomimetic *in-vitro* artificial corneal replacement. Such a biomaterial was successfully created by the addition of corneal stromal components into a hydrogel matrix, which included collagen types I and V, and the glycosaminoglycans chondroitin sulphate and dermatan sulphate. Furthermore, the hydrogel matrix was formulated in such a way that the concentration of each component was proportional to their ratios within the natural cornea.

By combining these corneal stromal components into a simple collagenous hydrogel, this investigation created a hydrogel with enhanced light transmission due to the decreased diameter of the collagen fibrils. Furthermore, the hydrogel created is considered to be a biomimetic corneal biomaterial, since the diameters of the collagen fibrils are comparable with that of porcine corneal tissue. Additionally, we were able to demonstrate that the biomimetic corneal hydrogels had mechanical properties similar to simple collagen type I hydrogels and that the inclusion of collagen type V and CS/DS GAGs into a collagen type I hydrogel matrix provided an environment that supported the proliferation and survival of corneal keratocytes without excessive contraction and loss of transparency of the gel. Therefore, future investigations into *in-vitro* produced artificial corneal replacements should consider the inclusion of corneal stromal components within their makeup, in order to generate biomaterials and tissue engineered constructs with enhanced optical properties. Additionally, the created biomaterial may also provide a better model for *in-vitro* corneal stromal modelling in the future.

CHAPTER 6: Discussion – Elucidation of porcine corneal ultrastructure to inform the development of corneal xenografts or biomimetic replacements

6.1 INTRODUCTION

The cornea is the anterior most tissue of the eye which is a transparent window that maintains the shape of eye globe as well as being the major refractive organ of the eye, making it a multi-purpose tissue that allows light into the eye for sight (Nishida et al., 1997). The ability of the cornea to perform these roles is possible due to a unique collagenous extra cellular matrix (ECM) architecture found within the corneal stroma (Hassell and Birk, 2010, Freegard, 1997, Cox et al., 1970, Maurice, 1957). However, when this complex architecture is disrupted the transparency of the tissue decreases resulting in decreased vision. Corneal opacities require surgical intervention, however there remains a lack of artificial corneal replacements available to clinicians and there is a heavy reliance upon corneal transplantation.

Treating corneal blindness often requires corrective surgery such as corneal keratoplasty, however, corneal grafts have a failure rate of one in four after five years (NHS Blood & Transplant, 2014, Williams et al., 2006). Tissue engineering has the potential to provide artificial corneal tissues which could improve corneal transplantation rates tissues. Such artificially created constructs may become off-the-shelf products that can be *in-vitro*

manipulated to produce auto-graft material by the inclusion of corneal cells harvested from the patient

The concept of tissue engineered corneal constructs is an established treatment for limbal stem cell deficiency (NICE, 2007, Sharpe et al., 2007, Daya et al. 2005, James et al., 2001). Corneal epithelial stem cells are harvested from limbal epithelial biopsies, expanded *in-vitro* and re-engrafted onto a limbal stem cell deficient eye. However, this treatment is only suitable for eyes that are deficient in limbal epithelial cells and where stromal opacity is not an issue but there remains a lack of artificial stromal replacements that can be used as tissue engineered corneal replacements to regenerate the stroma.

This thesis aimed to elucidate upon the ultrastructure of porcine corneal tissue, so as to better understand its architecture and the mechanisms of transparency, which was accomplished through modelling the porcine using transmission electron microscopy. Furthermore, it aimed to use the knowledge gained to inform the development of a humanised porcine corneal xenograft material as well as the development of a biomimetic corneal biomaterial comprised of corneal stromal extra-cellular matrix components. These aims were achieved by developing methodologies to swell and dehydrate decellularised porcine corneal tissues in order to allow primary human cell infiltration into the matrices and the development of a transparent biomaterial comprised of stromal extra-cellular matrix components. Accordingly, this thesis was able to demonstrate the potential of artificial corneal replacement to treat corneal opacities in the future.

6.2 ELUCIDATION OF PORCINE CORNEAL ULTRASTRUCTURE

Porcine corneal tissue is currently under investigation as a corneal xenograft, yet no full-depth three-dimensional analysis of the porcine stromal extra cellular matrix architecture had previously been carried out. Hence, porcine corneal tissue was selected to elucidate upon the architecture of the stromal extra cellular matrix. In order to visualise the porcine corneal ultra-structure transmission electron microscopy was determined to be the most suitable technique. This was because electron microscopes are able to resolve nanometre scale structures (Goodhew et al., 2001), and as such were able to resolve the individual collagen fibrils and collagen lamella architecture of the stroma. In addition, by sequentially imaging a vertical slice through the tissue a full depth profile of the central porcine corneal stroma could be produced.

6.2.1 Porcine Corneal Stromal Architecture

The corneal stromal ECM is transparent due to the thin nature and even spacing of the collagen fibrils, which is the product of heterogeneous collagen type I and V fibres (Smith and Birk, 2012) together with keratan sulphate and chondroitin/dermatan sulphate proteoglycan fibril spacers (Parfitt et al., 2010, Knupp et al., 2009). The collagen fibrils are then formed into lamella sheets that provide structural integrity to the corneal stroma tissue (Meek and Boote, 2009, Hayes et al., 2007, Radner & Mallinger, 2000).

Transmission electron microscope imaging of the individual collagen fibrils of the porcine corneal stromal ECM demonstrated the uniform nature of the collagen fibrils. The thin

and uniform nature of the porcine collagen fibrils was attributed to the collagen-PG composition of the ECM (Parfitt et al., 2010, Knupp et al., 2009), and this was concluded to be important for the transparency of the tissue.

The arrangement of the collagen fibrils of the porcine corneal stromal tissue are in accordance with the quasi-crystalline arrangement, proposed by Cox, *et al* (1970), with the fibrils arranged into a pseudo-hexagonal arrangement, albeit not crystalline. This lack of crystallinity is most likely the product of the fluidic nature of the hydrogen-bonding between the proteoglycans of the corneal stroma (Parfitt, 2010; Knupp, 2009}. However, it is not detrimental to the transparency of the porcine corneal stroma, since the sum of the collagen fibril diameter and spacing is less than 200nm and there is suitable short range ordering to allow light waves to pass uninterrupted through the tissue.

TEM imaging the aligning sheets of collagen demonstrated the interweaving lamella sheets. Through the use of TEM, measurements of the lamellae thicknesses of the porcine stromal lamellae was possible, and revealed the posterior lamellae tend to be thicker than the anterior lamellae. However, the TEM imaging demonstrated that the lamella sheets of the porcine cornea are not strictly orthogonal as they converge/diverge and weave past one another throughout the stroma depth. Though, visualisation of the lamellae orientations revealed the level of interweaving of porcine corneal stromal lamellae was observed to be, subjectively, lesser in the posterior lamellae of the tissue than the anterior tissue. Studies regarding the preferential orientation of collagen lamellae within the porcine stromal tissue reveal the orthogonal arrangement of the tissue is preferential to the insertion of the rectus tendon into the superior, inferior, nasal and temporal poles of the eye (Meek and Boote, 2009, Hayes et al., 2007).

Recently there has been the proposition of an acellular pseudo layer at the posterior of the stroma, known as a Dua's layer, (Dua et al., 2014, Dua et al., 2013), however from the TEM images of the posterior lamellae revealed no evidence of the presence of an acellular. However, processing the tissue using the big-bubble technique as well as imaging of the full width of the posterior corneal stroma may be required to confirm the presence of this layer. Nevertheless, the observations made here are in accordance with the findings of Schlötzer-Schrehardt et al., 2014.

6.2.2 Comparability of Porcine, Rabbit and Human Corneal Stromal Extra Cellular Matrix Architectures

The architecture of the human corneal stromal extra cellular matrix is well defined within the literature (Akhtar, 2012, Radner and Mallinger, 2002, Radner et al., 1998) and has even been directly compared with rabbit corneal tissues in previous microscopic studies (Komai and Ushiki, 1991). Thus, in the current study, rabbit corneal stromal tissue was used as a direct comparison with porcine corneal tissue, from which an indirect assessment of the comparability of human and porcine corneal stromal tissues was made from the data published within the literature.

Through TEM observations, the stromal collagen fibril diameter and spacing of rabbit and porcine corneal stromal fibrils were observed to not be significantly different. Additionally, the rabbit lamellae were observed to be thinner than the posterior lamellae, in agreement with the observations made of the porcine lamellae. However, the level of interweaving between the porcine and rabbit tissues appeared to be different, with the

porcine tissue being more readily interwoven which would suggest a greater comparability with the human corneal stromal architecture.

Results reported for the comparison of human and rabbit corneal tissues (Komai and Ushiki, 1991) showed that the size and organisation of the collagen fibrils between the two species are similar, though rabbit corneal stromal tissues are less likely to interweave than human tissues. The difference in collagen lamella organisation between the two species has also been studied by optical coherence tomography and X-ray crystallography (Meek and Boote, 2009, Hirsch et al., 2001) which confirmed this observation.

This current investigation noted that the porcine collagen lamellae interweaved more than the rabbit corneal tissue, potentially making the porcine tissue similar to the human tissue. Furthermore, a statistical comparison of the published data for human stromal collagen fibril diameter and spacing, with porcine tissue was not significantly different. Hence porcine corneal tissue is potentially very comparable with human corneal tissue. In order to affirm the comparability of porcine corneal architecture with that of human corneal tissue presented herein a direct comparison between the two species is required by a future study.

6.2.3 Informing the Development of Artificial Corneal Replacements

Porcine tissue is currently being investigated as a potential source of donor tissue for porcine to human xenografting (Lee et al., 2014, Lynch and Ahearne, 2013, Fu et al., 2010, Hashimoto et al., 2010, Oh et al., 2009a, Oh et al., 2009b, Oh et al., 2009c); even though a

direct comparison of the stromal architecture of porcine and human tissues had not previously been made. Hence a comparison of the elucidated porcine corneal stromal architecture with human tissue was required. The comparability of porcine and human tissues indicates that porcine tissue would be a suitable material for a corneal xenograft. As such, porcine tissue was selected as a potential route for the development of an artificial corneal replacement developed by tissue engineering.

In addition to this, the preserved nature of the collagen fibril uniformity across porcine, rabbit and human tissues, due to the heterogeneous collagen type I/V fibrils and proteoglycan, informs the need to control the fibril organisation within any artificial corneal replacement, since they are vital for tissue transparency. Hence, a novel biomaterial that mimics the collagen fibril composition was also developed.

6.3 DEVELOPMENT OF A HUMANISED PORCINE CORNEAL XENOGRAFT

Immunogenic incompatibilities, namely α -Gal epitopes found on the surface of porcine cells (Cooper, 2003, Tanemura et al., 2000), between porcine and human tissues make the use of porcine xenografts unsuitable at the current time (Zhiqiang et al., 2007, Amano et al., 2003). However, removing the α -Gal, by decellularising the tissue, may make porcine corneal xenografts more suitable in the future. Additionally, tissue engineering has the potential to provide a humanised porcine corneal xenograft. Hence, to develop a humanised porcine corneal xenograft, this thesis has successfully decellularised porcine corneal tissue and used tissue engineering to re-introduce cells into the decellularised extra-cellular matrix using cues from foetal development.

6.3.1 Porcine Corneal Decellularisation

In order to decellularise the porcine corneal tissue, the decellularising agent needed to completely remove all the cells from the porcine corneal stroma, whilst not damaging the uniform collagen fibril arrangement. Previous studies have found detergents, such as 1% triton X100, to be very successful at decellularising corneal tissue (Lee et al., 2014, Lynch and Ahearne, 2013, Fu et al., 2010, Oh et al., 2009a, Oh et al., 2009b, Oh et al., 2009c). These treatments lyse cells while not being detrimental to collagen architecture.

The results presented herein concur with the use of detergents to decellularise porcine corneal tissues, since 1% triton X 100 was successful in being able to remove the porcine cellular materials, although immune-labelling using anti- α -Gal primary antibodies should be carried out in future investigations to confirm the complete removal of α -Gal. Additionally, through TEM imaging of the decellularised collagenous extra-cellular matrix, this thesis was able to demonstrate that the Triton-X100 detergent did not degrade the collagen fibrils of the extra-cellular matrix, since no significant difference was observed between decellularised porcine corneal tissues, compared with normal corneal stromal collagens tissues.

6.3.2 Infiltration of Human Cells into Decellularised Porcine Cornea Tissue

Once the porcine tissues were decellularised they may be suitable for providing a humanised artificial corneal replacement by incorporating primary human corneal fibroblasts into the decellularised stromal scaffold. By including primary human corneal

fibroblasts from the recipient into the decellularised porcine stromal scaffold there is the potential to provide an autograft-like artificial corneal replacement. There is also scope to provide a cultured epithelial layer either at the time of surgery, or as part of the *in-vitro* process. This could reduce the delay in surface re-epithelialisation as seen with other artificial corneal replacements (Fagerholm et al. 2010).

In order to infiltrate human corneal fibroblasts into the decellularised stromal tissue a novel approach of mimicking foetal development and the infiltration of keratocyte precursor cells into a swollen primary corneal extra cellular matrix was taken (Ruberti and Zieske, 2008). Using foetal development to infiltrate cells into the decellularised tissue was theorised to enable primary cell contact inhibition. This would prevent over saturation of cells within the scaffold, which may occur using the technique proposed by Yoeuruk et al. 2012 of injecting cells directly into the matrix.

To mimic foetal development the corneal tissue was swollen using PBS during the decellularising process. PBS was used since corneal tissue swells in this medium (Doughty, 2000). This was also observed within the decellularised porcine corneal tissue used for this thesis since the collagen fibril spacing became significantly enlarged.

The swollen stromal scaffolds were then incubated with primary human corneal fibroblasts, and the cells were observed to re-infiltrate into the scaffolds. The cells were cultured in serum, hence it is likely that the cells have transformed into a myofibroblastic phenotype, though this has not been confirmed. Therefore further work is required to characterise the phenotype of the cells and specialised culture methods may be required to ensure the cells maintain a keratocyte phenotype. Additionally the rate of migration into the decellularised tissue is not known and will also require investigation.

Nevertheless this study has demonstrated a novel way to reintroduce cells into decellularised porcine corneal tissues through mimicking foetal development *in-vitro*. This indicates the potential for the swollen stromal scaffolds to provide a suitable environment for primary human corneal fibroblasts, as well as the potential to provide humanised xenograft material for donation.

Swelling corneal tissue in PBS was detrimental to the transparency of the decellularised stroma, as a result of disruption of the quasi-crystalline uniform collagen architecture. It was also detrimental to the orthogonal arrangement of the collagen lamella sheets. This was the result of tissue oedema, due to the loss of hydration control by the endothelium and the proteoglycan swelling pressure (Lynch and Ahearne, 2013, Zhang et al., 2006; Doughty, 2000). Therefore, transparency needed to be restored for the humanised porcine corneal tissue to be suitable as a corneal graft.

To restore transparency currently used eye banking techniques, such as immersing the swollen tissue in 5% dextran (Armitage, 2011; Pels, 1983) were employed to dehydrate the tissue.

Dehydrating the decellularised porcine corneal tissues visibly improved the level of transparency was compared with swollen tissues. Also using 5% dextran was not detrimental to the collagen type I/V-proteoglycan extra-cellular matrix, since the mean fibril diameter was maintained at widths comparable to human corneal stromal collagens. Furthermore, the dextran solution partially restored the interweaving lamella architecture of the decellularised porcine corneal tissues. However, the 5% dextran was not able to fully restore tissue transparency and a slight haziness remained within the

tissues. This was due to enlarged collagen fibril spacings causing the collagen fibrils to not conform to the uniform architecture required for transparency.

The level of dehydration was not as great has been reported for clinical studies, (Armitage, 2011; Pels, 1983). This was most likely due to the lack of hydration control mechanisms that the endothelial cells would normally exert upon the corneal stroma (Zhang et al., 2006) since these cells were removed prior to decellularisation. Hence there is a need to optimise the dextran concentration to reduce the level of oedema within the swollen decellularised corneal tissues.

This is the first time such an observation has been made on porcine xenograft material, and demonstrates the potential for swelling and dehydrating decellularised porcine corneal tissue to be infiltrated with human cells and mimicking corneal foetal development, for the development of a humanised porcine corneal xenograft. However, the effect of the dehydrating dextran solution on the cells was not studied and will also be required in any future work in order to ensure the hypo-osmotic effects of the dextran is not detrimental to the cells.

6.4 DEVELOPMENT OF BIOMIMETIC CORNEAL REPLACEMENTS

An alternative approach to the development of a corneal replacement was to develop an *in-vitro* biomimetic artificial corneal replacement. The development of a completely *in-vitro* engineered corneal stromal construct could potentially provide clinicians with a corneal replacement that can be tailor made to a specific size or shape, and can be

seeded with an individual's own cells to provide a pseudo-autograft capable of regenerating the cornea. Additionally an *in-vitro* produced corneal replacement could have certain advantages over corneal xenograft material, including improved control of the manufacture processes, reducing product-to-product variation, and reduced potential for the transmission of non-detectable infective agent, such as vCJD-prion. An added benefit of the development of a tissue engineered corneal replacement is that the product could be useful as an alternative model to animal testing in, for example, safety assessments of during the development of novel drug therapies.

The development of an artificial corneal replacement is not an easy undertaking, since for an *in-vitro* corneal replacement to be successful the tissue must become suitably incorporated into the host corneal tissue, without being detrimental to the host. Moreover any artificial corneal replacement needs to be able to maintain the structure of the eye globe and most importantly be transparent.

6.4.1 Potential for an Improved Artificial Corneal Replacement

Of all the collagen based biomaterials, the construct closest to providing a usable novel corneal replacement to clinicians is a recombinant human type III cross-linked hydrogel, developed by May Griffith and her group, which is currently in phase 1 clinical trials (Fagerholm et al., 2014, Lagali et al., 2011, Fagerholm et al., 2010). This biomaterial is created by reconstituting recombinant human collagen type III, derived from yeast cultures, into a hydrogel that is then stabilised by cross-linking the collagen with 1-ethyl-

3-(3-dimethyl amino propyl) carbodiimide (EDAC) and N-hydroxysuccinimide (NHS) (McLaughlin et al., 2009a).

This biomaterial is created from collagen type III, which is not found in high quantities in the normal cornea. Additionally, many of the *in-vitro* produced corneal replacements currently being researched are often constructed from a sole collagen type, such as collagen type I (Acun and Hasirci, 2014, Xiao et al., 2014, Builles et al., 2010, Levis et al., 2010, Torbet et al., 2007). Torbet et al., (2007) reported struggling to control the diameter of collagen fibrils as a result of increasing the collagen concentration resulting in reduced biomaterial transparency.

6.4.2 Biomimetic Corneal Replacements

Subsequent to elucidation of the porcine corneal stromal architecture, it was determined that the transparency of the cornea was the product of the uniform arrangement of the collagen fibrils. This is the product of heterogeneous collagen type I/V fibrils and proteoglycan extra cellular matrix constituents fibre (Smith and Birk, 2012; Quantock and Young, 2008).

This thesis has demonstrated the first biomimetic corneal biomaterial created from collagen types I and V along with chondroitin/dermatan glycosaminoglycans to provide an improved artificial corneal replacement. By including collagen type V into a collagenous hydrogel the percentage of light transmission and hence transparency significantly improved across all wavelengths of light when compared with a collagen type I hydrogel.

The improved transparency is likely to be the product of heterogeneous collagen type I and type V collagen fibrils forming within the hydrogel construct since the diameter of the fibrils within the collagen type I/V hydrogel were significantly thinner than in the collagen type I alone hydrogel and comparable with that of the normal cornea. Therefore, the addition of collagen type V should be considered for collagenous based artificial corneal replacements.

The heterogeneous nature of the collagen type I/V fibrils was not studied, and may need to be confirmed, in order to better characterise the transparent properties of the hydrogels. However, previous work on corneal tissues have shown that collagen type V limits the diameter of fibrous collagen matrices due to a globular domain that prevents aggregation of additional fibrous tropocollagens to the collagen fibre (Smith and Birk, 2012).

When CS/DS GAGs were added to the collagen type I/V hydrogel matrix, there was also a significant reduction to the collagen fibril diameter, which was most likely due to the GAGs binding to the collagen fibrils (Quantock and Young, 2008), preventing additional collagen fibrils aggregating to the fibre. The addition of the CS/DS GAGs to the biomaterial did result in a slight reduction to the transparency of the construct. The cause of the reduction in transparency of the biomaterial when CS/DS GAGs were included within its composition could not be determined, though it is thought the lack of keratan sulphate within the biomaterial may play a part. This was theorised to be the case since corneal tissues with improper GAG expression often suffer from a reduced level of transparency (Quantock and Young, 2008). This is due to an atypical imbibition of fluid

into the corneal stroma. Further investigation is required to determine whether the inclusion of KS GAGs to the biomaterial construct would improve the transparency.

For a corneal replacement to be successful, the replacement needs to be suitably integrated into the host tissue, without being detrimental to the host. When the collagen type I/V plus CS/DS GAG hydrogels had primary human corneal cells encapsulated into the hydrogel construct the cells were observed to be well integrated into the collagenous architecture. Additionally, the cells were observed to have the elongated morphology that is typical of fibroblast cells attached to a substrate. It was assumed that the collagenous hydrogel scaffold would not be toxic to the fibroblasts as it has been demonstrated to not be in previous studies (Shevchenko, R. V. et al., 2014). The initial tissue culture observations made herein correlate with collagenous structures being non-toxic to cells. However, this should be confirmed by quantifying the cell proliferation within the gels. The phenotype of the cells also needs to be confirmed to ensure the cells maintain a keratocyte phenotype.

After 7-days in tissue culture, a significant level of gel contraction was observed. This was the product of the keratocytes remodelling the biomaterial architecture and resulted in a significant reduction in biomaterial transparency. However, including collagen type V and CS/DS GAGs to the hydrogel construct was not detrimental to the biomechanical properties of the hydrogel, as assessed by rheological measurements.

It is likely these gels will need to be cross-linked in order to improve their structural integrity as has previously been required by other collagenous biomaterials (Brown et al., 2005; Griffith et al., 1999). Though, the inconclusive nature of the rheology results requires further analysis to better characterise the mechanical properties. This will also

enable a better indication of how these novel collagen biomaterials compare with previously published corneal biomaterials, in terms of their mechanical properties as well as that of the normal cornea.

6.5 CONCLUDING REMARKS

The transparent nature of corneal tissue and the lack of a gold standard treatment for corneal opacities necessitates research to better understand the mechanisms of corneal transparency and to inform the development of artificial corneal replacements. By elucidating the structure of the porcine corneal stroma, this thesis has been able to conclude that the orthogonal arrangement of the collagen lamellae enables the corneal stroma to maintain the structure of the eye globe, while the uniform nature of stromal collagens is vital to the transparency of the stroma, though a fully crystalline architecture is not necessary.

The conclusions regarding the uniform nature of the collagen fibrils was supported by the work that was carried out for the development of artificial corneal replacements, since disrupting the uniform porcine stromal collagen architecture by swelling the tissue with phosphate buffered saline reduced the transparency of the tissue. Additionally, the biomimetic corneal stromal biomaterial created during this thesis had an improved transparency due to thinner collagen fibrils. Hence, it is the stromal extra cellular matrix composition, and the uniform nature of the collagen arrangement that it provides, which enables the tissue to be transparent.

In addition to this, the elucidation of the porcine corneal tissue architecture has demonstrated that porcine corneal tissue is comparable with human corneal tissue and therefore a potential source of corneal xenograft material. Moreover, this thesis was able to demonstrate human cell re-population of decellularised porcine extra cellular matrix tissue and therefore the potential for decellularised porcine corneal tissue to provide a suitable scaffold for the development of humanised corneal xenograft material.

Likewise, an *in-vitro* produced artificial corneal replacement has the potential to provide clinicians with an artificial corneal stromal replacement, which can be turned into a tissue engineered corneal construct by incorporating primary human corneal fibroblasts into the biomaterial, and even the potential for the addition of an epithelial layer. Furthermore, by creating a biomaterial with corneal stromal extra cellular matrix components, this thesis has produced a biomaterial with improved optical properties and this biomimetic hydrogel may provide a better model for *in-vitro* corneal stromal studies in the future. Therefore future biomaterials created for corneal tissue engineering and *in-vitro* corneal stromal modelling should consider including the additional collagen types and proteoglycans found within the corneal stroma.

REFERENCES

- Abad, E., Lorente, G., Gavara, N., Morales, M., Gual, A. & Gasull, X. (2008) Activation of store-operated Ca^{2+} channels in trabecular meshwork cells. *Investigative Ophthalmology & Visual Science*, 49 (2), 677-686.
- Acun, A. & Hasirci, V. (2014) Construction of a collagen-based, split-thickness cornea substitute. *Journal of Biomaterials Science-Polymer Edition*, 25 (11), 1110-1132.
- Ahmad, S. (2012) Concise review: limbal stem cell deficiency, dysfunction, and distress. *Stem Cells Transl Med*, 1 (2), 110-5.
- Ahmadiankia, N., Ebrahimi, M., Hosseini, A. & Baharvand, H. (2009) Effects of different extracellular matrices and co-cultures on human limbal stem cell expansion *in-vitro*. *Cell Biology International*, 33 (9), 978-987.
- Akhtar, S. (2012) Effect of processing methods for transmission electron microscopy on corneal collagen fibrils diameter and spacing. *Microscopy Research and Technique*, 75 (10), 1420-1424.
- Amano, S., Shimomura, N., Kaji, Y., Ishii, K., Yamagami, S. & Araie, M. (2003) Antigenicity of porcine cornea as xenograft. *Current Eye Research*, 26 (6), 313-318.
- Armitage, W. J. (2011) Preservation of Human Cornea. *Transfusion Medicine and Hemotherapy*, 38 (2), 143-147.
- Armitage, W. J., Tullo, A. B. & Larkin, D. F. (2006) The first successful full-thickness corneal transplant: a commentary on Eduard Zirm's landmark paper of 1906. *Br J Ophthalmol*, 90 (10), 1222-3.
- Bairaktaris, G., Lewis, D., Fullwood, N. J., Nieduszynski, I. A., Marcyniuk, B., Quantock, A. J. & Ridgway, A. E. A. (1998) An ultrastructural investigation into proteoglycan distribution in human corneas. *Cornea*, 17 (4), 396-402.
- Bard, J. B. L. & Higginson, K. (1977) Fibroblast-Collagen interaction in the formation of the secondary stroma of the chick cornea. *Journal of Cell Biology*, 74 (3), 816-827.
- Baum, J. P., Maurice, D. M. & Mccarey, B. E. (1984) The Active and Passive Transport of Water Across the Corneal Endothelium. *Experimental Eye Research*, 39 (3), 335-342.
- Beebe, D. C. & Masters, B. R. (1996) Cell lineage and the differentiation of corneal epithelial cells. *Investigative Ophthalmology & Visual Science*, 37 (9), 1815-1825.
- Benedek, G. B. (1971) Theory of Transparency of the Eye. *Applied Optics*, 10 (3), 459-&.
- Beuerman, R. W. & Pedroza, L. (1996) Ultrastructure of the human cornea. *Microscopy Research and Technique*, 33 (4), 320-335.
- Bidanset, D. J., Guidry, C., Rosenberg, L. C., Choi, H. U., Timpl, R. & Hook, M. (1992) Binding of the Proteoglycan Decorin to Collagen Type VI. *Journal of Biological Chemistry*, 267 (8), 5250-5256.

- Birk, D. E. (2001) Type V collagen: heterotypic type I/V collagen interactions in the regulation of fibril assembly. *Micron*, 32 (3), 223-237.
- Bonanno, J. A. (2012) Molecular mechanisms underlying the corneal endothelial pump. *Experimental Eye Research*, 95 (1), 2-7.
- Boote, C., Dennis, S., Huang, Y. F., Quantock, A. J. & Meek, K. M. (2005) Lamellar orientation in human cornea in relation to mechanical properties. *Journal of Structural Biology*, 149 (1), 1-6.
- Boulze Pankert, M., Goyer, B., Zaguia, F., Bareille, M., Perron, M. C., Liu, X., Cameron, J. D., Proulx, S. & Brunette, I. (2014) Biocompatibility and functionality of a tissue-engineered living corneal stroma transplanted in the feline eye. *Invest Ophthalmol Vis Sci*.
- Bourne, W. M. (1976) Specular microscopy of human corneal endothelium *in-vivo*, *Am. J. of Ophthalmol.* 81 (3) 319-323
- Brown, R. A., Wiseman, M., Chuo, C. B., Cheema, U. & Nazhat, S. N. (2005) Ultrarapid engineering of biomimetic materials and tissues: Fabrication of nano- and microstructures by plastic compression. *Advanced Functional Materials*, 15 (11), 1762-1770.
- Builles, N., Janin-Manificat, H., Malbouyres, M., Justin, V., Rovere, M. R., Pellegrini, G., Torbet, J., Hulmes, D. J. S., Burillon, C., Damour, O. & Ruggiero, F. (2010) Use of magnetically oriented orthogonal collagen scaffolds for hemi-corneal reconstruction and regeneration. *Biomaterials*, 31 (32), 8313-8322.
- Castroviejo, R. (1950) Total Penetrating Keratoplasty: Preliminary Report. *Transactions of the American Ophthalmological Society*, 48, 297-312.
- Chandran, P. L. & Barocas, V. H. (2004) Microstructural mechanics of collagen gels in confined compression: Poroelasticity, viscoelasticity, and collapse. *Journal of Biomechanical Engineering-Transactions of the Asme*, 126 (2), 152-166.
- Chen, J. J. Y. & Tseng, S. C. G. (1990) Corneal Epithelial Wound Healing in Partial Limbal Deficiency. *Investigative Ophthalmology & Visual Science*, 31 (7), 1301-1314.
- Chen, J. J. Y. & Tseng, S. C. G. (1991) Abnormal corneal epithelial wound healing in partial-thickness removal of limbal epithelium. *Investigative Ophthalmology & Visual Science*, 32 (8), 2219-2233.
- Chen, Q., Fitch, J. M., Gibney, E. & Linsenmayer, T. F. (1993) Type II Collagen During Cartilage and Corneal Development: Immunohistochemical Analysis With an Anti-Telopeptide Antibody. *Developmental Dynamics*, 196 (1), 47-53.
- Cho, H. I., Covington, H. I. & Cintron, C. (1990) Immunolocalization of Type VI Collagen in Developing and Healing Rabbit Cornea. *Investigative Ophthalmology & Visual Science*, 31 (6), 1096-1102.
- Cintron, C., Covington, H. I. & Kublin, C. L. (1990) Morphologic Analyses of Proteoglycans in Rabbit Corneal Scars. *Investigative Ophthalmology & Visual Science*, 31 (9), 1789-1798.

- Cintron, C., Hong, B. S. & Kublin, C. L. (1981) Quantitative analysis of collagen from normal developing corneas and corneal scars. *Current Eye Research*, 1 (1), 1-8.
- Cintron, C., Szamier, R. B., Hassinger, L. C. & Kublin, C. L. (1982) Scanning Electron Microscopy of Rabbit Corneal Scars. *Investigative Ophthalmology & Visual Science*, 23 (1), 50-63.
- Cisneros, D. A., Hung, C., Franz, C. A. & Muller, D. J. (2006) Observing growth steps of collagen self-assembly by time-lapse high-resolution atomic force microscopy. *Journal of Structural Biology*, 154 (3), 232-245.
- Connon, C. J., Dutch, J., Chen, B., Hopkinson, A., Mehta, J. S., Nakamura, T., Kinoshita, S. & Meek, K. M. (2010) The variation in transparency of amniotic membrane used in ocular surface regeneration. *British Journal of Ophthalmology*, 94 (8), 1057-1061.
- Cooper, D. K. C. (2003) Clinical xenotransplantation - how close are we? *Lancet*, 362 (9383), 557-559.
- Cox, J. L., Farrell, R. A., Hart, R. W. & Langham, M. E. (1970) The transparency of the mammalian cornea. *Journal of Physiology-London*, 210 (3), 601-&.
- Crabb, R. A. B., Chau, E. P., Evans, M. C., Barocas, V. H. & Hubel, A. (2006) Biomechanical and microstructural characteristics of a collagen film-based corneal stroma equivalent. *Tissue Engineering*, 12 (6), 1565-1575.
- Cvekl, A. & Tamm, E. R. (2004) Anterior eye development and ocular mesenchyme: new insights from mouse models and human diseases. *Bioessays*, 26 (4), 374-386.
- Dartt, D. A. (2009) Neural regulation of lacrimal gland secretory processes: Relevance in dry eye diseases. *Progress in Retinal and Eye Research*, 28 (3), 155-177.
- Davanger, M. & Evensen, A. (1971) Role of the Pericorneal Papillary Structure in Renewal of Corneal Epithelium. *Nature*, 229 (5286), 560-&.
- Davison, P. F. & Galbavy, E. J. (1986) Connective Tissue Remodeling in Corneal and Scleral Wounds. *Investigative Ophthalmology & Visual Science*, 27 (10), 1478-1484.
- Daya, S. M., Watson, A., Sharpe, J. R., Giledi, S., Rowe, A., Martin, R. & James, S. E. (2005) Outcomes and DNA analysis of ex vivo expanded stem cell allograft for ocular surface reconstruction. *Ophthalmology*, 112 (3), 470-477.
- DEFRA, 2006, Animal Welfare Act, www.legislation.gov.uk/ukpga/2006/45/contents (accessed 15th June 2015)
- Dikstein, S. & Maurice, D. M. (1972) The Metabolic Basis to the Fluid Pump of the Cornea. *Journal of Physiology-London*, 221 (1), 29.
- Doane, M. G., Dohlman, C. H. & Bearse, G. (1996) Fabrication of a keratoprosthesis. *Cornea*, 15 (2), 179-184.
- Doughty, M. J. (2000) Swelling of the collagen-keratocyte matrix of the bovine corneal stroma ex vivo in various solutions and its relationship to tissue thickness. *Tissue & Cell*, 32 (6), 478-493.

- Dropcova, S., Denyer, S. P., Lloyd, A. W., Gard, P. R., Hanlon, G. W., Mikhalovsky, S. V., Sandeman, S., Olliff, C. J. & Faragher, R. G. A. (1999) A standard strain of human ocular keratocytes. *Ophthalmic Research*, 31 (1), 33-41.
- Du, Y. D., Funderburgh, M. L., Sundarraj, N. & Funderburgh, J. L. (2005) Multipotent stem cells in human corneal stroma. *Stem Cells*, 23 (9), 1266-1275.
- Dua, H. S. & Azuara-Blanco, A. (2000) Limbal stem cells of the corneal epithelium. *Survey of Ophthalmology*, 44 (5), 415-425.
- Dua, H. S., Faraj, L. A., Branch, M. J., Yeung, A. M., Elalfy, M. S., Said, D. G., Gray, T. & Lowe, J. (2014) The collagen matrix of the human trabecular meshwork is an extension of the novel pre-Descemet's layer (Dua's layer). *British Journal of Ophthalmology*, 98 (5), 691-697.
- Dua, H. S., Faraj, L. A., Said, D. G., Gray, T. & Lowe, J. (2013) Human Corneal Anatomy Redefined A Novel Pre-Descemet's Layer (Dua's Layer). *Ophthalmology*, 120 (9), 1778-1785.
- Duan, D., Klenkler, B. J. & Sheardown, H. (2006) Progress in the development of a corneal replacement: keratoprotheses and tissue-engineered corneas. *Expert Review of Medical Devices*, 3 (1), 59-72.
- Dupps, W. J. & Wilson, S. E. (2006) Biomechanics and wound healing in the cornea. *Experimental Eye Research*, 83 (4), 709-720.
- Engelmann, K., Bednarz, J. & Valtink, M. (2004) Prospects for endothelial transplantation. *Experimental Eye Research*, 78 (3), 573-578.
- Executive, N. (1999) Variant Creutzfeldt-Jakob Disease (vCJD): Minimising the Risk of Transmission.
- Fagerholm, P., Lagali, N. S., Ong, J. A., Merrett, K., Jackson, W. B., Polarek, J. W., Suuronen, E., Liu, Y. W., Brunette, I., Griffith, M. (2014) Stable corneal regeneration four years after implantation of a cell-free recombinant human collagen scaffold, *Biomaterials*, 35 (8) 2420-2427.
- Fagerholm, P., Lagali, N. S., Merrett, K., Jackson, W. B., Munger, R., Liu, Y. W., Polarek, J. W., Soderqvist, M. & Griffith, M. (2010) A Biosynthetic Alternative to Human Donor Tissue for Inducing Corneal Regeneration: 24-Month Follow-Up of a Phase 1 Clinical Study. *Science Translational Medicine*, 2 (46), 8.
- Fini, M. E., Girard, M. T. & Matsubara, M. (1992) Collagenolytic/gelatinolytic enzymes in corneal wound healing. *Acta Ophthalmol Suppl*, (202), 26-33.
- Fitch, J., Fini, M. E., Beebe, D. C. & Linsenmayer, T. F. (1998) Collagen type IX and developmentally regulated swelling of the avian primary corneal stroma. *Developmental Dynamics*, 212 (1), 27-37.
- Fitch, J. M., Birk, D. E., Linsenmayer, C. & Linsenmayer, T. F. (1990) The spatial organization of Descemet's membrane-associated type IV collagen in the avian cornea. *Journal of Cell Biology*, 110 (4), 1457-1468.

- Fitch, J. M., Linsenmayer, C. M. & Linsenmayer, T. F. (1994) Collagen Fibril Assembly in the Developing Avian Primary Corneal Stroma. *Investigative Ophthalmology & Visual Science*, 35 (3), 862-869.
- Freegard, T. J. (1997) The physical basis of transparency of the normal cornea. *Eye*, 11, 465-471.
- Friedrichs, J., Taubenberger, A., Franz, C. M. & Muller, D. J. (2007) Cellular remodelling of individual collagen fibrils visualized by time-lapse AFM. *Journal of Molecular Biology*, 372 (3), 594-607.
- Fu, Y., Fan, X. Q., Chen, P., Shao, C. Y. & Lu, W. J. (2010) Reconstruction of a Tissue-Engineered Cornea with Porcine Corneal Acellular Matrix as the Scaffold. *Cells Tissues Organs*, 191 (3), 193-202.
- Fukuda, K., Chikama, T., Nakamura, M. & Nishida, T. (1999) Differential distribution of subchains of the basement membrane components type IV collagen and laminin among the amniotic membrane, cornea, and conjunctiva. *Cornea*, 18 (1), 73-79.
- Funderburgh, J. L. (2000) Keratan sulfate: structure, biosynthesis, and function. *Glycobiology*, 10 (10), 951-958.
- Funderburgh, J. L., Caterson, B. & Conrad, G. W. (1986) Keratan sulfate proteoglycan during embryonic development of the chicken cornea. *Developmental Biology*, 116 (2), 267-277.
- Gain, P., Thuret, G., Chiquet, C., Rizzi, P., Pugnet, J. L., Acquart, S., Colpart, J. J., Le Petit, J. C. & Maugery, J. (2002) Cornea procurement from very old donors: post organ culture cornea outcome and recipient graft outcome. *British Journal of Ophthalmology*, 86 (4), 404-411.
- Gal, R., Dontchev, M., Beck, R., Mannis, M., Holland, E., Kollman, C., Dunn, S., Heck, E., Lass, J., Montoya, M., Schultze, R., Stulting, D., Sugar, A., Sugar, J., Tennant, B. & Verdier, D. (2008) The effect of donor age on corneal transplantation outcome: Results of the cornea donor study. *Ophthalmology*, 115 (4), 620-626.
- Germundsson, J., Karanis, G., Fagerholm, P. & Lagali, N. (2013) Age-Related Thinning of Bowman's Layer in the Human Cornea *In-vivo*. *Investigative Ophthalmology & Visual Science*, 54 (9), 6143-6149.
- Gipson, I. K., Spurrmichaud, S. J. & Tisdale, A. S. (1987) Anchoring Fibrils Form a Complex Network in Human and Rabbit Cornea. *Investigative Ophthalmology & Visual Science*, 28 (2), 212-220.
- Goldman, J. N. & Benedek, G. B. (1967) The relationship between morphology and transparency in the non-swelling corneal stroma of the shark. *Invest Ophthalmol*, 6 ((6)), 574-600.
- Goldman, J. N., Benedek, G. B., Dohlman, C. H. & Kravitt, B. (1968) Structural alterations affecting transparency in swollen human corneas. *Investigative Ophthalmology*, 7 (5), 501-&.
- Gomaa, A., Comyn, O. & Liu, C. (2010) Keratoprotheses in clinical practice - a review. *Clinical and Experimental Ophthalmology*, 38 (2), 211-226.

- Goodhew, P. J., Humphreys, J. & Beanland, R. (2001) *Electron Microscopy and Analysis*, Taylor & Frances.
- Gordon, M. K., Foley, J. W., Linsenmayer, T. F. & Fitch, J. M. (1996) Temporal expression of types XII and XIV collagen mRNA and protein during avian corneal development. *Developmental Dynamics*, 206 (1), 49-58.
- Gordon, M. K. & Hahn, R. A. (2010) Collagens. *Cell and Tissue Research*, 339 (1), 247-257.
- Gough, J. E., Scotchford, C. A. & Downes, S. (2002) Cytotoxicity of glutaraldehyde crosslinked collagen/poly(vinyl alcohol) films is by the mechanism of apoptosis. *Journal of Biomedical Materials Research*, 61 (1), 121-130.
- Gregory, J. D., Coster, L. & Damle, S. P. (1982) Proteoglycans of Rabbit Corneal Stroma: Isolation and partial characterization. *Journal of Biological Chemistry*, 257 (12), 6965-6970.
- Griffith, M., Hakim, M., Shimmura, S., Watsky, M. A., Li, F. F., Carlsson, D., Doillon, C. J., Nakamura, M., Suuronen, E., Shinozaki, N., Nakata, K. & Sheardown, H. (2002) Artificial human corneas - Scaffolds for transplantation and host regeneration. *Cornea*, 21 (7), S54-S61.
- Griffith, M., Osborne, R., Munger, R., Xiong, X. J., Doillon, C. J., Laycock, N. L. C., Hakim, M., Song, Y. & Watsky, M. A. (1999) Functional human corneal equivalents constructed from cell lines. *Science*, 286 (5447), 2169-2172.
- Guo, X. Q., Hutcheon, A. E. K., Melotti, S. A., Zieske, J. D., Trinkaus-Randall, V. & Ruberti, J. W. (2007) Morphologic characterization of organized extracellular matrix deposition by ascorbic acid-stimulated human corneal fibroblasts. *Investigative Ophthalmology & Visual Science*, 48 (9), 4050-4060.
- Hashimoto, Y., Funamoto, S., Sasaki, S., Honda, T., Hattori, S., Nam, K., Kimura, T., Mochizuki, M., Fujisato, T., Kobayashi, H. & Kishida, A. (2010) Preparation and characterization of decellularized cornea using high-hydrostatic pressurization for corneal tissue engineering. *Biomaterials*, 31 (14), 3941-8.
- Hashimoto, Y., Shieh, T. Y., Aoyama, H., Izawa, Y. & Hayakawa, T. (1986) ISOLATION AND CHARACTERIZATION OF TYPE-V COLLAGEN FROM HUMAN POSTBURN GRANULATION TISSUES. *Journal of Investigative Dermatology*, 87 (4), 540-543.
- Hassell, J. R. & Birk, D. E. (2010) The molecular basis of corneal transparency. *Experimental Eye Research*, 91 (3), 326-335.
- Hassell, J. R., Cintron, C., Kublin, C. & Newsome, D. A. (1983) Proteoglycan changes during restoration of transparency in corneal scars. *Archives of Biochemistry and Biophysics*, 222 (2), 362-369.
- Hayashi, M., Ninomiya, Y., Hayashi, K., Linsenmayer, T. F., Olsen, B. R. & Trelstad, R. L. (1988) Secretion of collagen types I and II by epithelial and endothelial cells in the developing chick cornea demonstrated by in situ hybridization and immunohistochemistry. *Development*, 103 (1), 27-36.
- Hayes, S., Boote, C., Lewis, J., Sheppard, J., Abahussin, M., Quantock, A. J., Purslow, C., Votruba, M. & Meek, K. M. (2007) Comparative study of fibrillar collagen

- arrangement in the corneas of primates and other mammals. *Anatomical Record-Advances in Integrative Anatomy and Evolutionary Biology*, 290, 1542-1550.
- Herse, P. R. (1990) Corneal Hydration Control in Normal and Alloxon-Induced Diabetic Rabbits. *Investigative Ophthalmology & Visual Science*, 31 (11), 2205-2213.
- Hirsch, M., Prenant, G. & Renard, G. (2001) Three-dimensional supramolecular organization of the extracellular matrix in human and rabbit corneal stroma, as revealed by ultrarapid-freezing and deep-etching methods. *Experimental Eye Research*, 72 (2), 123-135.
- Home Office, (2013), Research and Testing Using Animals, <https://www.gov.uk/research-and-testing-using-animals>, (accessed 15th June 2015)
- Huang, A. J. W. & Tseng, S. C. G. (1991) Corneal Epithelial Wound Healing in the Absence of Limbal Epithelium. *Investigative Ophthalmology & Visual Science*, 32 (1), 96-105.
- Huh, M. I., Lee, Y. M., Seo, S. K., Kang, B. S., Chang, Y., Lee, Y. S., Fini, M. E., Kang, S. S. & Jung, J. C. (2007) Roles of MMP/TIMP in regulating matrix swelling and cell migration during chick corneal development. *Journal of Cellular Biochemistry*, 101 (5), 1222-1237.
- Ishizaki, M., Westerhausenlarson, A., Kino, J., Hayashi, T. & Kao, W. W. Y. (1993) Distribution of Collagen IV in Human Ocular Tissues. *Investigative Ophthalmology & Visual Science*, 34 (9), 2680-2689.
- James, S. E., Rowe, A., Ilari, L., Daya, S. & Martin, R. (2001) The potential for eye bank limbal rings to generate cultured corneal epithelial allografts. *Cornea*, 20 (5), 488-494.
- Janin-Manificat, H., Rovere, M. R., Galiacy, S. D., Malecaze, F., Hulmes, D. J. S., Moali, C. & Damour, O. (2012) Development of ex vivo organ culture models to mimic human corneal scarring. *Molecular Vision*, 18 (294-97), 2896-2908.
- Johnson, D. H., Bourne, W. M. & Campbell, J. (1982) The Ultrastructure of Descemet's membrane I: Changes with age in normal cornea. *Archives of Ophthalmology*, 100 (12), 1942-1947.
- Jonkman, M. F. & Bouwes Bavinck, J. N. (1993) Vooruitgang in onderzoek naar epidermolysis bullosa. *Tijdschr Dermatol Venereol*.
- Joyce, N. C. & Zhu, C. C. (2004) Human corneal endothelial cell proliferation: potential for use in regenerative medicine. *Cornea*, 23 (8 Suppl), S8-S19.
- Kaufman, H. E. E. A. (2000) *Part II, Clinical Science*, Butterworth-Heinemann.
- Kenyon, K. R. (1989) Limbal autograft transplantation for chemical and thermal burns. *Dev Ophthalmol*, 18, 53-8.
- Kenyon, K. R. & Tseng, S. C. G. (1989) Limbal autograft transplantation for ocular surface disorders. *Ophthalmology*, 96 (5), 709-723.
- Khan, B. F., Harissi-Dagher, M., Khan, D. M. & Dohlman, C. H. (2007) Advances in Boston keratoprosthesis: enhancing retention and prevention of infection and inflammation. *Int Ophthalmol Clin*, 47 (2), 61-71.

- Kipling, D., Jones, D. L., Smith, S. K., Giles, P. J., Jennert-Burston, K., Ibrahim, B., Sheerin, A. N. P., Evans, A. J. C., Rhys-Williams, W. & Faragher, R. G. A. (2009) A transcriptomic analysis of the EK1.Br strain of human fibroblastoid keratocytes: The effects of growth, quiescence and senescence. *Experimental Eye Research*, 88 (2), 277-285.
- Kivela, T. & Uusitalo, M. (1998) Structure, development and function of cytoskeletal elements in non-neuronal cells of the human eye. *Progress in Retinal and Eye Research*, 17 (3), 385-428.
- Knupp, C., Pinali, C., Lewis, P. N., Parfitt, G. J., Young, R. D., Meek, K. M. & Quantock, A. J. (2009) The Architecture of the Cornea and Structural Basis of its Transparency. *Advances in Protein Chemistry and Structural Biology, Vol 78*. San Diego, Elsevier Academic Press Inc.
- Komai, Y. & Ushiki, T. (1991) The three-dimensional organisation of collagen fibrils in the human cornea and sclera. *Investigative Ophthalmology & Visual Science*, 32 (8), 2244-2258.
- Krenzer, K. L. & Freddo, T. F. (1997) Cytokeratin expression in normal human bulbar conjunctiva obtained by impression cytology. *Invest Ophthalmol Vis Sci*, 38 (1), 142-52.
- Kruse, F. E., Chen, J. J. Y., Tsai, R. J. F. & Tseng, S. C. G. (1990) Conjunctival Transdifferentiation Is due to the Incomplete Removal of Limbal Basal Epithelium. *Investigative Ophthalmology & Visual Science*, 31 (9), 1903-1913.
- Lagali, N., Fagerholm, P. & Griffith, M. (2011) Biosynthetic corneas: prospects for supplementing the human donor cornea supply. *Expert Review of Medical Devices*, 8 (2), 127-130.
- Lee, W., Miyagawa, Y., Long, C., Cooper, D. K. & Hara, H. (2014) A comparison of three methods of decellularization of pig corneas to reduce immunogenicity. *Int J Ophthalmol*, 7 (4), 587-93.
- Lehrer, M. S., Sun, T. T. & Lavker, R. M. (1998) Strategies of epithelial repair: modulation of stem cell and transit amplifying cell proliferation. *Journal of Cell Science*, 111, 2867-2875.
- Levis, H. & Daniels, J. T. (2009) New technologies in limbal epithelial stem cell transplantation. *Current Opinion in Biotechnology*, 20 (5), 593-597.
- Levis, H. J., Brown, R. A. & Daniels, J. T. (2010) Plastic compressed collagen as a biomimetic substrate for human limbal epithelial cell culture. *Biomaterials*, 31 (30), 7726-7737.
- Lewis, P. N., Pinali, C., Young, R. D., Meek, K. M., Quantock, A. J. & Knupp, C. (2010) Structural interactions between collagen and proteoglycans are elucidated by three-dimensional electron tomography of bovine cornea. *Structure*, 18 (2), 239-45.
- Li, F. F., Carlsson, D., Lohmann, C., Suuronen, E., Vascotto, S., Kobuch, K., Sheardown, H., Munger, R., Nakamura, M. & Griffith, M. (2003) Cellular and nerve regeneration within a biosynthetic extracellular matrix for corneal transplantation. *Proceedings*

of the National Academy of Sciences of the United States of America, 100 (26), 15346-15351.

- Li, W., Hayashida, Y., Chen, Y. T. & Tseng, S. C. G. (2007a) Niche regulation of corneal epithelial stem cells at the limbus. *Cell Research*, 17 (1), 26-36.
- Li, W., Sabater, A. L., Chen, Y. T., Hayashida, Y., Chen, S. Y., He, H. & Tseng, S. C. G. (2007b) A novel method of isolation, preservation, and expansion of human corneal endothelial cells. *Investigative Ophthalmology & Visual Science*, 48 (2), 614-620.
- Linsenmayer, T. F., Fitch, J. M., Gordon, M. K., Cai, C. X., Igoe, F., Marchant, J. K. & Birk, D. E. (1998) Development and roles of collagenous matrices in the embryonic avian cornea. *Progress in Retinal and Eye Research*, 17 (2), 231-265.
- Linsenmayer, T. F., Gibney, E., Gordon, M. K., Marchant, J. K., Hayashi, M. & Fitch, J. M. (1990) Extracellular Matrices of the Developing Chick Retina and Cornea: Localization of mRNAs for Collagen Types II and IX by in Situ Hybridization. *Investigative Ophthalmology & Visual Science*, 31 (7), 1271-1276.
- Liu, W., Merrett, K., Griffith, M., Fagerholm, P., Dravida, S., Heyne, B., Scaiano, J. C., Watsky, M. A., Shinozaki, N., Lagali, N., Munger, R. & Li, F. (2008) Recombinant human collagen for tissue engineered corneal substitutes. *Biomaterials*, 29 (9), 1147-1158.
- Liu, Y., Griffith, M., Watsky, M. A., Forrester, J. V., Kuffova, L., Grant, D., Merrett, K. & Carlsson, D. J. (2006a) Properties of porcine and recombinant human collagen matrices for optically clear tissue engineering applications. *Biomacromolecules*, 7 (6), 1819-1828.
- Liu, Y. W., Gan, L. H., Carlsson, D. J., Fagerholm, P., Lagali, N., Watsky, M. A., Munger, R., Hodge, W. G., Priest, D. & Griffith, M. (2006b) A simple, cross-linked collagen tissue substitute for corneal implantation. *Investigative Ophthalmology & Visual Science*, 47 (5), 1869-1875.
- Luo, H., Lu, Y., Wu, T., Zhang, M., Zhang, Y. & Jin, Y. (2013) Construction of tissue-engineered cornea composed of amniotic epithelial cells and acellular porcine cornea for treating corneal alkali burn. *Biomaterials*, 34 (28), 6748-59.
- Lynch, A. P. & Ahearne, M. (2013) Strategies for developing decellularized corneal scaffolds. *Experimental Eye Research*, 108, 42-47.
- Marieb, E. N. (2004) The Special Senses. *Human Anatomy and Physiology*.
- Matsubara, M., Girard, M. T., Kublin, C. L., Cintron, C. & Fini, M. E. (1991a) Differential roles for two gelatinolytic enzymes of the matrix metalloproteinase family in the remodelling cornea. *Developmental Biology*, 147 (2), 425-439.
- Matsubara, M., Zieske, J. D. & Fini, M. E. (1991b) Mechanism of Basement Membrane Dissolution Preceding Corneal Ulceration. *Investigative Ophthalmology & Visual Science*, 32 (13), 3221-3237.
- Maurice, D. M. (1957) The structure and transparency of the cornea. *Journal of Physiology-London*, 136 (2), 263-&.

- Mcgowan, S. L., Edelhauser, H. F., Pfister, R. R. & Whitehart, D. R. (2007) Stem cell markers in the human posterior limbus and corneal endothelium of unwounded and wounded corneas. *Molecular Vision*, 13, 1984-2000.
- Mclaughlin, C. R., Acosta, M. C., Luna, C., Liu, W., Belmonte, C., Griffith, M. & Gallar, J. (2009a) Regeneration of functional nerves within full thickness collagen-phosphorylcholine corneal substitute implants in guinea pigs. *Biomaterials*.
- Mclaughlin, C. R., Tsai, R. J. F., Latorre, M. A. & Griffith, M. (2009b) Bioengineered corneas for transplantation and *in-vitro* toxicology. *Frontiers in Bioscience*, 14, 3326-3337.
- Mclaughlin, J. S., Linsenmayer, T. F. & Birk, D. E. (1989) Type V collagen synthesis and deposition by chicken embryo corneal fibroblasts *in-vitro*. *Journal of Cell Science*, 94, 371-379.
- Meek, K. M. & Boote, C. (2004) The organization of collagen in the corneal stroma. *Experimental Eye Research*, 78 (3), 503-512.
- Meek, K. M. & Boote, C. (2009) The use of X-ray scattering techniques to quantify the orientation and distribution of collagen in the corneal stroma. *Progress in Retinal and Eye Research*, 28 (5), 369-392.
- Meek, K. M. & Fullwood, N. J. (2001) Corneal and scleral collagens - a microscopist's perspective. *Micron*, 32 (3), 261-272.
- Meng, I. D. & Kurose, M. (2013) The role of corneal afferent neurons in regulating tears under normal and dry eye conditions. *Experimental Eye Research*, 117, 79-87.
- Merrett, K., Fagerholm, P., Mclaughlin, C. R., Dravida, S., Lagali, N., Shinozaki, N., Watsky, M. A., Munger, R., Kato, Y., Li, F. F., Marmo, C. J. & Griffith, M. (2008) Tissue-engineered recombinant human collagen-based corneal substitutes for implantation: Performance of type I versus type III collagen. *Investigative Ophthalmology & Visual Science*, 49 (9), 3887-3894.
- Mi, S., Chen, B., Wright, B. & Connon, C. (2010a) Plastic compression of a collagen gel forms a much improved scaffold for ocular surface tissue engineering over conventional collagen gels. *J Biomed Mater Res A*, 95 (2), 447-53.
- Mi, S. L., Chen, B., Wright, B. & Connon, C. J. (2010b) Ex Vivo Construction of an Artificial Ocular Surface by Combination of Corneal Limbal Epithelial Cells and a Compressed Collagen Scaffold Containing Keratocytes. *Tissue Engineering Part A*, 16 (6), 2091-2100.
- Mimura, T., Yamagami, S. & Amano, S. (2013) Corneal endothelial regeneration and tissue engineering. *Progress in Retinal and Eye Research*, 35, 1-17.
- Muller, L. J., Pels, E., Schurmans, L. & Vrensen, G. (2004) A new three-dimensional model of the organization of proteoglycans and collagen fibrils in the human corneal stroma. *Experimental Eye Research*, 78 (3), 493-501.
- Muller, L. J., Pels, L. & Vrensen, G. (1995) Novel Aspects of the Ultrastructural Organization of Human Corneal Keratocytes. *Investigative Ophthalmology & Visual Science*, 36 (13), 2557-2567.

- Nelson, J. D. & J.D., C. (1997) The Conjunctiva: Anatomy and physiology. IN KRACHMER, J. H. E. A. (Ed.) *Cornea*.
- NHS Blood and Transplant, (2012) Organ Donation and Transplantation - Activity figures for the UK as at 23rd March 2012. NHS Blood & Transplant.
- NHS Blood and Transplant, (2014) Organ Donation and Transplantation: Activity Report 2013/14. NHS Blood & Transplant.
- NICE (National Institute for Health and Clinical Excellence) (2007) Tissue-Cultured Limbal Stem Cell Allograft Transplantation for Regrowth of Corneal Epithelium. *NICE Guidance Interventional Procedures, IPG216*, pp. 1-10, 2007
- Nishida, T., Al., E. & Al, E. (1997) Basic Science: Cornea. IN KRACHMER, J. H. E. A. (Ed.) *Cornea*.
- Nishida, T., Yasumoto, K., Otori, T. & Desaki, J. (1988) The Network Structure of Corneal Fibroblasts in the Rat as Revealed by Scanning Electron Microscopy. *Investigative Ophthalmology & Visual Science*, 29 (12), 1887-1890.
- O'callaghan, A. R. & Daniels, J. T. (2011) Concise Review: Limbal Epithelial Stem Cell Therapy: Controversies and Challenges. *Stem Cells*, 29 (12), 1923-1932.
- O'neal, M. R. & Polse, K. A. (1985) *In-vivo* Assessment of Mechanisms Controlling Corneal Hydration. *Investigative Ophthalmology & Visual Science*, 26 (6), 849-856.
- O'sullivan, F. & Clynes, M. (2007) Limbal stem cells, a review of their identification and culture for clinical use. *Cytotechnology*, 53 (1-3), 101-106.
- Oh, J., Kim, M., Ko, J., Lee, H., Park, C., Kim, S., Wee, W. & Lee, J. (2009a) Histological differences in full-thickness vs. lamellar corneal pig-to-rabbit xenotransplantation. *Vet Ophthalmol*, 12 (2), 78-82.
- Oh, J., Kim, M., Lee, H., Ko, J., Wee, W. & Lee, J. (2009b) Comparative observation of freeze-thaw-induced damage in pig, rabbit, and human corneal stroma. *Vet Ophthalmol*, 12 Suppl 1, 50-6.
- Oh, J. Y., Kim, M. K., Lee, H. J., Ko, J. H., Wee, W. R. & Lee, J. H. (2009c) Processing Porcine Cornea for Biomedical Applications. *Tissue Engineering Part C-Methods*, 15 (4), 635-645.
- Ordonez, P. & Di Girolamo, N. (2012) Limbal Epithelial Stem Cells: Role of the Niche Microenvironment. *Stem Cells*, 30 (2), 100-107.
- Pang, K. P., Du, L. Q. & Wu, X. Y. (2010) A rabbit anterior cornea replacement derived from acellular porcine cornea matrix, epithelial cells and keratocytes. *Biomaterials*, 31 (28), 7257-7265.
- Parfitt, G. J., Pinali, C., Young, R. D., Quantock, A. J. & Knupp, C. (2010) Three-dimensional reconstruction of collagen-proteoglycan interactions in the mouse corneal stroma by electron tomography. *J Struct Biol*, 170 (2), 392-7.
- Pascolini, D. & Mariotti, S. P. (2012) Global estimates of visual impairment: 2010. *Br J Ophthalmol*, 96 (5), 614-8.

- Pellegrini, G., Traverso, C. E., Franzi, A. T., Zingirian, M., Cancedda, R. & De Luca, M. (1997) Long-term restoration of damaged corneal surfaces with autologous cultivated corneal epithelium. *Lancet*, 349 (9057), 990-3.
- Pels, E. & Schuchard, Y. (1983) ORGAN-CULTURE PRESERVATION OF HUMAN CORNEAS. *Documenta Ophthalmologica*, 56 (1-2), 147-153.
- Pinnamaneni, N. & Funderburgh, J. L. (2012) Concise Review: Stem Cells in the Corneal Stroma. *Stem Cells*, 30 (6), 1059-1063.
- Pleyer, U. & Schlickeiser, S. (2009) The taming of the shrew? The immunology of corneal transplantation. *Acta Ophthalmologica*, 87 (5), 488-497.
- Poddar, R. Cortés, D. E., Werner, J. S., Mannis, M. J., Zawadski, R. J., (2013) Three-dimensional anterior segment imaging in patients with type 1 Boston Keratoprosthesis with switchable depth range swept source optical coherence tomography. *Journal of Biomedical Optics*, 18 (8)
- Proulx, S., Uwamaliya, J. D., Carrier, P., Deschambeault, A., Audet, C., Giasson, C. J., Guerin, S. L., Auger, F. A. & Germain, L. (2010) Reconstruction of a human cornea by the self-assembly approach of tissue engineering using the three native cell types. *Molecular Vision*, 16 (234-36), 2192-2201.
- Quantock, A. J. & Young, R. D. (2008) Development of the Corneal Stroma, and the Collagen-Proteoglycan Associations That Help Define Its Structure and Function. *Developmental Dynamics*, 237 (10), 2607-2621.
- Radner, W. & Mallinger, R. (2002) Interlacing of collagen lamellae in the midstroma of the human cornea. *Cornea*, 21 (6), 598-601.
- Radner, W., Zehetmayer, M., Aufreiter, R. & Mallinger, R. (1998) Interlacing and cross-angle distribution of collagen lamellae in the human cornea. *Cornea*, 17 (5), 537-543.
- Ramaesh, T., Collinson, J. M., Ramaesh, K., Kaufman, M. H., West, J. D. & Dhillon, B. (2003) Corneal abnormalities in Pax6(+/-) small eye mice mimic human aniridia-related keratopathy. *Investigative Ophthalmology & Visual Science*, 44 (5), 1871-1878.
- Rawe, I. M., Tuft, S. J. & Meek, K. M. (1992) Proteoglycan and collagen morphology in superficially scarred rabbit cornea. *Histochemical Journal*, 24 (6), 311-318.
- Robert, L., Legeais, J. M., Robert, A. M. & Renard, G. (2001) Corneal collagens. *Pathologie Biologie*, 49 (4), 353-363.
- Rubaltelli, E., Barra, P., Canova, D., Germani, G., Tomat, S., Ancona, E., Cozzi, E., Rumiati, R., (2009) People's attitudes toward xenotransplantation: affective reactions and the influence of evaluation context. *Xenotransplantation*, 16 (3), 129-134
- Ruberti, J. W. & Zieske, J. D. (2008) Prelude to corneal tissue engineering - Gaining control of collagen organization. *Progress in Retinal and Eye Research*, 27 (5), 549-577.
- Sasaki, S., Funamoto, S., Hashimoto, Y., Kimura, T., Honda, T., Hattori, S., Kobayashi, H., Kishida, A. & Mochizuki, M. (2009) *In-vivo* evaluation of a novel scaffold for artificial corneas prepared by using ultrahigh hydrostatic pressure to decellularize porcine corneas. *Molecular Vision*, 15 (216-18), 2022-2028.

- Schermer, A., Galvin, S. & Sun, T. T. (1986) Differentiation-related Expression of a Major 64K Corneal Keratin *In-vivo* and In Culture Suggests Limbal Location of Corneal Epithelial Stem Cells. *Journal of Cell Biology*, 103 (1), 49-62.
- Schlitt, H.J., Brunkhorst, R. Haverich, A., Raab, R., (1999), Attitude of patients towards transplantation of xenogenic organs, *Langenbecks Archives of Surgery*, 384 (4), 384-391
- Schlotzer-Schrehardt, U. & Kruse, F. E. (2005) Identification and characterization of limbal stem cells. *Experimental Eye Research*, 81 (3), 247-264.
- Schlötzer-Schrehardt, U., Bachmann, B. O., Tourtas, T., Torricelli, A. A., Singh, A., González, S., Mei, H., Deng, S. X., Wilson, S. E. & Kruse, F. E. (2014) Ultrastructure of the Posterior Corneal Stroma. *Ophthalmology*.
- Scott, J. E. (1995) Extracellular matrix, supramolecular organisation and shape. *J Anat*, 187 (Pt 2), 259-69.
- Scott, J. E. (2001) Structure and function in extracellular matrices depend on interactions between anionic glycosaminoglycans. *Pathol Biol (Paris)*, 49 (4), 284-9.
- Scott, J. E. & Bosworth, T. R. (1990) A comparative biochemical and ultrastructural study of proteoglycan-collagen interactions in corneal stroma. *Biochemical Journal*, 270 (2), 491-497.
- Scott, J. E. & Haigh, M. (1985) Small'-proteoglycan:collagen interactions: keratan sulphate proteoglycan associates with rabbit corneal collagen fibrils at the 'a' and 'c' bands. *Bioscience Reports*, 5 (9), 765-774.
- Shao, Y., Quyang, L. W., Zhou, Y. P., Tang, J., Tan, Y. H., Liu, Q. P., Lin, Z. R., Yin, T. T., Qiu, F. F. & Liu, Z. G. (2010) Preparation and physical properties of a novel biocompatible porcine corneal acellularized matrix. *In-vitro Cellular & Developmental Biology-Animal*, 46 (7), 600-605.
- Shao, Y., Yu, Y., Pei, C. G., Qu, Y. L., Gao, G. P., Yang, J. L., Zhou, Q., Yang, L. & Liu, Q. P. (2012) The expression and distribution of alpha -Gal gene in various species ocular surface tissue. *International Journal of Ophthalmology*, 5 (5), 543-548.
- Sharpe, J. R., Daya, S. M., Dimitriadi, M., Martin, R. & James, S. E. (2007) Survival of cultured allogeneic limbal epithelial cells following corneal repair. *Tissue Engineering*, 13 (1), 123-132.
- Shevchenko, R. V., Eenma, M., Rowshanravan, B., Allan, I. U., Savina, I. N., Illsley, M., Salmon, M., James, S. L., Mikhalovsky, S. V., James, S. E., (2014) The in-vitro characterization of a gelatin scaffold, prepared by cryogelation and assessed in vivo as a dermal replacement in wound repair. *Acta Biomaterialia*, 10, 3156-3166.
- Singh, G., Bohnke, M., Vondomarus, D. & Draeger, J. (1985) ENDOTHELIAL-CELL DENSITIES IN CORNEAL DONOR MATERIAL. *Annals of Ophthalmology*, 17 (10), 627-631.
- Smith, S. M. & Birk, D. E. (2012) Focus on Molecules: Collagens V and XI. *Experimental Eye Research*, 98, 105-106.
- Stoiber, J., Csaky, D., Schedle, A., Ruckhofer, J. & Grabner, G. (2002) Histopathologic findings in explanted osteo-odontokeratoprosthesis. *Cornea*, 21 (4), 400-404.

- Stults, C. L. M., Macher, B. A., Bhatti, R., Srivastava, O. P. & Hindsgaul, O. (1999) Characterization of the substrate specificity of alpha 1,3galactosyltransferase utilizing modified N-acetyllactosamine disaccharides. *Glycobiology*, 9 (7), 661-668.
- Swamynathan, S., Kenchegowda, D. & Piatigorsky, J. (2011) Regulation of Corneal Epithelial Barrier Function by Kruppel-like Transcription Factor 4. *Investigative Ophthalmology & Visual Science*, 52 (3), 1762-1769.
- Tan, A. N., Tan, D. T., Tan, X. W. & Mehta, J. S. (2012) Osteo-odonto Keratoprosthesis: Systematic Review of Surgical Outcomes and Complication Rates. *Ocular Surface*, 10 (1), 15-25.
- Tanemura, M., Maruyama, S. & Galili, U. (2000) Differential expression of alpha-gal epitopes (Gal alpha 1-3Gal beta 1-4GlcNac-R) on pig and mouse organs. *Transplantation*, 69 (1), 187-190.
- Thoft, R. A. & Friend, J. (1983) The X, Y, Z Hypothesis of Corneal Epithelial Maintenance. *Investigative Ophthalmology & Visual Science*, 24 (10), 1442-1443.
- Torbet, J., Malbouyres, M., Builles, N., Justin, V., Roulet, M., Damour, O., Oldberg, A., Ruggiero, F. & Hulmes, D. J. S. (2007) Orthogonal scaffold of magnetically aligned collagen lamellae for corneal stroma reconstruction. *Biomaterials*, 28, 4268-4276.
- Trowbridge, J. M. & Gallo, R. L. (2002) Dermatan sulfate: new functions from an old glycosaminoglycan. *Glycobiology*, 12 (9), 117R-25R.
- Tsai, R. J., Li, L. M. & Chen, J. K. (2000) Reconstruction of damaged corneas by transplantation of autologous limbal epithelial cells. *New England Journal of Medicine*, 343 (2), 86-93.
- Tsai, R. J. F., Sun, T. T. & Tseng, S. C. G. (1990) Comparison of limbal and conjunctival autograft transplantation in corneal surface reconstruction in rabbits. *Ophthalmology*, 97 (4), 446-455.
- Tseng, S. C. G., Smuckler, D. & Stern, R. (1982) Comparison of Collagen Types in Adult and Fetal Bovine Cornea. *Journal of Biological Chemistry*, 257 (5), 2627-2633.
- Tuft, S. J. & Coster, D. J. (1990) THE CORNEAL ENDOTHELIUM. *Eye*, 4, 389-424.
- Ueda, A., Nishida, T., Otori, T. & Fujita, H. (1987) Electron-microscopic studies on the presence of gap junctions between corneal fibroblasts in rabbits. *Cell and Tissue Research*, 249 (2), 473-475.
- Verdier, D. D. (1997) Penetrating Keratoplasty: Technique. IN KRACHMER, J. H. E. A. (Ed.) *Cornea*.
- Vrana, E., Builles, N., Hindie, M., Damour, O., Aydinli, A. & Hasirci, V. (2008) Contact guidance enhances the quality of a tissue engineered corneal stroma. *Journal of Biomedical Materials Research Part A*, 84A (2), 454-463.
- Vrana, N. E., Builles, N., Kocak, H., Gulay, P., Justin, V., Malbouyres, A., Ruggiero, F., Damour, O. & Hasirci, V. (2007a) EDAC/NHS cross-linked collagen foams as scaffolds for artificial corneal stroma. *Journal of Biomaterials Science-Polymer Edition*, 18 (12), 1527-1545.

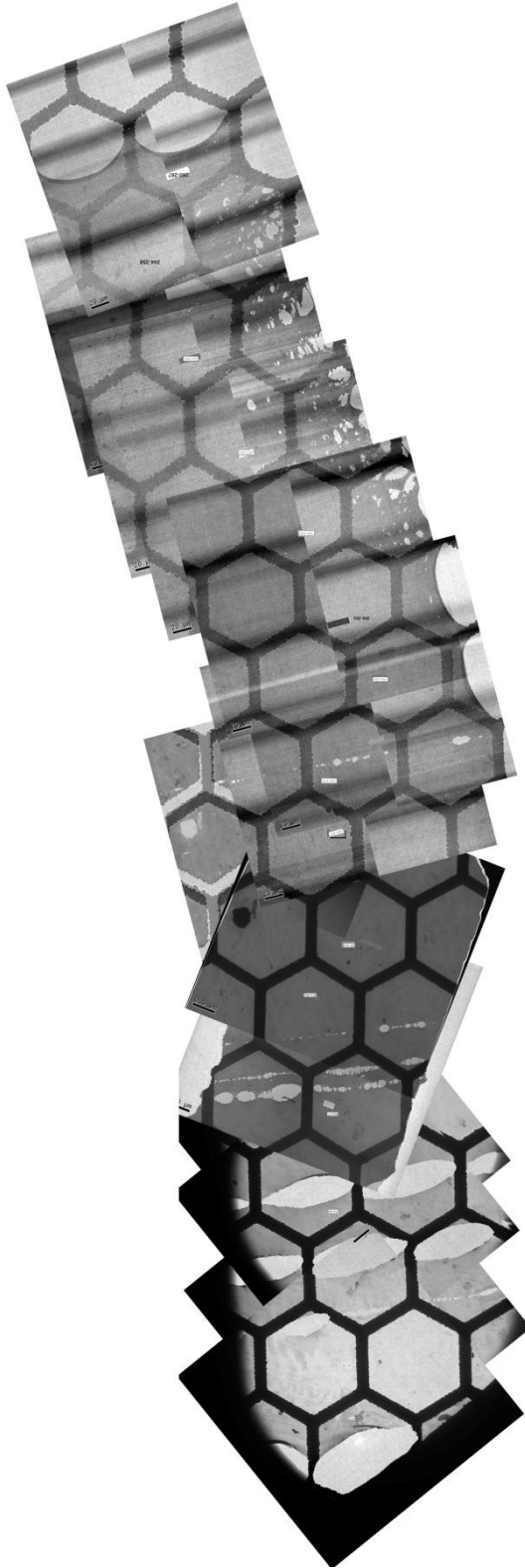
- Vrana, N. E., Elsheikh, A., Builles, N., Damour, O. & Hasirci, V. (2007b) Effect of human corneal keratocytes and retinal pigment epithelial cells on the mechanical properties of micropatterned collagen films. *Biomaterials*, 28, 4303-4310.
- Watson, P. G. & Young, R. D. (2004) Scleral structure, organisation and disease. A review. *Experimental Eye Research*, 78 (3), 609-623.
- Whikehart, D., Parikh, C., Vaughn, A., Mishler, K. & Edelhauser, H. (2005) Evidence suggesting the existence of stem cells for the human corneal endothelium. *Molecular Vision*, 11 (97), 816-824.
- Wiebe, J. P. & Dinsdale, C. J. (1991) INHIBITION OF CELL-PROLIFERATION BY GLYCEROL. *Life Sciences*, 48 (16), 1511-1517.
- Williams, K. A., Esterman, A. J., Bartlett, C., Holland, H., Hornsby, N. B., Coster, D. J. & Australian Corneal Graft, R. (2006) How effective is penetrating corneal transplantation? Factors influencing long-term outcome in multivariate analysis. *Transplantation*, 81 (6), 896-901.
- Wilson, S. E. & Hong, J. W. (2000) Bowman's layer structure and function - Critical or dispensable to corneal function? A hypothesis. *Cornea*, 19 (4), 417-420.
- Wray, L. S. & Orwin, E. J. (2009) Recreating the Microenvironment of the Native Cornea for Tissue Engineering Applications. *Tissue Engineering Part A*, 15 (7), 1463-1472.
- Xiao, X. H., Pan, S. Y., Liu, X. N., Zhu, X. P., Connon, C. J., Wu, J. & Mi, S. L. (2014) *In-vivo* study of the biocompatibility of a novel compressed collagen hydrogel scaffold for artificial corneas. *Journal of Biomedical Materials Research Part A*, 102 (6), 1782-1787.
- Yoeruek, E., Bayyoud, T., Maurus, C., Hofmann, J., Spitzer, M. S., Bartz-Schmidt, K. U. & Szurman, P. (2012) Decellularization of porcine corneas and repopulation with human corneal cells for tissue-engineered xenografts. *Acta Ophthalmologica*, 90 (2), e125-e131.
- Zeng, Y. J., Yang, J., Huang, K., Lee, Z. H. & Lee, X. Y. (2001) A comparison of biomechanical properties between human and porcine cornea. *Journal of Biomechanics*, 34 (4), 533-537.
- Zhang, Y. T., Schmack, I., Dawson, D. G., Grossniklaus, H. E., Conrad, A. H., Kariya, Y., Suzuki, K., Edelhauser, H. F. & Conrad, G. W. (2006) Keratan sulfate and chondroitin/dermatan sulfate in maximally recovered hypocellular stromal interface scars of postmortem human LASIK corneas. *Investigative Ophthalmology & Visual Science*, 47 (6), 2390-2396.
- Zhiqiang, P., Cun, S., Ying, J., Ningli, W. & Li, W. (2007) WZS-pig is a potential donor alternative in corneal xenotransplantation. *Xenotransplantation*, 14 (6), 603-11.
- Zhou, Y., Wu, Z., Ge, J. A., Wan, P. X., Li, N. Y., Xiang, P., Gao, Q. Y. & Wang, Z. C. (2011) Development and Characterization of Acellular Porcine Corneal Matrix Using Sodium Dodecylsulfate. *Cornea*, 30 (1), 73-82.

- Zimmermann, D. R., Trueb, B., Winterhalter, K. H., Witmer, R. & Fischer, R. W. (1986) Type VI collagen is a major component of the human cornea. *Febs Letters*, 197 (1-2), 55-58.
- Zuidema, J. M., Rivet, C.J., Gilbert, R. J., Morrison, F. A., (2013) A protocol for rheological characterisation of hydrogels for tissue engineering strategies. *Journal of Biomedical Materials B: Applied Biomaterials*, 102 (2), 1063-1073.

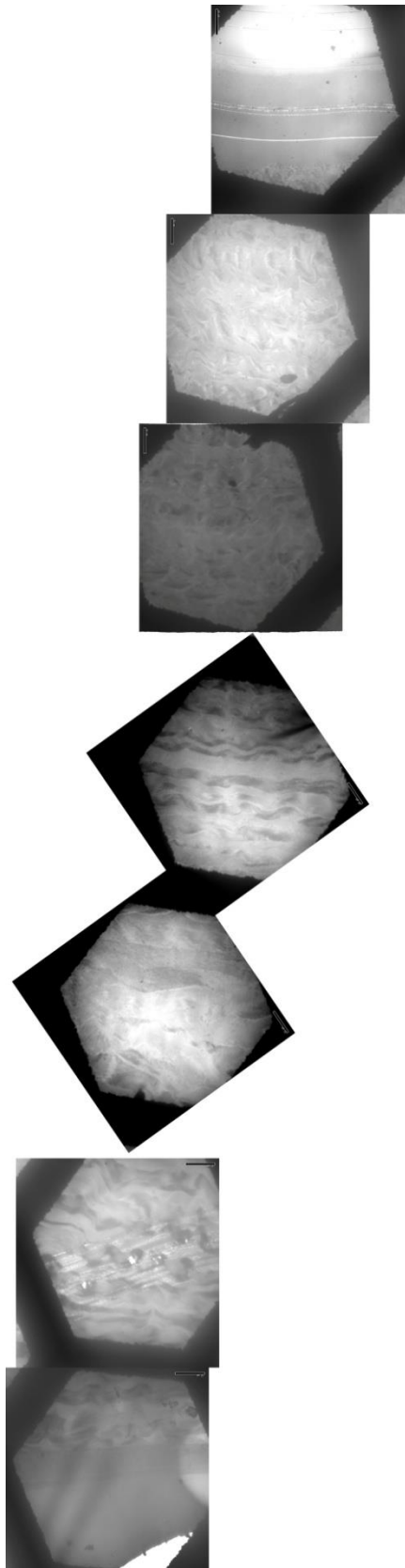
APPENDICES

The following appended data are supplied as additional evidence of the results presented above and are referred to as appropriate within the text.

APPENDIX A



Appendix A(i): Composite TEM micrograph taken in low magnification mode of the full depth profile of the porcine cornea



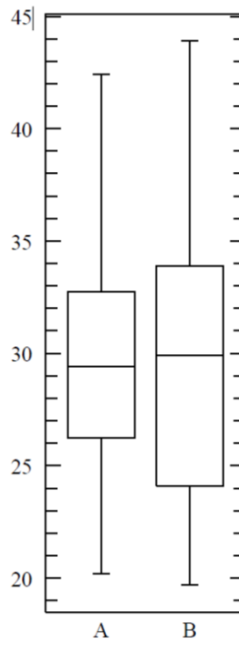
Appendix A(ii): Composite TEM micrograph taken in low magnification mode of the full depth profile of the rabbit cornea

	Porcine corneal stromal tissue						Rabbit corneal stromal tissue					
	C1 Diameter	C1 Spacing	C2 Diameter	C2 Spacing	C3 Diameter	C3 Spacing	C1 Diameter	C1 Spacing	C2 Diameter	C2 Spacing	C3 Diameter	C3 Spacing
Mean	30.9	34.0	26.1	32.3	31.0	36.3	29.9	35.9	31.1	35.1	26.1	29.5
SD	4.0	13.4	3.5	11.7	4.1	12.4	4.9	10.8	5.4	9.4	4.7	11.9
Number of fibrils measured	80	82	70	96	82	88	35	37	37	37	35	36

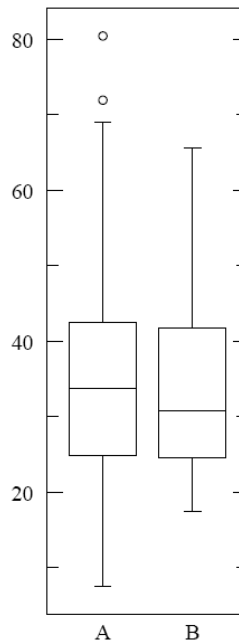
Statistics

	Porcine corneal stromal tissue		Rabbit corneal stromal tissue	
	Diameter	Spacing	Diameter	Spacing
Number of organisms	3		3	
Number of fibrils measured	232	266	107	110
Mean	29.5	34.1	29.1	33.5
SD	4.5	12.5	5.4	11.0
Minimum	20.2	7.5	19.7	17.5
Maximum	42.4	80.4	43.9	65.5

Appendix A(iii): The raw measured diameter and spacing of collagen fibrils of the porcine and rabbit corneal stroma. At least 30 fibril diameters and spacing were measured for each of the three corneas supplied for TEM analysis.



Appendix A(iv): Boxplot of the collagen fibril diameters of porcine (A) versus rabbit (B) corneal stromal tissues; $p=0.44$



Appendix A(v): Boxplot of the collagen fibril spacings of porcine (A) versus rabbit (B) corneal stromal tissues: $p=0.66$

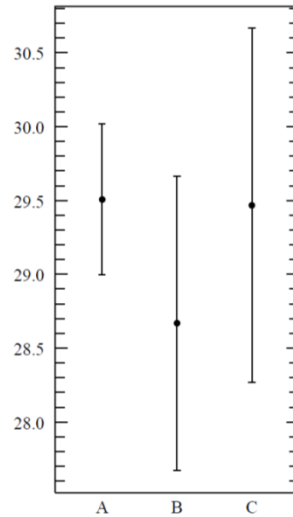
APPENDIX B

	Decellularised/swollen porcine corneal tissue						Swollen corneal tissue					
	Cornea 1		Cornea 2		Cornea 3		Cornea 1		Cornea 2		Cornea 3	
	Diameter	Spacing	Diameter	Spacing	Diameter	Spacing	Diameter	Spacing	Diameter	Spacing	Diameter	Spacing
Mean	27.7	63.2	28.6	75.7	29.5	73.6	28.0	48.9	27.5	47.2	25.5	136.5
SD	1.6	25.2	2.1	26.5	3.1	30.1	1.8	36.8	2.5	30.5	2.0	45.3
n	24.0	38.0	25.0	40.0	24.0	38.0	11.0	12.0	12.0	24.0	11.0	17.0
Min	24.4	25.9	25.0	25.9	25.9	28.2	25.4	11.6	23.8	3.1	21.0	45.3
Max	30.0	115.7	34.1	121.4	39.7	121.4	31.3	110	32.9	100.1	27.8	209.0

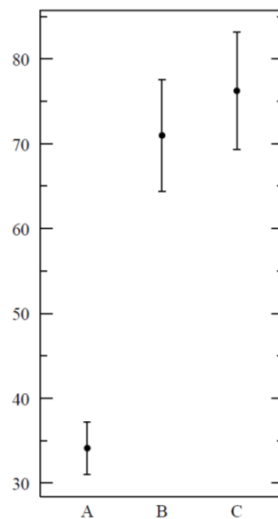
	Dextran treated decellularised/swollen porcine corneal tissue						Dextran treated swollen porcine corneal tissue					
	Cornea 1		Cornea 2		Cornea 3		Cornea 1		Cornea 2		Cornea 3	
	Diameter	Spacing	Diameter	Spacing	Diameter	Spacing	Diameter	Spacing	Diameter	Spacing	Diameter	Spacing
Mean	26.5	53.0	28.6	56.8	28.1	57.7	29.7	46.1	30.4	48.1	30.9	55.4
SD	2.2	21.6	3.7	26.6	2.7	21.7	3.3	23.1	3.3	27.2	3.4	27.2
n	29.0	41.0	29.0	50.0	30.0	47.0	42.0	125.0	34.0	127.0	36.0	44.0
Min	23.2	13.8	21.9	4.4	22.3	16.0	23.5	8.2	24.8	9.4	25.9	9.7
Max	33.8	88.5	39.6	97.4	32.8	97.6	37.9	100.0	36.8	168.2	37.3	103.4

	Statistics									
	Normal Porcine Corneal Stromal Tissue		Decellularised/swollen tissue		Swollen corneal tissue		Dextran treated decellularised/swollen tissue		Dextran treated swollen tissue	
	Diameter	Spacing	Diameter	Spacing	Diameter	Spacing	Diameter	Spacing	Diameter	Spacing
N	3		3		3		3		3	
Mean	29.5	34.1	28.6	70.9	27.0	76.2	27.7	56.0	30.3	48.3
SD	4.5	12.5	2.4	27.8	2.4	55.5	3.0	23.5	3.3	25.7
n	232	266	73	116	34	53	88	138	112	296
Min	20.2	7.5	24.4	25.9	21.0	3.1	21.9	4.4	23.5	8.2
Max	42.4	80.4	39.7	121.4	32.9	209.0	39.6	97.6	37.9	168.2
P-Value			0.33	<0.0001 (0.52)	0.33	<0.0001 (0.52)	0.24	<0.0001 (0.94)	0.24	<0.0001 (0.94)

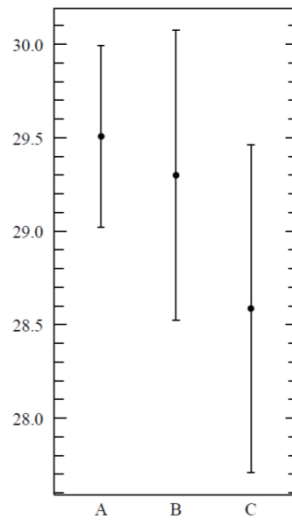
Appendix B(i): The raw measured diameter and spacing of collagen fibrils of swollen porcine corneal stromal tissue



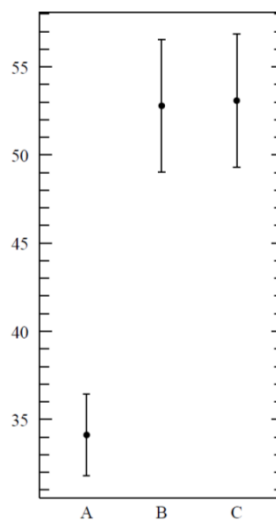
Appendix B(ii): Two-way ANOVA 95% confidence interval plot of the mean collagen fibril diameter (nm) of normal porcine stromal fibrils (A), 1%triton x100 in PBS decellularised and swollen porcine stromal tissues (B), and PBS swollen porcine stromal tissues (C)



Appendix B(iii): Two-way ANOVA 95% confidence interval plot of the mean collagen fibril spacing (nm) of normal porcine stromal fibrils (A), 1%triton x100 in PBS decellularised and swollen porcine stromal tissues (B), and PBS swollen porcine stromal tissues (C)



Appendix B(iv): Two-way ANOVA 95% confidence interval plot of the mean collagen fibril diameter (nm) of normal porcine stromal fibrils (A), 1%triton x100 in PBS decellularised and swollen porcine stromal tissues (B), and PBS swollen porcine stromal tissues (C) after dextran treatment



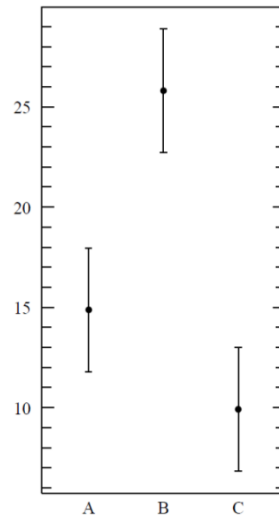
Appendix B(v): Two-way ANOVA 95% confidence interval plot of the mean collagen fibril spacing (nm) of normal porcine stromal fibrils (A), 1%triton x100 in PBS decellularised and swollen porcine stromal tissues (B), and PBS swollen porcine stromal tissues (C) after dextran treatment

APPENDIX C

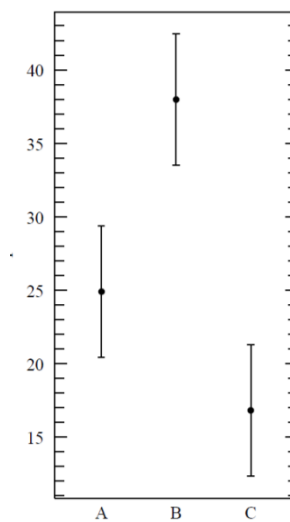
Wavelength	Col I/V + GAG			Col I/V			Col I			Neutralised blank		
	Absorbance	% transmission	SD	Absorbance	% transmission	SD	Absorbance	% transmission	SD	Absorbance	% transmission	SD
405nm (Violet)	0.832	14.73	2.29	0.593	25.51	4.47	1.025	9.45	3.51	0.651	22.78	5.29
450nm (Blue)	0.609	24.61	4.19	0.425	37.63	5.76	0.792	16.16	5.33	0.816	15.90	5.67
490nm (Green)	0.494	32.04	5.51	0.405	39.34	5.36	0.672	21.29	5.47	0.538	29.55	6.91
595nm (Yellow)	0.319	47.97	8.23	0.291	51.19	6.09	0.444	35.99	6.13	0.330	47.20	7.68
750nm (Red)	0.173	67.09	11.43	0.163	68.71	7.33	0.247	56.67	7.23	0.319	48.53	8.09

Appendix C(i): The raw measured mean absorbance data and calculated % light transmittance of a biomimetic artificial corneal replacement.

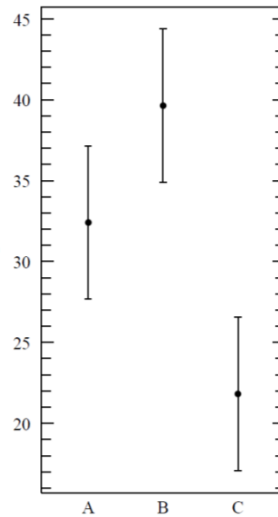
$$\% \text{ light transmittance} = 10^{-\text{Absorbance}} \times 100$$



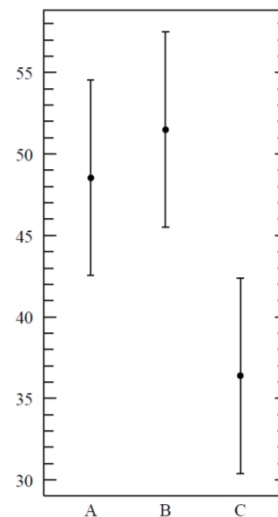
Appendix C(ii): Two-way ANOVA 95% confidence interval plot of the mean % light transmittance of collagen type I/V-CS/DS GAG (A), collagen type I/V (B) and collagen type I (C) hydrogels at 405nm



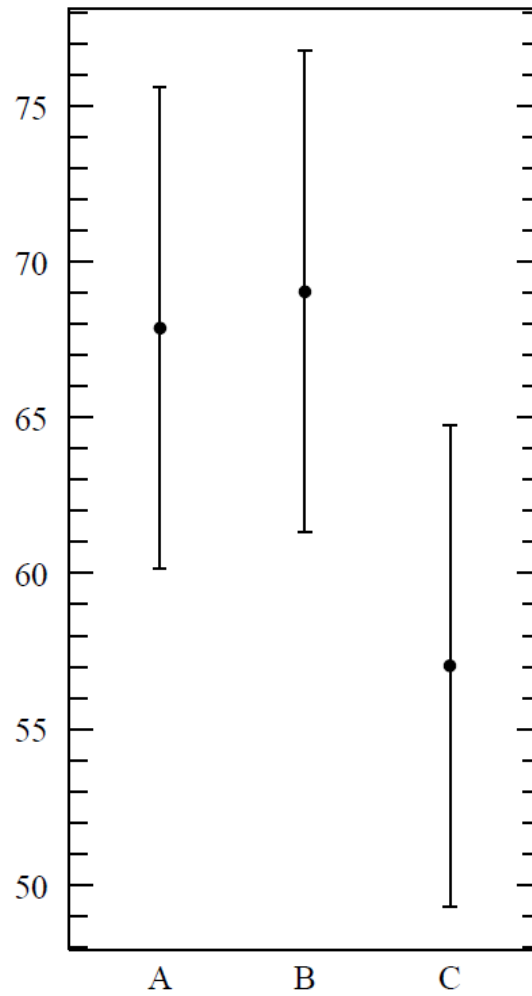
Appendix C(iii): Two-way ANOVA 95% confidence interval plot of the mean % light transmittance of collagen type I/V-CS/DS GAG (A), collagen type I/V (B) and collagen type I (C) hydrogels at 450nm



Appendix C(iv): Two-way ANOVA 95% confidence interval plot of the mean % light transmittance of collagen type I/V-CS/DS GAG (A), collagen type I/V (B) and collagen type I (C) hydrogels at 490nm



Appendix C(v): Two-way ANOVA 95% confidence interval plot of the mean % light transmittance of collagen type I/V-CS/DS GAG (A), collagen type I/V (B) and collagen type I (C) hydrogels at 595nm

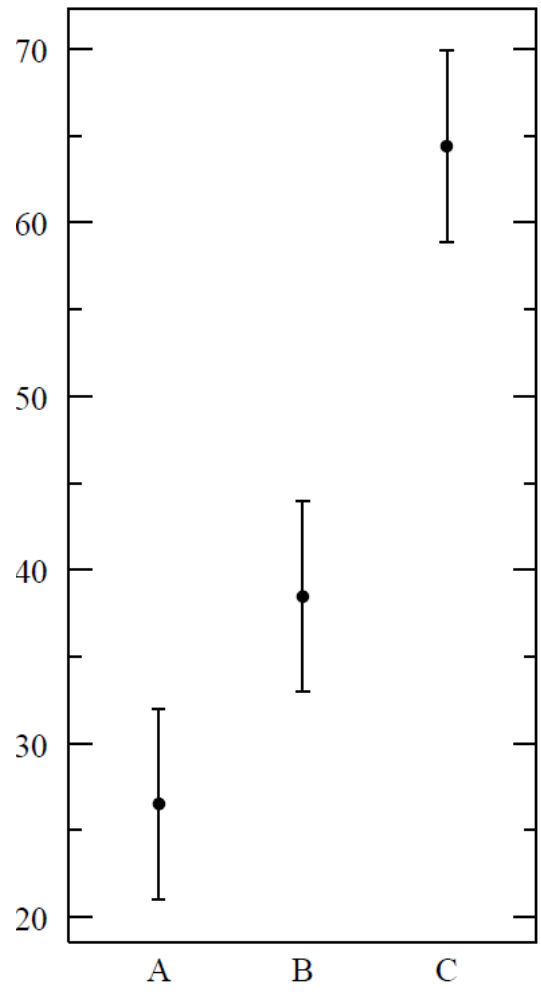


Appendix C(vi): Two-way ANOVA 95% confidence interval plot of the mean % light transmittance of collagen type I/V-CS/DS GAG (A), collagen type I/V (B) and collagen type I (C) hydrogels at 750nm

	Collagen type I/V-GAG hydrogel			Collagen type I/V hydrogel			Collagen type I hydrogel		
	Hydrogel 1	Hydrogel 2	Hydrogel 3	Hydrogel 1	Hydrogel 2	Hydrogel 3	Hydrogel 1	Hydrogel 2	Hydrogel 3
Mean	26.4	24.0	29.2	40.1	37.7	40.5	67.5	74.0	51.7
SD	6.4	5.8	5.8	18.6	21.3	27.9	36.1	19.1	15.9
n	15	15	15	20	15	20	15	15	15
Min	17.2	15.2	18.2	6.3	20.3	15.7	32.3	40.2	32.9
Max	40.3	35.0	39.5	85.7	103.9	146.8	146.8	96.8	78.9

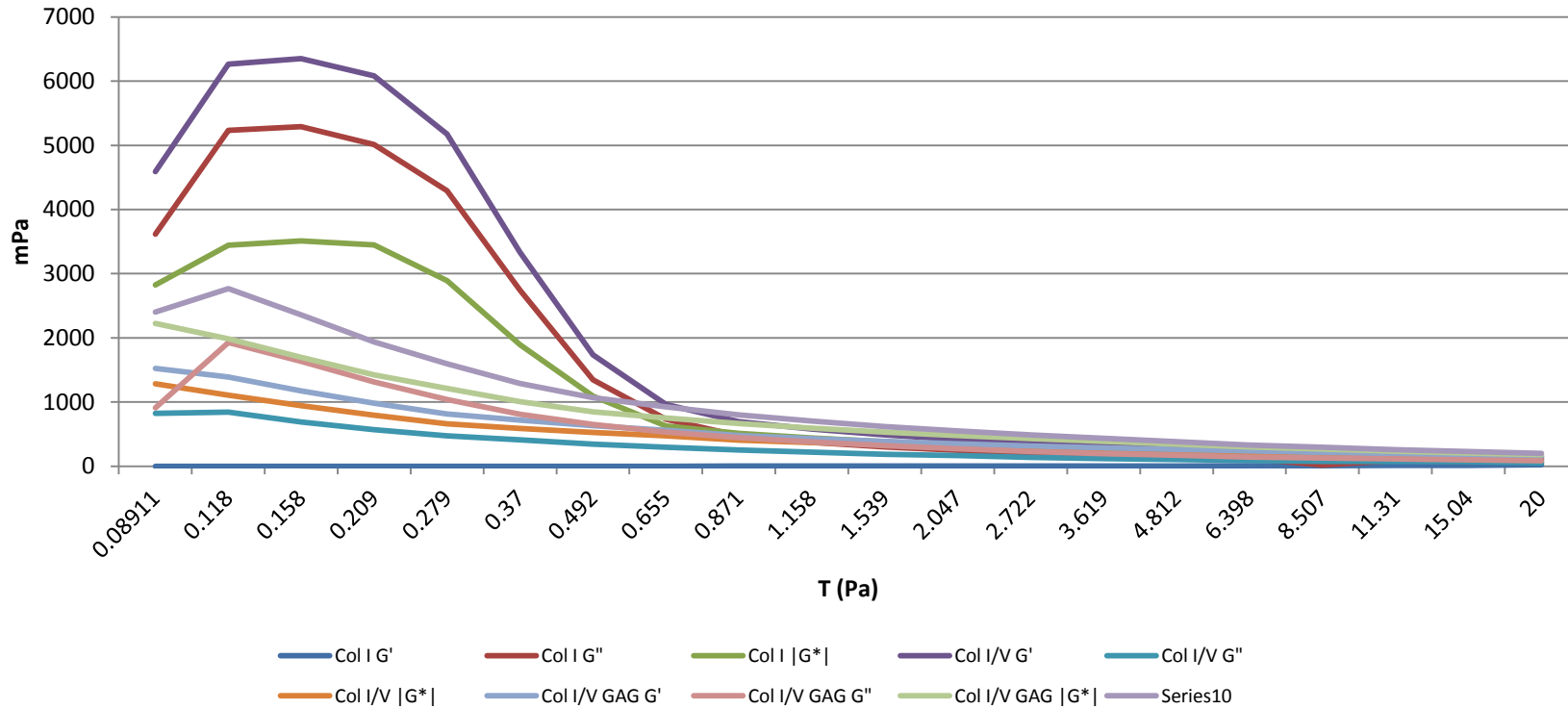
	Collagen type I/V-GAG hydrogel	Collagen type I/V hydrogel	Collagen type I hydrogel
Mean	26.5	38.5	64.4
SD	6.3	17.5	26.5
n	45	45	45
Min	15.2	6.3	32.3
Max	40.3	103.9	146.8

Appendix C(vii): The raw measured fibril diameters of a novel biomimetic corneal replacement



Appendix C(viii): Two-way ANOVA 95% confidence interval plot of the mean fibril diameters of a novel biomimetic corneal replacement

Shear stress sweep test of biomimetic collagen hydrogels



Appendix C(ix): Shear stress sweep test of biomimetic corneal collagen hydrogels.

T (Pa)	ω {rad/s}	Frequency [Hz]	Collagen I		Collagen I/V		Collagen I/V - GAG	
			Mean	SD	Mean	SD	Mean	SD
0.2	0.628	0.1	1.62E+03	2.30E+03	2.52E+03	3.60E+03	1.23E+02	1.19E+02
0.2	0.838	0.133	2.36E+03	3.54E+03	2.12E+03	2.70E+03	2.23E+02	2.39E+02
0.2	1.117	0.178	2.86E+03	4.47E+03	1.08E+04	1.33E+04	3.91E+02	4.66E+02
0.2	1.49	0.237	2.70E+03	4.21E+03	2.55E+03	3.23E+03	3.89E+02	3.85E+02
0.2	1.987	0.316	3.43E+03	5.45E+03	2.24E+04	3.74E+04	5.75E+02	6.12E+02
0.2	2.65	0.422	3.83E+03	6.12E+03	2.95E+03	3.50E+03	6.65E+02	6.59E+02
0.2	3.533	0.562	3.88E+03	6.19E+03	3.26E+03	3.95E+03	7.97E+02	7.68E+02
0.2	4.712	0.75	4.38E+03	6.97E+03	3.62E+03	4.22E+03	8.57E+02	8.56E+02
0.2	6.283	1	4.80E+03	7.47E+03	4.01E+03	4.62E+03	1.09E+03	8.87E+02
0.2	8.379	1.334	5.37E+03	8.06E+03	4.51E+03	4.96E+03	1.29E+03	8.74E+02
0.2	11.17	1.778	5.77E+03	8.18E+03	5.11E+03	5.31E+03	1.68E+03	9.53E+02
0.2	14.9	2.371	6.58E+03	8.62E+03	6.09E+03	5.88E+03	2.23E+03	9.43E+02
0.2	19.87	3.162	7.18E+03	8.03E+03	6.67E+03	5.12E+03	3.16E+03	1.45E+03
0.2	26.5	4.217	7.26E+03	6.76E+03	8.42E+03	4.86E+03	5.03E+03	2.18E+03
0.2	35.33	5.623	9.04E+03	8.84E+03	1.06E+04	3.66E+03	7.26E+03	3.31E+03
0.2	47.12	7.499	1.18E+04	1.19E+04	6.02E+03	4.08E+03	1.11E+04	5.87E+03
0.2	62.83	10	1.64E+04	1.68E+04	1.31E+04	5.91E+03	1.67E+04	1.05E+04

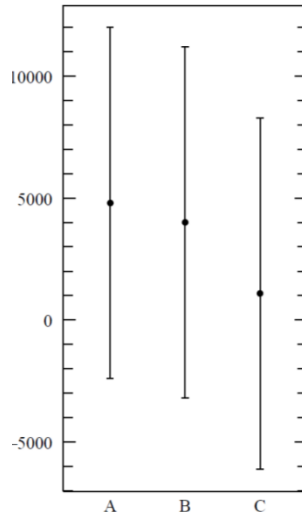
Appendix C(x): Storage modulus (G') data for biomimetic corneal collagen hydrogels collected using frequency sweep test rheology (n=3 in all cases)

T (Pa)	ω {rad/s}	Frequency [Hz]	Collagen I		Collagen I/V		Collagen I/V - GAG	
			Mean	SD	Mean	SD	Mean	SD
0.2	0.628	0.1	1.26E+03	1.52E+03	2.15E+03	2.47E+03	4.44E+02	4.50E+02
0.2	0.838	0.133	1.71E+03	2.38E+03	2.01E+03	2.11E+03	5.37E+02	5.32E+02
0.2	1.117	0.178	1.78E+03	2.60E+03	1.95E+03	1.92E+03	6.93E+02	7.12E+02
0.2	1.49	0.237	1.75E+03	2.52E+03	1.95E+03	1.79E+03	7.37E+02	6.95E+02
0.2	1.987	0.316	1.73E+03	2.45E+03	2.15E+03	1.81E+03	8.46E+02	7.90E+02
0.2	2.65	0.422	1.88E+03	2.68E+03	2.38E+03	2.04E+03	9.59E+02	8.85E+02
0.2	3.533	0.562	1.81E+03	2.58E+03	2.58E+03	2.23E+03	1.08E+03	1.01E+03
0.2	4.712	0.75	2.16E+03	3.11E+03	2.78E+03	2.27E+03	1.19E+03	1.10E+03
0.2	6.283	1	2.34E+03	3.25E+03	3.03E+03	2.39E+03	1.28E+03	1.13E+03
0.2	8.379	1.334	2.60E+03	3.47E+03	3.57E+03	2.92E+03	1.40E+03	1.16E+03
0.2	11.17	1.778	2.99E+03	3.93E+03	3.80E+03	2.99E+03	1.54E+03	1.15E+03
0.2	14.9	2.371	3.10E+03	4.54E+03	4.45E+03	3.38E+03	1.86E+03	1.56E+03
0.2	19.87	3.162	3.68E+03	4.22E+03	5.03E+03	3.32E+03	2.30E+03	2.08E+03
0.2	26.5	4.217	3.51E+03	3.72E+03	5.93E+03	4.03E+03	2.83E+03	2.95E+03
0.2	35.33	5.623	4.62E+03	4.94E+03	7.78E+03	5.10E+03	3.73E+03	4.07E+03
0.2	47.12	7.499	5.23E+03	6.23E+03	8.69E+03	6.03E+03	4.22E+03	5.65E+03
0.2	62.83	10	5.85E+03	8.36E+03	9.29E+03	7.10E+03	4.46E+03	7.06E+03

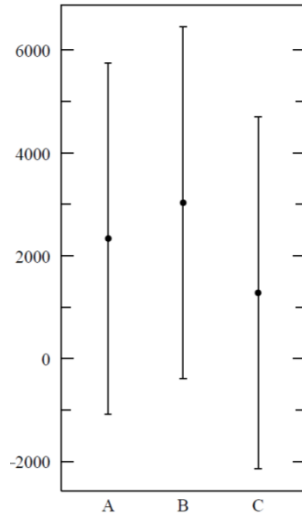
Appendix C(xi): Loss modulus (G'') data for biomimetic corneal collagen hydrogels collected using frequency sweep test rheology (n=3 in all cases)

T (Pa)	ω {rad/s}	Frequency [Hz]	Collagen I		Collagen I/V		Collagen I/V - GAG	
			Mean	SD	Mean	SD	Mean	SD
0.2	0.628	0.1	2.07E+03	2.74E+03	3.34E+03	4.33E+03	4.61E+02	4.66E+02
0.2	0.838	0.133	2.92E+03	4.26E+03	2.94E+03	3.40E+03	5.82E+02	5.83E+02
0.2	1.117	0.178	3.38E+03	5.16E+03	3.02E+03	3.47E+03	7.98E+02	8.48E+02
0.2	1.49	0.237	3.23E+03	4.90E+03	3.25E+03	3.64E+03	8.34E+02	7.94E+02
0.2	1.987	0.316	6.38E+02	3.79E+02	3.56E+03	3.72E+03	1.02E+03	9.96E+02
0.2	2.65	0.422	4.29E+03	6.65E+03	3.83E+03	3.99E+03	1.17E+03	1.10E+03
0.2	3.533	0.562	4.30E+03	6.69E+03	6.88E+03	3.74E+03	1.34E+03	1.27E+03
0.2	4.712	0.75	4.90E+03	7.61E+03	4.62E+03	4.70E+03	1.51E+03	1.37E+03
0.2	6.283	1	5.35E+03	8.12E+03	5.10E+03	5.09E+03	1.68E+03	1.44E+03
0.2	8.379	1.334	5.98E+03	8.75E+03	5.47E+03	5.87E+03	1.91E+03	1.45E+03
0.2	11.17	1.778	6.51E+03	9.07E+03	6.42E+03	6.02E+03	2.28E+03	1.48E+03
0.2	14.9	2.371	7.41E+03	9.62E+03	7.59E+03	6.69E+03	3.54E+03	1.76E+03
0.2	19.87	3.162	7.89E+03	9.21E+03	8.39E+03	6.03E+03	3.97E+03	2.39E+03
0.2	26.5	4.217	8.07E+03	7.71E+03	1.03E+04	6.20E+03	5.92E+03	3.30E+03
0.2	35.33	5.623	1.02E+04	1.01E+04	1.23E+04	6.93E+03	8.42E+03	4.58E+03
0.2	47.12	7.499	1.29E+04	1.34E+04	1.43E+04	7.60E+03	1.24E+04	7.00E+03
0.2	62.83	10	1.75E+04	1.85E+04	1.65E+04	8.08E+03	1.79E+04	1.13E+04

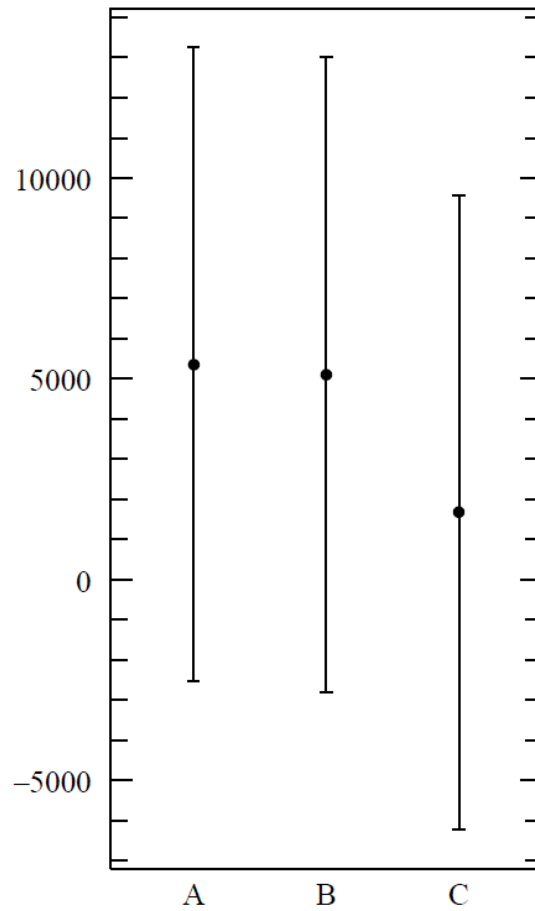
Appendix C(xii): Complex modulus ($|G^*|$) data for biomimetic corneal collagen hydrogels collected using frequency sweep test rheology (n=3
in all cases)



Appendix C(xiii): Two-way ANOVA 95% confidence interval plot of the storage modulus (G') data for collagen type I (A), collagen type I/V (B) and collagen type I/V-GAG (C) hydrogels collected using frequency sweep test rheology



Appendix C(xiv): Two-way ANOVA 95% confidence interval plot of the loss modulus (G'') data for collagen type I (A), collagen type I/V (B) and collagen type I/V-GAG (C) hydrogels collected using frequency sweep test rheology



Appendix C(xv): Two-way ANOVA 95% confidence interval plot of the complex modulus ($|G^*|$) data for collagen type I (A), collagen type I/V (B) and collagen type I/V-GAG (C) hydrogels collected using frequency sweep test rheology